

1-1-2001

Atom transfer radical polymerization : fundamentals, challenges, and application.

Young-Je, Kwark

University of Massachusetts Amherst

Follow this and additional works at: https://scholarworks.umass.edu/dissertations_1

Recommended Citation

Kwark, Young-Je, "Atom transfer radical polymerization : fundamentals, challenges, and application." (2001). *Doctoral Dissertations 1896 - February 2014*. 1024.

https://scholarworks.umass.edu/dissertations_1/1024

This Open Access Dissertation is brought to you for free and open access by ScholarWorks@UMass Amherst. It has been accepted for inclusion in Doctoral Dissertations 1896 - February 2014 by an authorized administrator of ScholarWorks@UMass Amherst. For more information, please contact scholarworks@library.umass.edu.

*

UMASS/AMHERST

*



312066 0275 8508 8

ATOM TRANSFER RADICAL POLYMERIZATION:
FUNDAMENTALS, CHALLENGES, AND APPLICATION

A Dissertation Presented

by

YOUNG-JE KWARK

Submitted to the Graduate School of the
University of Massachusetts Amherst in partial fulfillment
Of the requirements for the degree of

DOCTOR OF PHILOSOPHY

September 2001

Polymer Science and Engineering

© Copyright by Young-Je Kwark 2001

All Rights Reserved

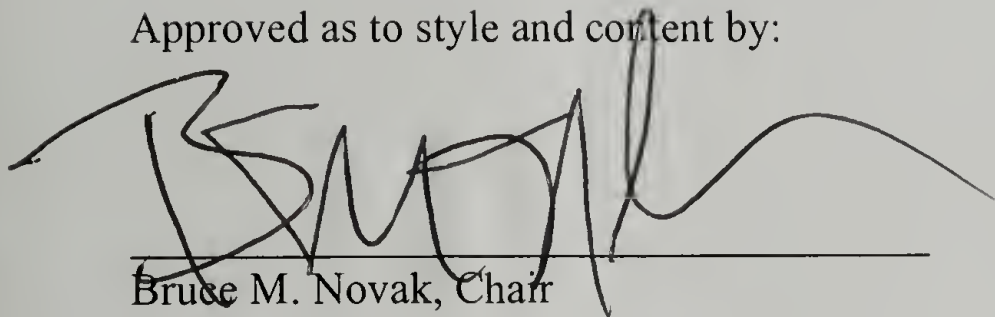
Atom Transfer Radical Polymerization:
Fundamentals, Challenges, and Application

A Dissertation Presented

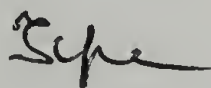
by

YOUNG-JE KWARK

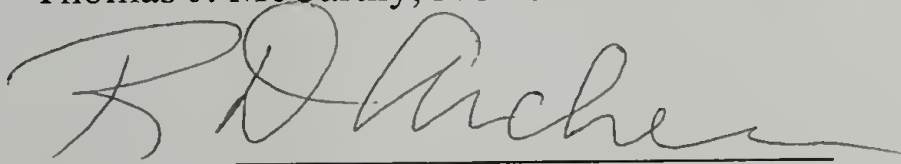
Approved as to style and content by:



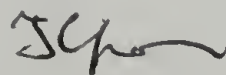
Bruce M. Novak, Chair



Thomas J. McCarthy, Member



Ronald D. Archer, Member



Thomas J. McCarthy, Department Head
Department of Polymer Science and
Engineering

DEDICATION

To my patient and loving wife.

ABSTRACT

ATOM TRANSFER RADICAL POLYMERIZATION:
FUNDAMENTALS, CHALLENGES, AND APPLICATION

SEPTEMBER 2001

YOUNG-JE KWARK, B.S. SEOUL NATIONAL UNIVERSITY

M.S., SEOUL NATIONAL UNIVERSITY

Ph.D., UNIVERSITY OF MASSACHUSETTS AMHERST

Directed by: Professor Bruce M. Novak

Various aspects of atom transfer radical polymerization (ATRP) were investigated. In an attempt to find a novel catalyst system for ATRP, we screened the activities of various metal complexes using a combinatorial approach. Several new catalyst systems including $\text{FeCl}_2/\text{bam}(\text{TMS})$ were found to be active ATRP catalysts in the polymerization of styrene and MMA. In order to make this combinatorial screening a viable method of quickly discovering usable systems, we tried to find a fast and reliable method to evaluate the catalysts. A parameter estimation method based on nonlinear regression was developed to evaluate various catalyst systems by determining kinetic parameters of polymerization. From our model system considering small molecular atom transfer addition reaction, we found that equilibrium constant of atom transfer reaction could be successfully estimated. A new model dealing polymerization itself was also developed, and we could demonstrate that each values of activation and deactivation reaction rate constant can be estimated unambiguously.

On screening the catalyst systems for ATRP, we found some titanium complexes gave a control in the polymerization of styrene without the aid of Group I-III cocatalysts. A series of experiments to elucidate the mechanism of polymerization all support that radical mechanism is involved in the polymerization using bis-(cyclopentadienyl)titanium dichloride. A possibility of ATRP mechanism was checked by isolating intermediate species. It is found that the polymerization is not followed the pure ATRP pathway, but is comprised of various competing reactions.

Several strategies has been developed to prepare polymers having higher order structure including branched, hyperbranched, star, and dendrigrafts. The combination of nitroxide mediated SFRP and ATRP techniques successfully provided relatively simple routes to from branched and hyperbranched polymers in controlled structures. To overcome this limitation of backbone polymer prepared by SFRP, a new strategy using protection-deprotection chemistry was employed. Among the various protected monomers tested, we could prepare branched polystyrene having controlled structure using *VBt*-BOC and 4-methyl styrene. As an example of diversity of this strategy, we also could prepare the branched acrylate polymer having controlled structure.

TABLE OF CONTENTS

	Page
ABSTRACT	v
LIST OF TABLES	xii
LIST OF FIGURES.....	xiv
LIST OF SCHEMES.....	xix
CHAPTER	
1. INTRODUCTION.....	1
1.1 Introduction.....	2
1.2 Controlled/"Living" Radical Polymerization.....	2
1.2.1 Nitroxide-Mediated Stable Free Radical Polymerization (SFRP)	7
1.2.2 Reversible Addition-Fragmentation Chain Transfer Process (RAFT).....	15
1.2.3 Atom Transfer Radical Polymerization (ATRP).....	17
1.3 Combinational Screening of Transition Metal Complexes for Activity as ATRP Catalysts	21
1.4 Conclusion.....	35
1.5 Experimental	40
1.5.1 Materials and Characterization.....	40
1.5.2 Preparation of Ligands	41
1.5.3 Combinatorial Screening of Catalyst Systems	45
1.5.3.1 Parallel Polymerizations.....	45
1.5.3.2 Kinetic Studies of the Polymerization of Styrene	45
1.5.3.3 Determination of Half-Wave Potential ($E_{1/2}$) of Metal Complexes using Cyclovoltametric Analysis	46
1.6 References	47
2. DETERMINATION OF KINETIC PARAMETERS OF ATRP.....	55
2.1 Introduction	56
2.2 Development of a Parameter Estimation Algorithm.....	60
2.2.1 Model Reactions.....	60
2.2.2 Development of the Algorithm	62

2.3	Checking the Approach	67
2.3.1	Checking the Model	67
2.3.2	Verifying the Parameter Estimation Algorithm	77
2.3.3	A Model to Estimate k_{act} and k_{deact}	92
2.4	Application to Experimental Data	97
2.4.1	Application to Available Literature Data	97
2.4.2	Data Collection	101
2.4.3	Determination of Kinetic Constants in ATRP for Various Polymerization Systems	105
2.5	Conclusion	111
2.6	Experimental	112
2.6.1	Materials and Characterization	112
2.6.2	Preparation of Model Compounds	113
2.6.3	Kinetic Study	116
2.6.3.1	ATRA of Styrene	116
2.6.3.2	ATRA of Methyl Methacrylate	117
2.7	References	119
3.	TITANIUM COMPLEXES AS CATALYSTS FOR CONTROLLED RADICAL POLYMERIZATION	121
3.1	Introduction	122
3.2	Controlled Polymerization of Styrene Using Titanium(IV) Complexes	129
3.2.1	Kinetics of Polymerization	130
3.2.2	Chain Extension Reaction	132
3.3	Verifying the Mechanism of the Polymerization using Titanium Complexes	133
3.3.1	Effects of the Radical Inhibitors	134
3.3.2	Effects of the Radical Chain Transfer Agents	136
3.3.3	Copolymerization of Styrene and Ethyl Vinyl Ether	138
3.3.4	Polymerization of Methyl Methacrylate	140
3.4	Polymerization of Styrene using Titanium(III) Complexes	141
3.5	Checking Atom Transfer Reaction	146
3.5.1	Isolation of the Activation Reaction	146

3.5.2 Isolation of the Deactivation Reaction	148
3.6 Conclusion.....	152
3.7 Experimental	153
3.7.1 Materials and Characterization.....	153
3.7.2 Polymerization	155
3.7.2.1 General Methods of Polymerization	155
3.7.2.2 Polymerization of Styrene Using Titanium(IV) Complexes.....	157
3.7.2.2.1 Kinetic Studies of the Polymerization of Styrene Using Various Titanium(IV) Complexes	157
3.7.2.2.2 Chain Extension Reaction.....	157
3.7.2.3 Verifying the Mechanism of the Polymerization Using Titanium Complexes	158
3.7.2.3.1 Polymerization of Styrene with Radical Inhibitors	158
3.7.2.3.2 Polymerization of Styrene with Radical Chain Transfer Agent.....	158
3.7.2.3.3 Copolymerization of Styrene with Ethyl Vinyl Ether..	158
3.7.2.3.2 Polymerization of Methyl Methacrylate	159
3.7.2.4 Polymerization of Styrene Using Titanium(III) Complexes (Cp ₂ TiCl).....	159
3.7.3 Checking Atom Transfer Reaction.....	159
3.7.3.1 Isolation of Activation Steps in ATRP.....	159
3.7.3.2 Isolation of Deactivation Steps in ATRP	160
3.8 References	161
4. PREPARATION OF POLYMERS HAVING VARIOUS ARCHITECTURES.....	165
4.1 Introduction	166
4.2 Preparation of Branched or Comb Polymers by the Sequential Use of Conventional Radical Polymerization and ATRP.....	171
4.3 Branched Polymers by the Sequential Use of Two Different Controlled Free Radical Polymerization Methods	173
4.4 Hyperbranched Polymers by the Sequential Use of Two Different Controlled Free Radical Polymerization Methods	178
4.5 Star-like Polymers by Two-Step Reaction Using ATRP Methods	182
4.6 Branched Polymers Using Protection-Deprotection Chemistry.....	183

4.6.1	Vinylbenzyltosylate (VBOTs)	187
4.6.2	Vinylbenzyl dimethyl- <i>t</i> -butylsilylether (VBOSi).....	188
4.6.3	Vinylbenzylalcohol (VBOH)	193
4.6.4	Vinylbenzyl- <i>t</i> -butylether (VBO <i>t</i> -Bu).....	195
4.6.5	Vinylbenzyl- <i>t</i> -butyloxycarbonate (VB <i>t</i> -BOC).....	197
4.6.5.1	Synthesis of VB <i>t</i> -BOC	198
4.6.5.2	Homopolymerization of VB <i>t</i> -BOC	199
4.6.5.3	Deprotection Reaction of Poly(VB <i>t</i> -BOC)	204
4.6.5.4	Preparation of Linear-Branched Block Copolymer	208
4.6.6	4-Methylstyrene	211
4.6.7	2-Isobutyryloxyethyl Methacrylate (IBEM)	216
4.7	Conclusion.....	219
4.8	Experimental	221
4.8.1	Characterizations.....	221
4.8.2	Materials.....	222
4.8.2.1	Preparation of Protected Monomers.....	222
4.8.3	Deprotection Reactions	227
4.8.3.1	Deprotection of <i>t</i> -Butyloxycarbonate Group.....	227
4.8.3.2	Bromination of Poly(4-methyl styrene)	227
4.8.3.2	Bromination of Poly(IBEM)	228
4.8.4	Polymerization	228
4.8.4.1	Preparation of Branched Polymers Using Conventional Radical Polymerization and ATRP Method.....	228
4.8.4.2	Preparation of Branched Polymers by the Sequential Use of Two Different Controlled Free Radical Polymerization Methods	229
4.8.4.3	Preparation of Hyperbranched Polymers by the Sequential Use of Two Different Controlled Free Radical Polymerization Methods	230
4.8.4.4	Preparation of Star Polymers by the Sequential Use of Two Different Controlled Free Radical Polymerization Methods	230
4.8.4.5	Branched Polymers Using Protection-Deprotection Chemistry..	231
4.8.4.5.1	General Procedure	231
4.8.4.5.2	Polymerization of Styrenes in the Presence of Additives Bearing the Same Functionalities	

as the Protecting Groups	231
4.8.4.5.3 Preparation of Linear-Branched Block Copolymer	232
4.8.4.5.4 Preparation of Branched PMMA.....	233
4.9 References	235
BIBLIOGRAPHY	238

LIST OF TABLES

Table	Page
1.1 Screening of the Metal Complexes for Activity as a Catalyst of the ATRP of Styrene	24
1.2 Screening of the Metal Complexes for Activity as a Catalyst of the ATRP of MMA.....	29
2.1 Values of the Parameters Used in the Simulation of Styrene ATRP	68
2.2 Values of the Parameters Used in the Simulation of Styrene ATRA.....	78
2.3 Effect of the Initial Guess on the Estimated Parameters.....	80
2.4 Parameter Estimation Using the Algorithm of Sequential Use of MINPACK and DSM.....	88
2.5 Effect of Reparameterization. Reparameterization was performed as $k'' = k'/10$...	89
2.6 Effect of reparameterization. Reparameterization was performed as $k'' = k' \times 10$...	89
2.7 Effect of Experimental Noise on the Estimated Parameters	90
2.8 Effect of the Number of Experimental Data on the Accuracy of Estimated Parameters	91
2.9 Parameter Estimation Based on Our New Model Using Polymerization Data (conversion, M_n , and PDI).....	95
2.10 Conditions of Reaction Used to Determine Chain End Degradation Rate Constants by Matyjaszewski, <i>et al.</i>	97
2.11 Result of Parameter Estimation Using Literature Data.....	98
2.12 Estimation of Kinetic Parameters in the ATRA of Styrene Using FeBr ₂ /PnBu ₃ Catalyst System	106
2.13 Estimation of Kinetic Parameters in the ATRA of Styrene Using RuCl ₂ (PPh ₃) ₃ /Al(O- <i>i</i> Pr) ₃ Catalyst System	107
2.14 Estimation of Kinetic Parameters in the ATRA of MMA Using FeBr ₂ /PnBu ₃ Catalyst System	108
2.15 Estimation of Kinetic Parameters in the ATRA of MMA Using	

	RuCl ₂ (PPh ₃) ₃ /Al(O- <i>i</i> Pr) ₃ Catalyst System	109
3.1	Polymerization of Styrene Under Various Conditions at 130 °C	130
3.2	Effect of Radical Scavenger on the Polymerization of Styrene Using Titanium Complexes	136
3.3	Effect of Radical Chain Transfer Agent (1-octanethiol, RSH) on the Polymerization of Styrene Using Titanium Complexes (a, Cp ₂ TiCl ₂ ; b, Cp*TiCl ₃) at 130 °C	138
3.4	Copolymerization of Styrene and Ethyl Vinyl Ether Using Various Titanium Complexes at 100 °C	139
3.5	Polymerization of Methyl Methacrylate (MMA) Using Titanium Complexes (a, Cp ₂ TiCl ₂ ; b, Cp*TiCl ₃)	140
3.6	Polymerization of Styrene Using Cp ₂ Ti ^{III} Cl and 1-Phenylethyl Chloride at Various Temperatures	143
4.1	Polymerization of VBOSi Under Various Conditions	191
4.2	Polymerization of VBt-BOC Under Various Conditions.....	201

LIST OF FIGURES

Figure	Page
1.1 Stable nitroxide radicals used in SFRP process	11
1.2 A shaker used in parallel syntheses of polymers to screen transition metal complexes for activity as an ATRP catalyst in combinatorial way	23
1.3 Kinetics of polymerization of styrene using various catalyst systems	32
1.4 Cyclovoltammograms of CuCl/4,4'-di-(4-ethylphenoxy)-2,2'-bipyridine (epy) in 0.1 M of Bu ₄ N·PF ₆ /DMF measured at different temperature. (a) 25 °C, (b) 50 °C, (c) 100 °C	37
1.5 Relationship between half-wave potential of metal complexes ($E_{1/2}$) and apparent rate constant of the polymerization (k_{app}) using these metal complexes. (□, heterogeneous system; ■, homogeneous system).....	38
1.6 Relationship between half-wave potential of metal complexes ($E_{1/2}$) and polydispersity index(PDI) of polymers prepared using these metal complexes. (□, heterogeneous system; ■, homogeneous system).....	39
2.1 First-order kinetic plot of monomer consumption in the ATRP of styrene simulations (---, Fischer's result), (—, this work).....	70
2.2 First-order kinetic plot of monomer consumption, as a function of time ^{2/3} , in the ATRP of styrene simulations (---, Fischer's result), (—, this work)	70
2.3 [Mt ⁿ⁺¹] as a function of time in the ATRP of styrene simulations (---, Fischer's result), (—, this work).....	72
2.4 [Mt ⁿ⁺¹] as a function of time ^{1/3} in the ATRP of styrene simulations (---, Fischer's result), (—, this work).....	72
2.5 First-order kinetic plot of monomer consumption in the ATRP of styrene; experiment (■) and simulation with (a) constant k_t (---); (b) diffusion-dependent k_t (—)	74
2.6 [Mt ⁿ⁺¹] as a function of time in the ATRP of styrene; experiment (■) and simulation with (a) constant k_t (---); (b) diffusion-dependent k_t (—).....	74
2.7 Concentrations of dormant species, deactivator, and active vs. time in a double-logarithmic plot.....	76
2.8 One-dimensional contour maps. Φ is the merit function defined by eq. 3	81

2.9	Extrema of a function in an interval. Points A, C, and G are local, but not global minima. Points B and F are local, but not global minima. The global maximum occurs at D. The global minimum is at E.....	83
2.10	Possible outcomes for a step in the downhill simplex method. The simplex at the beginning of the step, here a tetrahedron, is shown, top. The simplex at the end of the step can be any one of (a) a reflection away from the high point, (b) a reflection and expansion away from the high point, (c) a contraction along one dimension from the high point, or (d) a contraction along all dimensions towards the low point. (Ref. 16)	87
2.11	Simulated data of $\ln([M]_0/[M])$ (♦) and conversion () vs. time based on our new model using the same conditions in Table 1 except $k_{tc} = 0$	96
2.12	Number average degree of polymerization (X_n , ♦) and polydispersity (PDI,) simulated based on our new model using the same condition in Table 1 except $k_{tc} = 0$	96
2.13	First-order kinetic plot of 1-phenylethyl bromide (1-PEBr) consumption in the ATRA of styrene; experimental data (points) and simulation with estimated kinetic parameters (lines).....	100
2.14	First-order kinetic plot of monomer consumption in the ATRP of styrene; experimental data (points) and simulation (lines; ---, with the literature values of kinetic parameters and —, with estimated kinetic parameters).....	100
2.15	GC-MS spectrum of a typical reaction mixture of styrene ATRA	103
2.16	Convolution of various components over reaction time in the ATRA of styrene using $\text{FeBr}_2/\text{PnBu}_3$ catalyst system. Points (experimental data), lines (simulation with the estimated kinetic parameters)	106
2.17	Convolution of various components over reaction time in the ATRA of styrene using $\text{RuCl}_2(\text{PPh}_3)_3/\text{Al}(\text{O-}i\text{Pr})_3$ catalyst system. Points (experimental data), lines (simulation with the estimated kinetic parameters).....	107
2.18	Convolution of various components over reaction time in the ATRA of MMA using $\text{FeBr}_2/\text{PnBu}_3$ catalyst system. Points (experimental data), lines (simulation with the estimated kinetic parameters).....	108
2.19	Convolution of various components over reaction time in the ATRA of MMA using $\text{RuCl}_2(\text{PPh}_3)_3/\text{Al}(\text{O-}i\text{Pr})_3$ catalyst system. Points (experimental data), lines (simulation with the estimated kinetic parameters)	109
2.20	First-order kinetic plot of monomer consumption in the ATRP of styrene	

	using $\text{FeBr}_2/\text{PnBu}_3$ catalyst. Experimental data (points) and simulation with the estimated rate constants by parameter estimation approach (line).....	110
3.1	Transition metals of which complexes have been used as ATRP catalysts	128
3.2	Kinetic of the polymerization of styrene using various titanium complexes at 130°C , (a) Cp_2TiCl_2 (\blacklozenge , ---); (b) Cp^*TiCl_3 (\blacksquare , —); (c) $\text{Cp}^*_2\text{TiCl}_2$ (\blacktriangle , - · -)..	131
3.3	Plots of number average molecular weight (M_n , \blacklozenge , —) and polydispersity index (PDI, \blacksquare , ---) of the polymer and monomer conversion for the polymerization of styrene using Cp_2TiCl_2 at 130°C	131
3.4	GPC traces of (a) initial polystyrene before the chain extension reaction; (b) final polystyrene after the reaction using Cp_2TiCl_2	133
3.5	$^1\text{H-NMR}$ spectrum of poly(methyl methacrylate) prepared using (a) Cp_2TiCl_2 ; (b) benzoyl peroxide.....	141
3.6	Kinetic plots of $\ln([\text{M}]_0/[\text{M}])$ vs. time for the bulk polymerization of styrene using Cp_2TiCl_2 at 90°C	145
3.7	Plots of molecular weight and polydispersity of the polymer and monomer conversion for the polymerization of styrene using Cp_2TiCl_2 at 90°C	145
3.8	$^1\text{H-NMR}$ spectrum of Cp_2TiCl_2 and 1-phenylethyl chloride in toluene- d_8	147
3.9	$^1\text{H-NMR}$ spectrum after reaction between 1-phenylethyl-TEMPO adduct and Cp_2TiCl_2 at 130°C in toluene- d_8	150
4.1	Polymer architectures that have been prepared to date.....	167
4.2	Polymer architectures involving two monomers, A (\circ) and B (\bullet).....	168
4.3	GPC chromatograms of (a) backbone polymer prepared by conventional free radical polymerization method and (b) branched polymer by ATRP	173
4.4	GPC chromatograms of (a) backbone polymer prepared by nitroxide-mediated SFRP method and (b) branched polymer by ATRP.....	175
4.5	GPC chromatograms of linear-branched block copolymers prepared by the sequential use of two different controlled free radical polymerization methods: (a) initial polystyrene by nitroxide-mediated SFRP method (---); (b) linear block copoly(styrene- <i>b</i> -vinylbenzyl chloride) (—); and (c) linear-branched block copolymers ()	177
4.6	Plots of of molecular weight vs. radius of gyration of the polymer measured by	

GPC-LS, linear polystyrene (◆, slope = 0.472) and hyperbranched poly(vinylbenzyl chloride) (+, slope = 0.082)	179
4.7 ¹ H-NMR spectrum of hyperbranched poly(vinylbenzyl chloride).....	180
4.8 GPC chromatograms of (a) poly(vinylbenzyl chloride) and (b) styrene-poly(vinylbenzyl chloride) copolymer	180
4.9 GPC chromatograms of poly(vinylbenzyl chloride) (—) and the star-like polymer (---).....	183
4.10 GC chromatogram of VBOSi	190
4.11 ¹ H-NMR spectrum of VBOSi	190
4.12 GPC chromatogram of poly(vinylbenzyl alcohol)	194
4.13 GPC chromatogram of polystyrene prepared in the presence of benzyl alcohol ...	194
4.14 GC chromatogram of VBO <i>t</i> -Bu	196
4.15 ¹ H-NMR spectrum of VBO <i>t</i> -Bu.....	196
4.16 GPC chromatogram of poly(vinylbenzyl <i>t</i> -butylether) polymerized at (a) 130 °C and (b) 110 °C	197
4.17 ¹ H-NMR spectrum of VB <i>t</i> -BOC	200
4.18 GC chromatogram of VB <i>t</i> -BOC	200
4.19 GPC chromatogram of poly(VB <i>t</i> -BOC) prepared using CuCl/pby as a catalyst at 130 °C, (a) Run 1, (b) Run 2, (c) Run 5	202
4.20 GPC chromatogram of polystyrene prepared in the presence of Bz <i>t</i> -BOC (Run 7).....	202
4.21 Deprotection reaction of <i>t</i> -BOC group.....	207
4.22 GPC chromatograms of linear-branched block copolymer, (a) initial polystyrene, (b) copoly[styrene- <i>b</i> -(styrene/VB <i>t</i> -BOC)] backbone, (c1) linear-branched block copolymer having polystyrene branches, (c2) linear-branched block copolymer having PMMA branches	210
4.23 GPC chromatograms of linear-branched block copolymer, (a) initial polystyrene, (b) copoly[styrene- <i>b</i> -(styrene/4-methylstyrene)] backbone, (c) linear-branched block copolymer having polystyrene branches	215

- 4.24 GPC chromatograms of linear-branched block copolymer, (a) initial polystyrene, (b) copoly[styrene-*b*-(styrene/4-methylstyrene)] backbone, (c) linear-branched block copolymer having PMMA branches 216
- 4.25 GPC chromatograms of branched PMMA. (a) backbone copoly(MMA /IBEM), (b) branched PMMA 218
- 4.26 ¹H-NMR spectrums for, (a) copoly(MMA/IBEM), (b) brominated copolymer 218

LIST OF SCHEMES

Scheme	Page
1.1 Mechanism of RAFT.....	15
1.2 Pathway of ATRP.....	18
2.1 Model reactions of ATRP	60
2.2 Self-Initiation of Styrene	61
2.3 Self-Initiation of MMA	62
2.4 Algorithm of Parameter Estimation	66
2.5 Algorithm of Parameter Estimation Using MINPACK and DSM.....	86
2.6 Preparation of Model Compounds in ATRA of Styrene.....	104
2.7 Preparation of Model Compounds in ATRA of MMA	104
3.1 Isolation of the Activation Reaction.....	146
3.2 Preparation of 1-phenylethyl-TEMPO adduct	148
3.3 Isolation of the Deactivation Reaction.....	149
3.4 Degradation of 1- phenylethyl-TEMPO adduct	150
3.5 Degradation of polymer chain ends	151
3.6 Degradation of Ti-alkyl compound.....	151
4.1 Preparation of Branched Polymers by the Sequential Use of Two Different Controlled Free Radical Polymerization Methods.....	174
4.2 Preparation of Linear-Branched Block Copolymer by the Sequential Use of Two Different Controlled Free Radical Polymerization Methods	176
4.3 Preparation of Hyperbranched Polymers by the Sequential Use of Two Different Controlled Free Radical Polymerization Methods	181
4.4 Preparation of Star-Like Polymers by Two-Step Reaction Using ATRP Methods.....	182

4.5	Preparation of Branched and Hyperbranched Polymers Using Protection-Deprotection Chemistry	186
4.6	Candidate Structures for Protected Styrene	186
4.7	Preparation of VBOH.....	187
4.8	Attempts to Prepare VBOTs	188
4.9	Preparation of VBOSi	189
4.10	Preparation of VBO <i>t</i> -Bu.....	195
4.11	Literature Methods of <i>t</i> -butyloxycarbonylation of Hydroxyls and Thiols.....	198
4.12	Preparation of VB <i>t</i> -BOC	199
4.13	Deprotection of Poly(VB <i>t</i> -BOC)	206
4.14	Preparation of Linear-Branched Block Copolymer Using VB <i>t</i> -BOC.....	209
4.15	Preparation of Linear-Branched Block Copolymer Using 4-Methylstyrene	212
4.16	Preparation of Branched PMMA Using IBEM.....	217

CHAPTER 1
INTRODUCTION

1.1 Introduction

Polymerization of vinyl monomers is of enormous industrial importance. These vinyl polymers are mostly thermoplastics and they are used in a wide variety of applications. Many vinyl monomers are polymerized by free radical, ionic, and coordination polymerization mechanism. For several reasons, radical polymerization has significant advantages over ionic and coordination polymerizations. The reaction conditions are usually not as demanding, they exhibit a tolerance of trace impurities, and it is possible to polymerize a variety of monomers by radical polymerization. As a consequence of these characteristics, it is possible to prepare high molecular weight polymers without removing the stabilizers present in commercial monomers, in the presence of trace amounts of oxygen, in solvents that have not been rigorously dried, or even in aqueous media. Today, free radical polymerization accounts for a large portion of mass-produced polymers.

Despite the limitations of ionic systems, they were easier to bring under control because of the number of influential variables available (solvent polarity, counter ions, etc.) that can be manipulated. However, these same variables are either unattainable or ineffective at modulating the reactivity of radicals, hence, historically it has been difficult to control these polymerizations, which is the main deficiency of conventional free radical polymerization.

1.2 Controlled/“Living” Radical Polymerization

The first report of controlling radical polymerization was made in 1969 by Borsig, *et al.* They used bulky diaryl and triaryl ester groups on methacrylate monomers and

observed during their polymerization, an increase of molecular weight with conversion and the formation of block copolymers.¹ However, the relationship between molecular weight and conversion was not linear, initiation efficiencies was low, and polydispersities of the product polymers were always relatively high. This could result from a slow but continuous initiation of the bulky organic radicals. This system was later extensively investigated by Braun,² and improved by Crivello³ and Otsu.⁴ However, reports of work on this system have been rare in recent years.

Lee *et al.* reported that the polymerization of methyl methacrylate (MMA) initiated by benzoyl peroxide (BPO) in the presence of chromium(III) acetate resulted an increase of molecular weight with conversion, and they claimed the formation of block copolymers.⁵ They proposed a mechanism that propagation proceeds via radicals coordinated to Cr^{2+} and termination is depressed due to the screening of growing radicals by the chromium. This system was later criticized by Hungenberg, *et al.*⁶ who presented evidence of the formation of additional free radicals from the reaction of Cr^{III} cation intermediates with BPO. Thus, the polymerization of MMA in this system could be a normal radical one with free and uncomplexed radicals, and the increase of the molecular weight with conversion can be explained by the decreasing rate of the radical forming reactions and the onset of the gel effect. Similar system was reported by Mandare, *et al.* in the polymerization of vinyl acetate and MMA.⁷ They used macrocyclic polyamine ligands to stabilize the highest metal oxidation state leading to a change in the redox potential of $\text{Cr}^{2+}/\text{Cr}^{3+}$ couples, and observed a linear first order kinetic plot of monomer conversion, increase of molecular weight with conversion, and a relatively lower polydispersity. Similar approaches involving formation of persistent radicals from

transition metal compounds, including cobalt dimethylglyoxime and cobalt porphyrin, to polymerize acrylates in a controlled way have been reported.⁸ High molecular weight polyacrylates with very low polydispersities were prepared. Some organocobalt compounds can catalyze free radical chain transfer, thereby regulating molecular weight in free radical polymerization of MMA and styrene.⁹ The chain transfer process proceeds with abstraction of a hydrogen atom from a polymeric radical and its transfer to a new monomer, thereby constituting initiation of a new polymer chain. However, for cobalt complexes with suitable ligands including substituted porphyrines, β -H abstraction of cobalt-polymer chain is effectively prohibited by the steric constraints imposed by these ligands. Other examples of controlled radical polymerization by forming stable persistent radicals include the use of organoaluminum compound and the formation of hypervalent phosphoranyl radicals. Mardare, *et al.* reported controlled polymerization of vinyl acetate using an $\text{AlR}_3/\text{bpy}/\text{TEMPO}$ system.¹⁰ The idea of using hypervalent phosphoranyl radicals in the controlled radical polymerization was based on the studies of reactions involving free radicals and trivalent phosphorous compounds such as alkyl (aryl) phosphines or phosphites.¹¹ It was possible to achieve a partial control in the polymerization of vinyl acetate initiated by BPO in the presence of phosphites or phosphates.¹² The first order kinetic plot of monomer conversion vs. polymerization time was linear, indicating that the concentration of the growing radicals does not vary during polymerization. Molecular weight and polydispersity of the prepared poly(vinyl acetate) do not vary with conversion, whereas when BPO alone was used as initiator, a strong decrease of molecular weights as well as a significant increase of polydispersities with conversion was noticed. However, as evidenced by the fact that the molecular weight does not vary with conversion, chain transfer reactions are involved during the

polymerization, which reduces considerably the control. In recent years, this system has been criticized for its non-reducability.¹³

The use of term “living radical polymerization” was coined by Otsu, *et al.* during his work on the iniferter mechanism in 1982.¹⁴ In this article, they proposed calling the organic disulfide initiator with chain transfer and termination as *initiator - transfer agent - terminator (iniferter)*. They used tetraethylthiuram disulfide in the thermal or photo polymerization of styrene and MMA, and obtained α,ω -functionalized polymers having initiator fragments and the chain termini. Later, They also found that S-alkyl dithiocarbamate groups undergo reversible photodissociation to a reactive alkyl radical and an inert dithiocarbamate radical.¹⁵ They exploited this property of the dithiocarbamates in the formation of block and graft copolymer by irradiating a monomer in the presence of a suitable initiator. However, the use of dithiocarbamates has the drawback of decomposition, which leads to a loss of the living nature of the chain end. For example, dithiocarbamate polymer chain ends can decompose to CS₂ and dialkyl amino radical, and this radical can initiate further polymerization at slow rate.¹⁶

In 1985, Rizzardo *et al.* introduced the concept of stable free radical polymerization by using persistent nitroxyl radicals.¹⁷ At first, the main reaction responsible for the formation of well-defined polymers in these systems was described as the degenerative transfer of alkoxyamine between polymer chains. However, since the first publication of Georges, *et al.*,¹⁸ the control of polymerization is ascribed to a reversible homolytic cleavage of the polymer chain – TEMPO adduct (the detailed

mechanism will be discussed later in the section). Since then, the nitroxide-mediated systems are among the most studied of all controlled radical polymerization systems.

A different approach to achieve a controlled free radical polymerization based on degenerative transfer reactions was reported. This is very similar to the inifer system in carbocationic polymerization and group transfer polymerization in the anionic polymerization of methacrylates. The control in the polymerization is achieved not by establishing equilibrium between dormant and active species having very low equilibrium constant, but by the thermodynamically neutral exchange of a group between the growing radicals, present at very low concentrations, and a dormant species, present at much higher concentrations. If the exchange reactions are very fast relative to propagation reaction, the resulting polymers could have low polydispersity. Various alkyl iodides were used as transfer agents. Examples include the use of perfluorinated alkyl iodides in the polymerization of fluorinated alkenes¹⁹ and various alkyl iodides in the polymerization of styrene and acrylates.²⁰ Relatively recently, Rizzardo, *et al.* used thiocarbonylthio compounds as transfer agents in the free radical polymerizations.²¹ This approach has the basis on the degenerative transfer, and is called reversible addition-fragmentation chain transfer (RAFT) process. It is very versatile, and many monomers can be polymerized in a control manner by using this approach.

In 1995 two research groups independently reported a similar controlled radical polymerization technique, the atom transfer radical polymerization (ATRP) method. They were based on catalytic systems used for atom transfer radical addition reaction (ATRA), or the well-known Kharasch reaction, an efficient method of forming carbon-carbon

bonds between organic halides and alkenes.²² The first reported by Sawamoto *et al.*, uses $\text{RuCl}_2(\text{PPh}_3)_3/\text{Al}(\text{O-}i\text{Pr})_3$ as a catalyst system in the polymerization of MMA initiated by CCl_4 .²³ The second system reported by Matyjaszewski, *et al.*, is the polymerization of styrene catalyzed by $\text{CuCl}/2,2'$ -bipyridine (bpy) in the presence of 1-phenylethyl chloride as an initiator.²⁴ Since these first reports, there have been many reports on ATRP of styrenic, acrylates, methacrylates, and acrylonitrile by using various transition metal complexes, including nickel, iron, palladium, and rhodium. Compared with other controlled radical polymerization methods, ATRP is very versatile. This method provides control in the polymerization of many different monomers under various reaction conditions, and makes it possible to prepare polymers having a wide range of architectures including blocks, grafts, gradient copolymers,²⁵ stars, combs, branched, and hyperbranched (co)polymers.²⁶

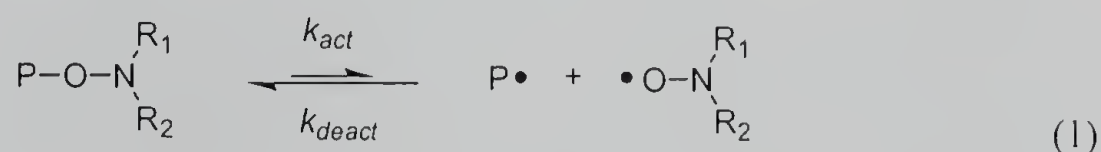
In next sections, we want to review in detail the three main types of controlled radical polymerizations: (i) nitroxide-mediated stable free radical polymerization, which employs stable nitroxyl radicals; (ii) reversible addition-fragmentation chain transfer polymerization, which uses dithioesters together with a free radical initiator; and (iii) atom transfer radical polymerization, which uses complexes of transition metals in conjunction with alkyl halides.

1.2.1 Nitroxide-Mediated Stable Free Radical Polymerization (SFRP)

Most controlled radical polymerization methods, including the nitroxide-mediated SFRP, employ the basic strategy of achieving control by establishing equilibrium, having very low equilibrium constant, between dormant and active species. In radical reactions,

termination is the most important chain breaking process. Because termination reactions are second order in active radical concentration, and propagation reactions are first order, the ratio of termination over propagation reaction decreases with decreasing concentration of active radicals. Although termination reactions cannot be eliminated completely, the contribution of termination can be significantly lowered by this approach, and it becomes possible to control the polymer architectures. The concept of employing equilibria between dormant and active species was first used in the cationic ring-opening polymerization of tetrahydrofuran.²⁷ This idea has subsequently been successfully used in carbocationic polymerizations,²⁸ although a “pseudocationic mechanism”,²⁹ “invisible species”,³⁰ and “stretched-covalent bonds”³¹ were all postulated initially.

Various compounds have been reported as trapping agents of active radicals to form the dormant species. Among them, the SFRP method uses stable persistent radicals for this purpose, and most of these are nitroxide radicals (eq 1).



The ability of nitroxides to trap carbon-centered radicals has been known for some time, and nitroxides have been used as scavengers to inhibit polymerization or polymer degradation.³² The stable nitroxide radicals do not initiate the growth of any extra polymer chains, but they react with organic radicals very fast at near diffusion-controlled rates. On the other hand, the alkoxyamine C-O bond is also known to be relatively unstable.³³ Upon heating, it readily cleaves homolytically to yield a carbon-centered

radical species and a nitroxide. In the beginning of this process, the relative weak bond formed by the coupling of the primary radical and nitroxides breaks at high temperatures, and the monomer adds to the carbon based radical soon after. Eventually, the propagating radical is reversibly trapped by the nitroxide radical. These reactions can repeat until all the monomer is consumed. During this process, a very small instantaneous concentration of propagating free radicals produced by reinitiation is moderated by the nitroxides and leads to the stepwise growth of the chains. Consequently, termination reactions are minimized, and polymers with narrow polydispersities are obtained.

The labile bond between the alkyl group and scavenger should homolytically and reversibly cleave at elevated temperature. Hence, most of the controlled radical polymerizations require high temperatures ($> 100\text{ }^{\circ}\text{C}$). Although the ratio of the rate constant of propagation to that of termination increases with temperature, leading to better control, the probability of other side reactions such as transfer and decomposition of dormant species increases simultaneously. Thus, a temperature range must be adjusted to match the requirements of each particular system. The resulting polymers possess molecular weights inversely proportional to the concentration of alkoxyamines, and the rates of the polymerizations are determined by the stationary concentration of the growing radicals.

In the SFRP system, it appears that the equilibrium position between dormant and active species is mostly affected by the bond energy in the dormant species,³⁴ although rate enhancement was noted in the presence of some additives that either shift the equilibrium towards radicals or decompose the scavengers.³⁵ A variety of nitroxides has

been used in SFRP processes. Some of those found most effective in early studies include 1,1,3,3-tetraethyl-2,3-dihydro-1*H*-isoindolin-2-yloxy (1), 2,2,6,6-tetramethyl-1-piperidin-1-yl-1-oxyl (TEMPO) (2), and di-*t*-butyl nitroxide (3) (Figure 1.1).³⁶ There are some disadvantages associated with the use of many of these compounds in nitroxide-mediated polymerization, and include the availability of the nitroxide (i.e., expense or difficulty of synthesis: only TEMPO and some derivatives are commercially available), and their propensity to undergo side reactions (e.g., disproportionation between propagating species and nitroxide). To achieve SFRP system having higher activity and reduced side reactions, various nitroxide compounds have been synthesized and utilized in the controlled radical polymerization. Examples include derivatives of 2,2,5,5-tetraalkylimidazolidin-4-one-1-oxyl (4 and 5), nitronyl nitroxide (6),³⁷ five-membered cyclic nitroxides (7),³⁸ asymmetric nitroxides such as 2,5-dimethyl-2,5-diphenylpyrrolidin-1-oxyl (8),³⁹ acyclic β -phosphonylated nitroxides (9),⁴⁰ and 2,5- and 2,6-dispiro nitroxides (10-12).⁴¹ Other stable radicals such as cyanoxyl radicals ($\bullet\text{OC}\equiv\text{N}$)⁴² and triazoliny radicals⁴³ have also been used as trapping agents.

Since the initial report by Georges *et al.* in 1993,¹⁸ bimolecular initiating systems have been used in the SFRP processes, that involve a mixture of a traditional radical initiator, such as BPO or azobis(isobutyronitrile) (AIBN), and a stable nitroxide free radical. For the polymerization of styrene-based monomers, that undergo autoinitiation at elevated temperatures, SFRP in the absence of initiators can be performed.⁴⁴ Also, alkoxyamines prepared in advance have successfully been employed as unimolecular initiators for SFRP.^{45,46,47,48,49,50,51} Using the preformed alkoxyamines as initiators has

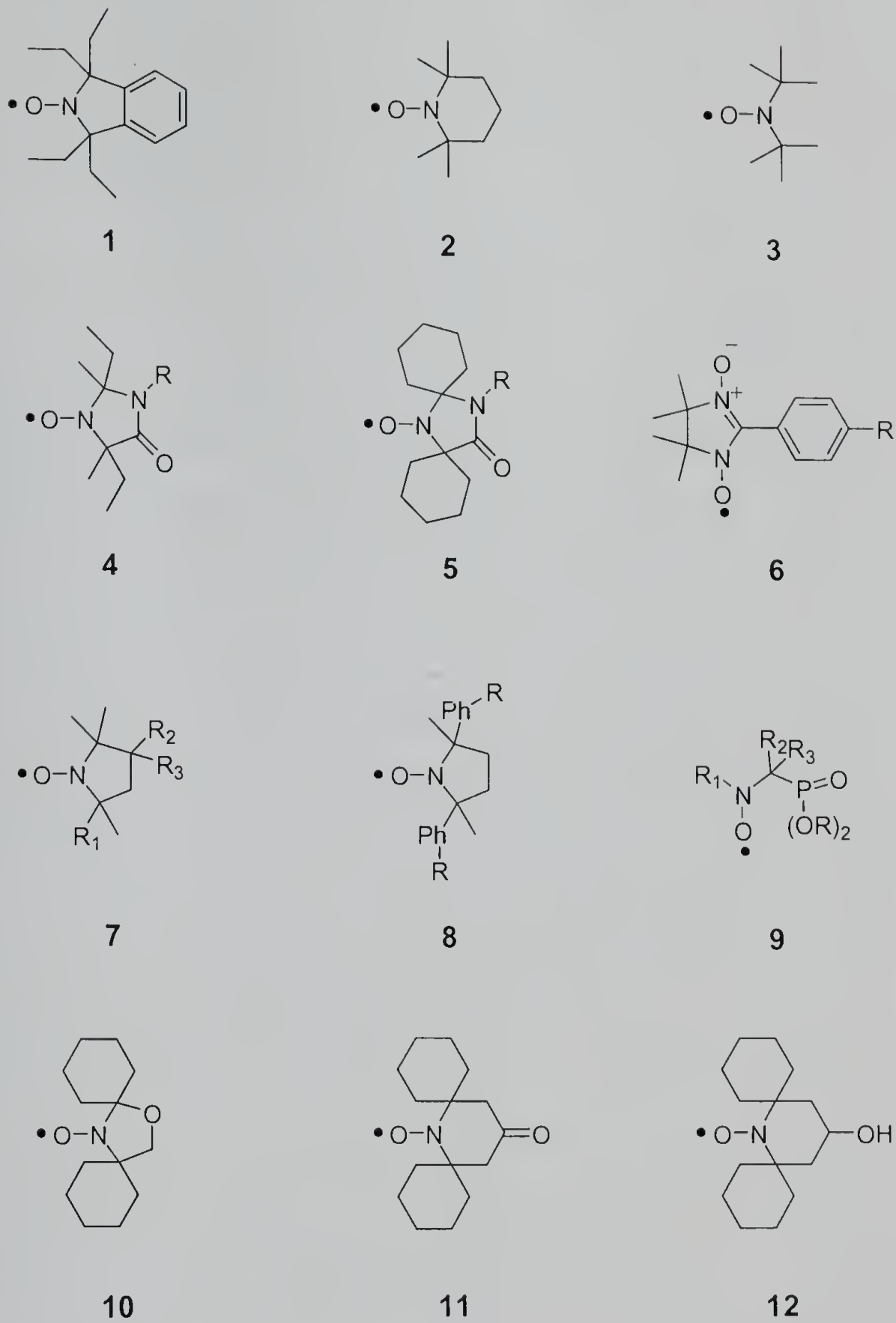


Figure 1.1 Stable nitroxide radicals used in SFRP process.

the advantage of a fixed stoichiometry between the organic initiator and the nitroxide radical, while in the two component free radical initiated SFRP, a ratio of initiator/nitroxide of 1/1.3 is typically used in order to account for the low initiator efficiency and autoinitiated chains.

Nitroxide-mediated SFRP is still limited to only a few monomers, and it is particularly well suited for styrene^{34a, 52} and styrene derivatives.⁵³ The controlled polymerization of acrylates has long been considered a challenge, and there have been efforts to achieve controlled radical polymerization of these and other non-styrenic monomers using the SFRP method. For example, Yoshida *et al.* prepared an aminoxy-terminated polystyrene, and used it to initiate the radical polymerization of methyl, ethyl, and butyl acrylate to afford the corresponding block copolymers.⁵⁴ Fukuda *et al.* synthesized a block copolymer of styrene and acrylonitrile to produce a random copolymer with narrow polydispersity by carrying out the free radical polymerization in the presence of nitroxide stable free radical, TEMPO.⁵⁵ Georges, *et al.* performed homopolymerization of acrylate monomers and copolymerization with styrene using TEMPO or TEMPO derivatives, but relatively broad molar mass distributions were observed (polydispersity index(PDI) > 1.5).⁵⁶ Lokaj *et al.* prepared poly[styrene-*b*-(2-(dimethylamino) ethyl methacrylate)] block copolymers by SFRP.⁵⁷ Listigovers *et al.* synthesized low molecular weight polyacrylate homopolymers as well as polystyrene-polyacrylate diblocks, polyacrylate-polyacrylate diblocks, and polyacrylate-polyacrylate-polyacrylate triblocks via nitroxide-mediated living polymerization.⁵⁸ Steenbock *et al.* attempted to initiate living radical polymerization of MMA using polystyrene having a TEMPO end group as a macroinitiator by the addition of camphorsulfonic acid and found

that the copolymer was contaminated with high levels of homo-polystyrene.⁵⁹ Recently, Burguiere *et al.* synthesized ω -unsaturated poly[styrene-*b*-(*n*-butyl methacrylate)] block copolymers using TEMPO-mediated controlled radical polymerization with low monomer conversions.⁶⁰ Yousi, *et al.* synthesized well-defined block copolymers from styrene with acrylates, vinyl acetate, and *N,N*-dimethylacrylamide by TEMPO-mediated controlled radical polymerization.⁶¹ However, relatively broad molar mass distributions were observed for the homopolymerization of acrylates, and narrow molecular weight distribution was observed only for the copolymerization with styrene. In the case of nitroxide-mediated polymerization of methacrylates, low monomer conversions were always found because the alkoxyamines formed are totally converted after a short polymerization time into dead polymer chains by a β -hydrogen transfer reaction from the propagating radicals to TEMPO (also referred to as a disproportionation reaction). This reaction leads to the corresponding hydroxylamine and to an ω -unsaturated polymer. Benoit, *et al.* used phosphonylated nitroxide stable radical in the polymerization of *n*-butyl acrylate.⁶² Phosphonylated nitroxide that carry substituents in the α -position that introduce strong electronic and steric effects, and weaken the -C-ON- bond in the alkoxyamine are prepared. These active alkoxyamines make it possible to reduce polymerization temperature, and, as a consequence, decrease the effect of side reactions, which diminishes the living character of polymer chains and broadens the molecular weight distribution of the product polymers.

The controlled polymerization of 1,3-dienes has also encountered difficulty. A relatively successful approach has been developed by the Xerox group in which TEMPO-

terminated polystyrene chains were chain-extended with 1,3-dienes to give block copolymers.⁶³ Alternatively, the same group reported that isoprene could be homopolymerized at 145 °C to moderate conversions in the presence of TEMPO and a reducing agent such as acetol to give polyisoprenes with PDIs ranging from 1.36 to 1.53.⁶⁴ The difficulties associated with both procedures are evidenced by polydispersities that are higher than those normally obtained with nitroxide-mediated procedures and that moderate conversions are obtained at high polymerization temperatures. A reasonable explanation for the observed difficulty in the homopolymerization of dienes may be a preponderance in these systems for irreversible termination reactions leading to a buildup of excess TEMPO as the polymerization proceeds. According to the persistent radical mechanism proposed by Fischer,⁶⁵ this excess nitroxide should dramatically slow the reaction and lead to incomplete conversion and nonliving behavior. Benoit *et al.* used alkoxyamine initiators based on a 2,2,5-trimethyl-4-phenyl-3-azahexane-3-oxo skeleton, and successfully synthesized a wide range of 1,3-diene-based homo-, random, and block copolymers.⁶⁶ Because these α -hydrogen nitroxides can decompose via disproportionation, the buildup of excess nitroxide in these systems will thereby be prevented, and the polymerization is free to proceed to higher conversion and display low polydispersities.

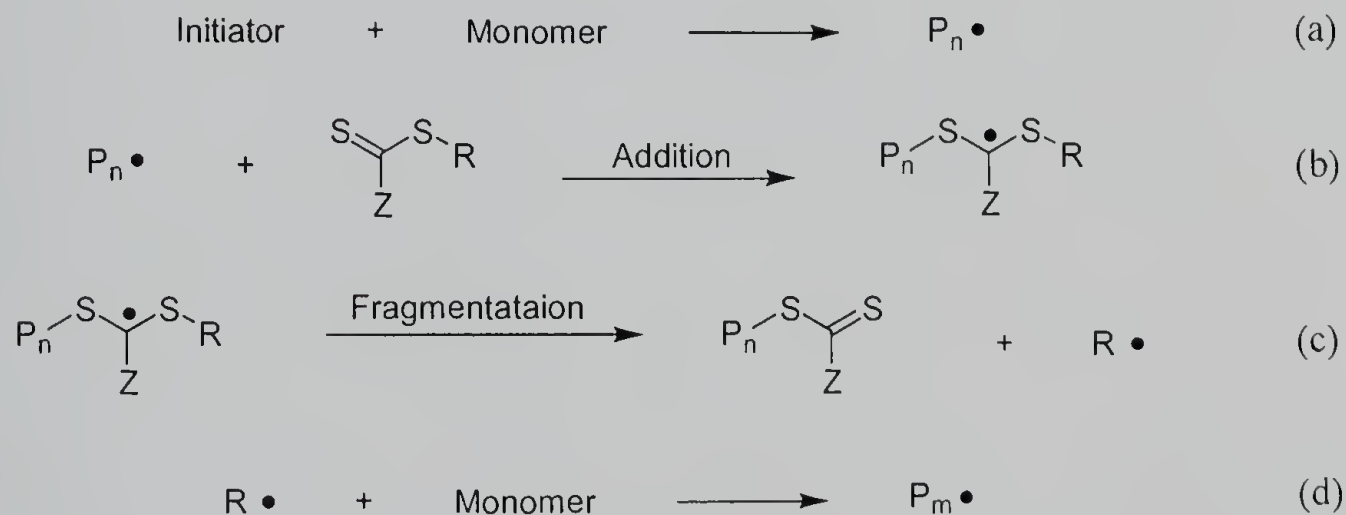
In addition to these monomers, nitroxide-mediated SFRP has slowly been expanded to other monomers, including more exotic monomers,⁶⁷ 4-vinylpyridine,⁶⁸ and *N*-vinylcarbazole.^{58,69} The main advantages of nitroxide-mediated SFRP include its simplicity and the fact that it does not require a metal catalyst. However, it has drawbacks

including the limitation of applicable monomers (despite the recent progress), the expensive, and difficult syntheses of the alkoxyamine initiators.

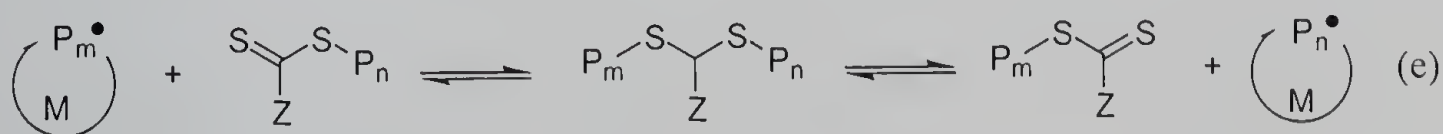
1.2.2 Reversible Addition-Fragmentation Chain Transfer Process (RAFT)

RAFT is a special case of degenerative transfer. The RAFT process involves the combination of monomer, a good solvent for both monomer and polymer, an azo- or peroxy- initiator, and the essential reversible transfer agent. A simplified mechanism is given in Scheme 1.1. The transfer agent (dithioester) reacts with the propagating radical ($P_n\bullet$) to give another transfer agent and the species $R\bullet$, which reinitiates polymerization (b and c). The living behavior involves a reversible addition-fragmentation sequence between the active and dormant species with the $S=C(Z)S$ - chain transfer moiety (e).

Scheme 1.1 Mechanism of RAFT



Overall Equation



The RAFT process has distinct advantages over other controlled free-radical living processes (e.g., nitroxide-mediate SFRP, reversible atom and group transfer) in that it can be used for a wide range of monomers, including *N*-isopropylacrylamide,⁷⁰ methacrylic acid, styrenesulfonic acid sodium salt, 2-hydroxyethyl methacrylate, 2-(dimethylamino)ethyl methacrylate, and most importantly, vinyl acetate.⁷¹ These monomers can be polymerized in a wide range of solvents under a wide range of experimental conditions. The products, whether homopolymers, random copolymers, gradient, or block copolymers,⁷² are of controlled molecular weight and generally have very narrow polydispersities (usually PDI < 1.2, and sometimes < 1.1).⁷³

In order for a dithioester compound to be effective as a RAFT agent, it needs to meet the following requirements; (i) both rates of addition and fragmentation must be fast relative to the rate of propagation, and (ii) the expelled radical (R•) must be capable of reinitiating polymerization. The first requirement ensures the rapid consumption of the initial RAFT agent and fast equilibration of the dormant and active species, while the second ensures the continuity of the chain process. By changing the substituents of dithioester compounds (Z and/or R in Scheme I), it is possible to prepare chain transfer agents fulfilling these requirements in the polymerizations of various monomers, and consequently, to prepare polymers with controlled molecular weight and low polydispersity. The RAFT process is simple like nitroxide-mediate and does not require any metal catalyst. The advantage of RAFT is illustrated by the fact that the greatest number of monomers can be polymerized in controlled way compared to other controlled radical polymerization methods. A potential disadvantage of RAFT, and degenerative

transfer polymerization methods in general, is that a concentration of low molecular weight radicals is always present and available for unwanted termination reactions.

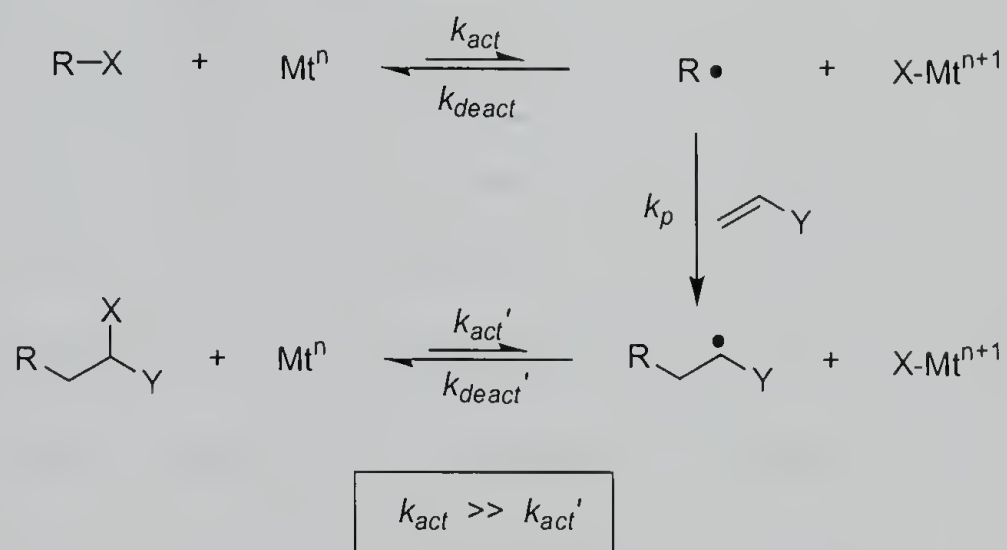
1.2.3 Atom Transfer Radical Polymerization (ATRP)

ATRP is an extension of atom transfer radical addition (ATRA) reaction used in organic synthesis. It has long been difficult to control organic radical reactions, which suffer among other things, the low yields of desired products caused by radical termination reactions. However, the Kharasch addition of alkyl halides to alkenes initiated by small amount of peroxides or light,⁷⁴ and atom transfer addition catalyzed by transition metals led to highly chemoselective 1:1 adducts in high yields.⁷⁵

In ATRA catalyzed by transition metals, a metal complex in lower oxidation state undergoes a single electron oxidation with concomitant abstraction of a halogen atom from an alkyl halide reagent. This reaction generates an organic radical and a metal complex in a higher oxidation state, and substituents on the organic halide can facilitate the reaction by stabilizing the resulting organic radical. This radical can then add to an alkene in either an inter- or intramolecular fashion and then reabstract a halogen atom from the higher-oxidation state metal complex to reform the original lower-oxidation state metal complex and the halogenated product (Scheme 1.2). Compounds derived from the inter-radical reaction (i.e., termination) comprise very little of the product, because the metal complex in higher oxidation state acts as a persistent radical and controls the concentration of the intermediate radicals in accord with the "persistent radical effect",⁶⁵ which will be explained in detail in the next chapter. Substrates for this reaction are typically chosen such that if addition occurs, then the newly formed radical is much less

stabilized than the initial radical and will essentially react irreversibly with the higher-oxidation state metal complex to form an inactive alkyl halide product ($k_{act} \gg k_{act}'$). Thus, in ATRA, usually only one addition step occurs; however, if the starting and product alkyl halides possess similar reactivities toward atom transfer, then it should be possible to repeat the catalytic cycle and add multiple unsaturated groups as in a polymerization reaction: a “side reaction” that was rigorously avoided by the small molecular practitioners.

Scheme 1.2 Pathway of ATRP



The initial reports on ATRP by Sawamoto, *et al.* and Matyjaszewski, *et al.* used two of the most well-known ATRA catalysts for their controlled radical polymerization, $\text{RuCl}_2(\text{PPh}_3)_3$ and CuCl/bpy , respectively. Sawamoto, *et al.* polymerized MMA with CCl_4 as an initiator and a modified the catalyst system by adding Lewis acids such as methylaluminum bis(2,6-di-*t*-butylphenoxide). With this combination, they prepared poly(methyl methacrylate)s having controlled molecular weight and narrow molecular weight distributions.²³ Matyjaszewski, *et al.* prepared polystyrenes having controlled

structures using a CuX (X = Cl, Br)/bpy catalyst system in combination with either 1-phenylethyl chloride or bromide at high temperature (130 °C for X = Cl, 110 °C for X = Br).²⁴ The catalyst system was later improved by adding solubilizing side chains to the 4,4'-positions of the bpy ligand, which makes the polymerization a homogeneous process, and as a result, the prepared polystyrene has PDI comparable to those found for the most carefully performed living anionic polymerizations (1.05 or less).⁷⁶

Since their early reports, research on ATRP have been numerous, and ATRP has become one of the most studied subjects in current synthetic polymer chemistry. The research areas in ATRP are diverse and cover such topics as elucidation of the mechanism of the catalytic reactions, improvement of system by changing various components of ATRP, and preparation of polymers having a variety of new architectures. One of the merits of ATRP is its generality. Not only limited to styrene and MMA, but a variety of acrylates, acrylonitrile,⁷⁷ acrylamide,⁷⁸ dienes,⁷⁹ and 4-vinyl pyridine⁸⁰ have all been successfully polymerized by ATRP. The ATRP system is composed of many components that comprise the entire polymerization system, and this fact provides a plenty of room for modulating the polymerization conditions to make it suitable for use with particular monomers. This is not a technique for all monomers, however, and there have been difficulties in polymerizing less reactive monomers that propagate through non-stabilized radicals such as ethylene, α -olefins, vinyl chloride and vinyl acetate: though copolymerization is sometimes successful. Moreover, acidic monomers are also problematic in controlled polymerization by ATRP process because of the possible deactivation of metal complexes from the reaction with the acid functionalities. Recently, Armes, *et al.* demonstrated that methacrylic acid⁸¹ and 4-vinyl benzoic acid⁸² could be

polymerized in its sodium salt form by ATRP in aqueous solution even at low temperature, and thus opens a new direction in the polymerization of hydrophilic monomers by ATRP.

The initiation step is required to be fast compared to the propagation steps in order to achieve low polydispersity in controlled radical polymerization. In ATRP, mostly alkyl halides and related compounds have been used as initiators. For fast and efficient initiation reaction, polyhalogenated compounds (CCl_4 and CHCl_3)²³ and compounds with weak R-X bonds, such as N-X, O-X, and S-X (tosyl chlorides),⁸³ have been used as initiators. Alkyl halides that are close structural analogues to the growing ends that are generated from the respected monomers are also known to be very effective initiators for preparing polymers with low polydispersities.⁸⁴

Metal complexes are the most important component of ATRP systems because they govern the formation of radicals and concentration of the propagating radicals. The metal complex must undergo reversibly single electron redox reactions via an inner-sphere electron transfer process. In doing so, the metal must change its coordination number by one (e.g. from 4 to 5) in order to accommodate the ligand transfer. In addition, metal complex should selectively participate in this atom transfer reaction over other potential reactions such as oxidative addition, reductive elimination, β -H elimination, or outer-sphere electron transfer. To date, a variety of transition metals, mostly late metals, bearing a wide range of ligands have been reported as successful ATRP catalyst systems. Some of these are extensions of well-known ATRA catalysts, however, many new metal-

ligand complexes have been developed as ATRP catalyst system, and the quest to find more active and efficient catalysts continues.

ATRP has been successful in the polymerization of a large number of monomers under a variety of reaction conditions. They have been carried out in bulk, solution, dispersion, and emulsion⁸⁵ conditions, at temperature ranging from -15°C ⁸⁶ to 130°C , and in the presence of a variety of additives and functional groups - even with oxygen in some cases.⁸⁷ Halogen-containing initiators can be derived from a range of commercially available compounds. A characteristic of ATRP is that the transfer group is a simple halogen atom, and it remains the end group of the dormant polymer chains, and the halogen end groups can be displaced by other useful functional groups using $\text{S}_{\text{N}}2$, $\text{S}_{\text{N}}1$, radical, and other efficient chemistries.⁸⁸ A disadvantage of ATRP is metal contamination of the polymer. After the polymerization, the transition metal catalyst must be removed from the final polymerization product, and if at all possible, recycled.

1.3 Combinatorial Screening of Transition Metal Complexes for Activity As An ATRP Catalyst

In order to find a catalyst system that provides both excellent control and high activity in ATRP, we screened various metal complexes as ATRP catalysts using a combinatorial approach. Combinatorial chemistry is a novel and innovative way of rapidly generating and screening a large number of related compounds. One of the first reports of its use was by Furka, *et al.* at an international meeting in 1988,⁸⁹ and later by three research groups publishing in the open literature in 1991.⁹⁰ One of the characteristics of combinatorial synthesis is that a reaction is performed with many

synthetic building blocks at once – in parallel or in a mixture – rather than sequentially with just one building block at a time. All possible combinations are formed in each step, so that a large number of products, a so-called library, are obtained from only a few reactants. The combinatorial approach has been effectively applied in the pharmaceutical industries, and recently, its application has been expanded to the discovery of new materials. A few papers and reviews have appeared covering the areas of electronic materials,⁹¹ catalysts,⁹² and organic materials.⁹³ The strategy underlying the combinatorial approach is to accelerate discovery by rapidly creating arrays of candidates and rapidly evaluating these candidates for suitability in a desired application. The latter requirement of rapid evaluation has inhibited the exploitation of combinatorial approaches in the areas of polymer chemistry. There have been a limited number of reports of adapting combinatorial approaches to polymerization studies. Symix technology group developed an automated serial chromatograph and flow-injection analytical techniques to analyze polymers prepared by parallel synthesis with the goal of achieving high-throughput screening,⁹⁴ and used this method in the ATRP process.⁹⁵ Hawker, *et al.* used combinatorial approaches to identify an efficient alkoxyamine compounds for use as initiators in nitroxide-mediated SFRP.⁹⁶

In an effort to find efficient catalyst systems for ATRP in timely fashion, we applied combinatorial approaches to an array of ATRP catalysts. In order to achieve the parallel synthesis of polymers, a new polymerization setup was used. In our group, it was found that 8 mL vials with Teflon-lined cap are sufficiently airtight for even an extended period of time.⁹⁷ We prepared the polymerization mixtures in vials in a drybox under inert atmosphere. After sealing with Teflon-lined caps, the vials were removed from the

drybox, and placed in a shaker thermostated at the desired temperature. The shaker employed has total 96 wells, thus making it possible to test 96 different polymerization systems at the same time (Figure 1.2).



Figure 1.2 A shaker used in parallel syntheses of polymers to screen transition metal complexes for activity as an ATRP catalyst in combinatorial way.

A large array of metals, ligands, and halogens were tested for both styrene and MMA polymerizations. The metals investigated included Group IV (titanium and zirconium complexes) through Group X (copper). Ligands were mostly modular in type and included bipyridines, iminopyridines, phosphines, and amines. Physical parameters of merit measured included reaction rate (yield of polymer or monomer conversion over time), molecular weight (experimental vs. theoretical), and PDI (Table 1.1 and 1.2). Interestingly, very small changes in catalyst structure could make big differences in properties of polymers prepared. For example, polystyrene prepared using FeCl_2/bpy catalyst system had uncontrolled molecular weight and broad molecular weight distribution ($M_n = 146,000$ (target 10,000); $\text{PDI} = 1.67$), whereas polystyrene from the $\text{FeCl}_2/4,4'$ -di-*t*-butyl-2,2'-bipyridine (bpy^*) showed controlled molecular weight and low

Table 1.1 Screening of the Metal Complexes for Activity as a Catalyst of the ATRP of Styrene^a

	bpy ^b				bpy ^{*b}				dNbpy ^b			
	time (h) ^c	Conv. ^d	M_n ($\times 10^4$)	PDI	time (h) ^c	Conv. ^d	M_n ($\times 10^4$)	PDI	time (h) ^c	Conv. ^d	M_n ($\times 10^4$)	PDI
MnCl ₂									1.7	high	21.0	1.63
FeCl ₂	2.5	high	14.6	1.67	1	high	1.02	1.28	3.5	high	3.36	1.95
CoCl ₂	2	high	18.2	1.58	2	high	18.3	1.53	1.7	high	17.3	1.57
NiCl ₂	2	high	17.5	1.65	2.5	high	19.8	1.49	3	high	10.1	1.56
CuCl	8	high	1.39	1.21	8	high	1.09	1.08	3	high	1.45	1.09
[Cu(Otf)] ₂ . benzene ^b	2	high	2.12	1.37	8	high	1.44	1.12				
RuCl ₂ .COD ^b									4.5	high	4.51	2.01

^a Conditions: 130 °C in shaker; 8 mL vials under Argon; Initiator, 1-phenylethyl chloride; MtCl_n: ligand : initiator : styrene = 1 : 2 : 1 : 100

^b [Cu(Otf)]₂.benzene, copper(I)triflate dimer benzene complex; Ru Cl₂.COD, ruthenium dichloride cyclooctadiene complex; bpy, 2,2'-bipyridine; bpy*, 4,4'-di-*t*-butyl-2,2'-bipyridine, dNbpy, 4,4'-di-5-nonyl-2,2'-bipyridine

^c Time; time at which THF was added to stop the polymerization

^d Approximate conversion: low – reaction mixture remained fluid; high – reaction mixture very viscous or solid

Table 1.1 Continued^a

	PPI ^b				OPI ^b				API ^b				BPI ^b			
	time (h) ^c	Conv. ^d	M_n ($\times 10^4$)	PDI	time (h) ^c	Conv. ^d	M_n ($\times 10^4$)	PDI	time (h) ^c	Conv. ^d	M_n ($\times 10^4$)	PDI	time (h) ^c	Conv. ^d	M_n ($\times 10^4$)	PDI
MnCl ₂									7	high	5.3	1.17				
FeCl ₂	2	high	5.24	1.40	2	high	1.96	1.30	4	high	1.55	1.12	2	high	2.73	1.38
CoCl ₂	2	high	14.5	1.38	2	high	8.09	1.27	7	high	3.5	1.43	2.5	high	8.69	1.23
NiCl ₂	8	high	10.4	1.37	2	high	4.61	1.23	7	high	4.73	1.28	8	high	6.04	1.19
CuCl	2	high	2.23	1.66	1	high	1.94	1.22	7	high	4.44	1.66	1	high	1.65	1.15
[Cu(Otf)] ₂ ·benzene ^b	2	high	2.56	1.54	2.5	high	1.82	1.45					1	high	2.2	1.16
RuCl ₂ ·COD ^b									7	high	5.56	1.13				

^a Conditions: 130 °C in shaker; 8 mL vials under Argon; Initiator, 1-phenylethyl chloride; MtCl_n: ligand: initiator: styrene = 1:2:1:100

^b [Cu(Otf)]₂·benzene, copper(II) triflate dimer benzene complex; RuCl₂·COD, ruthenium dichloride cyclooctadiene complex; PPI, *M*-(*n*-propyl)-2-pyridylmethanimine; OPI, *M*-(*n*-octyl)-2-pyridylmethanimine; API, *M*-phenyl-2-pyridylmethanimine; BPI, *M*-benzyl-2-pyridylmethanimine

^c Time; time at which THF was added to stop the polymerization

^d Approximate conversion: low – reaction mixture remained fluid; high – reaction mixture very viscous or solid

Table 1.1 Continued^a

	3 eq PnBu ₃ ^b				1 eq bam(TMS) ^b				2 eq bam(TMS) ^b			
	time (h) ^c	Conv. ^d	M _n (x10 ⁴)	PDI	time (h) ^c	M _n (x10 ⁴)	M _n (x10 ⁴)	PDI	time (h) ^c	Conv. ^d	M _n (x10 ⁴)	PDI
MnCl ₂	1.7	high	15.3	1.49	1.7	high	15.9	1.63	1.7	high	17.5	1.61
FeCl ₂	1.5	high	2.15 ^e	1.40 ^e	0.5	high	1.52	1.15	0.5	high	1.58	1.18
CoCl ₂	1.7	high	12.7 ^e	1.40 ^e	1.7	high	13.6	1.66	1.7	high	14.2	1.6
NiCl ₂	3	high	2.4	1.59	1.5	high	14.8	1.51	1.5	high	15.1	1.61
CuCl	7	high	3.68	1.54	1.5	high	10.1	1.57	1.5	high	10.9	1.57
RuCl ₂ :COD ^b	5	high	1.84	2.53	1.5	high	6.25	1.69	1.5	high	7.28	1.65

^a Conditions: 130 °C in shaker; 8 mL vials under Argon; Initiator, 1-phenylethyl chloride; MtCl_n: initiator; styrene = 1 : 1 : 100

^b RuCl₂:COD, ruthenium dichloride cyclooctadiene complex; PnBu₃, tri-*n*-butyl-phosphine; bam(TMS), tris(trimethylsilyl)benzamide

^c Time; time at which THF was added to stop the polymerization

^d Approximate conversion: low – reaction mixture remained fluid; high – reaction mixture very viscous or solid

^e Multiple peaks – major one shown

Table 1.1 Continued^a

	bpy ^b			bpy ^{a,b}			dNbpy ^b				1 eq MADP ^b				
	time (h) ^c	Conv. ^d	M_n ($\times 10^4$)	time (h) ^c	Conv. ^d	M_n ($\times 10^4$)	PDI	time (h) ^c	Conv. ^d	M_n ($\times 10^4$)	PDI	time (h) ^c	Conv. ^d	M_n ($\times 10^4$)	PDI
MnBr ₂	38	low	4.01	38	low	3.58	1.59	38	low	13.3	1.87	7.5	high	17.4	1.44
FeBr ₂	38	low	1.05	38	low	8.00 ^e	1.43 ^e	38	low	12.8 ^e	1.26 ^e	7.5	high	2.85	1.61
CoBr ₂	38	low	3.77	38	low	7.52	1.83	38	low	7.86	2.6	7.5	high	15	1.44
NiBr ₂	6	high	33.7	6	high	31.40	1.58	6	high	32.5	1.5	7.5	high	15.3	1.47
CuBr	9	high	0.81	9	high	0.80	1.03	9	high	1.16	1.03	19	high	7.53	1.59
CuBr ₂ dms ^b	9	high	0.77	22	high	0.96	1.05	6	high	1.14	1.03				

^a Conditions: 110 °C in shaker; 8 mL vials under Argon; Initiator, 1-phenylethyl bromide; MtBr_n: ligand; initiator: styrene = 1:2:1:100

^b CuBr₂dms, copper(D) bromide complex; bpy, 2,2'-bipyridine; bpy*, 4,4'-di-*t*-butyl-2,2'-bipyridine; dNbpy, 4,4'-di-5-nonyl-2,2'-bipyridine; MADP, *N*-isopropyl-2-(isopropylamino)treponimin

^c Time; time at which THF was added to stop the polymerization

^d Approximate conversion: low – reaction mixture remained fluid, high – reaction mixture very viscous or solid

^e Multiple peaks – major one shown

Table 1.1 Continued^a

	PPI ^b				OPI ^b				BPI ^b				API ^b			
	time (h) ^c	Conv. ^d	M_n ($\times 10^4$)	PDI	time (h) ^c	Conv. ^d	M_n ($\times 10^4$)	PDI	time (h) ^c	Conv. ^d	M_n ($\times 10^4$)	PDI	time (h) ^c	Conv. ^d	M_n ($\times 10^4$)	PDI
MnBr ₂	22	high	18.1	1.24	22	high	14.8	1.27	10	high	9.02	1.31	42	high	5.6	1.62
FeBr ₂	22	high	14.5	1.19	4	high	3.15	1.43	4	high	5.01	1.33	19	high	1.77	1.15
CoBr ₂	22	high	14.3	1.23	4	high	7.00	1.38	6	high	8.08	1.31	42	high	4.89	1.45
NiBr ₂	38	high	16.3	1.16	4	high	7.03	1.29	10	high	9.31	1.3	19	high	4.68	1.31
CuBr	9	high	1.61	1.20	3	high	1.70	1.16	4	high	1.21	1.06	19	high	3.55	1.49
CuBr.dms ^b	9	high	1.49	1.24	3	high	1.47	1.13	4	high	1.26	1.04				

^a Conditions: 110 °C in shaker; 8 mL vials under Argon; Initiator, 1-phenylethyl bromide; MtBr_n: ligand; initiator : styrene = 1 : 2 : 1 : 100

^b CuBr.dms, copper(I) bromide complex; PPI, *N*-(*n*-propyl)-2-pyridylmethanimine; OPI, *N*-(*n*-octyl)-2-pyridylmethanimine; API, *N*-phenyl-2-pyridylmethanimine; BPI, *N*-benzyl-2-pyridylmethanimine

^c Time; time at which THF was added to stop the polymerization

^d Approximate conversion: low – reaction mixture remained fluid; high – reaction mixture very viscous or solid

Table 1.2 Screening of the Metal Complexes for Activity as a Catalyst of the ATRP of MMA^a

	bpy ^b			dNbpy ^b			pby ^b			epy ^b					
	time (h) ^c	Conv. (%)	M_n ($\times 10^4$)	time (h) ^c	Conv. (%)	M_n ($\times 10^4$)	PDI	time (h) ^c	Conv. (%)	M_n ($\times 10^4$)	PDI	time (h) ^c	Conv. (%)	M_n ($\times 10^4$)	PDI
FeBr ₂	100	49	no polymer	25		0.856	1.683	100	52	0.76	1.90	12	65	1.07	1.38
CoBr ₂	48	73	51.0	100	58	4.100	2.777	100	51	e	e	100	50	e	e
NiBr ₂	100	52	e	100	56	1.336 ^d	1.222 ^d	100	48	1.11	2.00	100	54	1.34	1.66
CuBr	1	71	0.95	1	67	1.292	1.446	1	63	0.88	1.28	1	93	1.02	1.22

^a Conditions: 90 °C in shaker, 8 mL vials under Argon; Initiator, methyl α -bromoisoobutyrate; MtBr_n: ligand; initiator : MMA = 1 : 2 : 1 : 100

^b bpy, 2,2'-bipyridine; dNbpy, 4,4'-di-5-nonyl-2,2'-bipyridine; pby, 4,4'-di-phenoxy-2,2'-bipyridine; epy, 4,4'-di-(4-ethylphenoxy)-2,2'-bipyridine

^c Time; time at which THF was added to stop the polymerization

^d Multiple peaks – major one shown

^e cannot be determined due to the high noise level

Table 1.2 Continued^a

	PPI ^b				OPI ^b				API ^b			
	time (h) ^c	Conv. (%)	M_n ($\times 10^4$)	PDI	time (h) ^c	Conv. (%)	M_n ($\times 10^4$)	PDI	time (h) ^c	Conv. (%)	M_n ($\times 10^4$)	PDI
FeBr ₂	48	62	28.4	2.04	2	44	27.5	1.83	100	51	1.17	1.71
CoBr ₂	25		21.6	3.41	7	44	12.76 ^d	2.771 ^d	12	50	17.7	2.26
NiBr ₂	48		25.7	2.12	3	47	85.3	1.53	4	41	110	1.59
CuBr	1	52	0.74	1.16	2	70	0.85	1.13	12	-	no polymer	

^a Conditions: 90 °C in shaker; 8 mL vials under Argon; Initiator, methyl α -bromoisobutyrate; MtBr_n ligand; initiator : MMA = 1 : 2 : 1 : 100

^b PPI, *N*-(*n*-propyl)-2-pyridylmethanimine; OPI, *N*-(*n*-octyl)-2-pyridylmethanimine; API, *N*-phenyl-2-pyridylmethanimine

^c Time; time at which THF was added to stop the polymerization

^d Multiple peaks – major one shown

Table 1.2 Continued^a

	3 eq PnBu ₃ ^b			3 eq PPh ₃ ^b			2 eq dppe ^b					
	time (h) ^c	Conv. (%)	M_n (x10 ⁴)	PDI	time (h) ^c	Conv. (%)	M_n (x10 ⁴)	PDI	time (h) ^c	Conv. (%)	M_n (x10 ⁴)	PDI
FeBr ₂	1	97	3.53 ^d	1.65 ^d	1	65	0.96 ^d	1.45 ^d	1	77	1.54 ^d	1.84 ^d
CoBr ₂	1	68	4.06 ^d	2.04 ^d	2	54	0.40 ^d	1.56 ^d	2	61	0.69 ^d	1.92 ^d
NiBr ₂	1	56	4.18	2.38	2	68	0.80	1.17	1	60	15.4	2.26
CuBr	1	-	5.10	1.92	12	-	47.1	1.89	7	-	2.24 ^d	1.81 ^d

^a Conditions: 90 °C in shaker; 8 mL vials under Argon; Initiator, methyl α -bromoisobutyrate; MtBr_n initiator : MMA = 1 : 1 : 100

^b PnBu₃, tri-*n*-butyl-phosphine; PPh₃, triphenylphosphine; dppe, 1,2-diphenylphosphinoethane

^c Time; time at which THF was added to stop the polymerization

^d Multiple peaks – major one shown

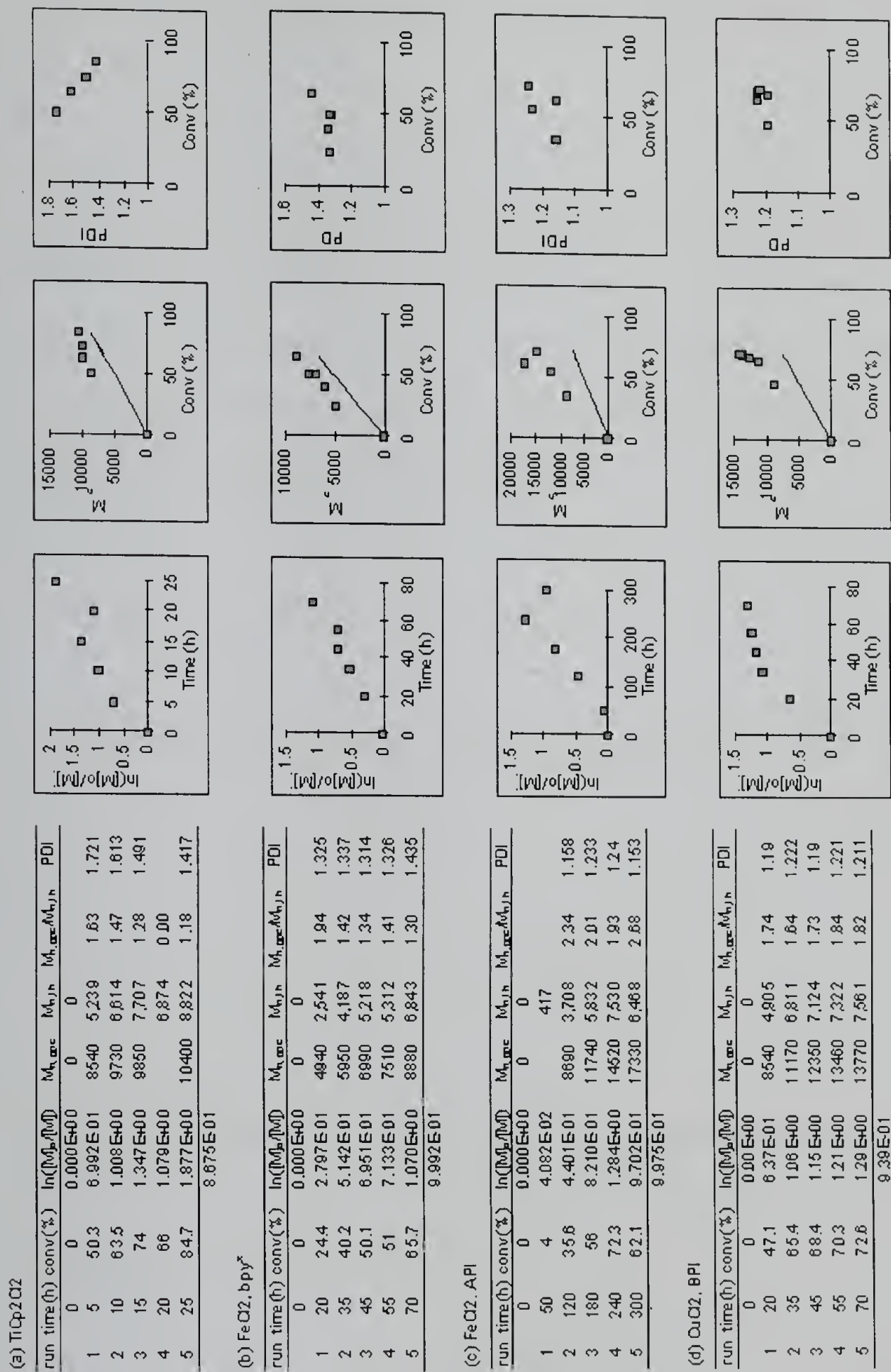
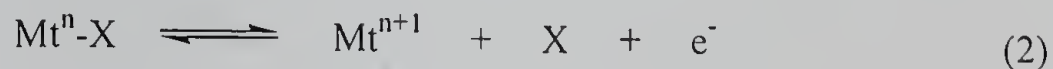


Figure 1.3 Kinetics of polymerization of styrene using various catalyst system

polydispersity ($M_n = 10,000$ (target 10,000); PDI = 1.28). We also performed more detailed kinetic studies of some of the catalyst system that showed some degree of control (Figure 1.3).

To make this a viable method of quickly discovering usable systems, we had to find a method to evaluate the catalysts. Because single electron redox couples are intimately involved in the catalytic cycle, we tried to find a correlation between catalytic activity and redox potential of the metal complexes. In electrochemical analysis, redox process of metal complex can be expressed by eq 2.



The chemical potential of the redox reaction can be predicted using Nernst equation (eq 3).

$$E = E^0 + \frac{RT}{nF} \ln \frac{[\text{Mt}^n]}{[\text{Mt}^{n+1}]} \quad (3)$$

The half-wave potential, $E_{1/2}$, is defined as a chemical potential when the redox couple have same concentrations ($[\text{Mt}^n] = [\text{Mt}^{n+1}]$). Hence, it equal to the standard potential or the chemical potential at the equilibrium state, E^0 , (eq 4).

$$E_{1/2} = E^0 = \frac{RT}{nF} \ln \left(\frac{[\text{Mt}^n]}{[\text{Mt}^{n+1}]} \right)_{eq} \quad (4)$$

Therefore, a metal complex with a higher value of $E_{1/2}$ has a higher equilibrium concentration of low-oxidation state metal complex, and this constitutes a shift of the position of equilibrium in the atom transfer reaction to the dormant species. It will decrease the concentration of active radical species, and reduce the rate of polymerization. In turn, it will also decrease the termination reaction, and lower the polydispersity of product polymer.

The half-wave potentials of metal complexes were determined by cyclic voltammetric (CV) analysis. As an example, Figure 1.4 shows the cyclic voltammogram of CuCl/4,4'-di-(4-ethylphenyl)-2,2'-bipyridine (epy) in DMF. The wave is assigned to the Cu^I/Cu^{II} redox couple. Interestingly, the results differed as a function of temperature. The CuCl/epy showed only quasi-reversible behavior at room temperature, but at higher temperature, it showed near perfect electrochemically reversible cycles. The values of half-wave potential also changed from -0.32 at 50 °C to -0.30 at 100 °C. The similar behavior was observed for other metal complexes as well. Therefore, for proper comparisons between electrochemical behavior and ATRP characteristics, we collected the $E_{1/2}$ data at 100 °C, a temperature that is close to the polymerization temperature used.

Figure 1.5 shows the relationship between the $E_{1/2}$ of several metal complexes and the apparent rate constant of the polymerization (k_{app}). The k_{app} was calculated from the slope of the first order kinetic plot of monomer conversion as a function of polymerization time as shown in Figure 1.3. It can be seen that there is rough relationship

of increasing k_{app} by increasing $E_{1/2}$, but it is not significant. Even among the homogeneous system (filled squares), the correlation is very weak. The same is seen in the plot of half-wave potential of the metal complexes and the PDI of polymers prepared using these metal complexes (Figure 1.6). The lack of correlations can be explained by a closer look at the mechanism of the redox reaction. Atom transfer radical reactions are inner-sphere redox processes. The inner-sphere mechanism involves the reversible forming and breaking of a metal-ligand bond. The ligands, halogen atoms in ATRP, is transferred through intermediate bridging species between the metal and organic radical, thus the redox reaction is affected by the bridging ligand and the relative stability of intermediate. On the other hand, the CV electrochemical redox reaction is an outer-sphere electron transfer process, in which there is no bridging intermediate or ligand transfer involved. Therefore, these two processes are totally different, and are sensitive to different factors. There have been two similar attempts to find a correlation between electrochemical measurements and polymerization behavior using metal complexes.⁹⁸ Although they used same metal and changed only the ligands, the correlations were not good.

1.4 Conclusion

We screened the activities of various metal complexes as ATRP catalysts using a combinatorial approach in order to find a catalyst system that provides both excellent control and high activity in ATRP. Several new catalyst systems including $\text{FeCl}_2/\text{bam}(\text{TMS})$ were found to be active ATRP catalysts in the polymerization of styrene and MMA. However, in order to make this combinatorial screening a viable method of quickly discovering usable systems, we had to find a fast and reliable method

to evaluate the catalysts. As an initial attempt, we tried to find a correlation between catalytic activity and redox potential of the metal complexes because one electron redox couples are intimately involved in the catalytic cycle of ATRP. It can be seen that there is rough relationship of increasing k_{app} by increasing $E_{1/2}$, but it is not significant. The same is seen in the plot of half-wave potential of the metal complexes and the polydispersity index of polymers prepared using these metal complexes. Therefore, the development of a new evaluation method of catalyst system was highly desired.

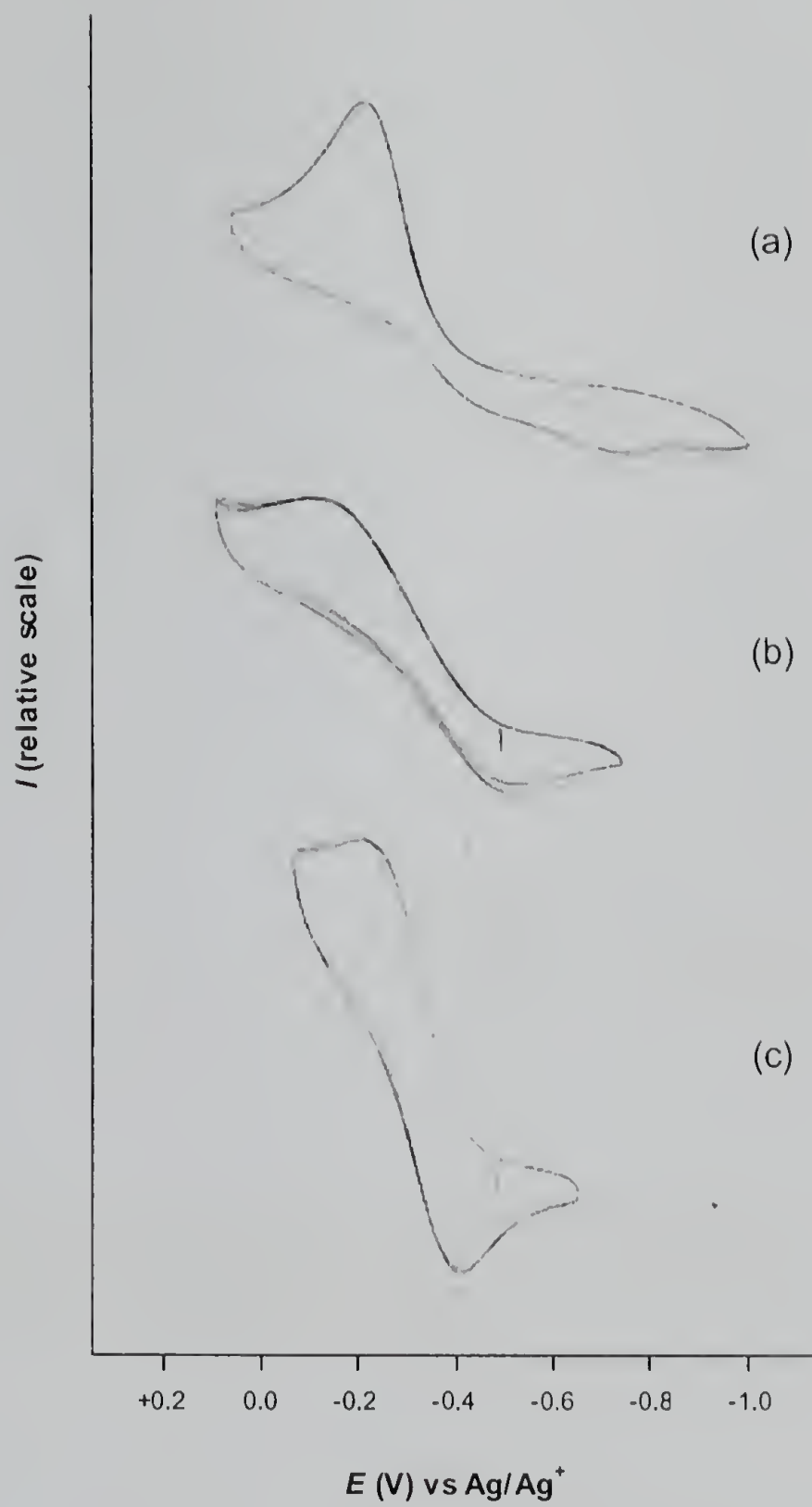


Figure 1.4 Cyclic voltammograms of CuCl/4,4'-di-(4-ethylphenoxy)-2,2'-bipyridine (epy) in 0.1 M of Bu₄N·PF₆/DMF measured at different temperature. (a) 25 °C, (b) 50 °C, (c) 100 °C.

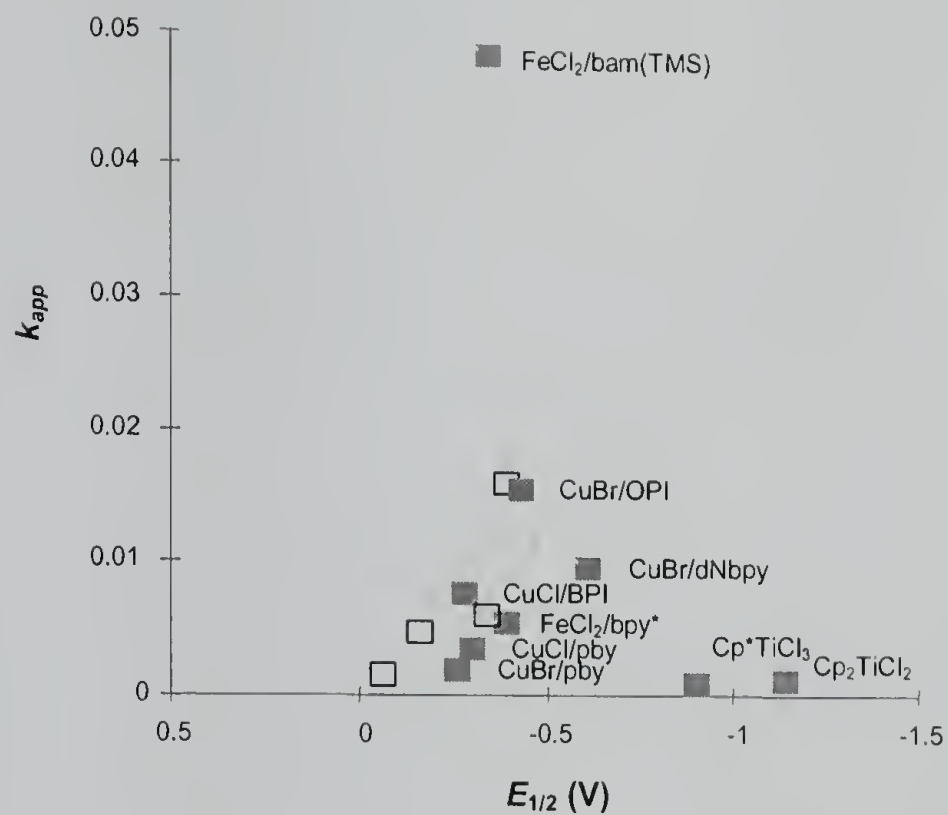


Figure 1.5 Relationship between half-wave potential of metal complexes ($E_{1/2}$) and apparent rate constant of the polymerization (k_{app}) using these metal complexes. (□, heterogeneous system; ■, homogeneous system).

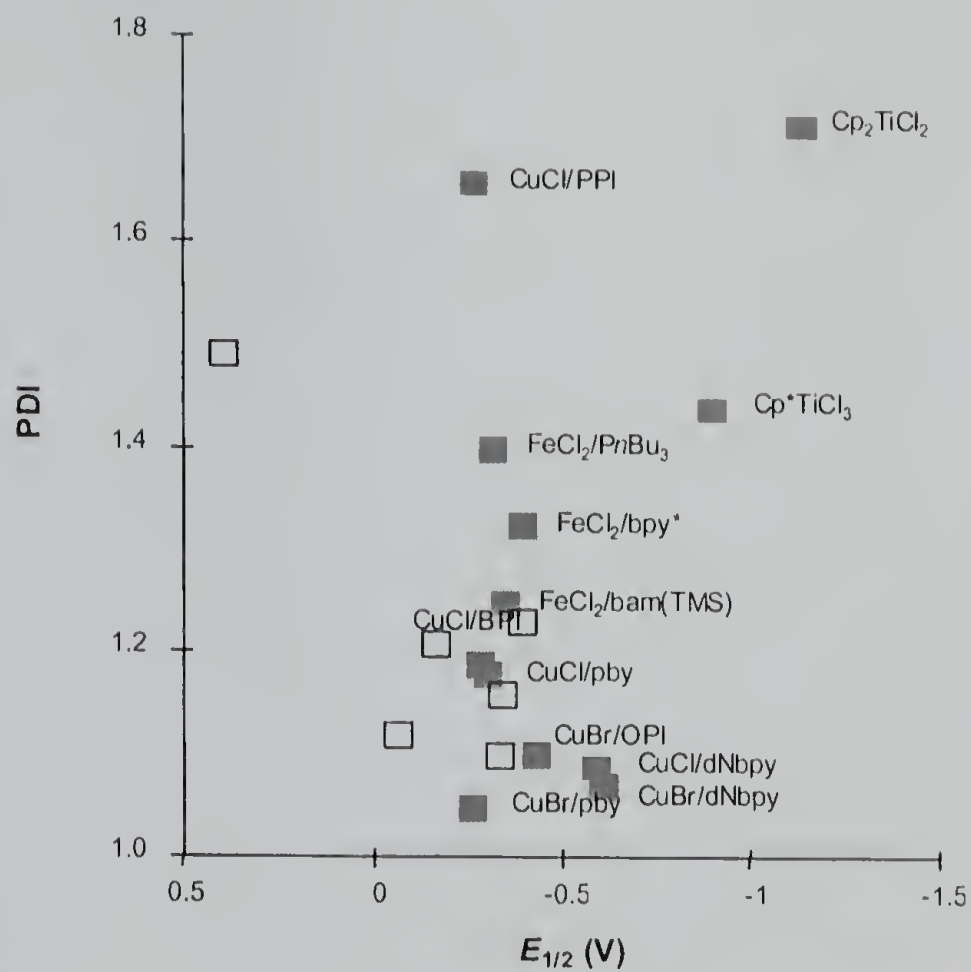


Figure 1.6 Relationship between half-wave potential of metal complexes ($E_{1/2}$) and polydispersity index(PDI) of polymers prepared using these metal complexes. (□, heterogeneous system; ■, homogeneous system).

1.5 Experimental

1.5.1 Materials and Characterizations

IR spectra of samples were measured with either a Perkin-Elmer 1600 series FTIR or a Jasco FT/IR-410 spectrometer as thin films coated on NaCl plates. ^1H and ^{13}C NMR spectra were measured in CDCl_3 . Spectra were recorded on either a Varian 200, Bruker 200, 300, or GE 300 spectrometer. ^1H NMR spectra were measured at 200 or 300 MHz. Proton decoupled ^{13}C NMR spectra were recorded at 75 MHz. ^1H chemical shift (δ) was referenced to a selected resonance of residual protons in the solvent employed. ^{13}C chemical shift (δ) was referenced to the carbon resonance of the solvent employed. Gel permeation chromatography/light scattering (GPC/LS) were performed using Hewlett-Packard (HP) 1050 series liquid chromatography pump equipped with a Wyatt Dawn DSP-F laser photometer, a Wyatt/Optilab interferometer and a Waters 746 data module integrator. Tetrahydrofuran (THF) was used as the mobile phase. Samples were prepared as 0.5 – 2 % (w/v) solution in THF and passed through 0.45 μm filters prior to injection. Residual metal complexes were removed by passing the polymer solution through active alumina column. Separations were effected by a multiple series of Polymer laboratory Mixed C columns and 100 Å Waters Ultrastaygel columns in series at a flow rate of 1 mL/min at 25 °C. Residual metal complexes were removed by passing the polymer solution through active alumina column before analysis. Gas chromatography (GC) was performed using either a HP 5890 equipped with MS detector, or a HP 6890 with a FID detector. Non-polar HP-5 or medium polar HP-INNOWAX capillary column were used for the separation. The sample was diluted in diethyl ether, THF, or methylene chloride, and directly injected into GC without any further purification. Cyclovoltametry was

performed using PAR Scanning Potentiostat Model 362 equipped with PAR Plotter Model RE 150.

Materials were obtained from commercial suppliers and used without further purification, unless otherwise noted. Styrene and methyl methacrylate were dried over CaH_2 overnight, and distilled twice under reduced pressure from CaH_2 prior to use. 1-Phenylethyl bromide (1-PEBr) and methyl α -bromoisobutyrate (MIB-Br) were purchased from Aldrich Chemical and distilled twice under reduced pressure prior to use. 1-Phenylethyl chloride (1-PECl) was prepared following literature procedures.⁹⁹ All metal halides and metal complexes was purchased and used without further purification. Tetrabutylammonium hexafluorophosphate ($\text{Bu}_4\text{N}\cdot\text{PF}_6$) was purified by recrystallization from ethylalcohol/water, and further dried over P_2O_5 .

1.5.2 Preparation of Ligands

Pentamethyldiethylenetetraamine (PMDETA), tri-*n*-butyl-phosphine (PnBu_3), triphenyl-phosphine (PPh_3), and ethylenebis(diphenylphosphine) (dppe) were purchased from commercial supplier and used without further purification. Bipyridine (bpy) was purchased from Aldrich, and purifies by recrystallization from ethyl alcohol. 4,4'-Di-*t*-butyl-2,2'-bipyridine (bpy*),¹⁰⁰ 4,4'-di-5-nonyl-2,2'-bipyridine (dNbpy),¹⁰¹ 4,4'-di-nitro-2,2'-bipyridine,¹⁰² 4,4'-di-phenoxy-2,2'-bipyridine (pby),¹⁰² *N*-(*n*-propyl)-2-pyridylmethanimine (PPI), and *N*-(*n*-octyl)-2-pyridyl-methanimine (OPI),¹⁰³ *N*-isopropyl-2-(isopropylamino)-treponimin (MADI),¹⁰⁴ tris[2-(dimethyl-amino)ethyl]amine (Me6-TREN),¹⁰⁵ and tris(tri-methylsilyl)benzamidine (bam(TMS))¹⁰⁶ were prepared following literature procedures.

4,4'-Di-(4-ethylphenoxy)-2,2'-bipyridine (epy). To a solution of 30 g (0.25 mol) of 4-ethylphenol in 100 mL of nitrobenzene was added 1.5 g (0.65 mol) of sodium metal. The mixture was stirred at 60 °C for 1 day, and then a solution of 5 g (0.018 mol) of 4,4'-di-nitro-2,2'-bipyridine in 150 mL of nitrobenzene was added. The mixture was stirred at 70 °C for 1 day, cooled to room temperature, and then poured into 1 L of diethylether. The mixture was neutralized with acetic acid and cooling, filtration afforded an ether-insoluble solid. A suspension of the latter in 250 mL of water was acidified to pH ~ 4 by adding few drops of concentrated sulfuric acid. The suspension was filtered and dried under vacuum to yield 4.86 g (64 %) of 4,4'-di-(4-ethylphenoxy)-2,2'-bipyridine-1,1'-dioxide as a solid. m.p. 211-213 °C. ¹H NMR (CDCl₃): δ 8.19 (d, 2H), 7.24 (m, 6H), 7.02 (m, 4H), 2.66 (q, 2H), 1.25 (t, 6H). IR (neat): 3026, 2964, 1602, 1506, 1476, 1440, 1286, 1234, 1218 cm⁻¹.

To a suspension of 3 g (7 mmol) of 4,4'-di-(4-ethylphenoxy)-2,2'-bipyridine-1,1'-dioxide in 75 mL of dry chloroform was added 18 mL of phosphorous trichloride (0.19 mol) in a ice-bath. After the mixture had been allowed to reflux for 3 h, it was cooled to room temperature. After the removal of chloroform, the crude product was added in acetone. The acetone-insoluble solid was filtered and dissolved in water. Neutralized of the latter solution with 25 % sodium hydroxide caused separation of a solid precipitate that, after cooling of the mixture, was isolated by filtration and dried under vacuum. Recrystallization from absolute ethanol afforded a 1.23 g (44 %) of 4,4'-di-(4-ethylphenoxy)-2,2'-bipyridine as white crystals. ¹H NMR (CDCl₃): δ 8.46 (d, 2H), 7.95

(d, 2H), 7.24 (d, 4H), 7.04 (d, 4H), 6.82 (q, 2H), 2.68 (q, 2H), 1.27 (t, 6H). IR (neat): 3024, 2961, 1581, 1556, 1504, 1452, 1382, 1280, 1231, 1200 cm^{-1} .

4,4'-Di-(4-methoxyphenoxy)-2,2'-bipyridine (mpy). To a solution of 30 g (0.25 mol) of 4-methoxyphenol in 100 mL of nitrobenzene was added 1.5 g (0.65 mol) of sodium metal. The mixture was stirred at 65 °C for 2 day, and then a solution of 5 g (0.018 mol) of 4,4'-di-nitro-2,2'-bipyridine in 150 mL of nitrobenzene was added. The mixture was stirred at 80 °C for 30 h, cooled to room temperature, and then poured into 1 L of diethylether. The mixture was neutralized with acetic acid and cooling, filtration afforded an ether-insoluble solid. A suspension of the latter in 250 mL of water was acidified to pH ~ 4 by adding few drops of concentrated sulfuric acid. The suspension was filtered and dried under vacuum to yield 5.6 g (73 %) of 4,4'-di-(4-methoxyphenoxy)-2,2'-bipyridine-1,1'-dioxide as a solid. ^1H NMR (CDCl_3): δ 8.19 (d, 2H), 7.20 (d, 2H), 7.04 (m, 4H), 6.92 (m, 4H), 6.87 (q, 2H), 3.81 (s, 6H). IR (neat): 3026, 1619, 1504, 1465, 1438, 1284, 1244, 1218, 1201, 1033 cm^{-1} .

To a suspension of 4 g (9.3 mmol) of 4,4'-di-(4-methoxyphenoxy)-2,2'-bipyridine-1,1'-dioxide in 100 mL of dry chloroform was added 24 mL of phosphorous trichloride (0.25 mol) in a ice-bath. After the mixture had been allowed to reflux for 3 h, it was cooled and poured into a mixture of ice and water. After phase separation, the chloroform layer was extracted repeatedly with distilled water, and aqueous extracts were combined with the water layer from the reaction mixture. Neutralized of the aqueous solution with 40 % potassium hydroxide caused separation of a solid precipitate that, after

cooling of the mixture, was isolated by filtration and dried under vacuum. Recrystallization from dichloroethane afforded a 1.58 g (43 %) of 4,4'-di-(4-methoxyphenoxy)-2,2'-bipyridine as white crystals. ^1H NMR (CDCl_3): δ 8.44 (d, 2H), 7.89 (d, 2H), 7.06 (m, 4H), 6.96 (m, 4H), 6.80 (q, 2H), 3.84 (s, 6H). IR (neat): 1580, 1502, 1451, 1274, 1247, 1225, 1194, 1034 cm^{-1} .

***N*-Phenyl-2-pyridylmethanimine (API).** An excess of aniline (23 mL, 0.25 mol) was added dropwise to a stirred solution of pyridine-2-carboxaldehyde (20 mL, 0.21 mol) in diethyl ether (20 mL) cooled in an ice bath. After complete addition of the amine, anhydrous magnesium sulfate (5 g) was added and the slurry stirred for 2 h at 25 °C. The solution was filtered, solvent removed, and the product purified by distillation under reduced pressure to give a golden yellow oil. Yield: 35.8 g (96.7 %). Bp 114 °C/2 Torr. ^1H NMR (CDCl_3): δ 8.69-8.61 (m, 10H), 4.78 (s, 2H). IR (neat): 1650 cm^{-1}

***N*-Benzyl-2-pyridylmethanimine (BPI).** An excess of benzylamine (27 mL, 0.25 mol) was added dropwise to a stirred solution of pyridine-2-carboxaldehyde (20 mL, 0.21 mol) in diethyl ether (20 mL) cooled in an ice bath. After complete addition of the amine, anhydrous magnesium sulfate (5 g) was added and the slurry stirred for 2 h at 25 °C. The solution was filtered, solvent removed, and the product purified by distillation under reduced pressure to give a golden yellow oil. Yield: 35.8 g (96.7 %). Bp 123 °C/0.2 Torr. ^1H NMR (CDCl_3): δ 8.53 (s, 1H), 7.23 (m, 5H). IR (neat): 1648 cm^{-1} .

1.5.3 Combinatorial Screening of Catalyst Systems

1.5.3.1 Parallel Polymerizations

A series of 8 mL vials having a Teflon-lined airtight caps were charged with monomer (2×10^{-3} mol), initiator (2×10^{-5} mol), metal halide (2×10^{-5} mol), ligand ($1\sim 3 \times 10^{-5}$ mol), and phenyl ether (2×10^{-4} mol) in a drybox under inert atmosphere. The vials were removed from the drybox, further sealed with Teflon tape, and put into a shaker thermostated at the desired temperature. The polymerizations proceeded in the shaker operated at 250 rpm, and after set time, the reaction was quenched by immersion in liquid nitrogen. The vial was then opened, and THF or methylene chloride was added to dissolve/dilute the polymerization mixture. Conversion was checked either by gravimetry after precipitating polymeric product from methanol and drying overnight under vacuum, or by directly injecting this solution into a GC and determining the remaining monomer content. For other characterization such as GPC and NMR, the polymer was purified from the catalyst by repeated dissolving in THF-precipitating from methanol and/or by passing it through a short column of active alumina column.

1.5.3.2 Kinetic Studies of the Polymerization of Styrene

In a drybox, a homogeneous solution of transition metal (1×10^{-4} mol), ligand ($1\sim 3 \times 10^{-4}$ mol), 1-PEX (X = Br or Cl; 1×10^{-4} mol), styrene (1×10^{-2} mol) was prepared. The solution was then divided into five vials and fit with airtight caps having Teflon linings. The vials were removed from the drybox, and further sealed with Teflon tape. The polymerization proceeded in a shaker thermostated at 110 °C (X = Br) or 130 °C (X = Cl), operated at 250 rpm. After set intervals, the reactions were quenched by

immersion of the vials in liquid nitrogen. The vials were then opened, and THF was added to dissolve/dilute the polymerization mixture. Conversion was checked by gravimetry, and the number average molecular weight and polydispersity of the product polymer were determined by GPC analysis following general procedures.

1.5.3.3 Determination of Half-wave Potential ($E_{1/2}$) of Metal Complexes Using Cyclic Voltammetric Analysis

All materials and solvents for cyclic voltammetric analysis were purified and dried as moisture-free. All manipulation was performed in a drybox under a nitrogen atmosphere. 0.1 M of silver nitrate solution in acetonitrile was used as salt bridge in the reference cell. 5 mM of metal complex was dissolved in DMF or methylene chloride containing 0.1 M of $\text{Bu}_4\text{N}\cdot\text{PF}_6$. After stirring about 30 min to insure complete dissolution of metal complex and temperature stabilization, the voltage was scanned at the rate of 0.1 V/s, and the current response was plotted by x-y plotter.

1.6 References

1. Borsig, E.; Lazar, M.; Capla, M.; Florian, S. *Angew. Makromol. Chem.* **1969**, *9*, 89.
2. Braun, D. *Macromol. Symp.* **1996**, *111*, 63.
3. Crivello, J. V.; Lee, J. L.; Conlon, D. A. *J. Polym. Sci., Polym. Chem.* **1986**, *24*, 1251.
4. Yamada, B.; Tanaka, H.; Konishi, K.; Otsu, T. *J. Macromol. Sci.- Pure & Appl. Chem.* **1994**, *31*, 351.
5. (a) Lee, M.; Minoura, Y. *J. Chem Soc. Faraday Trans I* **1978**, *74*, 1726. (b) Lee, M.; Utsumi, K.; Minoura, Y. *J. Chem Soc. Faraday Trans I* **1979**, *75*, 1821.
6. Hungenberg, K.-D.; Bandermann, F. *Makromol. Chem.* **1983**, *184*, 1423.
7. Mandare, D.; Gaynor, S.; Matyjaszewski, K. *Polym. Prepr. (Am. Chem. Soc., Div. Polym. Chem.)* **1994**, *35(1)*, 700.
8. (a) Arvanitopoulos, L. D.; Greuel, M. P.; Harwood, H. J. *Polym. Prepr. (Am. Chem. Soc., Div. Polym. Chem.)* **1994**, *35(2)*, 549. (b) Wayland, B. B.; Poszmik, G.; Mukerjee, S. L.; Fryd, M. *J. Am. Chem. Soc.* **1994**, *116*, 7943.
9. Burezyk, A. F.; O'Driscoll, K. F.; Rempel, G. L. *J. Polym. Sci., Polym. Chem. Ed.* **1984**, *22*, 3255.
10. Mandare, D.; Matyjaszewski, K. *Macromolecules* **1994**, *27*, 645.
11. Davis, A. G.; Griller, D.; Roberts, B. P. *J. Chem. Soc. Perkin Trans. II* **1972**, 2229.
12. Greszta, D.; Mandare, D.; Matyjaszewski, K. *Polym. Prepr. (Am. Chem. Soc., Div. Polym. Chem.)* **1994**, *35(1)*, 466.
13. Personal communication with Bruce Novak.
14. Otsu, T.; Yoshida, M. *Makromol. Chem. Rapid Commun.* **1982**, *3*, 127.
15. Otsu, T.; Kuriyama, A. *Polym. J.* **1988**, *17*, 97.
16. Turner, S. R.; Blevins, R. W. *Macromolecules* **1990**, *23*, 1856.
17. (a) Solomon, D. H.; Rizzardo, E.; Cacioli, P. US Patent 4,581,529, 1985. (b) Rizzardo, E. *Chem. Aust.* **1987**, *54*, 32.

-
18. Georges, M. K.; Veregin, R. P. N.; Kazmaier, P. M.; Hamer, G. K. *Macromolecules* **1993**, *26*, 2987.
 19. Yutani, Y.; Tatemoto, M. Eur. Pat. Appl. 0489370A1, 1991.
 20. (a) Matyjaszewski, K.; Gaynor, S.; Wang, J.-S. *Macromolecules* **1995**, *28*, 2093. (b) Gaynor, S.; Wang, J.-S.; Matyjaszewski, K. *Macromolecules* **1995**, *28*, 8051.
 21. (a) Le, T. P.; Moad, G.; Rizzardo, E.; Thang, S. H. PCT Int. Appl. WO 9801478 A1 980115. (b) Chiefari, J.; Chong, Y. K.; Ercole, F.; Krstina, J.; Jeffery, J.; Le, T. P. T.; Mayadunne, R. T. A.; Meijs, G. F.; Moad, C. L.; Moad, G.; Rizzardo, E.; Thang, S. H. *Macromolecules* **1998**, *31*, 5559.
 22. Curran, D. P. *Comprehensive Organic Synthesis*; Trost, B. M., Fleming, I., Eds.; Pergamon: Oxford, UK, 1991; Vol. 4, p175.
 23. Kato, M.; Kamigaito, M.; Sawamoto, M.; Higashimura, T. *Macromolecules* **1995**, *28*, 1721.
 24. Wang, J.-S.; Matyjaszewski, K. *J. Am. Chem. Soc.* **1995**, *117*, 5614.
 25. Gaynor, S.; Matyjaszewski, K. *Polym. Prepr. (Am. Chem. Soc., Div. Polym. Chem.)* **1997**, *38(1)*, 758.
 26. (a) Gaynor, S.; Balchandani, P.; Kulfan, A.; Podwika, M.; Matyjaszewski, K. *Polym. Prepr. (Am. Chem. Soc., Div. Polym. Chem.)* **1997**, *38(1)*, 496. (b) Matyjaszewski, K.; Gaynor, S. *Polym. Mat. Sci. Eng.* **1997**, *77*, 210.
 27. Penczek, S.; Matyjaszewski, K. *J. Polym. Sci., Polym. Symp.* **1976**, *56*, 255.
 28. Matyjaszewski, K., Ed. *Cationic Polymerizations: Mechanism, Synthesis and Applications*; Marcel Dekker: New York, 1996.
 29. Gandini, A.; Plesch, P. H. *J. Chem. Soc.* **1965**, 4826.
 30. Sawamoto, M.; Higashimura, T. *Macromolecules* **1978**, *11*, 51.
 31. Kennedy, J. P.; Ivan, B. *Designed polymers by Carbocationic Macromolecular Engineering. Theory and Practice*; Hanser: Munich, 1992.
 32. (a) Bowry, V. W.; Ingold, K. U. *J. Am. Chem. Soc.* **1992**, *114*, 4992. (b) Chateaneuf, J.; Lusztyk, J.; Ingold, K. U. *J. Org. Chem.* **1988**, *53*, 1629. (c) Beckwith, A. J.; Bowry, V. W.; Ingold, K. U. *J. Am. Chem. Soc.* **1992**, *114*, 4983. (d) Rizzardo, E.; Solomon, D. H. *Polym. Bull.* **1979**, *1*, 529. (e) Moad, G.; Rizzardo, E.; Solomon, D. H. *Macromolecules* **1982**, *15*, 909. (f) Moad, G.;

-
- Rizzardo, E.; Solomon, D. H. *J. Macromol. Sci., Chem.* **1982**, *A17*, 51. (g)
Moad, G.; Rizzardo, E.; Solomon, D. H. *Polym. Bull.* **1982**, *6*, 589.
33. (a) Kovtun, G. A.; Aleksandrov, A. L.; Golubev, V. A. *Izv. Akad. Nauk SSSR, Ser. Khim.* **1973**, 2197. (b) Howard, J. A.; Tait, J. C. *J. Org. Chem.* **1978**, *43*, 4279. (c) Ingold, K. U. In *Free Radicals*; Kochi, J. K., Ed.; Wiley: New York, 1973; Vol. 1, Chapter 2.
34. (a) Georges, M. K.; Veregin, R. P. N.; Kazmaier, M. K.; Hamer, G. K. *Trends in Polym. Sci.* **1994**, *2*, 66. (b) Kazmaier, M. K.; Moffat, K. A.; Georges, M. K.; Veregin, R. P. N.; Hamer, G. K. *Macromolecules* **1995**, *28*, 1841. (c) Moad, G.; Rizzardo, E. *Macromolecules* **1995**, *28*, 8722.
35. (a) Georges, M. K.; Veregin, R. P. N.; Kazmaier, M. K.; Hamer, G. K.; Saban, M. *Macromolecules* **1994**, *27*, 7228; (b) Odell, P. G.; Veregin, R. P. N.; Michalak, L. M.; Brousmiche, D.; Georges, M. K. *Macromolecules* **1995**, *28*, 8453; (c) Baldovi, M. V.; Mohtat, N.; Scaiano, J. C. *Macromolecules* **1996**, *29*, 5497; (d) Grezta, D.; Matyjaszewski, K. *J. Polym. Sci. A. Polym. Chem.* **1997**, *35*, 1857; (e) Fukuda, T.; Terauchi, T.; Goto, A.; Ohno, K.; Tsujii, Y.; Miyamoto, T. *Macromolecules* **1996**, *29*, 6393. (f) Malmström, E.; Miller, R. D.; Hawker, C. J. *Tetrahedron* **1997**, *53*, 15225.
36. For reviews, see: (a) Otsu, T.; Matsumoto, A. *Adv. Polym. Sci.* **1998**, *136*, 75. (b) Colombani, D. *Prog. Polym. Sci.* **1997**, *22*, 1649. (c) Rizzardo, E.; Moad, G. *Living Radical Polymerization*; Salamone, J. C., Ed.; CRC Press: Boca Raton, FL, 1996; Vol. 5, p 3834. (d) Moad, G.; Solomon, D. H. *The Chemistry of Free Radical Polymerization*; Pergamon: Oxford, 1995; p 335. (e) Georges, M. K.; Veregin, R. P. N.; Kazmaier, P. M.; Hamer, G. K. *Trends Polym. Sci.* **1994**, *2*, 66. (f) Malmström, E. E.; Hawker, C. J. *Macromol. Chem. Phys.* **1998**, *199*, 923.
37. Shigemoto, T.; Matyjaszewski, K. *Macromol. Rapid. Commun.* **1997**, *17*, 347.
38. Yamada, B.; Miura, Y.; Nobukane, Y.; Aota, M., In *Controlled Radical Polymerization*; Matyjaszewski, K., Ed.; ACS Symp. Ser. No. 685; American Chemical Society: Washington, DC, 1998; Chap. 12.
39. Puts, R. D.; Sogah, D. Y. *Macromolecules* **1996**, *29*, 3323.
40. Grimaldi, G.; Finet, J.-P.; Moigne, F. L.; Zeghdaoui, A.; Tordo, P.; Benoit, D.; Fontanille, M.; Gnanou, Y. *Macromolecules* **2000**, *33*, 1141.
41. Miura, Y.; Nakamura, N.; Taniguchi, I. *Macromolecules* **2001**, *34*, 447.
42. Grande, D.; Baskaran, S.; Baskaran, C.; Gnanou, Y.; Chaikof, E. L. *Macromolecules* **2000**, *33*, 1123.

-
43. Mullen, K.; Steenbock, M.; Klapper, M. *Polym. Prepr. (Am. Chem. Soc., Div. Polym. Chem.)* **1999**, *40*(2), 321.
44. (a) Georges, M. K.; Kee, R. A.; Veregin, R. P. N.; Hamer, G. K.; Kazmaier, M. K. *J. Phys. Org. Chem.* **1995**, *8*, 301. (b) Gaynor, S.; Greszta, D.; Mandare, D.; Teodorescu, M.; Matyjaszewski, K. *J. Macromol. Sci., Pure Appl. Chem.* **1994**, *A31*, 1561. (c) Matyjaszewski, K.; Gaynor, S.; Greszta, D.; Mandare, D.; Shigemoto, T. *Makromol. Symp.* **1995**, *98*, 73. (d) Greszta, D.; Matyjaszewski, K. *Macromolecules* **1996**, *29*, 7661. (e) Devonport, W.; Michalak, L.; Malmström, E.; Mate, M.; Kurdi, B.; Hawker, C. J.; Barclay, G. G.; Sinta, R. *Macromolecules* **1997**, *30*, 1929.
45. (a) Veregin, R. P. N.; Georges, M. K.; Hamer, G. K.; Kazmaier, M. K. *Macromolecules* **1995**, *28*, 4391. (b) Connolly, T. J.; Maldoví, M. V.; Mohtat, N.; Scaiano, J. C. *Tetra. Lett.* **1996**, *37*, 4919. (c) Skene, W. G.; Scaiano, J. C.; Listigovers, N. A.; Kazmaier, M. K.; Georges, M. K. *Macromolecules* **2000**, *33*, 5065.
46. Abrol, S.; Kambouris, P. A.; Looney, M. G.; Solomon, D. H. *Macromol. Rapid Commun.* **1997**, *18*, 755.
47. (a) Hawker, C. J. *J. Am. Chem. Soc.* **1994**, *116*, 11185. (b) Hawker, C. J.; Hendrick, J. L. *Macromolecules* **1995**, *28*, 2993. (c) Hawker, C. J.; Elce, E.; Dao, J.; Volksen, W.; Russell, T. P.; Barclay, G. G. *Macromolecules* **1996**, *29*, 2686. (d) Hawker, C. J.; Barclay, G. G.; Orellana, A.; Dao, J.; Devenport, W. *Macromolecules* **1996**, *29*, 5245.
48. (a) Kobatake, S.; Harwood, H. J.; Quirk, R. P.; Priddy, D. B. *Macromolecules* **1997**, *30*, 4239. (b) Li, I. Q.; Howell, B. A.; Matyjaszewski, K.; Shigemoto, T.; Smith, P. B.; Priddy, D. B. *Macromolecules* **1995**, *28*, 6692. (c) Howell, B. A.; Priddy, D. B.; Li, I. Q.; Smith, P. B.; Kastl, P. E. *Polym. Bull.* **1996**, *37*, 451. (d) Li, I. Q.; Howell, B. A.; Koster, R. A.; Priddy, D. B. *Macromolecules* **1996**, *29*, 8554.
49. (a) Calata, J. M.; Bubel, F.; Hammouch, S. O. *Macromolecules* **1995**, *28*, 8441. (b) Hammouch, S. O.; Calata, J. M. *Macromol. Rapid Commun.* **1996**, *17*, 149. (c) Hammouch, S. O.; Calata, J. M. *Macromol. Rapid Commun.* **1996**, *17*, 683.
50. Braslau, R.; Burrill, L. C.; Siano, M.; Naik, N.; Howden, R. K.; Mahal, L. K. *Macromolecules* **1997**, *30*, 7348.
51. (a) Miura, Y.; Hirota, K.; Moto, H.; Yamada, B. *Macromolecules* **1998**, *31*, 4659. (b) Miura, Y.; Hirota, K.; Moto, H.; Yamada, B. *Macromolecules* **1999**, *32*, 8356.

-
52. Hawker, C. J. *Trends Polym. Sci.* **1996**, *4*, 183.
53. (a) Jousset, S.; Hammouch, S. O.; Catala, J.-M.; *Macromolecules* **1997**, *30*, 6685: (b) Bertin, D.; Boutevin, B. *Polym. Bull.* **1996**, *37*, 337: (c) Keoshkerian, B.; Georges, M. K.; Boils-Boissier, D. *Macromolecules* **1995**, *28*, 6381: (d) Gao, B.; Chen, X.; Ivan, B.; Kops, J.; Batsberg, W. *Macromol. Rapid Commun.* **1997**, *18*, 1095: (e) Kazmaier, M. K.; Daimon, K.; Georges, M. K.; Hamer, G. K.; Veregin, R. P. N. *Macromolecules* **1997**, *30*, 2228.
54. Yoshida, E.; Ishizone, T.; Hirao, A.; Nakahama, S.; Takata, T.; Endo, T. *Macromolecules* **1994**, *27*, 3119.
55. Fukuda, T.; Terauchi, T.; Goto, A.; Tsujii, Y.; Miyamoto, T. *Macromolecules* **1996**, *29*, 3050.
56. (a) Georges, M. K.; Listigovers, N. A.; Odell, P. G.; Hamer, G. K.; Quinlan, M. H.; Veregin, R. P. N. *Polym. Prepr. (Am. Chem. Soc., Div. Polym. Chem.)* **1997**, *38* (1) 454. (b) Odell, P. G.; Rabien, A.; Michalak, L. M.; Veregin, R. P. N.; Quinlan, M. H.; Moffat, K. A.; MacLeod, P. J.; Listigovers, N. A.; Honeyman, C. H.; Georges, M. K. *Polym. Prepr. (Am. Chem. Soc., Div. Polym. Chem.)* **1997**, *38* (2), 414. (c) Keoshkerian, B.; Georges, M.; Quinlan, M.; Veregin, R.; Goodbrand, B. *Macromolecules* **1998**, *31*, 7559.
57. Lokaj, J.; Vlcek, D.; Kriz, J. *Macromolecules* **1997**, *30*, 7644.
58. Listigovers, N. A.; Georges, M. K.; Odell, P. G.; Keoshkerian, B. *Macromolecules* **1996**, *29*, 8992.
59. Steenbock, M.; Klapper, M.; Mullen, K.; Pinhal, N.; Hubirck, M. *Acta Polym.* **1996**, *47*, 276.
60. Burguiere, C.; Dourges, M. A.; Charleux, B.; Vairon, J. P. *Macromolecules* **1999**, *32*, 3883.
61. Yousi, Z.; Jian, L.; Rongchuan, Z.; Jianliang, Y.; Lizong, D.; Lansun, Z. *Macromolecules* **2000**, *33*, 4745.
62. (a) Benoit, D.; Grimaldi, S.; Finet, J.; Tordo, P.; Fontanille, M.; Gnanou, Y. *Polym. Prepr. (Am. Chem. Soc., Div. Polym. Chem.)* **1997**, *38* (1), 729. (b) Benoit, D.; Grimaldi, S.; Finet, J.; Tordo, P.; Fontanille, M.; Gnanou, Y. In *Controlled Radical Polymerization*; Matyjaszewski, K., Ed.; ACS Symp. Ser. No. 685; American Chemical Society: Washington, DC, 1998; p 225.
63. Georges, M. K.; Hamer, G. K.; Listigovers, N. A. *Macromolecules* **1998**, *31*, 9087.

-
64. Keoshkerian, B.; Georges, M. K.; Quinlan, M.; Veregin, R.; Goodbrand, B. *Macromolecules*, **1998**, *31*, 7559.
65. Fischer, J. *J. Am. Chem. Soc.* **1986**, *108*, 3925.
66. Benoit, D.; Harth, E.; Fox, P.; Waymouth, R. M.; Hawker, C. J. *Macromolecules*, **2000**, *33*, 363.
67. Jia, X.; Mingqian, L.; Han, S.; Wang, C.; Wei, Y. *Mater. Lett.* **1997**, *31*, 137.
68. (a) Bohrisch, J.; Wendler, U.; Jaeger, W. *Macromol. Rapid Commun.* **1997**, 975.
(b) Fischer, A.; Brembilla, A.; Lochon, P. *Macromolecules* **1999**, *32*, 6069.
69. Baethge, H.; Butz, S.; Schmidt-Naake, G. *Macromol. Rapid Commun.* **1997**, *18*, 911.
70. Ganachaud, F.; Monteiro, M. J.; Gilbert, R. G.; Dourges, M.-A.; Thang, S. H.; Rizzardo, E. *Macromolecules* **2000**, *33*, 6738.
71. Rizzardo, E.; Chiefari, J.; Mayadunne, R. T. A.; Moad, G.; Thang, S. H. *Polym. Prepr. (Am. Chem. Soc., Div. Polym. Chem.)* **1999**, *40* (2) 342.
72. Chong, Y. K.; Le, T. P. T.; Moad, G.; Rizzardo, E.; Thang, S. H. *Macromolecules* **1999**, *32*, 2071.
73. (a) Le, T. P.; Moad, G.; Rizzardo, E.; Thang, S. H. PCT Int. Appl. WO 9801478 A1 980115; *Chem. Abstr.* **1998**, *128*, 115390. (b) Chiefari, J.; Chong, Y. K.; Ercole, F.; Krstina, J.; Jeffery, J.; Le, T. P. T.; Mayadunne, R. T. A.; Meijs, G. F.; Moad, C. L.; Moad, G.; Rizzardo, E.; Thang, S. H. *Macromolecules* **1998**, *31*, 5559. (c) Rizzardo, E.; Chiefari, J.; Chong, Y. K.; Ercole, F.; Krstina, J.; Jeffery, J.; Le, T. P. T.; Mayadunne, R. T. A.; Meijs, G. F.; Moad, C. L.; Moad, G.; Thang, S. H. *Macromol. Symp.*, in press. (d) Chong, Y. K.; Le, T. P. T.; Moad, G.; Rizzardo, E.; Thang, S. H. *Macromolecules* **1999**, *32*, 2071. (e) Mayadunne, R. T. A.; Rizzardo, E.; Chiefari, J.; Krstina, J.; Moad, G.; Postma, A.; Thang, S. H. *Macromolecules* **2000**, *33*, 243.
74. Kharasch, M. S.; Jensen, E. U.; Urry, W. H. *Science* **1945**, *102*, 128.
75. (a) Minisci, F. *Acc. Chem. Res.* **1975**, *8*, 165. (b) Curran, D. P. *Synthesis* **1988**, 489.
76. Pattern, T. E.; Xia, J.; Abernathy, T.; Matyjaszewski, K. *Science* **1996**, *272*, 866.
77. Matyjaszewski, K.; Jo, S. M.; Paik, H.-J.; Shipp, D. A. *Macromolecules* **1999**, *32*, 6431.

-
78. Teodorescu, M.; Matyjaszewski, K. *Polym. Prepr. (Am. Chem. Soc., Div. Polym. Chem.)* **1999**, *40* (2) 428.
79. Matyjaszewski, K.; Wang, J. S. *WO 96/30421* **1996**.
80. Xia, J.; Zhang, X.; Matyjaszewski, K. *Macromolecules* **1999**, *32*, 3531.
81. Ashford, E. J.; Naldi, V.; O'Dell, R.; Billingham, N. C.; Armes, S. P. *Chem. Commun.* **1999**, 1285.
82. Wang, X.-S.; Jackson, R. A.; Armes, S. P. *Macromolecules* **2000**, *33*, 255.
83. Percec, V.; Kim, H.-J.; Barboiu, B. *Macromolecules* **1997**, *30*, 6702.
84. Matyjaszewski, K.; Wang, J.-L.; Grimaud, T.; Shipp, D. A. *Macromolecules* **1998**, *31*, 1527.
85. Gaynor, S. G.; Qiu, J.; Matyjaszewski, K. *Macromolecules* **1998**, *31*, 5951.
86. Haddleton, D. M.; Kukulj, D.; Duncalf, D. J.; Heming, A. M.; Shooter, A. J. *Macromolecules* **1998**, *31*, 5201.
87. Matyjaszewski, K.; Coca, S.; Gaynor, S. G.; Wei, M.; Woodworth, B. E. *Macromolecules* **1998**, *31*, 5967.
88. Matyjaszewski, K.; Coessens, V.; Nakagawa, Y.; Xia, J.; Qiu, J.; Gaynor, S. G.; Coca, S.; Jasieczek, C. In *Functional Polymers: Modern Synthetic Methods and Novel Structures*; Patil, A. O., Schulz, D. N., Novak, B. M., Eds.; American Chemical Society Symposium Series 704; American Chemical Society: Washington, DC, 1998; pp 16-27.
89. Furka, A.; Sebestyén, F.; Asgedom, M.; Dibo, G. *Abstr. 14th Int. Congr. Biochem., Prague, 1988; Abstr. 10th Int. Symp. Med. Chem., Budapest, 1988*.
90. (a) Furka, A.; Sebestyén, F.; Asgedom, M.; Dibo, G. *Int. J. Pept. Protein Res.* **1991**, *37*, 487. (b) Houghten, R. A.; Pinilla, C.; Blondelle, S. E.; Appel, J. R.; Dooley, C. T.; Cuervo, J. H. *Nature* **1991**, *354*, 84. (c) Lam, K.; Salmon, S.; Hersh, E.; Hruby, V.; Kazmierski, W.; Knapp, R. *Nature* **1991**, *354*, 82.
91. (a) Xiang, X.-D.; Sun, X.; Briceño, G.; Lou, Y.; Wang, K.; Chang, H.; Wallace-Freedman, W. G. Chen, S.; Schultz, P. G. *Science* **1995**, *268*, 1738. (b) Briceño, G.; Chang, H.; Sun, X.; Schultz, P. G. *Science* **1995**, *270*, 273. (c) Danielson, E.; Golden, J.; McFarland, E. W.; Reaves, C. M.; Weinberg, W. H.; Wu, X. D. *Nature* **1997**, *389*, 944.
92. Jandeleit, B.; Weinberg, W. H. *Chem. Ind.* **1998**, 795.

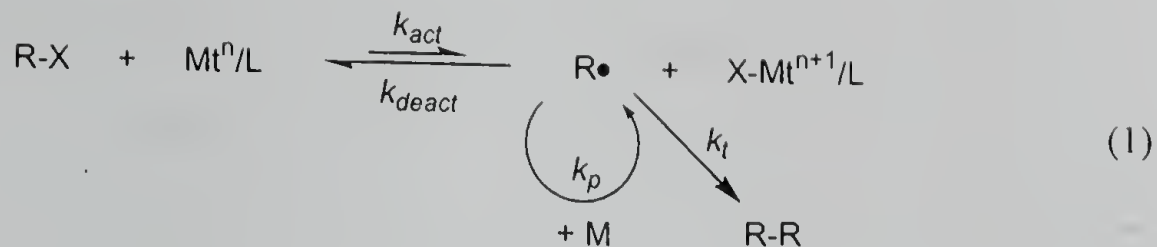
-
93. Brocchini, S.; James, K.; Tangpasuthadol, V.; Kohn, J. *J. Am. Chem. Soc.* **1997**, *119*, 4553.
 94. Petro, M.; Safir, A. L.; Nielson, R. B. *Polym. Prepr. (Am. Chem. Soc., Div. Polym. Chem.)* **1999**, *40* (2) 702.
 95. Nielsen, R. B.; Safir, A. L.; Petro, M.; Lee, T. S.; Huefner, P. *Polym. Mater. Sci. Eng.* **1999**, *80*, 92.
 96. Hawker, C. J.; Benoit, D.; Harth, E.; Nielson, R. B.; Klarner, G.; Petro, M., A presentation held in ACS national meeting in San Francisco, 2000.
 97. Goh, C.; Novak, B. M., unpublished data.
 98. (a) Ando, T.; Kamigaito, M.; Sawamoto, M. *Macromolecules*, **2000**, *33*, 5825. (b) Matyjaszewski, K. A presentation held in ACS national meeting in New Orleans, 1999.
 99. Landini, D.; Rolla, F. *J. Org. Chem.* **1980**, *45*, 3527.
 100. Hadda, T. B.; Bozec, H. L. *Polyhedron* **1988**, *7*, 575.
 101. Matyjaszewski, K.; Patten, T. E.; Xia, J. *J. Am. Chem. Soc.* **1997**, *119*, 674.
 102. Maerker, C.; Case, F. H. *J. Am. Chem. Soc.* **1958**, *80*, 2745.
 103. Haddleton, D. M.; Crossman, M. C.; Dana, B. H.; Duncalf, D. J.; Heming, A. M.; Kukulj, D.; Shooter, A. J. *Macromolecules*, **1999**, *32*, 2110.
 104. Diar, *Inorg. Chem.* **1995**, *34*, 6100.
 105. Ciampolini, M.; Nardi, N. *Inorg. Chem.* **1966**, *5*, 41.
 106. Boeré, R. T.; Oakley, R. T.; Reed, R. W. *J. Organomet. Chem.* **1987**, *331*, 161.

CHAPTER 2

DETERMINATION OF KINETIC PARAMETERS OF ATRP

2.1 Introduction

The key kinetic feature of controlled radical polymerizations is the reduction of the concentration of active chain ends by establishing dynamic equilibrium between active radicals and dormant species. In turn, this reduced radical concentration suppresses the rate of the bimolecular termination reactions. Moreover, the termination reactions between activated radical species are suppressed by the *persistent radical effect*, a concept proposed by Fischer *et al.*¹ The *persistent radical effect* occurs when concentrations of transient and persistent radicals are formed at equal rates in a single step. Because the transient radicals can undergo fast termination via coupling and/or disproportionation, their concentration decreases, and the concentration of the persistent radical builds up. Eventually, the concentration of persistent radical is sufficiently large that the rate at which the propagating radicals react with the persistent radicals in a deactivation (or reversible termination) step is much faster than the rate at which the propagating radicals react with each other in an irreversible termination step. Thus, addition chemistry can be performed involving free-radical intermediates, which is highly selective for addition over radical coupling and disproportionation. Of the various controlled radical polymerizations, atom transfer radical polymerization (ATRP) involves dormant chain molecules terminated by a halogen atom. This halogen atom is reversibly transferred to a metal catalyst through a single-electron oxidation process, and thereby propagating radicals are formed together with the complex in its oxidized form (eq 1). The active radicals then propagate to higher molecular weight chain, irreversibly terminate to lose their activity, or reversibly terminated by accepting halogen atom from oxidized metal catalyst until activated again sometime later.



Various metals and ligands have been used as catalysts for ATRP. Determining the kinetic parameters of these catalysts allows for the quantification of their efficiency. In ATRP, there are at least two important kinetic parameters. The first is the equilibrium constant ($K_{eq} = k_{act}/k_{deact}$) of the atom transfer reaction, which determines the K_{eq} of active radicals propagating at any one time with the reaction. The radical concentration needs to be optimized between an upper and lower limit: The concentration has to be low enough to make the polymerization controllable (suppress bimolecular termination), but high enough to have reasonable reaction rates. The second important kinetic parameter is the ratio of the deactivation rate constant (k_{deact}) to propagation rate constant (k_p), which should have a low value in order to produce polymers having low polydispersities. These kinetic parameters are affected by various factors including the catalyst system, monomer, temperature, and other reaction conditions.

Several research groups have attempted to determine these rate constants. Matyjaszewski, *et al.* determined the K_{eq} of various systems from the first-order kinetic plots of monomer consumption.² The plots are apparently linear for some catalyst systems, and with a few assumptions such as a fast pre-equilibrium, insignificant termination reactions, and a steady-state concentration of propagating radicals, the K_{eq} of atom transfer reaction can be determined from the slope of the plots. Fischer reported analytical solutions for the relation between K_{eq} with the monomer consumption and

polydispersity of the polymer.³ Although this is a more deliberate approach with fewer assumptions, the results showed discrepancies with real polymerization data. One explanation for this disparity was reported by Shipp *et al.* by considering diffusion controlled termination reactions.⁴

The activation rate constant (k_{act}) has been determined by several methods. Fukuda, *et al.*⁵ measured the k_{act} of polystyryl bromide catalyzed by copper(I) bromide using a gel permeation chromatography curve-resolution method. Fukuda also used NMR techniques to determine the k_{act} of various initiators in combination with a copper(I) catalyst.⁶ In this later scheme, the carbon radical formed by the atom transfer step is capped by a nitroxyl radical to form alkoxyamine. Two other research groups also used a similar strategy of capping the propagating radical with nitroxyl radical in order to isolate the activation process. Chambard, *et al.*⁷ measured the k_{act} of polystyrene and poly(butyl acrylate) macroinitiators with HPLC analysis, and Matyjaszewski, *et al.*⁸ calculated the k_{act} of benzyl bromide and 1-phenylethyl bromide by monitoring the formation of the corresponding alkoxyamine adducts using HPLC.

Even though there have been several experimental approaches used to determine the kinetic parameters in ATRP, most of them are based on many unrealistic assumptions, that include fast formation of the equilibrium, a steady-state approximation of the concentration of radical and metal complexes, and no side reactions including the radical coupling termination reaction in some examples. Moreover, the literature method used to determine the K_{eq} is only effective for a polymerization system that shows linearity in the first-order kinetic plot of monomer consumption. Because all the actual systems reported

are less than ideal, there is no way to accurately determine the kinetic parameters of these monomer-catalyst combinations. Our purpose is to find a relationship between the characteristics of a catalyst system and its efficiency as an ATRP catalyst. This goal challenged us to find a new method determining the kinetic parameters of ATRP. Furthermore, the method developed herein should be useful for any type of polymerization system.

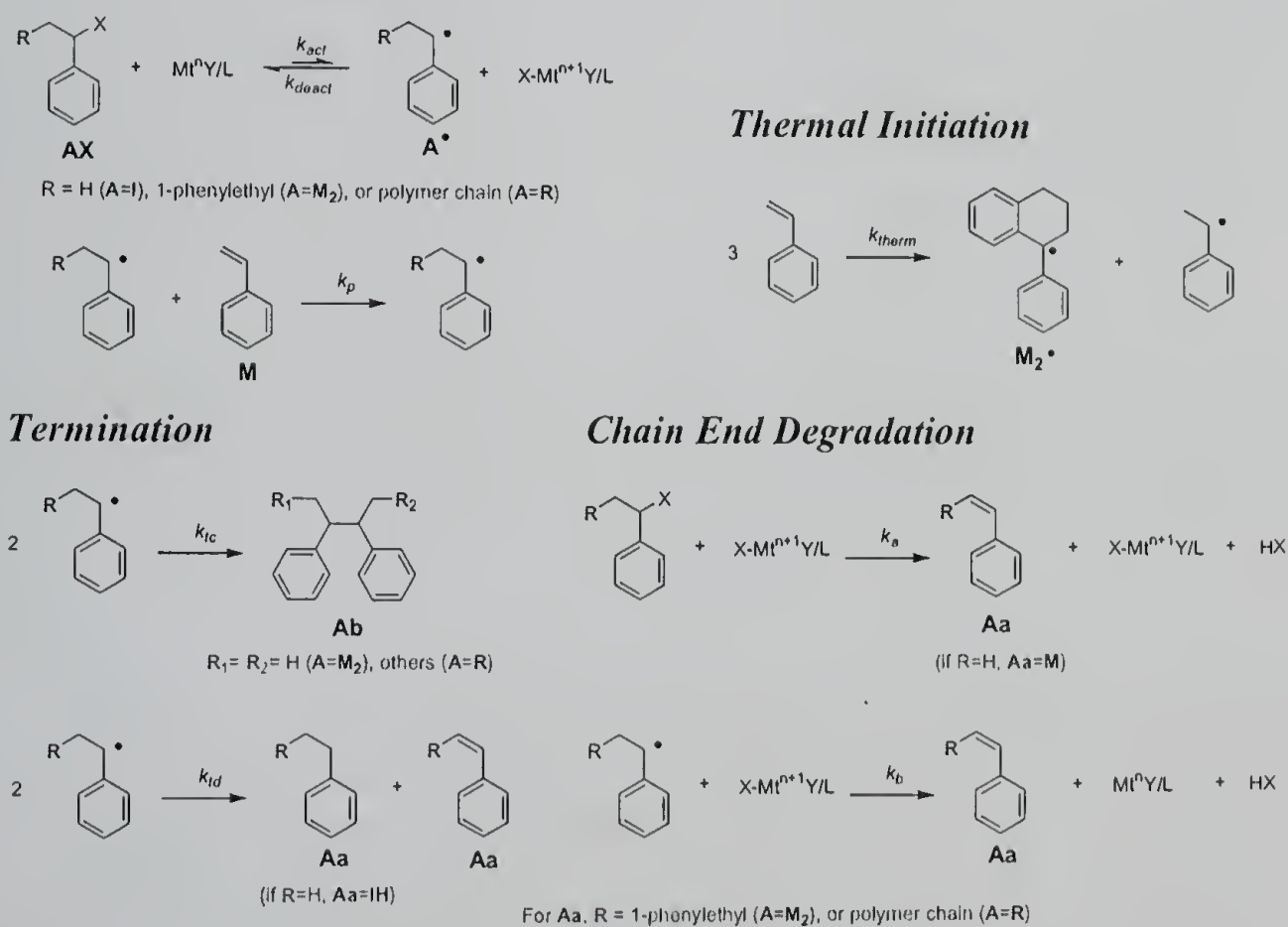
Parameter estimation algorithms have been widely used in the kinetic studies of chemical reactions. The development of these algorithms started from the linear system, but because most chemical reactions are nonlinear, it required converting the nonlinear equations to linear equations by redefining the variables. By virtue of the progress of computer technology, it has been possible to calculate very complex system in a reasonable time, and this has initiated the development of parameter estimation algorithms for complex nonlinear systems. A variety of algorithm has been reported, and they have been successfully used in the polymerization area.⁹ Parameter estimation algorithm has many advantages: The estimation algorithm can use all experimental data carried out under different conditions, and allows the estimation of all the parameters of the model. Moreover, the model involves fundamental parameters of the process, and there is no limitation on the number and character of estimatable parameters. In this section, we are going to apply this parameter estimation algorithm to determine important rate constants of ATRP.

2.2 Development of a Parameter Estimation Algorithm

2.2.1 Model Reactions

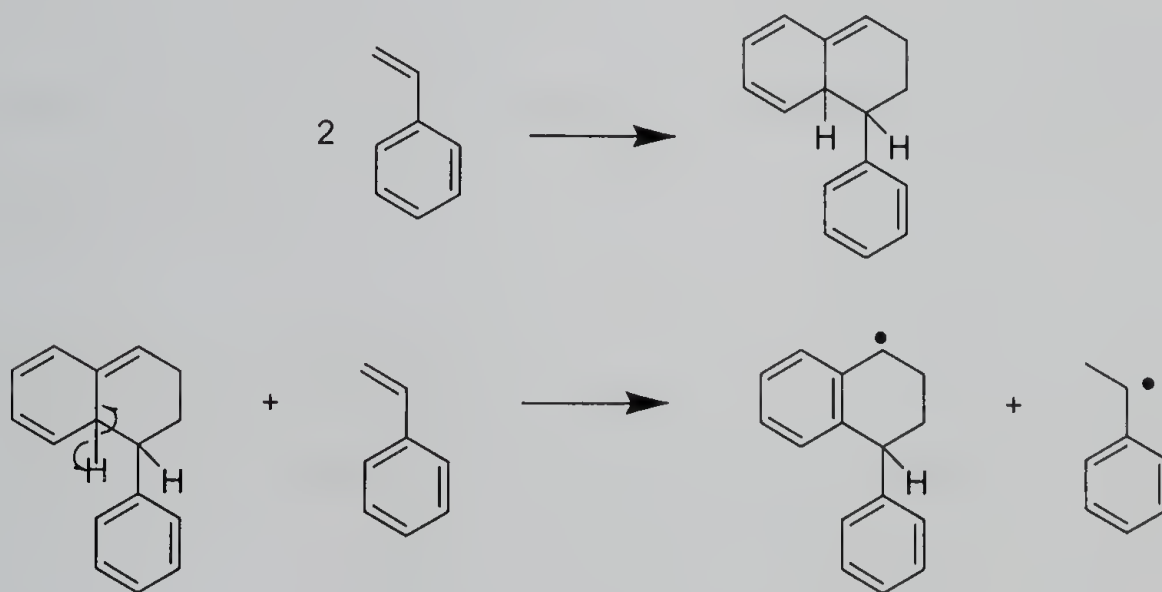
The first step of developing an algorithm is to establish the model reactions that fully as possible describe the polymerization reactions. One of the merits of our current approach is that there is no limitation on the number and character of estimatable parameters. In other words, it is possible to incorporate every possible reaction into this model. Scheme 2.1 outlines the general model for the polymerization of styrene used in our analysis. Included are the following reactions and associated rate constants/coefficients: (a) activation and deactivation of the dormant and active species (k_{act} , k_{deact} , K_{eq}), (b) propagation (k_p), (c) thermal initiation (k_{therm}), (d) termination of two radicals by both combination and disproportionation (k_{tc} , k_{td}), and (e) chain end degradation (k_a , k_b).

Scheme 2.1 Model reactions of ATRP



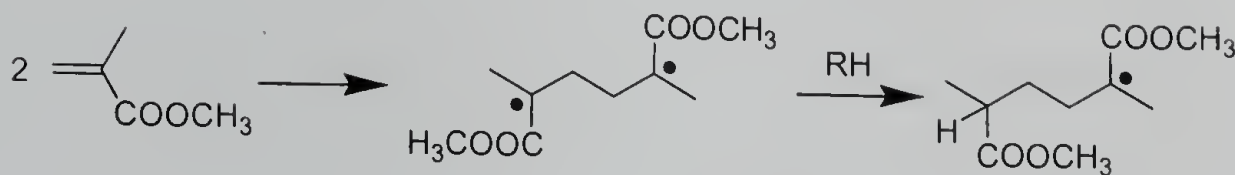
Many monomers undergo a spontaneous polymerization when heated in the “apparent” absence of catalysts or initiators. In most cases, the polymerizations are actually initiated by the thermal homolytic cleavage of impurities. However, a select number of monomers have been shown to undergo self-initiated polymerization, examples include styrene, methyl methacrylate (MMA), acenaphthylene, 2-vinylthiophene, and 2-vinylfuran.¹⁰ The self-initiation mechanism for the styrene polymerization involves the formation of a Diels-Alder dimer of styrene followed by the transfer of a hydrogen atom from the dimer to another styrene monomer (Scheme 2.2).¹¹ All aspects of this reaction have not been completely examined, but the kinetic data shows that the rate of reaction is close to being third order in the concentration of monomer.

Scheme 2.2 Self-Initiation of Styrene



For MMA, the self-initiation mechanism appears to involve the initial formation of a biradical by reaction of two monomers followed by hydrogen transfer from some species in the reaction system to convert the biradical to a monoradical (Scheme 2.3).¹²

Scheme 2.3 Self-Initiation of MMA



In addition to the self-initiation processes, spontaneous termination of the growing chains is also of concern. The chain-end degradation mechanism was suggested by Matyjaszewski, *et al.*¹³ in an effort to explain the molecular weight limit of ATRP of styrene. There are two types of chain-end degradation reactions. One involves the reaction between the dormant species (halogen capped chains) and metal complex in the high oxidation state to generate a terminal double bond and hydrogen halide, HX. The other proposed is the reaction between active radical and a metal complex in the high oxidation state to generate a terminal double bond, HX, and reduced a metal complex. Even though these reactions may be negligible under many normal polymerization conditions, they are very important in our model systems, because we run at high catalyst concentrations and low monomer concentrations.

2.2.2 Development of the Algorithm

Based on this kinetic model, we developed an algorithm to estimate the parameters of the various kinetic steps. First, the model reactions were described with a set of ordinary differential equations with a general formula of

$$\frac{dy}{dt} = f(t, y) \quad (2)$$

where y is the vector of dependant variables, and t is the independent variable, time.

The algorithm is composed of two main sub-algorithms; the numerical integration of the ordinary differential equations, and parameter estimation. Various numerical integration algorithms have been developed according to the characteristics of the differential equations: ordinary or partial, linear or nonlinear, explicit or implicit, and stiff or nonstiff. Among the various choices, we used LSODE (Livermore Solver for Ordinary Differential Equations) Fortran solver in ODEPACK developed by Hindmarsh.¹⁴ LSODE solves both stiff and nonstiff systems of the form $dy/dt = f$. In the stiff case, it treats the Jacobian matrix df/dy as either a full or a banded matrix, and as either user-supplied or internally approximated by difference quotient. It uses Adams methods (predictor-corrector) in the nonstiff case, and Backward Differentiation Formula (BDF) methods in the stiff case. The linear systems that arise are solved by direct methods (LU factor/solve). Because our system is comprised of nonlinear, stiff, ordinary differential equations, we used the BDF method and internally approximated Jacobian matrix df/dy .

For any parameter estimation algorithm, we must choose a merit function that measures the agreement between the data and the model for a particular choice of parameters. The parameters of the model are then adjusted to achieve a minimum in the merit function, and ultimately, yield the best-fit parameters. We used the familiar least-square fit, and the merit function (Φ) used was a root of the residual sum of squares (eq 3).

$$\Phi = \sqrt{\sum_{i=1}^m [y_e - y_c^h]^2} = \sqrt{\|y_e - y_c^h\|^2} \quad (3)$$

where m is the number of total data points, y_e is the experimental data, and y_c^h is the model prediction using the set of parameters h .

Eq 3 is nonlinear with respect to the parameters, and therefore the search for the set of values of the parameters is carried out in an iterative way. Given a set of parameters, \mathbf{K}^h , the new parameters of next step that give smaller merit function is calculated as follows,

$$\mathbf{K}^{h+1} = \mathbf{K}^h + \Delta\mathbf{K}^{h+1} \quad (4)$$

Where $\Delta\mathbf{K}^{h+1}$ is the correction vector that is calculated according to the Levenberg-Marquardt method.¹⁵

$$\Delta\mathbf{K}^{h+1} = (\mathbf{A}^T\mathbf{A} + \lambda\mathbf{I})^{-1} \mathbf{A}^T (y_e - y_c^h) \quad (5)$$

where \mathbf{I} is the identity matrix, λ is a scalar that is chosen at each iteration, so that the new parameters will result in a lower merit function in the following iteration, and \mathbf{A} is a Jacobian matrix of partial derivatives of y with respect to \mathbf{K} evaluated at all m points where experimental observation are available:

$$\mathbf{A} = \begin{bmatrix} \frac{\partial y_1}{\partial K_1} & \dots & \frac{\partial y_1}{\partial K_n} \\ \dots & \dots & \dots \\ \frac{\partial y_m}{\partial K_1} & \dots & \frac{\partial y_m}{\partial K_n} \end{bmatrix} \quad (6)$$

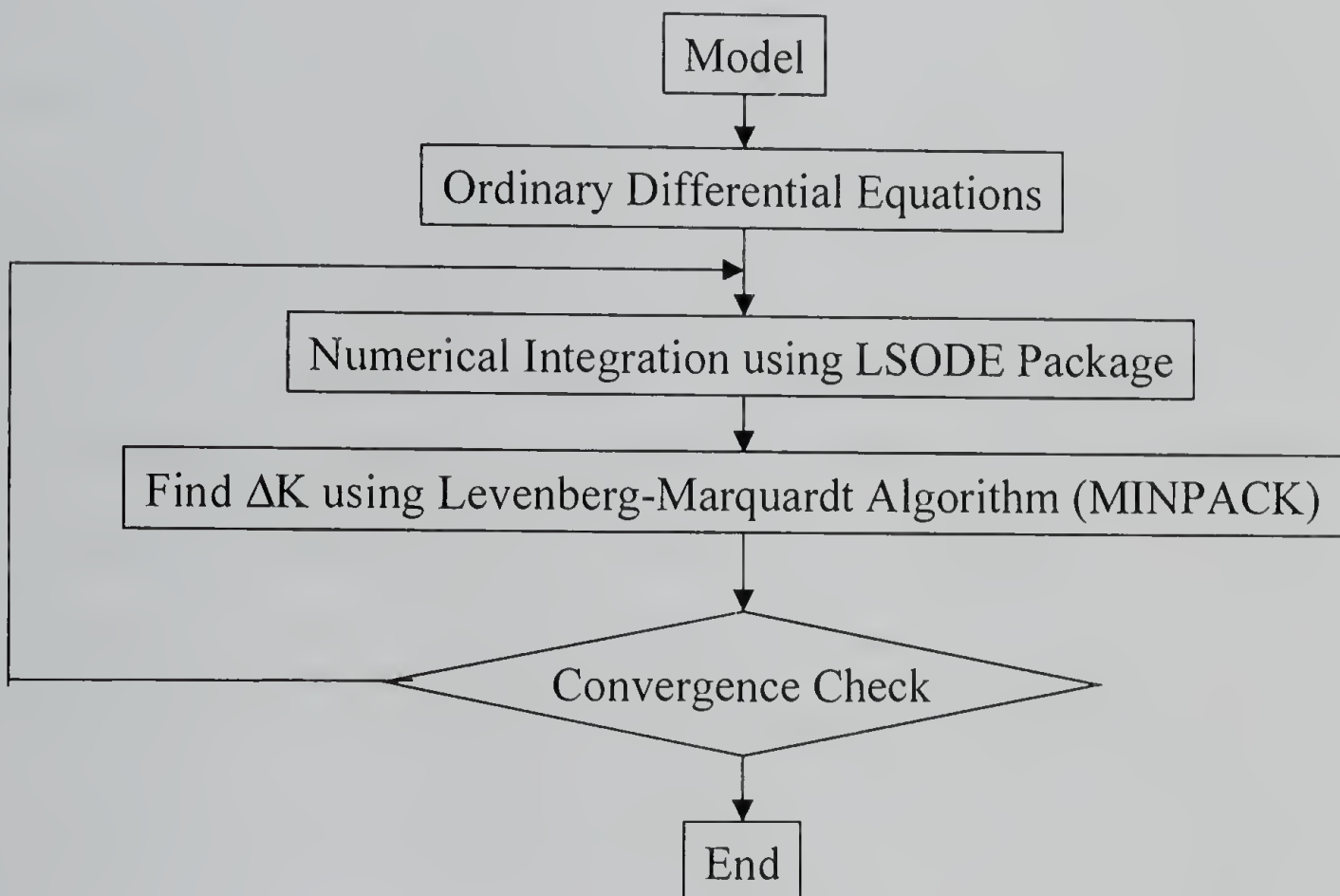
We used MINPACK package that is based on previously described algorithm. This package has been developed by Moré, *et al.*¹⁶ at Argonne National Laboratory, and includes software for solving nonlinear equations and nonlinear least squares problems. Among the choices, we used the 'lmdif' solver that handles nonlinear least squares problem using internally approximate Jacobian matrix calculated by a forward-difference approximation. Scheme 2.4 summarizes the parameter estimation algorithm.

The algorithm involves the following steps:

1. Assume initial guesses for the parameters of \mathbf{K} .
2. Integrate the ordinary differential equations using parameter \mathbf{K}^h and initial conditions with LSODE package to obtain the profiles of \mathbf{y}_c^h .
3. Calculate the merit function and Jacobian matrix \mathbf{A} by a forward-difference approximation.
4. Use eq 5 to obtain the correction vector $\Delta \mathbf{K}^{h+1}$.
5. Evaluate the new estimate of the parameters \mathbf{K}^{h+1} from eq 4.
6. Repeat step 2 through 5 until convergence is reached determined in a way of either
 - a. Φ is small enough;
 - b. Φ does not change anymore;

c. ΔK^{h+1} becomes very small.

Scheme 2.4 Algorithm of Parameter Estimation



2.3 Checking the Approach

2.3.1 Checking the Model

Before applying the algorithm to real problems, we had to check the validity of the approach. In this regard, we checked both model and the parameter estimation algorithm. First, we checked the validity of our model reactions. Even though we took into account many possible reactions in the model system, the model is unlikely to be perfect. To check this, we simulated a polymerization using conventional ATRP conditions, and compared our results with Fisher's report on ATRP kinetics.³

Table 2.1 is the list of the parameters used in the simulation of the polymerization of styrene. We used literature values for the rate constants of the various reactions in our ATRP scheme. It is practically impossible to describe the polymerization in terms of all the differing lengths of polymer chains with a finite number of differential equations, even though there is software called "Predici" actually doing it.¹⁷ However, if the average molecular weight or polydispersity is not the focal point of the problem, it is not necessary to describe all of the components with different chain lengths separately. We simplified the differential equation by considering only monomeric and dimeric units. The oligomers higher than trimer were not discriminated from each other, and they all were considered as polymer chains (i.e., for this treatment, we assumed that the reactivity is the same for all chains having different lengths.).

Figure 2.1 shows the first-order kinetic plot of monomer consumption for a styrene ATRP simulation. The simulation shows curvature throughout the

Table 2.1 Values of the Parameters Used in the Simulation of Styrene ATRP

$[RX]_0$ (M)	8.7×10^{-2}
$[M]_0$ (M)	8.7
$[Mt^nY/L]_0$ (M)	8.7×10^{-2}
$[XMt^{n+1}Y/L]_0$ (M)	0
Temperature ($^{\circ}C$)	110
k_{act} ($M^{-1} s^{-1}$)	.45
k_{deact} ($M^{-1} s^{-1}$)	1.1×10^7
k_p ($M^{-1} s^{-1}$)	1.6×10^3
k_{tc} ($M^{-1} s^{-1}$)	1.0×10^9
k_{td} ($M^{-1} s^{-1}$)	1.0×10^8
k_{therm} ($M^{-1} s^{-1}$)	4.8×10^{-11}
k_a ($M^{-1} s^{-1}$)	1.0×10^{-4}
k_b ($M^{-1} s^{-1}$)	1.63×10^3

polymerization. The experimental data of styrene ATRP, however, showed a linear relationship in this plot, which indicates that the concentration of the active radical is constant and follows the relationships;

$$R_p = -\frac{d[M]}{dt} = k_p [R \cdot][M]$$

$$\ln\left(\frac{[M]_0}{[M]}\right) = k_p [R \cdot] t \quad (7)$$

Fischer, however, has shown that the first-order kinetics with respect to monomer consumption should result in nonlinear relationship considering the concept of *persistent radical effect*.³ Fischer's analysis divided the reaction time into three segments:^{3,18} (1) very short times ($<10^{-3}$ s), (2) intermediate times ($\sim 10^{-3}$ s $< t < 5 \times 10^2$ h), and (3) very long times ($>3 \times 10^3$ years). Of practical interest is the intermediate regime only, where it was shown the monomer consumption should follow eq 8.³

$$\ln\left(\frac{[M]_0}{[M]}\right) = \frac{3}{2} k_p ([RX]_0 [Mt^n]_0)^{1/3} \left(\frac{k_{act}}{k_{deact} 2k_t}\right)^{1/3} t^{2/3} \quad (8)$$

Figure 2.2 plots the first-order kinetics as a function of $t^{2/3}$. This graph shows a linear relationship similar to Fischer's results in the low conversion region. However, there is curvature at higher conversion, and the conversion is lower than Fischer's result for the whole region.

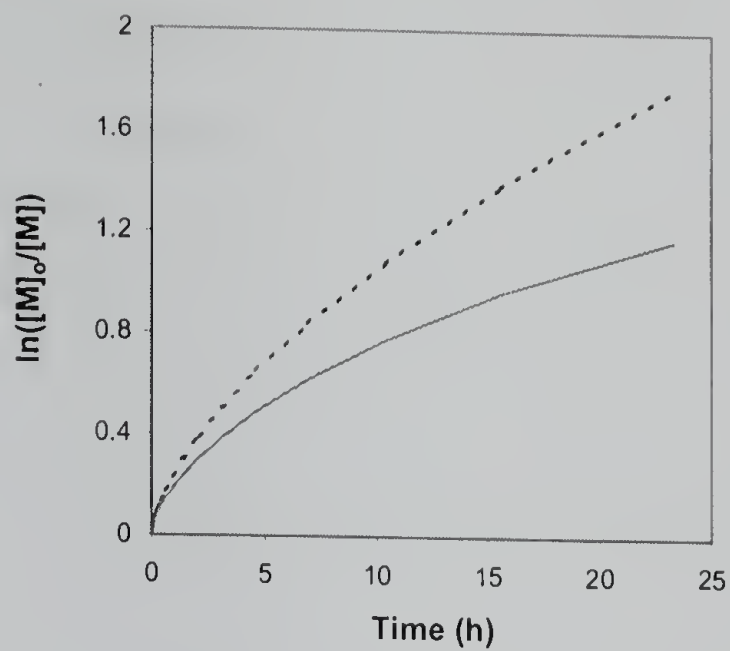


Figure 2.1 First-order kinetic plot of monomer consumption in the ATRP of styrene simulations (---, Fischer's result), (—, this work).

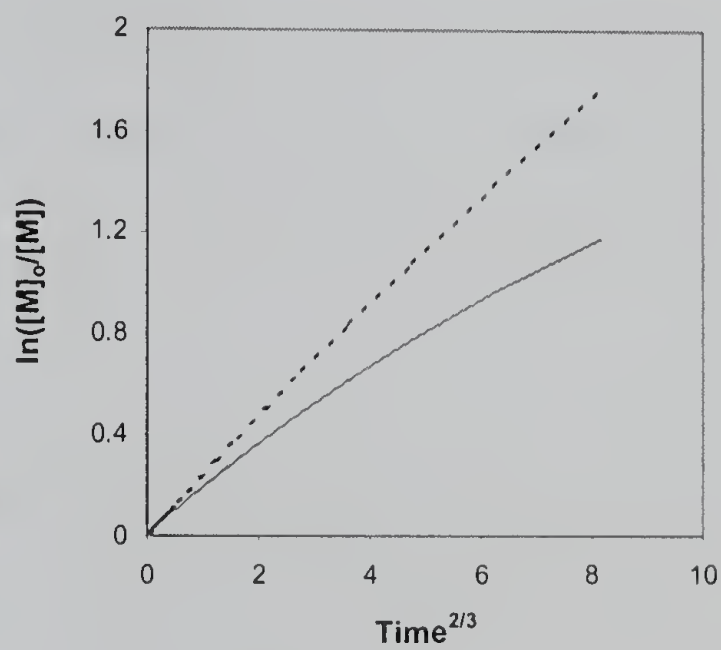


Figure 2.2 First-order kinetic plot of monomer consumption, as a function of time^{2/3}, in the ATRP of styrene simulations (---, Fischer's result), (—, this work).

The differences may be attributable to the fact that we included more side reaction in our model, (such as the chain-end degradation reactions) than did Fischer in his study. These side reactions act to decrease the concentration of active radicals further than in Fischer's model, and results in decreasing the monomer conversion over all times. Figure 2.3 shows the relationship between the concentration of the low oxidation state-metal complexes and time. Our results generally agree with Fischer's analyses that the concentration of metal complexes at higher oxidation state ($[Mt^{n+1}]$) is increased as a function of $t^{1/3}$. This decrease follows eq 9 with a deviation at the higher conversion region as we saw on the first-order kinetic plot of monomer consumption.

$$[Mt^{n+1}] = ([RX]_0[Mt^n]_0)^{2/3} \left(\frac{3k_{act}^2 2k_t}{k_{deact}^2} \right)^{1/3} t^{1/3} \quad (9)$$

Figure 2.4 plots $[Mt^{n+1}]$ as a function of $t^{1/3}$. This graph also shows a linear relationship similar to Fischer's results in the low conversion region. However, there is curvature at higher conversion, and $[Mt^{n+1}]$ is higher than Fischer's result for whole region.

One explanation for the disagreements between experimental data and these simulations was offered by Shipp *et al.* who considered diffusion controlled termination reactions.⁴ At high monomer conversion, the viscosity of the medium increases dramatically, and this affects the rates of several of the reactions involved in the polymerization. Because the bimolecular termination reactions involve the diffusion of

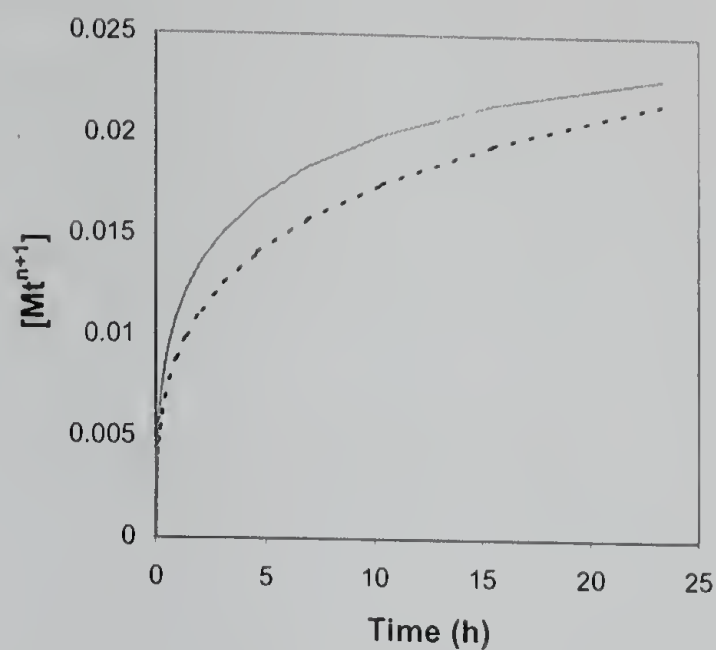


Figure 2.3 $[Mt^{n+1}]$ as a function of time in the ATRP of styrene simulations (---, Fischer's result), (—, this work).

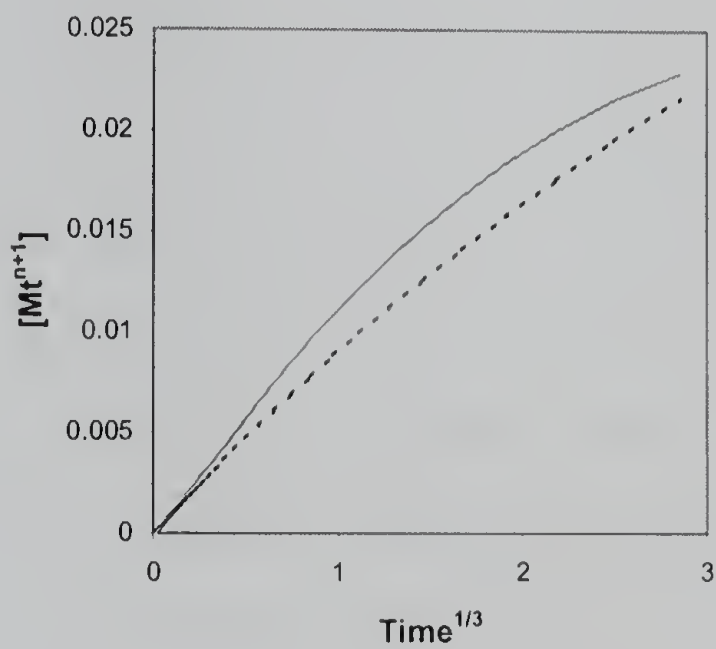


Figure 2.4 $[Mt^{n+1}]$ as a function of time^{1/3} in the ATRP of styrene simulations (---, Fischer's result), (—, this work).

two polymer chains, they may be affected significantly by the viscosity of the reaction medium. Shipp *et al.* used a simple scaling relationship of the form of eq 10, which is based upon the empirical equations describing diffusion coefficients of oligomeric methacrylates and styrenes in polymer solutions.¹⁹

$$k_t(DP) = k_t(0)DP^{-(0.65+0.02DP)} \quad (10)$$

where DP is calculated from conversion of monomer to polymer ($DP = \Delta[M]/[RX]_0$) and defining the initiator as the first unit.

Figure 2.5 is the plot of the first-order kinetics of monomer consumption in the styrene ATRP simulation taking into consideration the conversion dependent termination reaction constants. This analysis shows a similar linear relationship of $\ln([M]_0/[M])$ on polymerization time as the Shipp's analysis. The slight downhill curvature in the high conversion region is thought to be due to the side reactions, which include termination and chain-end degradation reactions. Because the curvature was prominent only at very high conversion (> 95 %), the plot was in better agreement with the experimental styrene ATRP data using the CuBr/dNbpy catalyst. Compared with the real data, the simulation with constant termination rate constants shows a much slower rate of polymerization. Hence, by inclusion of the diffusion dependent termination rate constants, the simulation gave better agreement with the real data, although there was still some discrepancy.

Figure 2.6 shows the relationship between $[Mt^{n+1}]$ and the polymerization time.

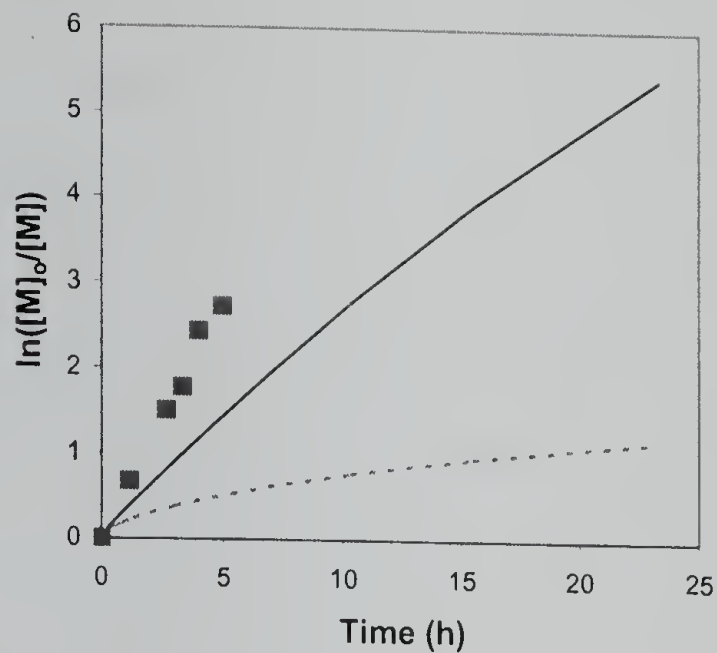


Figure 2.5 First-order kinetic plot of monomer consumption in the ATRP of styrene; experiment (■) and simulation with (a) constant k_t (---); (b) diffusion-dependent k_t (—).

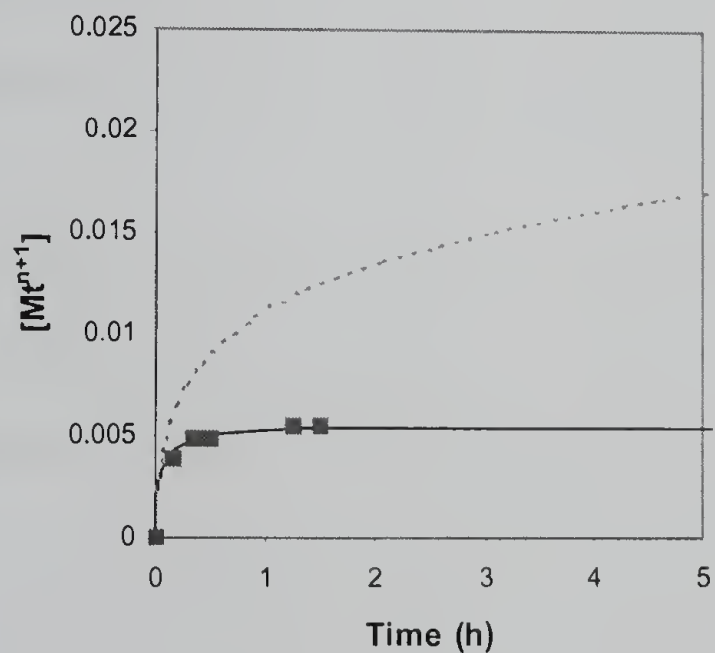


Figure 2.6 $[Mt^{n+1}]$ as a function of time in the ATRP of styrene; experiment (■) and simulation with (a) constant k_t (---); (b) diffusion-dependent k_t (—).

dramatically at the beginning of the polymerization and then levels out to be almost constant during the remainder of the reaction. In contrast, when a constant termination rate is used, $[Mt^{n+1}]$ continually increases. The increase of $[Mt^{n+1}]$ comes from the irreversible termination reactions between two radical species. The accumulated high oxidation state-metal complexes act as deactivator in ATRP, by suppressing the concentration of active radical species, which is the basic idea of *persistent radical effect*. Therefore, $[Mt^{n+1}]$ is highly related with the termination rate constants. In the case of a constant termination rate, the termination reaction is overestimated and is evidenced by the continual increase of $[Mt^{n+1}]$ throughout the polymerization. Because of this, the calculated polymerization rate is much slower than actual ATRP data. Kajiwara, *et al.* used electron paramagnetic resonance (EPR) methods to determine $[Mt^{n+1}]$.²⁰ Kajiwara's results showed that under the same condition as we used in our simulations, $[Mt^{n+1}]$ only slightly increased after a dramatic increase in the initial stage of polymerization, and reached a final concentration of 5-6 mM. Hence, the simulation that includes a diffusion-dependent termination rate was in excellent agreement with the EPR data.

Figure 2.7 shows the concentration of active radical, deactivator (Mt^{n+1}), and the dormant chains simulated with our model that includes the diffusion-dependent termination rate constants. In Fischer's analysis, the overall process is composed of three clearly distinguished stages; very short time, the intermediate $t^{1/3}$ dependence equilibrium regime, and very long times. The active radical and deactivator increase linearly, and equally, in the first short time region ($t < 10^{-3}$ s). The termination reactions then decrease the concentration of active radicals, and by doing so, increase the concentration of the deactivator. In this region, the equilibrium between active radicals and dormant chains is

finally established, and most of polymerization takes place ($\sim 10^{-3} \text{ s} < t < 5 \times 10^2 \text{ h}$). In the final “very long time” region ($t > 3 \times 10^3 \text{ years}$), the net change of the concentration of the active radicals is only governed by the self-termination. We could also find three similar stages of the process in our simulation, even though there were some differences in detail. The first stage is the same as in Fischer’s analysis that shows the linear, and equal, increase of active radicals and deactivators. However, both the intermediate stage, and the “very long time” stage do not follow the $t^{1/3}$ and t^{-1} dependence perfectly. Instead, they show complex behavior due to the inclusion of diffusion-dependent termination rate and chain end degradation side reactions.

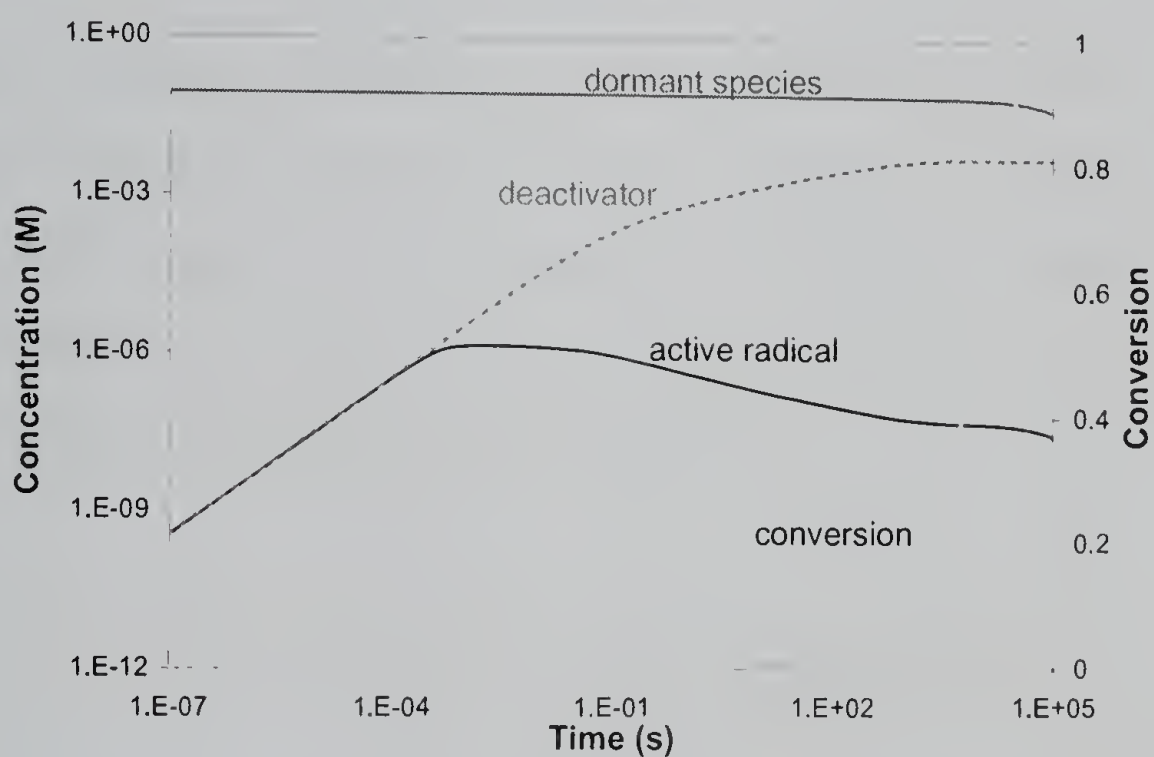


Figure 2.7 Concentrations of dormant species, deactivator, and active vs. time in a double-logarithmic plot.

2.3.2 Verifying the Parameter Estimation Algorithm

We used MINPACK package for the parameter estimation steps. The MINPACK is a universal package composed of many sub-solvers designed to address different problems, and many parameter estimation problems can be successfully solved with this package. However, in addition to make the necessary choices with the MINPACK package, we had to modify the program to make it suitable for our purposes. Therefore, prior to applying this modified program to real problems, we had to check the validity of the algorithm to ensure that the rate constants can be determined successfully with this new package.

In order to properly test this package, we used fabricated experimental data points that were generated by using literature rate constants. A set of nonlinear differential equations was derived from the mechanistic model, and numerically integrated using the reasonable literature rate constants. To then test the validity of our modified program, a series of "poor guesses" for the rate constants were refined using an iterative approach. The goodness of fit could then be evaluated by determining how close the calculated values matched the rate constants used to generate the data.

For accuracy and reliability of the parameter estimation approach, it is desirable to have data that relates to as many of the individual mechanistic steps as possible. For example, to estimate the thermal initiation rate constants successfully, we have to know the concentration of the dimeric product resulting from this step. In the polymerization itself, the pertinent data are the concentration of the monomer, molecular weight, and polydispersity of resulting polymer. It is, however, difficult to simulate molecular weight

and polydispersity of polymer because of the complex nature of the polymerization. We therefore used a simplified model system for this phase of the study. Specifically, small molecular atom transfer radical addition (ATRA) reactions were used as our testbed reactions. We used high initial concentrations of both initiator ($[IX]/[M] = 4$) and metal complexes ($[IX]/[Mt^n] = 10$). Under these reaction conditions, the concentration of the important components, including initiator (IX), dimeric dormant species (M_2X), and the termination dimeric product of initiator radical (M_2b), could be determined using standard characterization methods. It should be noted that because our model systems run at high catalyst concentrations and low monomer concentrations, the effect of the chain end degradation reactions becomes very important. Table 2.2 shows the reaction conditions and the values of rate constants used to generate the simulated data.

Table 2.2 Values of the Parameters Used in the Simulation of Styrene ATRA

$[IX]_0$ (M)	5.0×10^{-1}
$[M]_0$ (M)	1.25×10^{-1}
$[Mt^nY/L]_0$ (M)	5.0×10^{-2}
$[XMt^{n+1}Y/L]_0$ (M)	0
Temperature ($^{\circ}C$)	110

The system of differential equations depicting model reactions can be written as follows,

$$\frac{dS}{dt} = f(t, S, X, K) \quad (11)$$

where \mathbf{S} is the vector of the state variables, \mathbf{X} the vector of observable variables, and \mathbf{K} the vector of the estimatable parameters.

$$\begin{aligned} \mathbf{S} &= \{ I, IX, IH, M, M_2, M_2X, M_2a, M_2b, R, RX, Ra, Rb, Mt^n, Mt^{n+1}, HX \} \\ \mathbf{X} &= \{ IX, M, M_2X, M_2b \} \\ \mathbf{K} &= \{ k_{act}, k_{deact}, k_a, k_b, k_{therm} \} \end{aligned} \quad (12)$$

The easily determinable rate constants of propagation and termination were assumed to follow the literature values.

As a complicating factor in these calculations, the estimatable parameters have values of different orders of magnitudes. This value spread increases the stiff ratio of the Jacobian matrix in the parameter optimization step, and makes it difficult to find satisfactory solutions. To solve this problem and enhance the convergence of the algorithm, a reparameterization approach was used that required redefining the kinetic parameters in such a way that they all have similar values.

$$k_{deact}' = k_{deact}/10^7, k_a' = k_a/10^{-4}, k_b' = k_b/10^3, k_{therm}' = k_{therm}/10^{-11} \quad (13)$$

This reparameterization reduced the computing time, and allowed us to generate more reliable results.

Table 2.3 shows the first results of the parameter estimation. We started with several initial guesses with diverse values with the goal of identifying the global

minimum. The regression results showed that for all rate constants, different initial values resulted in fits of the data that were indistinguishable from one another. However, the ratio of k_{act} and k_{deact} , the equilibrium constant K_{eq} , converged quite well to the original value for most of the initial guesses. This result implied that although we could not successfully estimate each of the individual rate constants, it is possible to determine the K_{eq} from our model reactions and reaction conditions. There were several possible explanations for this unsuccessful parameter estimation scheme. The first reason is the sensitivities of the rate constants. If one reaction has a very small influence on the overall course of the reaction, it is hard to determine the rate constant corresponding to that step. The sensitivities of each of the rate constants could be checked by plotting the contour map of the merit function. We are attempting to estimate 5 different rate constants in ATRP, which means that the real contour map of our problem is 5-dimensional. Because it is impossible to visualize a 5-dimensional contour map, we simplified the problem into a series of 1-dimensional representations by holding other 4 rate constants fixed at the original values. This is not a true contour map, but it does allow us to get an idea about

Table 2.3 Effect of the Initial Guess on the Estimated Parameters

initial guesses					estimated parameters						Φ
k_{act}	k_{deact}	k_a	k_b	k_{therm}	k_{act}	k_{deact}	k_a	k_b	k_{therm}	K_{eq}	
0.5	0.5	0.5	0.5	0.5	0.335	0.818	1.493	0.579	0.014	4.099E-08	2.755E-02
1	1	1	1	1	0.911	2.240	1.275	1.022	0.919	4.067E-08	1.415E-02
5	5	5	5	5	2.424	8.124	0.001	10.531	5.614	2.984E-08	8.989E-01
0.5	1	5	1	0.5	0.723	1.773	1.144	1.321	0.001	4.076E-08	7.055E-03
1	5	0.5	5	1	2.216	5.489	0.001	2.879	0.390	4.038E-08	1.436E-01
5	0.5	1	0.5	5	0.010	0.018	1.816	0.010	0.001	5.641E-08	2.648E-01
original values					0.450	1.100	1.000	1.626	1.000	4.091E-08	

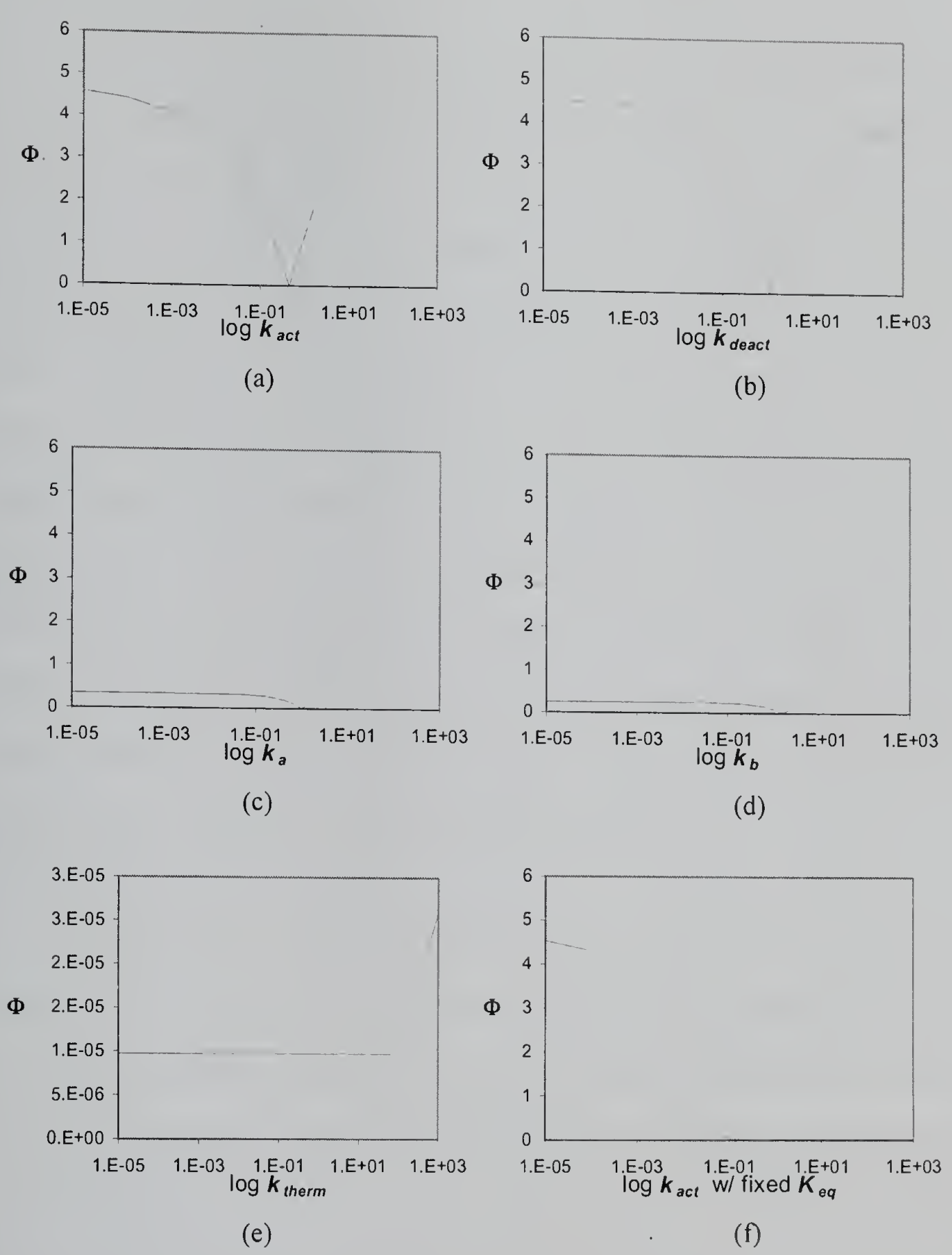


Figure 2.8 One-dimensional contour maps. Φ is the merit function defined by eq. 3.

the sensitivities of each of the rate constants.

Figure 2.8 shows the 1-dimensional contour maps of the merit function (Φ) in the parameter estimation algorithm. We held the other 4 rate constants at fixed values while allowing the parameter under investigation to vary. We can immediately see that k_{act} and k_{deact} are very sensitive, and shows big difference on value of merit function around the original values (8a and 8b), k_a and k_b are less sensitive (8c and 8d), and k_{therm} is extremely insensitive to the system (8e). Therefore, it was impossible to determine the thermal initiation rate constant of styrene with our model. One additional note is that when k_{act} or k_{deact} changes, K_{eq} also changes along with it because the other parameter is fixed at a constant value. In other word, the very sensitive parameter is not k_{act} or k_{deact} itself but the ratio of the two, K_{eq} . Figure 2.8f is the contour map generated by changing k_{act} with a fixed value of K_{eq} . In this case, the value k_{deact} must also change along with k_{act} in order to have the same value of K_{eq} . With a fixed value of K_{eq} , k_{act} is not so sensitive and the contour map shows a smooth valley around the original value.

The second explanation as to the failing of this parameter estimation scheme is the possibility of correlation between parameters. If there is a correlation between parameters, then they are not truly independent variables, and could not be determined at the same time. Being correlated, the individual values of k_{act} and k_{deact} were at best poorly estimated, but the ratio of them was successfully determined. This bolsters the idea that some correlation between two parameters may exist.

The third possibility is that the system gets trapped within local minimum before reaching the global minimum. We used two different convergent tests methods on the parameter estimation algorithm. The first test was designed to check how close the simulated data matched the experimental data, and the second one, checked how small the step length in a single cycle is. A very small step length means no practical improvement in convergent values, and further calculation is wasted. If the convergence test meets the first criteria, there is a higher probability of reaching the global minimum. However, convergence on the second test would indicate a high probability of local trapping. An extremum (maximum or minimum point) can be either *global* (truly the highest or lowest function value) or *local* (the highest or lowest in a finite neighborhood, but not outside the boundary of that neighborhood) (Figure 2.9). Finding a global extremum is, in general, a difficult problem. Two standard strategies are widely used: (i) find local extrema starting from widely varying starting values of the independent variables perhaps chosen quasi-randomly), and then pick the most extreme of these (if they are not all the same); or (ii) perturb a local extremum by taking a finite amplitude

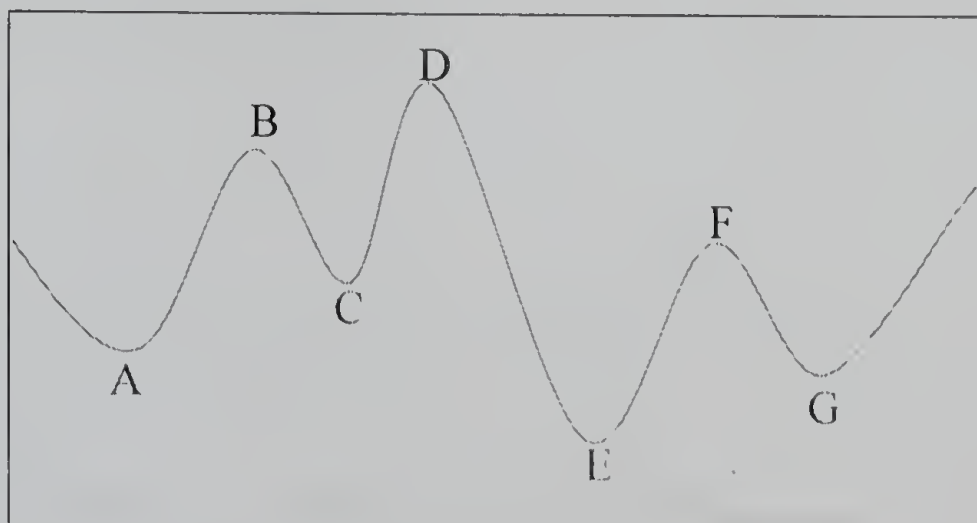


Figure 2.9 Extrema of a function in an interval. Points A, C, and G are local, but not global minima. Points B and F are local, but not global minima. The global maximum occurs at D. The global minimum is at E.

step away from it, and then monitor the response of the routine to see if it arrives at a better point, or “always” return to the same one. At first, we attempted to find global minimum using the second method. However, it was hard to determine the suitable amplitude of perturbation from the local minimum.

Downhill simplex method (DSM) Instead of taking finite amplitude steps away from the values generated from the MINPACK algorithm, we applied a secondary minimization algorithm as a perturbation. The secondary minimization algorithm has to be of a different character from the first MINPACK algorithm, and it doesn't have to be a particularly accurate minimization algorithm. In our strategy, the accuracy is derived from the first MINPACK algorithm because it is a special minimization algorithm developed for the parameter estimation problem. We used a simple minimization algorithm, the ‘Downhill Simplex Method (DSM)’ as our perturbation source.²¹ DSM is one of the multidimensional minimization solvers, and requires only function evaluations, not derivatives of them. DSM crawls downhill in a straightforward fashion with few if any special assumptions. This can be an extremely slow process, but it can also be extremely robust. Not to be overlooked is the fact that the code is concise and completely self-contained.

A *simplex* is a geometrical figure consisting in N dimensions of $N + 1$ points (or vertices) and all their interconnecting line segments, polygonal faces, etc. In two dimensions, a simplex is a triangle. In three dimensions, it is a tetrahedron, but not necessarily a regular tetrahedron. In general, we are only interested in simplexes that are nondegenerate, i.e., simplexes that enclose a finite inner N -dimensional volume. If any

point of a nondegenerate simplex is taken as the origin, then the N other points define vector directions that span the N -dimensional vector space.

In general, multidimensional minimization algorithms start from an initial guess, that is, an N -vector of independent variables as the first point. The algorithm then make its own way downhill through the unimaginable complexity of an N -dimensional topography, until it encounters a minimum. The DSM starts with not just a single point, but with $N + 1$ points, defining an initial simplex. From one of these points (it matters not which) as a initial starting point \mathbf{P}_0 , then we can take the other N points to be

$$\mathbf{P}_i = \mathbf{P}_0 + \lambda \mathbf{e}_i \quad (14)$$

where the \mathbf{e}_i 's are N unit vectors, and where λ is a constant which is a guess of the problem's characteristic length scale. The DSM now takes a series of steps, most steps just moving the point of the simplex where the function is largest ("highest point") through the opposite face of the simplex to a lower point. These steps are called reflections, and they are constructed to conserve the volume of the simplex (hence maintain its nondegeneracy). When it can do so, the method expands the simplex in one or another direction to take larger steps. When it reaches a "valley floor," the method contracts itself in the transverse direction and tries to slide down the valley. If there is a situation where the simplex is trying to "pass through the eye of a needle," it contracts itself in all directions, pulling itself in around its lowest (best) point. Figure 2.10 depicts the possible steps in the DSM.

Scheme 2.5 shows the newly designed algorithm for parameter estimation. After the MINPACK algorithm, the DSM runs with the result of the MINPACK as an initial point. The convergence of the DSM was also checked by two criteria, how small the decrease in the merit function value is, and how small the one step length is. These two minimization steps are called as a single cycle. The result obtained from the DSM is used again as a starting point of the MINPACK, and the program cycles again. The whole algorithm routine is terminated when two criteria are met. First, the algorithm will be terminated if the merit functional is smaller than an acceptable value. The other termination criterion is met when the step length in a cycle is too small to give an improvement on further calculation. The second check is performed at two times in a cycle, after the MINPACK calculation and after the DSM perturbation.

Scheme 2.5 Algorithm of Parameter Estimation Using MINPACK and DSM

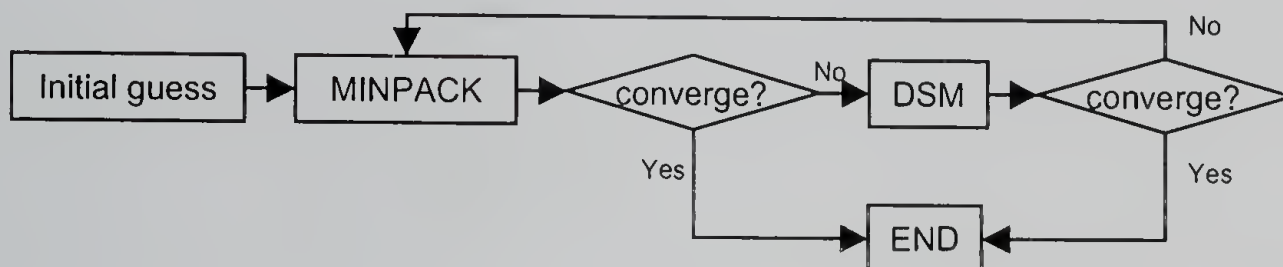


Table 2.4 is the results of the parameter estimation of ATRP using this new algorithm. From all of the initial guesses used, the algorithm successfully found the original values of the kinetic parameters except k_{therm} . As we have seen before, the k_{therm} has too low of a sensitivity to be estimated even with this new algorithm. With the new algorithm, we were successful in estimating not only K_{eq} but also each value of k_{act} and k_{deact} . The merit functions also had much smaller values than those of the older algorithm

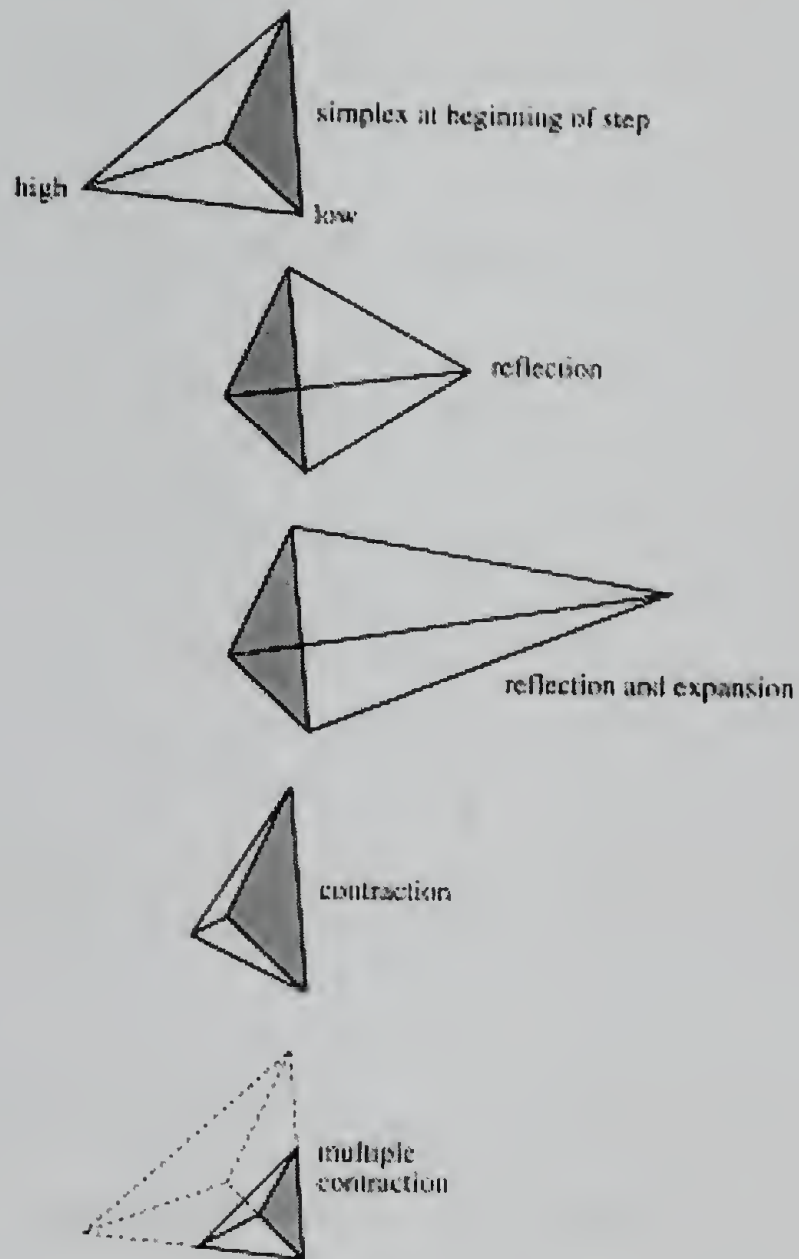


Figure 2.10 Possible outcomes for a step in the downhill simplex method. The simplex at the beginning of the step, here a tetrahedron, is shown, top. The simplex at the end of the step can be any one of (a) a reflection away from the high point, (b) a reflection and expansion away from the high point, (c) a contraction along one dimension from the high point, or (d) a contraction along all dimensions towards the low point. (Ref. 16).

that used only the MINPACK package. One thing to be noted is that the termination of the new algorithm was signaled not by how small the merit function becomes, but by how small the step or change of the merit function is. Therefore, the possibility of being trapped in a local minimum wasn't completely eliminated in the new algorithm.

Table 2.4 Parameter Estimation Using the Algorithm of Sequential Use of MINPACK and DSM

initial guesses					estimated parameters						Φ
k_{act}	k_{deact}	k_a	k_b	k_{therm}	k_{act}	k_{deact}	k_a	k_b	k_{therm}	K_{eq}	
0.5	0.5	0.5	0.5	0.5	0.444	1.084	1.000	1.630	0.088	4.091E-08	4.885E-05
1	1	1	1	1	0.437	1.069	1.000	1.629	0.001	4.092E-08	1.003E-04
5	5	5	5	5	0.462	1.129	1.000	1.630	0.001	4.090E-08	8.031E-05
0.5	1	5	1	0.5	0.462	1.130	1.000	1.630	1.681	4.090E-08	9.204E-05
1	5	0.5	5	1	0.457	1.116	1.000	1.630	0.013	4.091E-08	4.757E-05
5	0.5	1	0.5	5	0.460	1.124	1.000	1.628	0.052	4.090E-08	1.043E-04
original values					0.450	1.100	1.000	1.626	1.000	4.091E-08	

Effect of Reparameterization. In developing our parameter estimation algorithm, we used reparameterization of the estimatable rate constants to enhance the probability of convergence. The reparameterization was done based on the literature values of the rate constants. However, the literature values may not be correct, and for other polymerization systems, they could have values that are orders of magnitude different. If the convergence of the algorithm is affected by the reparameterization, the order of the reparameterization can affect the result of the parameter estimation. The results of the effect of reparameterization are presented in Table 5 and 6. Two different reparameterizations were made; $k'' = k' / 10$ in Table 5, $k'' = k' \times 10$ in Table 6. It can be

seen that the estimation of each parameters was not perfect for all initial guesses as when the original reparameterization was used. However, the K_{eq} was accurately estimated all the time. Moreover, if we combined the first strategy to find the global minimum, picking the most extreme among the many local minima starting from widely varying initial values of the parameters chosen quasi-randomly, we could also determine the values of each of the kinetic parameters.

Table 2.5 Effect of Reparameterization. Reparameterization was performed as $k'' = k' / 10$

initial guesses					estimated parameters						Φ
k_{act}	k_{deact}	k_a	k_b	k_{therm}	k_{act}	k_{deact}	k_a	k_b	k_{therm}	K_{eq}	
0.5	0.5	0.5	0.5	0.5	0.045	0.110	0.100	0.163	0.001	4.091E-08	4.725E-05
1	1	1	1	1	1.402	3.459	0.104	0.153	0.001	4.053E-08	3.516E-03
5	5	5	5	5	16.115	39.771	0.104	0.153	0.001	4.052E-08	3.660E-03
0.5	1	5	1	0.5	2.039	5.031	0.104	0.153	0.005	4.053E-08	2.076E-05
1	5	0.5	5	1	0.694	1.713	0.104	0.154	0.231	4.055E-08	3.559E-05
5	0.5	1	0.5	5	6.894	17.014	0.104	0.153	0.001	4.052E-08	1.184E-04
original values					0.045	0.110	0.100	0.163	0.480	4.091E-08	

Table 2.6 Effect of reparameterization. Reparameterization was performed as $k'' = k' \times 10$

initial guesses					estimated parameters						Φ
k_{act}	k_{deact}	k_a	k_b	k_{therm}	k_{act}	k_{deact}	k_a	k_b	k_{therm}	K_{eq}	
0.5	0.5	0.5	0.5	0.5	0.759	1.782	7.794	21.289	0.001	4.261E-08	1.899E-02
1	1	1	1	1	1.03E+03	2.53E+03	10.413	15.304	2.766	4.052E-08	3.060E-03
5	5	5	5	5	4.534	11.084	9.986	16.290	8.387	4.091E-08	9.951E-05
0.5	1	5	1	0.5	6.401E+04	1.580E+05	10.398	15.327	319.101	4.052E-08	3.008E-03
1	5	0.5	5	1	4.508	11.020	9.996	16.269	0.155	4.091E-08	3.129E-05
5	0.5	1	0.5	5	4.488	10.972	9.994	16.273	0.076	4.091E-08	2.941E-05
original values					4.500	11.100	10.000	16.230	48.000	4.054E-08	

Effect of Experimental Error. In generating simulated experimental data, we did not include experimental errors. However, real experimental data never results in a perfectly smooth curve, and there are always measurement errors incorporated. Therefore, it is worthwhile to check the behavior of parameter estimation approach when the data are affected by experimental errors. The experimental errors can be either or both random, statistical errors and/or systematic errors, such as wrong temperatures, poor fixing of starting time, or the wrong calibration of measurement apparatus. Because systematic errors are not the general case, our concern was limited to statistical errors. We used a Gaussian random number generator with a standard deviation, σ . The parameter estimation results shows that as σ is increased, the merit function of best fit is increased, and the estimated values of kinetic parameters deviate from the original values. However, K_{eq} is again successfully converged to the original value for all cases (Table 2.7). Hence, accurate results require accurate input.

Table 2.7 Effect of Experimental Noise on the Estimated Parameters

σ	k_{act}	k_{deact}	k_a	k_b	k_{therm}	K_{eq}	Φ
0.02	0.497	1.205	1.113	1.388	0.001	4.124E-08	1.352E-01
0.05	0.089	0.208	1.165	1.326	0.777	4.280E-08	3.371E-01
	0.450	1.100	1.000	1.626	4.800	4.091E-08	

Effect of the Size of the Experimental Data Set. Not only is the success of the parameter estimation highly dependent on the quality of the data, it is also dependent on the size of the data set. The more data are used, the more parameters that can be estimated. One example is the problematic k_{therm} . We have discussed the insensitivity of k_{therm} when the observable variables were $\{IX, M, M_2X, M_2b\}$. However, if we can get

data for the thermal initiation intermediate radical, k_{therm} could be estimated successfully. It is practically impossible to get concentration profiles of all the components in the model. We chose $\{IX, M, M_2X, M_2b\}$ as the set of observable variables, because we thought that they would be easy to determine by normal analytical methods. In some cases, however, the concentrations of dimeric species, M_2X, M_2b , are still too small to be measured unambiguously by any analytical method. It was thus advisable to check how the accuracy of estimated parameters is affected when there is a limit on the available data. As a check, we used the observable variables $\{IX, M\}$, as components constitute the main portion of reaction mixture, and their concentrations are most easily determined. Table 2.8 shows the results of parameter estimation using these two observable variables. It can be seen from the table that the value of K_{eq} converges to the original value for most of initial guesses, and each of the values of estimated parameters also approach the original values.

Table 2.8 Effect of the Number of Experimental Data on the Accuracy of Estimated Parameters

initial guesses					estimated parameters						Φ
k_{act}	k_{deact}	k_a	k_b	k_{therm}	k_{act}	k_{deact}	k_a	k_b	k_{therm}	K_{eq}	
0.5	0.5	0.5	0.5	0.5	0.336	0.822	0.996	1.640	0.001	4.089E-08	8.254E-05
1	1	1	1	1	0.859	2.097	1.006	1.605	1.075	4.095E-08	1.367E-04
5	5	5	5	5	0.282	0.689	0.992	1.651	0.248	4.088E-08	1.465E-04
0.5	1	5	1	0.5	0.644	1.573	1.004	1.612	0.001	4.093E-08	8.851E-05
1	5	0.5	5	1	4.117	10.046	1.012	1.586	0.068	4.098E-08	2.570E-04
5	0.5	1	0.5	5	12.787	2.294	0.214	0.567	0.001	5.574E-07	1.201E-01
original values					0.450	1.100	1.000	1.626	1.000	4.091E-08	

2.3.3 A Model to Estimate k_{act} and k_{deact}

The previous model was successful in estimating K_{eq} , which is one of the main parameters that govern the characteristics of the ATRP. However, it was difficult to determine each value of k_{act} and k_{deact} separately. The value of k_{deact} is important because it is the ratio of k_{deact}/k_p that influences the polydispersity of the polymer sample. Because the model discriminates only between dimeric species and higher oligomeric species, and the polydispersity, or the relative population of chains possessing different lengths was not taken into account, k_{deact} was not well estimated by the algorithm. Therefore, to find a model that gives a successful determination of k_{deact} , it is necessary to include factors describing polydispersity into the model. As we have already seen, it is practically impossible to describe all of the polymer chains with finite number of ordinary differential equations. We were therefore required to develop strategies to describe the polymerization in a much simpler way. The use of the time dependence of moments is one of the possible approaches. The number-average degree of polymerization, weight-average degree of polymerization, and ratio of them, the polydispersity index (PDI) of the polymer are defined by the following equations.

$$\begin{aligned}
 x_N &= \frac{\sum_i i n_i}{\sum_i n_i} = \frac{m_1(X)}{N} \\
 x_W &= \frac{\sum_i i w_i}{\sum_i w_i} = \frac{\sum_i i^2 n_i}{\sum_i i n_i} = \frac{m_2(X)}{m_1(X)} \\
 PDI &= \frac{x_W}{x_N} = \frac{m_2(X)/m_1(X)}{m_1(X)/N} = \frac{N m_2(X)}{m_1(X)^2}
 \end{aligned} \tag{15}$$

where the summations are over all the different sizes of polymer molecules from $i = 1$ to ∞ , n_i is the number of moles whose degree of polymerization is i , N is the total number of moles, w_i is the weight concentration of i molecules, and

$$m_k(X) = \sum_i i^k n_i \quad k = 1, 2 \quad (16)$$

It is, therefore, possible to describe the polymer characteristics including polydispersity in terms of moments. The development of ordinary differential equation using moments was straightforward except for one feature. We could not find a way to successfully include the termination reaction resulting from the combination between two radical species. The termination reaction by disproportionation was straightforward. The reaction between i -mer and j -mer radicals produce terminated products of i -mer and j -mer. This reaction does not affect the moments. However, the combination reactions between i -mer and j -mer radicals produce $(i+j)$ -mer of terminated product, and change the moments. The resulting derivatives of the moments including the summations of all the lengths chain were so complicated, we could not express them in simple ways. In present study, we elected to excluded the combination reaction from the model. This may not be such a bad approximation, because it is the chain termination steps that are largely excluded by the ATRP methodologies. We attempted to show the relationship between the rate constants and the molecular weight and polydispersity of the polymer, and pursued the possibility of determining the value of rate constants by our parameter estimation algorithm.

Figure 2.11 and 2.12 show the simulated results of polymerization using the new model with the same values of polymerization parameters as in Table 2.1. We employed 5 % of standard deviation in generating the data in order to mimic experimental error. The conversion and $\ln([M]_0/[M])$ vs. time curve shown in Figure 2.11 has small fluctuations, but generally follows the trend observed in real ATRP systems. The same is true for the molecular weight and polydispersity curves shown in Figure 2.12. The same strategy was used to check the validity of the parameter estimation algorithm. Using the simulated data as experimental ones, we checked to see if the algorithm could find the original values of rate constants used in the data simulation from any arbitrary initial guesses. The results are shown in Table 2.9. We were quite gratified to find that from a wide range of initial guesses, the algorithm successfully found the original values of k_{act} and k_{deact} . These results demonstrated that it is possible to determine the most important kinetic parameters in ATRP from normal polymerization data such as conversion, molecular weight, and polydispersity. Not surprisingly, the values of k_a and k_b were poorly determined by the algorithm. However, unlike the previous small molecular ATRA conditions, the chain end degradation reaction can be neglected in normal polymerizations. Therefore, the sensitivity of the chain end degradation rate constants on the polymerization result, especially conversion, molecular weight, and polydispersity, is too small to be estimated by the parameter estimation algorithm.

Table 2.9 Parameter Estimation Based on Our New Model Using Polymerization Data (conversion, M_n , and PDI)

initial guesses					estimated parameters						Φ
k_{act}	k_{deact}	k_a	k_b	k_{therm}	k_{act}	k_{deact}	k_a	k_b	k_{therm}	K_{eq}	
0.5	0.5	0.5	0.5	0.5	0.448	1.057	0.426	1.743	0.026	4.23E-08	1.611E-01
1	1	1	1	1	0.454	1.079	0.423	1.853	0.798	4.21E-08	1.609E-01
5	5	5	5	5	0.452	1.101	0.231	2.736	4.798	4.11E-08	1.602E-01
0.5	1	5	1	0.5	0.443	1.051	4.930	1.574	0.500	4.21E-08	1.610E-01
1	5	0.5	5	1	0.450	1.074	0.810	1.974	1.586	4.19E-08	1.606E-01
5	0.5	1	0.5	5	0.455	1.080	1.328	1.644	0.277	4.21E-08	1.610E-01
0.05	0.05	0.05	0.05	0.05	0.451	1.115	0.588	0.004	0.001	4.04E-08	1.702E-01
10	10	10	10	10	8.141	19.853	10.589	3.273	8.620	4.10E-08	2.446E-01
50	50	50	50	50	49.598	121.217	89.864	0.026	10.696	4.09E-08	2.518E-01
0.05	10	50	10	0.05	0.450	1.066	0.001	1.769	0.264	4.22E-08	1.610E-01
10	50	0.05	50	10	9.219	22.389	0.001	0.001	0.000	4.12E-08	2.571E-01
50	0.05	10	0.05	50	0.447	1.058	24.626	0.511	0.002	4.23E-08	1.610E-01
original values					0.450	1.100	1.623	1.000	4.800	4.09E-08	

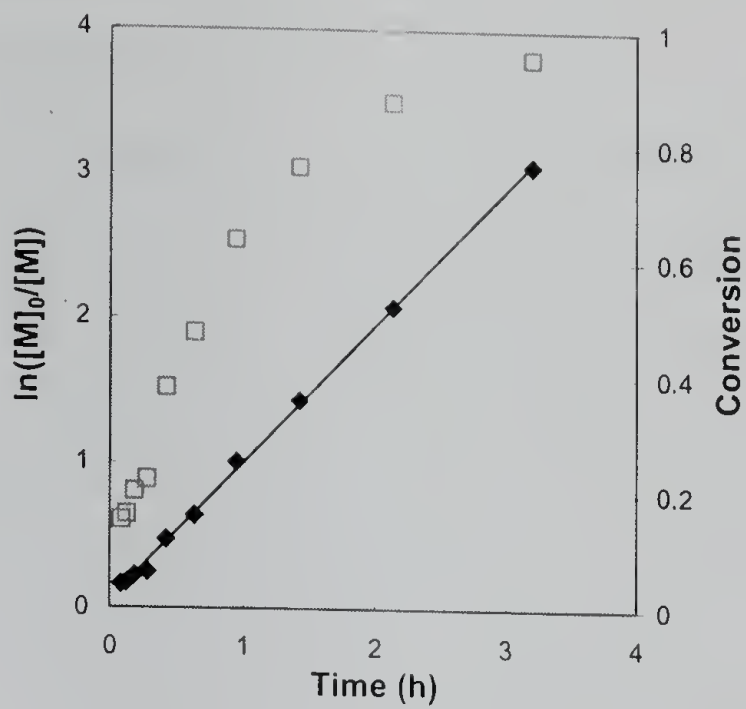


Figure 2.11 Simulated data of $\ln([M]_0/[M])$ (◆) and conversion (□) vs time based on our new model using the same conditions in Table 1 except $k_{tc} = 0$.

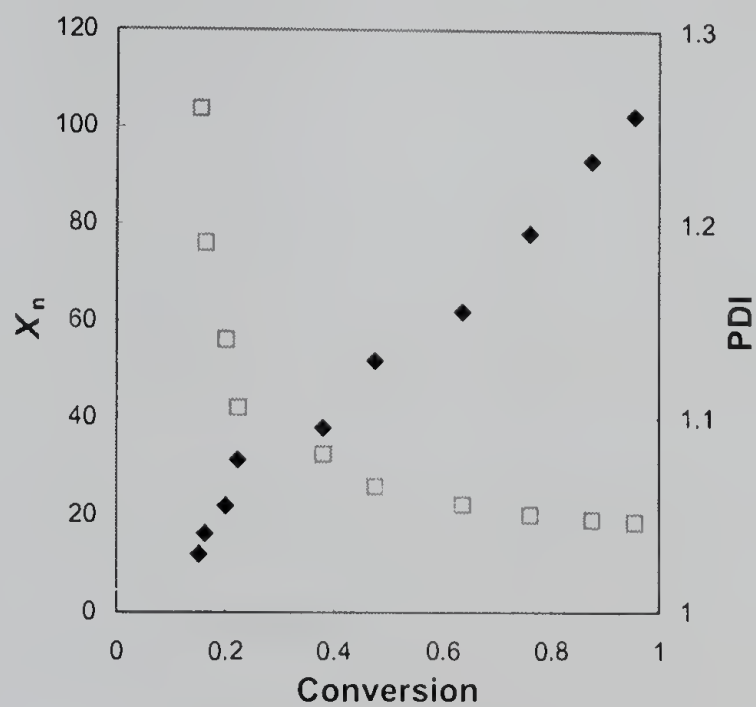


Figure 2.12 Number average degree of polymerization (X_n , ◆) and polydispersity (PDI, □) simulated based on our new model using the same condition in Table 1 except $k_{tc} = 0$.

2.4 Application to Experimental Data

2.4.1 Application to Available Literature Data

As we have seen in the previous section, the parameter estimation approach is a promising method to determine K_{eq} ATRP. Before applying the algorithm to the real data, it was firstly applied to the literature data. Most of the available literature data is on polymerization rather than ATRA reactions. Matyjaszewski, *et al.* tried to determine the chain end degradation rate constants.¹³ These side reactions are negligible in polymerization, but become meaningful at high conversion where the rate of polymerization is slow. To determine these side reaction rate constants, they used special reaction conditions (Table 2.10).

Table 2.10 Reaction Conditions Used to Determine Chain End Degradation Rate Constants by Matyjaszewski, *et al.*¹³

	Experiment A	Experiment B	Experiment C
$[IX]_0$ (M)	2.0×10^{-1}	2.0×10^{-1}	2.0×10^{-1}
$[M]_0$ (M)	0	0	0
$[Mt^nY/L]_0$ (M)	5.0×10^{-2}	5.0×10^{-2}	0
$[XMt^{n+1}Y/L]_0$ (M)	0	3.0×10^{-2}	3.0×10^{-2}

We used these same reaction data to determine the kinetic parameters in ATRP. As explained by Matyjaszewski, the only possible reaction under conditions of C is the degradation reaction of 1-phenylethyl bromide (IX) to form styrene (M) and HBr. Because there is no source of low oxidation state metal complexes, the activation reaction and the following propagation reaction cannot take place. Therefore, for this reaction

condition, the parameter estimation algorithm was not affected by the values of the other reaction parameters initially used, and it gave a highly converging value of the side reaction rate constant, k_b . This value was very close to the Matyjaszewski's result. The only difference between our model and the literature was that our model included the thermal initiation reaction resulting from the dimerization of styrene monomers. However, the thermal initiation reaction was of minimal consequence, and did not affect the value of k_b .

Table 2.11 Result of Parameter Estimation Using Literature Data

	k_{act}	k_{deact}	k_a	k_{therm}	K_{eq}	Φ
this work	5.78E-01	3.90E+06	6.62E+00	1.93E-09	1.481E-07	1.058E-01
literature	4.50E-01	1.10E+07	1.00E+04		4.091E-08	

From the data collected under conditions A and B, we determined the other rate constants using our parameter estimation algorithm (Table 2.11). The calculated values showed some differences from the literature values. These discrepancies could be explained in several ways. The first is on our assumption that the rate constants are constant throughout the polymerization. Our model was developed based on this assumption, and it certainly may not be entirely true. The other possibility is the assumptions made when determining the literature values. In order to calculate rate constants, Matyjaszewski made several assumptions such as constant values of $[Mt^n]$ and $[Mt^{n+1}]$, fast pre-equilibrium, and exclusion of side reactions including the termination reaction, all of which are not true in actuality. For an example, k_{deact} was calculated from the k_{act} , which was measured using a direct method, and the K_{eq} , which was determined

from the slope of linear first-order kinetic plot of monomer conversion in polymerization. The K_{eq} was measured under different conditions to k_{act} , with Mt^{n+1} ($= Cu^{II}X_2$) added at the beginning of the reaction so as to keep $[Cu^{II}X_2]$ constant.²² However, EPR data showed that this is not the case, and $[Cu^{II}X_2]$ does increase slightly.²⁰ This would lead to an underestimation of K_{eq} and thus an overestimation of k_{deact} . Figure 2.13 is the plot of simulated data using estimated rate constants. The simulation matches the real experimental data using the reaction condition in Table 2.10 with excellent accuracy. The polymerization results also plotted in Figure 2.14. The experimental data was taken from the literature.²² Among the two simulations, the one using newly estimated rate constants by the parameter estimation algorithm shows better agreement with the experimental data than the other using literature values of rate constants.

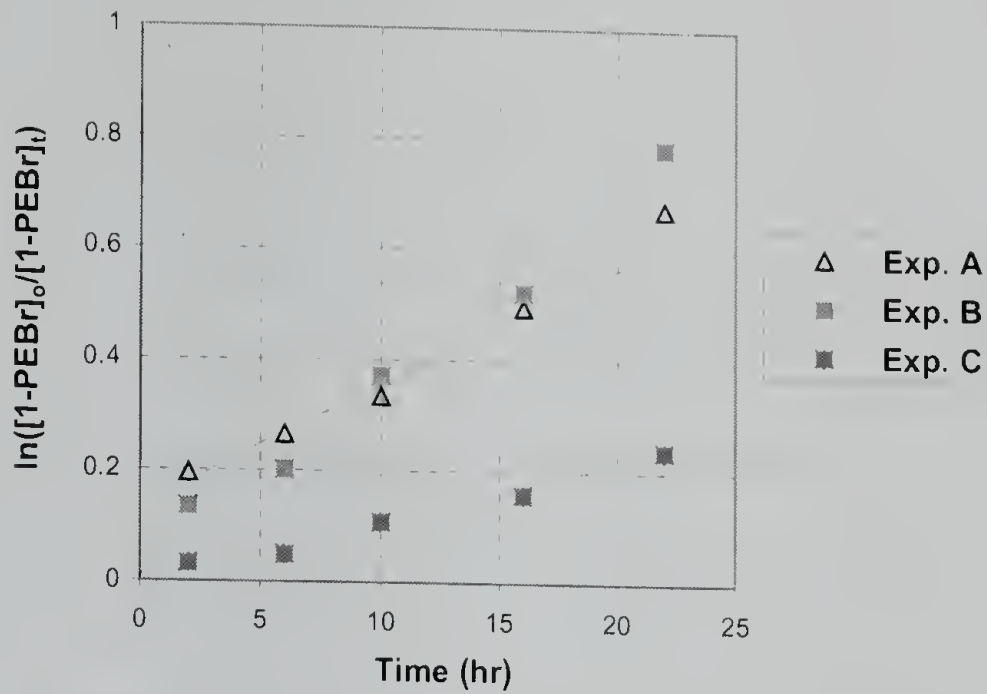


Figure 2.13 First-order kinetic plot of 1-phenylethyl bromide (1-PEBr) consumption in the ATRA of styrene; experimental data (points) and simulation with estimated kinetic parameters (lines).

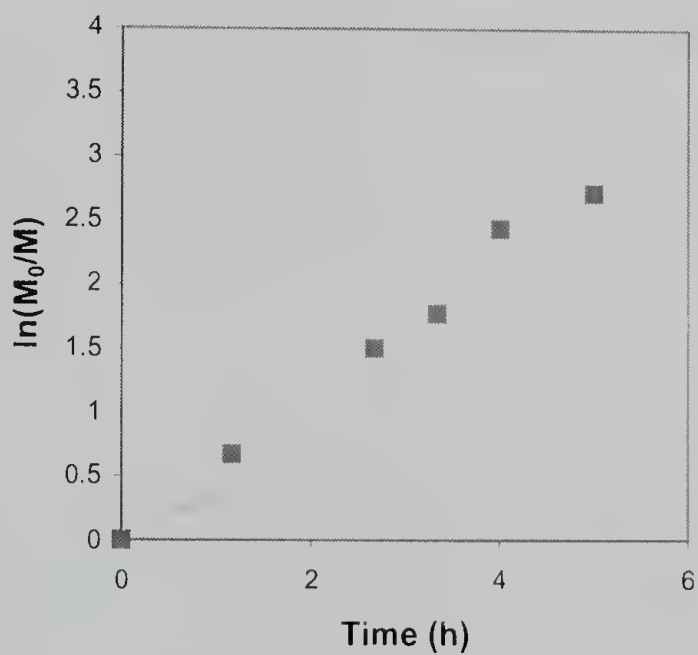


Figure 2.14 First-order kinetic plot of monomer consumption in the ATRP of styrene; experimental data (points) and simulation (lines; ---, with the literature values of kinetic parameters and —, with estimated kinetic parameters using our method).

2.4.2 Data Collection

To apply the parameter estimation algorithm to real systems, we had to find a suitable characterization method to measure the observable variables. The characterization method should be easy, fast, and because the model deals with small molecular components, it should be very sensitive to achieve sufficient resolution on as many of the different components possible. Many characterization methods were tested. NMR is one of the most widely used techniques for kinetic studies, and Matyjaszewski, *et al.* used ^1H -NMR in his study to determine chain end degradation rate constants. It is simple, fast, and sensitive for some specific components such as the vinyl proton of styrene monomer. However, some other components share similar characteristic chemical shifts, which makes it hard to distinguish them from each other. For example, the benzylic proton of 1-phenylethyl bromide has same chemical shift with the benzylic protons of the dimer and higher oligomers. In some catalyst systems, the ligand molecules may have similar chemical shifts with other reaction components. Therefore, the metal complexes should be removed before the characterization to get more reliable data. We also tried ^{13}C -NMR, however, it required very long data acquisition time for a single run, and the problems of metal complex removal and the discrimination of each component were not completely solved.

Because of the similarity in structure of the reaction components, spectroscopic techniques were found to be not suitable as characterization methods for our system. Chromatographic techniques were the next choice. Among them, GPC was not good enough because of the poor resolution of the components even when multiple 100 Å columns were employed. HPLC is very good technique to resolve small molecular

chemicals, and it gave fairly promising results on some test runs of our reaction system. One exception was the overlap of the peaks for styrene and 1-phenylethyl bromide. However, the development of suitable method of HPLC to achieve full resolution of components is a time-consuming job. Metal complexes also have to be removed before running so as not to contaminate the HPLC columns. Our method of choice turned out to be gas chromatography (GC). GC is simple, fast, and highly sensitive characterization method, and doesn't require any pre-treatment of the sample such as removal of the metal catalysts. If GC having a mass detector (GC-MS) is used, it is easy to identify each peak. The method development for GC is also relatively simple, and quantitative analysis can be done using internal standard without previous calibration. Due to its excellent sensitivity, there is the possibility of detecting many different reaction components that would help to increase the reliability of the parameter estimation algorithm (Figure 2.15).

For the peak identification in the GC spectrum using an FID detector, model compounds were prepared by separate syntheses. We synthesized the dimeric compounds by the atom transfer-propagation reaction (M_2X) and by the combinational termination reaction between initiator radicals (M_2b). Fortunately, the synthetic routes to these dimers were straightforward. Scheme 2.6 and 2.7 show the synthetic method of dimeric components for styrene and methyl methacrylate respectively.

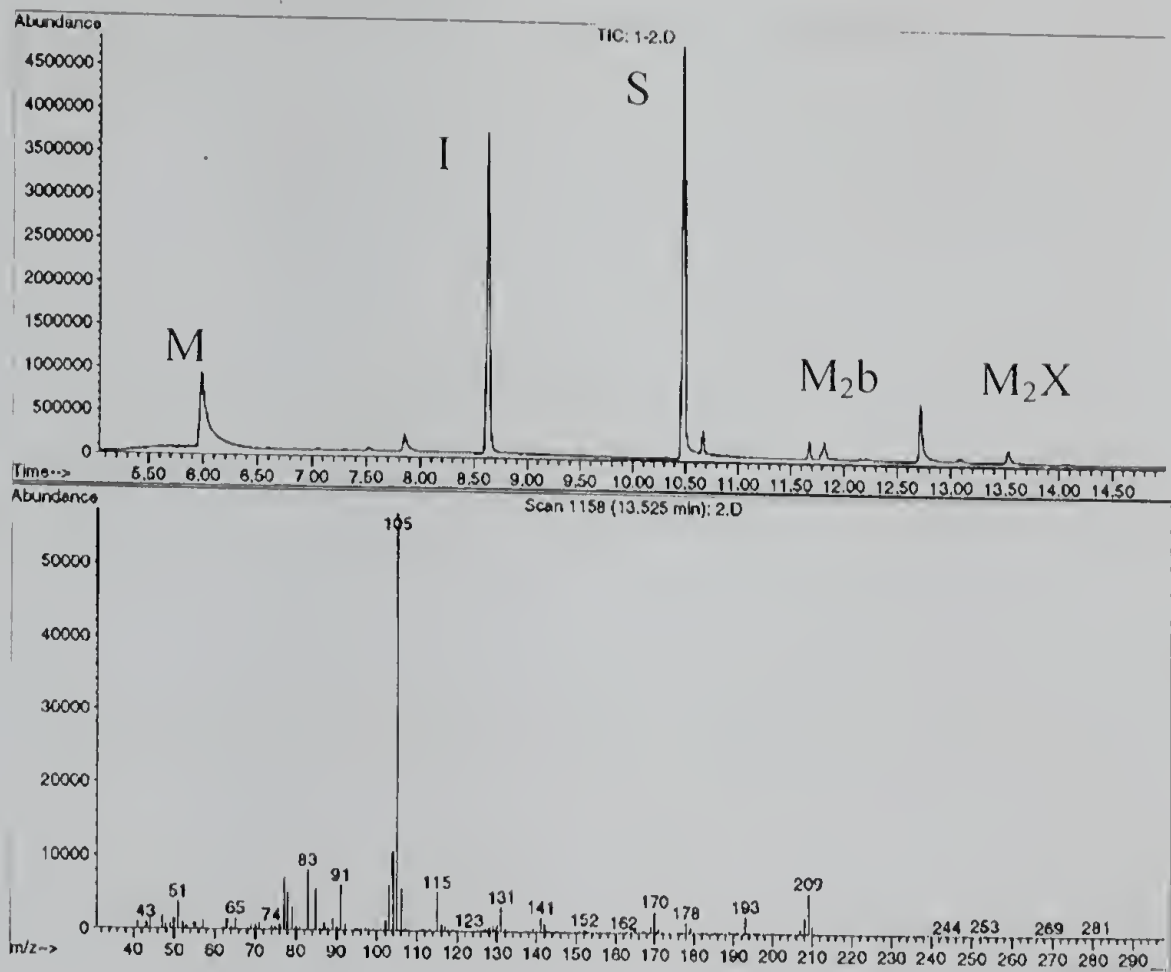
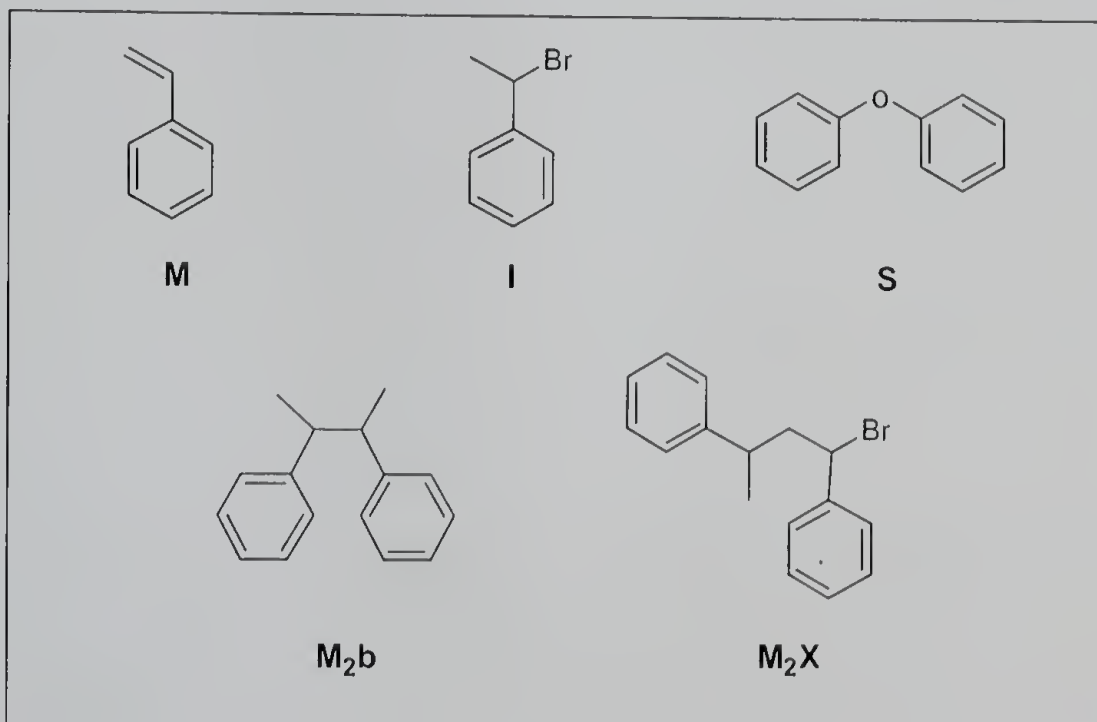
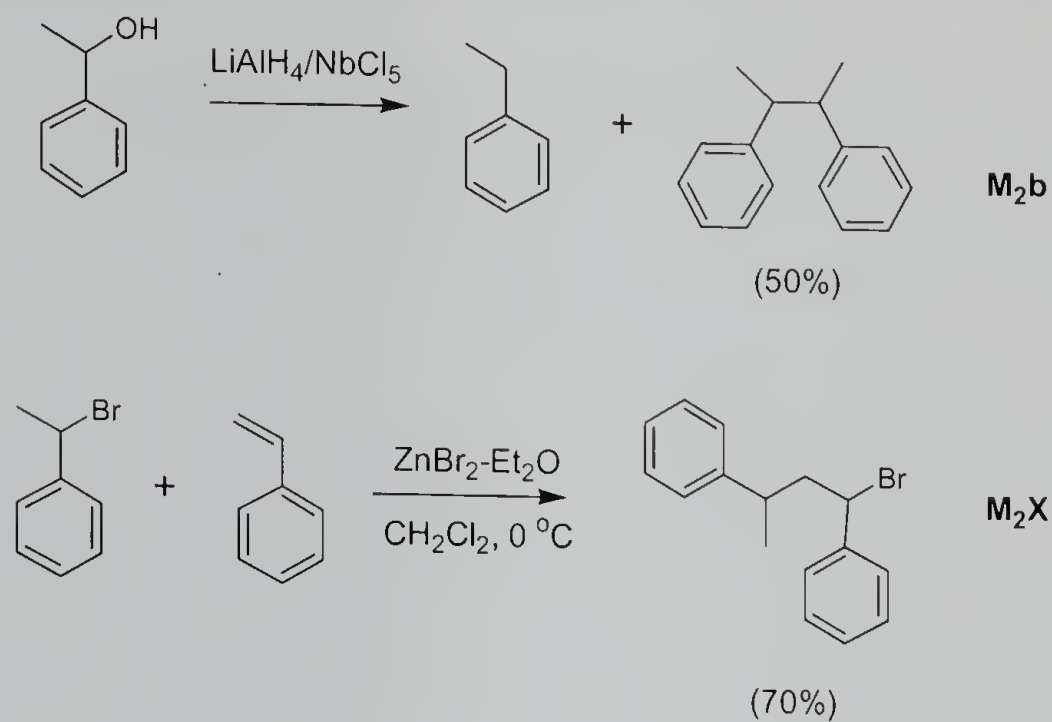


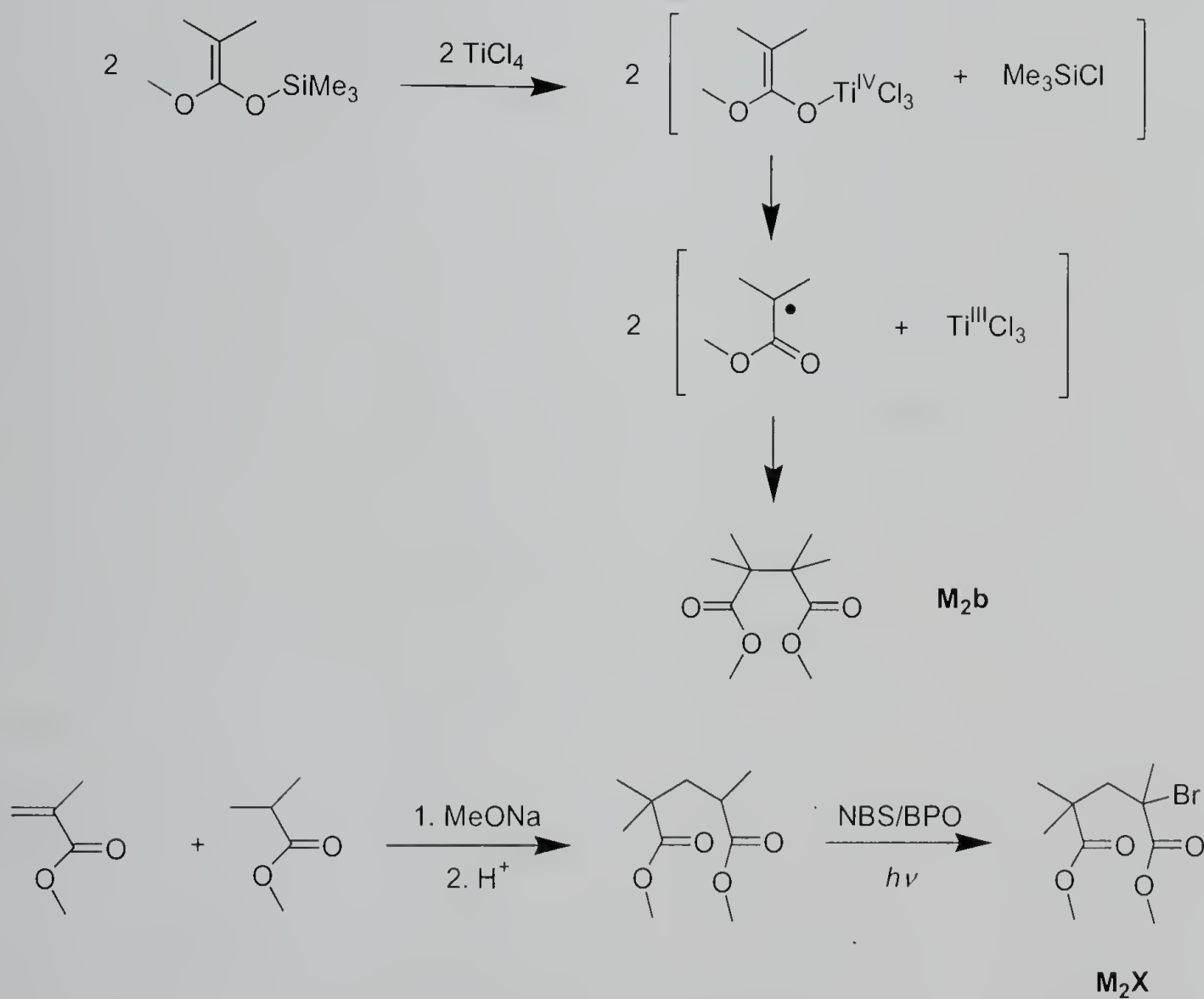
Figure 2.15 GC-MS spectrum of a typical reaction mixture of styrene ATRA.



Scheme 2.6 Preparation of Model Compounds in ATRA of Styrene



Scheme 2.7 Preparation of Model Compounds in ATRA of MMA



2.4.3 Determination of Kinetic Constants in ATRP for Various Polymerization Systems

Next we demonstrated the application of the parameter estimation approach to several atom transfer reaction systems in order to determine important kinetic rate constants of the reactions. The system include the atom transfer reactions of styrene and MMA using $\text{FeBr}_2/\text{PnBu}_3$ and $\text{RuCl}_2(\text{PPh}_3)_3/\text{Al}(\text{O-}i\text{Pr})_3$ as catalysts. Table 2.12-2.16 show the results of parameter estimations. For all cases, convergence to the global minima was not achieved from any initial guesses. Instead, by combining the first strategy to find the global minimum, picking the most extreme among the many local minima starting from widely varying initial values of the parameters chosen quasi-randomly, we determined the values of the kinetic parameters. Moreover, in most cases, we could observe some level of convergence to the values of the kinetic parameter at those points. Figure 2.16-2.19 shows the experimental data and the simulations using the estimated kinetic parameters of the convolution of various components over reaction time in the atom transfer reactions. The simulation results matched well with the experimental data. Using these estimated kinetic parameters, we also simulated the first order kinetic plots of monomer conversion as a function of time for the polymerization of styrene using $\text{FeBr}_2/\text{PnBu}_3$ catalyst, and compared with the literature values of the real experimental data (Figure 2.20).²³ The simulation and the experimental data show the excellent agreement, with a deviation at the higher conversion. These results demonstrate that the kinetic rate constants of ATRA or ATRP could be successfully determined by our parameter estimation approaches.

Table 2.12 Estimation of Kinetic Parameters in the ATRA of Styrene Using FeBr₂/PnBu₃ Catalyst System

initial guesses					estimated parameters						Φ
k_{act}	k_{deact}	k_a	k_b	k_{therm}	k_{act}	k_{deact}	k_a	k_b	k_{therm}	K_{eq}	
0.5	0.5	0.5	0.5	0.5	3.60E-3	3.21E-3	2.76E+0	1.34E-1	3.32E-2	1.121E-7	2.558E+0
1	1	1	1	1	3.62E-3	3.29E-3	2.68E+0	3.74E-2	1.70E-3	1.102E-7	2.562E+0
5	5	5	5	5	3.47E-3	6.43E-3	1.04E-3	1.11E+1	1.04E-3	5.397E-8	2.416E+0
0.5	1	5	1	0.5	6.67E-2	1.53E+0	1.04E+1	2.51E+0	2.46E-2	4.370E-9	3.695E+0
1	5	0.5	5	1	5.09E-1	1.41E+1	2.53E-3	7.45E+1	4.22E-2	3.624E-9	3.565E+0
5	0.5	1	0.5	5	3.45E-3	6.46E-3	1.25E-3	1.12E+1	4.81E-4	5.346E-8	2.416E+0

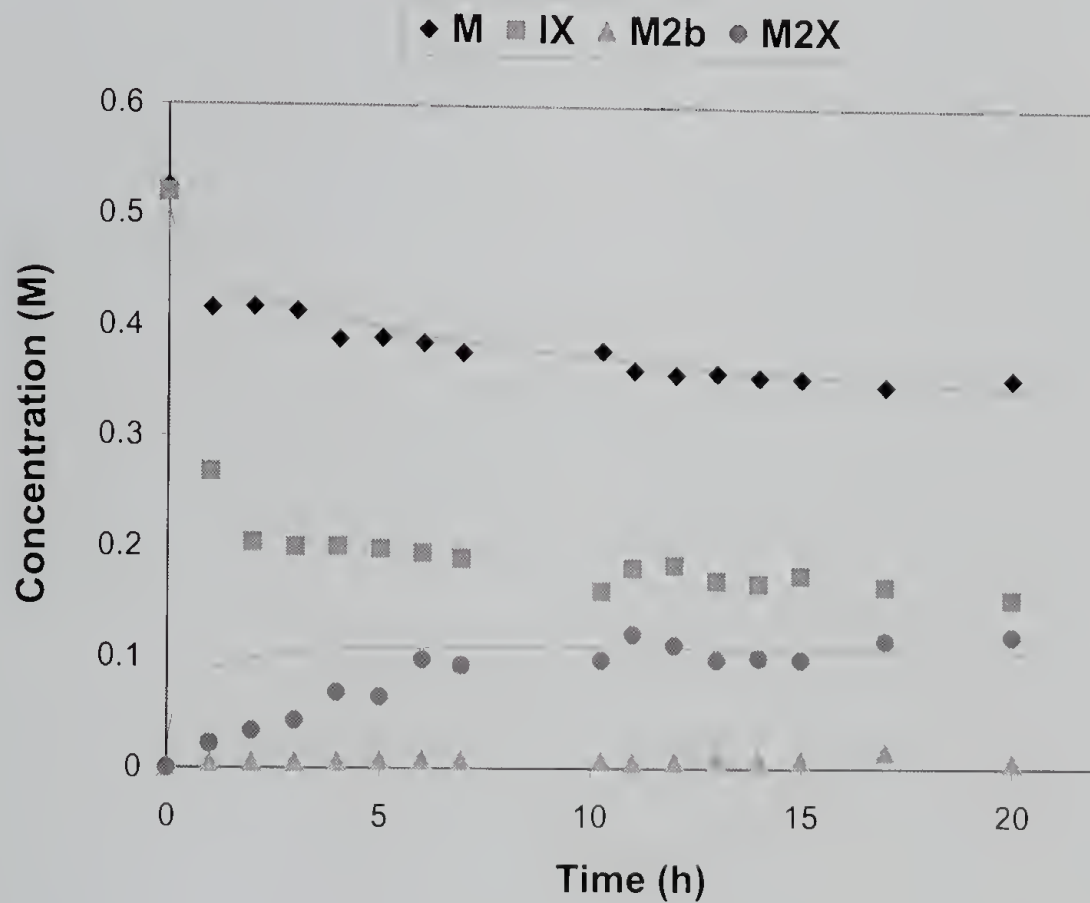


Figure 2.16 Convolution of various components over reaction time in the ATRA of styrene using FeBr₂/PnBu₃ catalyst system. Points (experimental data), lines (simulation with the estimated kinetic parameters).

Table 2.13 Estimation of Kinetic Parameters in the ATRA of Styrene Using $\text{RuCl}_2(\text{PPh}_3)_3/\text{Al}(\text{O-}i\text{Pr})_3$ Catalyst System

initial guesses					estimated parameters							Φ
k_{act}	k_{deact}	k_a	k_b	k_{therm}	k_{act}	k_{deact}	k_a	k_b	k_{therm}	K_{eq}		
0.5	0.5	0.5	0.5	0.5	1.08E+0	2.62E-1	1.89E-5	4.00E+0	1.07E-3	4.12E-7	4.77E-1	
1	1	1	1	1	2.19E+0	5.35E-1	1.10E-3	3.96E+0	2.76E-1	4.09E-7	4.76E-1	
5	5	5	5	5	1.24E+0	7.31E+0	1.62E-4	1.32E+1	4.62E+0	1.70E-8	5.36E-1	
0.5	1	5	1	0.5	3.47E+0	2.05E+1	9.72E-4	1.31E+1	1.03E-3	1.69E-8	5.36E-1	
1	5	0.5	5	1	1.76E+0	1.03E+1	2.04E-3	1.31E+1	3.36E+0	1.70E-8	5.36E-1	
5	0.5	1	0.5	5	7.91E+0	1.94E+0	6.71E-4	3.93E+0	4.87E+1	4.07E-7	4.75E-1	

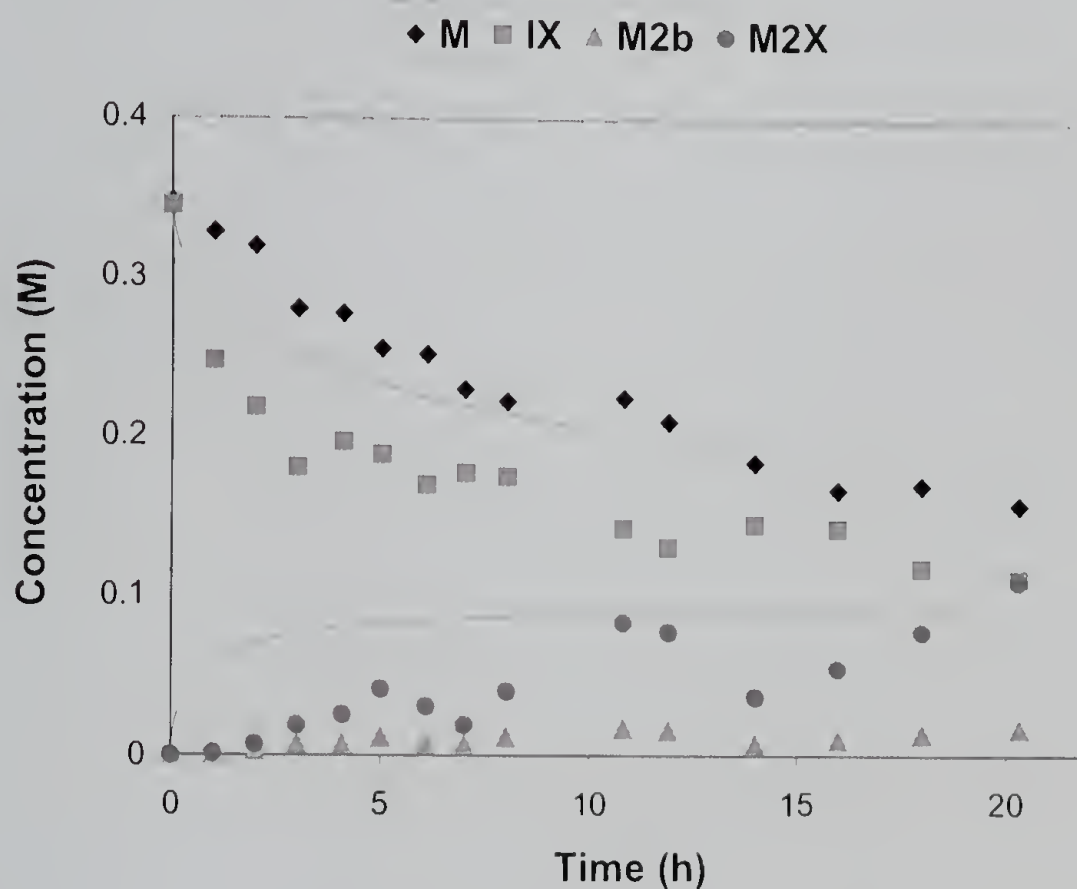


Figure 2.17 Convolution of various components over reaction time in the ATRA of styrene using $\text{RuCl}_2(\text{PPh}_3)_3/\text{Al}(\text{O-}i\text{Pr})_3$ catalyst system. Points (experimental data), lines (simulation with the estimated kinetic parameters).

Table 2.14 Estimation of Kinetic Parameters in the ATRA of MMA Using FeBr₂/PnBu₃ Catalyst System

initial guesses					estimated parameters						Φ
k_{act}	k_{deact}	k_a	k_b	k_{therm}	k_{act}	k_{deact}	k_a	k_b	k_{therm}	K_{eq}	
0.5	0.5	0.5	0.5	0.5	5.33E-3	5.86E-4	3.68E-1	5.12E-5	7.14E-4	9.094E-7	1.013E+0
1	1	1	1	1	4.83E+0	6.31E-1	1.51E-3	1.24E-3	1.25E+0	7.651E-7	2.753E+0
5	5	5	5	5	2.69E+1	4.55E+0	4.77E-1	1.58E-3	8.16E+0	5.908E-7	2.661E+0
0.5	1	5	1	0.5	5.52E-3	6.04E-4	3.65E-1	1.02E-3	1.58E+1	9.132E-7	1.013E+0
1	5	0.5	5	1	3.38E+0	5.65E-1	4.63E-1	1.50E-3	1.86E+0	5.980E-7	2.645E+0
5	0.5	1	0.5	5	6.11E+0	1.01E+0	4.52E-1	1.02E-5	6.28E+0	6.052E-7	2.652E+0

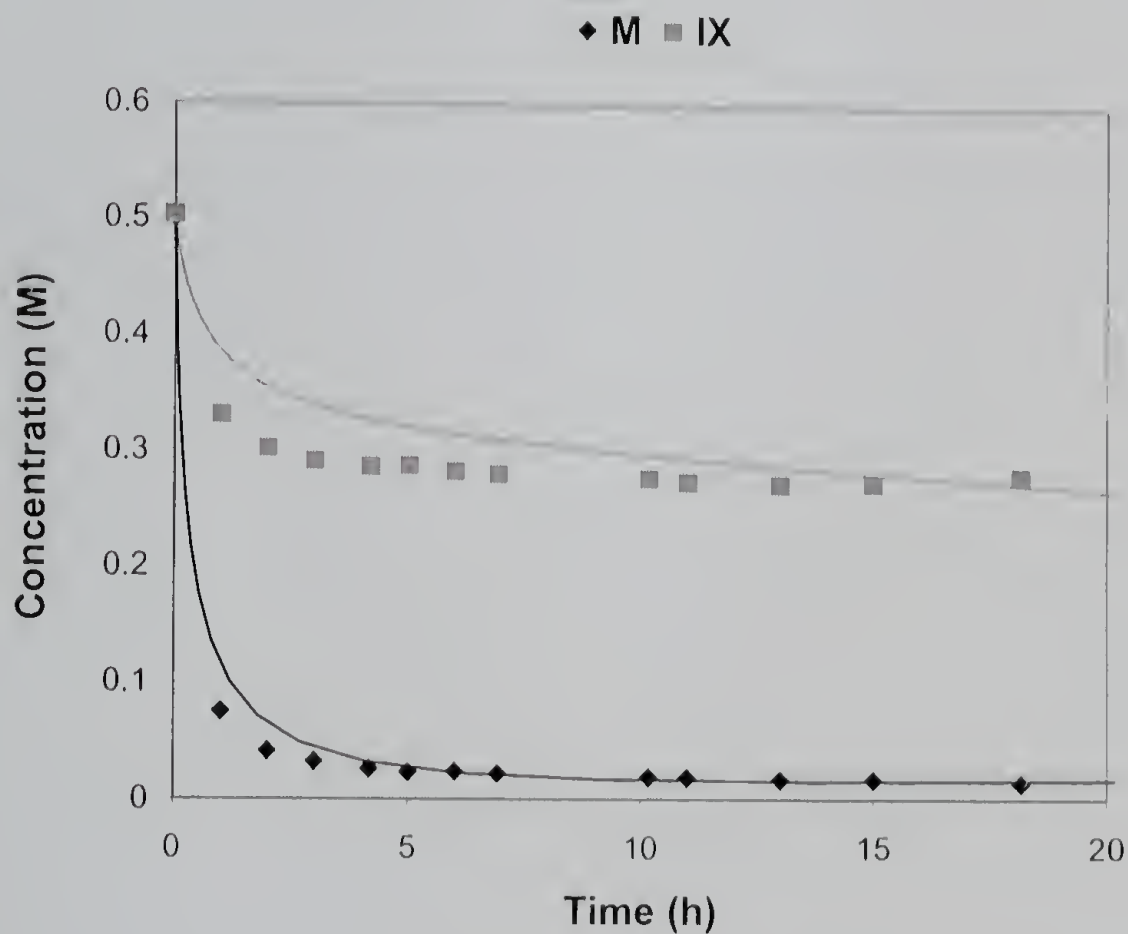


Figure 2.18 Convolution of various components over reaction time in the ATRA of MMA using FeBr₂/PnBu₃ catalyst system. Points (experimental data), lines (simulation with the estimated kinetic parameters).

Table 2.15 Estimation of Kinetic Parameters in the ATRA of MMA Using $\text{RuCl}_2(\text{PPh}_3)_3/\text{Al}(\text{O-}i\text{Pr})_3$ Catalyst System

initial guesses					estimated parameters							Φ
k_{act}	k_{deact}	k_a	k_b	k_{therm}	k_{act}	k_{deact}	k_a	k_b	k_{therm}	K_{eq}		
0.5	0.5	0.5	0.5	0.5	9.63E+1	8.16E+4	1.16E+2	3.18E+2	9.46E+4	1.180E-10	2.556E-1	
1	1	1	1	1	1.38E-2	9.64E-1	2.19E+1	7.94E-4	5.42E-1	1.435E-9	2.975E-1	
5	5	5	5	5	1.62E-2	1.13E+0	2.15E+1	1.05E-3	3.30E+1	1.426E-9	2.976E-1	
0.5	1	5	1	0.5	8.78E-2	6.30E+0	1.98E+1	1.18E-2	3.19E-1	1.394E-9	3.022E-1	
1	5	0.5	5	1	7.76E-1	5.58E+1	1.94E+1	1.03E-3	6.77E-3	1.392E-9	3.038E-1	
5	0.5	1	0.5	5	6.54E+0	7.70E-2	2.14E-1	9.73E-4	4.09E+1	8.494E-6	1.246E+0	

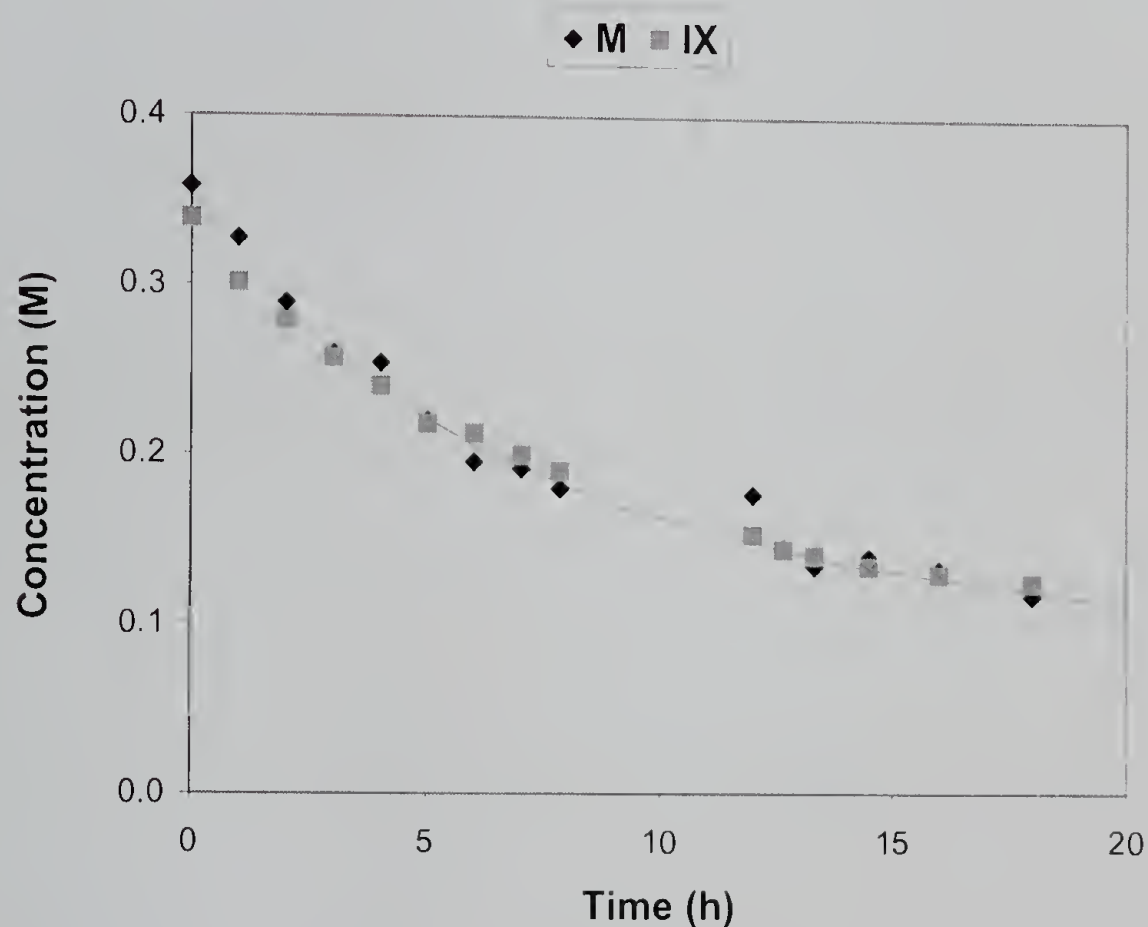


Figure 2.19 Convolution of various components over reaction time in the ATRA of MMA using $\text{RuCl}_2(\text{PPh}_3)_3/\text{Al}(\text{O-}i\text{Pr})_3$ catalyst system. Points (experimental data), lines (simulation with the estimated kinetic parameters).

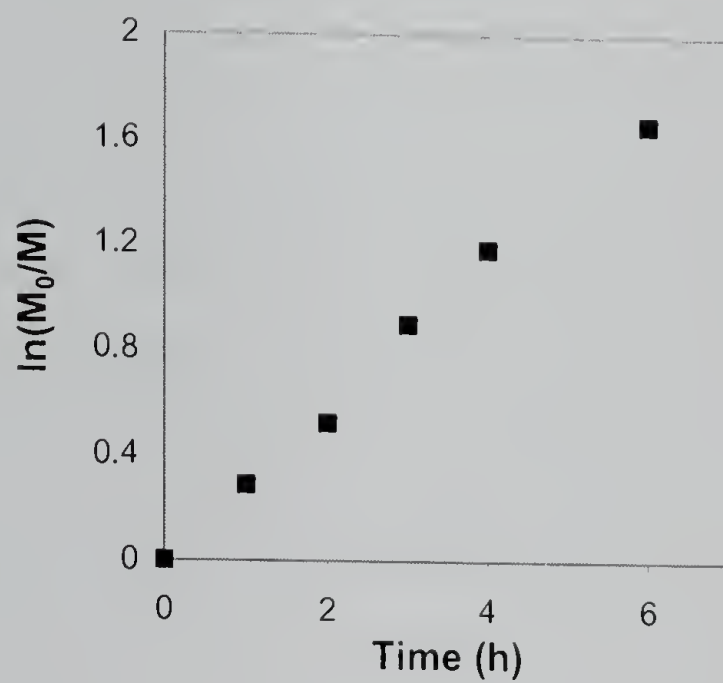


Figure 2.20 First-order kinetic plot of monomer consumption in the ATRP of styrene using $\text{FeBr}_2/\text{PnBu}_3$ catalyst. Experimental data (points) and simulation with the estimated rate constants by parameter estimation approach (line).

2.5 Conclusion

In this work, we report a new method to evaluate various catalyst systems by determining kinetic parameters of polymerization. We established the model reactions of ATRP including not only the atom transfer reaction and propagation reaction, but also other possible side reactions such as termination reaction, thermal initiation reaction, and chain degradation reactions. Simulations using this model show the good agreements with the other simulation results by Fisher and Matyjaszewski, and also agree well with the experimental data. Based on this model, we used a nonlinear regression method to get the important rate constants from atom transfer radical addition reactions. From the test the parameter estimation algorithm using the fabricated experimental data points that were generated by using literature rate constants, we found that it is possible to estimate equilibrium constant of atom transfer reaction. It was also found that the each value of activation rate constant and deactivation reaction constant is hard to be determined ubiquitously because the sensitivities of them are not high enough and there is a possibility of being trapped in the local minimum before reaching the global minimum. By applying downhill simplex method as a second minimization algorithm, the parameter estimation algorithm achieves higher propensity to reach global minimum, yet not all the time. The simulation results using kinetic rate constants determined by parameter estimation algorithm shows better agreement with the experimental data than that using literature values of rate constants. This is because the current method uses fewer assumptions than other literature methods in determining rate constants. We also demonstrated the determination of kinetic constants in the polymerization of styrene and MMA using various metal catalysts, and the simulations using these kinetic constants agree well with the experimental data.

2.6 Experimental

2.6.1 Materials and Characterizations

IR spectra were determined with either a Perkin-Elmer 1600 series FTIR or a Jasco FT/IR-410 spectrometer as thin films coated on NaCl plates. ^1H and ^{13}C NMR spectra were measured in CDCl_3 unless otherwise noted. Spectra were recorded on either a Varian 200, Bruker 200, 300, or GE 300 spectrometer. ^1H NMR spectra were measured at 200 or 300 MHz. Proton decoupled ^{13}C NMR spectra were recorded at 75 MHz. ^1H chemical shift (δ) were referenced to a selected resonance of residual protons in the solvent employed. ^{13}C chemical shift (δ) were referenced to the carbon resonance of the solvent employed. Gel permeation chromatography/light scattering (GPC/LS) were performed using Hewlett-Packard (HP) 1050 series liquid chromatography pump equipped with a Wyatt Dawn DSP-F laser photometer, a Wyatt/Optilab interferometer and a Waters 746 data module integrator. Tetrahydrofuran (THF) was used as the mobile phase. Samples were prepared as 0.5 - 2% (w/v) solution in THF and passed through 0.45 μm filters prior to injection. Residual metal complexes were removed by passing the polymer solution through active alumina column. Separations were effected by a multiple series of Polymer laboratory Mixed C columns and 100 Å Waters Ultrastyrigel columns in series at a flow rate of 1 mL/min at 25 °C. High performance liquid chromatography (HPLC) was performed using a Hewlett-Packard (HP) 1050 series liquid chromatography pump equipped with a HP model 1047 refractive index detector and a Waters 746 data module integrator. Separations were effected by a reverse phase non-polar Nucleosil C18 column using acetonitrile/water (3/1) mixture as the mobile phase. Residual metal complexes were removed by passing the polymer solution through active alumina column

before analysis. Gas chromatography (GC) was performed using either a HP 5890 equipped with MS detector, or a HP 6890 with a FID detector. Non-polar HP-5 or medium polar HP-INNOWAX capillary column were used for the separation. The sample was diluted in diethyl ether, THF, or methylene chloride, and directly injected into GC without any further purification.

Materials were obtained from commercial suppliers and used without further purification, unless otherwise noted. Styrene and MMA were dried over CaH_2 overnight, and distilled twice under reduced pressure from CaH_2 prior to use. 1-Phenylethyl bromide (1-PEBr) and methyl α -bromoisobutyrate (MIB-Br) were purchased from Aldrich Chemical and distilled twice under reduced pressure prior to use.

2.6.2 Preparation of Model Compounds

2,3-Diphenylbutane (St-M₂b). A solution of sodium aluminum hydride in THF (1.0 M, 12 mL) was added to a solution of niobium chloride (3.24 g, 12 mmol) in benzene-THF (40:1, 60 mL) at 0 °C under an argon atmosphere. Instantaneously, black suspension was formed with gas evolution. After 10 min, a solution of 1-phenyl ethanol (1.22 g, 10 mmol) in benzene (20 mL) was added dropwise and the resulting mixture was stirred at 80 °C for 30 min. The mixture was diluted with 120 mL of diethyl ether and treated with 3 mL of 15 % sodium hydroxide solution and anhydrous magnesium sulfate. The mixture was filtered through Celite 521 and remaining solid was washed repeatedly with diethyl ether. The filtrate and washings were mixed and washed with 1 N HCl, brine, and water. Purification by column chromatography using hexane as an eluent afforded

2,3-diphenylbutane in 60 % yield. $^1\text{H NMR}$ (CDCl_3): δ (ppm) 7.05-7.40 (m, 10H), 2.66-2.97 (m, 2H), 1.02 (d, 6H); MS (EI): m/z 210 (M^+), 178, 115, 105, 91, 77.

1-Bromo-1,3-diphenylbutane (St-M₂X). ZnBr_2 (6.67 g) was dissolved in 8 mL of diethyl ether. This solution was then diluted with 60 mL of methylene chloride at -78°C . To this solution a solution of 1-phenylethyl bromide (7.40 g, 40 mmol) in 20 mL of methylene chloride and a solution of styrene (4.17 g, 40 mmol) in 20 mL of methylene chloride were added. The mixture was allowed to warm to 0°C and after 10 h washed with aqueous ammonia. The organic layer was dried with magnesium sulfate, filtered, and evaporated to remove methylene chloride. Distillation under reduced pressure afforded 1-bromo-1,3-diphenylbutane. $^1\text{H NMR}$ (CDCl_3): δ ppm. MS (EI): m/z 289 (M^+), 115, 105, 91, 77.

Dimethyl tetramethylsuccinate (MMA-M₂b). To 5 g (28.7 mmol) of dimethylketene methyl trimethyl silyl acetal dissolved in a 28.7 mL of methylene chloride, 28.7 mL of 1 M solution of titanium tetrachloride in methylene chloride was added dropwise at room temperature. The mixture was stirred for 1 h at room temperature, and the resulting dark brown solution was poured into ice-water. The organic layer was separated, washed with water, dried over magnesium sulfate, and distilled under reduced pressure ($56\text{-}59^\circ\text{C}/100\text{mTorr}$) to afford 1.3 g (45 %) of dimethyl tetramethylsuccinate. IR (neat): 1727 cm^{-1} ; $^1\text{H NMR}$ (CDCl_3): δ (ppm) 3.89 (m, 6H), 1.47 (s, 12H); MS (EI): m/z 202 (M^+), 187.

2,4,4-Trimethylpentanedioic acid dimethyl ester. A 250 mL of 3-neck round bottom flask equipped with reflux condenser and Ar gas flow was charged with 75 mL (660 mmol) of methyl isobutyrate, 7.1 mL (66 mmol) of methyl methacrylate, 1.1884 g (22 mmol) of sodium methoxide, and 30 mL of isopropyl alcohol. The mixture was refluxed for 4 h under a steady flow of Ar, and cooled to room temperature. To this solution was added 13.1 N HCl. The organic layer was then extracted with methylene chloride, and dried over magnesium sulfate. After removing solvent by rotavap, distillation under reduced pressure afforded ~4 g of 2,4,4-trimethylpentanedioic acid dimethyl ester as a brown oil. The product was characterized and found to be not completely pure, but it was used in the next step without further purification. IR (neat): 1740, 1450, 1300, 1255, 1190, 1160, 1140 cm^{-1} . ^1H NMR (CDCl_3): δ (ppm) 3.62 (s, 6H), 2.48(ddq, 1H), 2.07 (dd, 1H), 1.63 (dd, 1H), 1.18 (s, 3H), 1.15 (s, 3H), 1.14 (s, 3H); MS (EI): m/z 203 (M^+), 171, 143.

2-Bromo-2,4,4-trimethylpentanedioic acid dimethyl ester (MMA-M₂X). A 100 mL of round-bottomed flask equipped with a magnetic stirr bar was charged with a heterogeneous mixture of 4 g of crude 2,4,4-trimethylpentanedioic acid dimethyl ester, 4 g of N-bromosuccinimide, 0.2 g of benzoyl peroxide, and 32 mL of carbon tetrachloride. The mixture was irradiated with UV light at 30 °C for 4 h. After reaction, the mixture was filtered, and evaporated under reduced pressure to give a sticky solid. This product was recrystallized several times from ethyl alcohol to afford 2-bromo-2,4,4-trimethylpentane-dioic acid dimethyl ester. IR (neat): 1730 cm^{-1} . ^1H NMR (CDCl_3): δ

(ppm) 3.78 (s, 3H), 3.68 (s, 3H), 2.78 (s, 2H), 1.90 (s, 3H), 1.23 (s, 3H), 1.08 (s, 3H); MS (EI): m/z 286 (M^+), 284, 254, 251, 226, 224, 204, 172, 144, 112, 103.

2.6.3 Kinetic study

2.6.3.1 ATRA of styrene

Iron(II) bromide / tri-*n*-butyl phosphine ($FeBr_2 / PnBu_3$) catalyst system. To a 25 mL Schlenk flask equipped with a magnetic stir bar was charged with 0.37 g of 1-PEBr (0.5 M), 0.21 g of styrene (0.5 M), 43 mg of $FeBr_2$ (0.05 M), 0.15 mL of $PnBu_3$ (0.15 M), 29 mg of decane (0.05 M), 3.4 mg of diphenylether (5×10^{-3} M), and 3.3 mL of toluene under inert atmosphere. A small portion of the mixture was diluted with THF in a scintillation vial. After removed from the drybox, the reaction flask was put in an oil bath thermostated at 110 °C. Just before heating a portion of the initial mixture in the vial was directly injected to GC to measure the concentration of each component. At appropriate time intervals, small aliquots were removed from the reaction mixture, and placed in liquid nitrogen to stop the reaction. The quenched THF solution was characterized with GC without further purification. The peaks were identified using model compounds in separate runs. The concentrations of styrene and 1-PEBr were calculated using decane as an internal standard, and the concentration of M_2b and M_2X were calculated using diphenylether as an internal standard.

Tris(triphenylphosphine)ruthenium(II) dichloride / aluminum tri(isopropoxide) ($RuCl_2(PPh_3)_3 / Al(O-iPr)_3$) catalyst system. A 25 mL Schlenk flask equipped with magnetic stir bar was charged with 0.37 g of 1-PEBr (3.3×10^{-1} M), 0.21 g of

styrene (3.3×10^{-1} M), 192 mg of $\text{RuCl}_2(\text{PPh}_3)_3$ (3.3×10^{-2} M), 163 mg of $\text{Al}(\text{O-}i\text{Pr})_3$ (1.3×10^{-1} M), 50 mg of decane (3.3×10^{-2} M), 10 mg of diphenylether (3.3×10^{-3} M), and 5.5 mL of toluene under inert atmosphere. A small portion of the mixture was diluted with THF in a scintillation vial. After removed from the drybox, and the reaction flask was put in an oil bath thermostated at 110 °C. Just before heating a portion of the initial mixture in the vial was directly injected to GC to measure the concentration of each component. At appropriate time intervals, small aliquots were removed from the reaction mixture, and placed in liquid nitrogen to stop the reaction. The quenched THF solution was characterized with GC without further purification. The concentrations of styrene and 1-PEBr were calculated using decane as an internal standard, and the concentration of M_2b and M_2X were calculated using diphenylether as an internal standard.

2.6.3.2 ATRA of MMA

Iron(II) bromide / tri-*n*-butyl phosphine (FeBr_2 / PnBu_3) catalyst system. A 25 mL Schlenk flask equipped with magnetic stir bar was charged with 0.36 g of MIB-Br (0.5 M), 0.2 g of MMA (0.5 M), 43 mg of FeBr_2 (0.05 M), 0.15 mL of PnBu_3 (0.15 M), 29 mg of decane (0.05 M), 3.4 mg of diphenylether (5×10^{-3} M), and 3.3 mL of toluene under inert atmosphere. A small portion of the mixture was diluted with THF in a scintillation vial. After removed from the drybox, and the reaction flask was put in an oil bath thermostated at 110 °C. Just before heating a portion of the initial mixture in the vial was directly injected to GC to measure the concentration of each component. At appropriate time intervals, small aliquots were removed from the reaction mixture, and placed in liquid nitrogen to stop the reaction. The quenched THF solution was

characterized with GC without further purification. The peaks were identified using model compounds in separate runs. However, peaks corresponding M_2b and M_2X overlapped and appeared with unidentified broad peak so that the calculation of their concentration was impossible. Therefore, only the concentrations of MMA and MIB-Br were used for the estimation of kinetic parameters in ATRP of MMA. The concentrations of MMA and MIB-Br were calculated using decane as an internal standard.

Tris(triphenylphosphine)ruthenium(II) dichloride / aluminum tri(isopropoxide) ($RuCl_2(PPh_3)_3 / Al(O-iPr)_3$) catalyst system. A 25 mL Schlenk flask equipped with magnetic stir bar was charged with 0.36 g of MIB-Br (3.3×10^{-1} M), 0.2 g of MMA (3.3×10^{-1} M), 192 mg of $RuCl_2(PPh_3)_3$ (3.3×10^{-2} M), 163 mg of $Al(O-iPr)_3$ (1.3×10^{-1} M), 50 mg of decane (3.3×10^{-2} M), 10 mg of diphenylether (3.3×10^{-3} M), and 5.5 mL of toluene under inert atmosphere. A small portion of the mixture was diluted with THF in a scintillation vial. After removed from the drybox, and the reaction flask was put in an oil bath thermostated at 110 °C. Just before heating a portion of the initial mixture in the vial was directly injected to GC to measure the concentration of each component. At appropriate time intervals, small aliquots were removed from the reaction mixture, and placed in liquid nitrogen to stop the reaction. The quenched THF solution was characterized with GC without further purification. The concentrations of MMA and MIB-Br were calculated using decane as an internal standard.

2.7 References

1. Fischer, H. *J. Am. Chem. Soc.* **1986**, *108*, 3925.
2. Matyjaszewski, K.; Patten, T. E.; Xia, J. *J. Am. Chem. Soc.* **1997**, *119*, 674.
3. (a) Fischer, H. *Macromolecules* **1997**, *30*, 5666. (b) Fischer, H. *J. Polym. Sci., Part A* **1999**, *37*, 1885.
4. Shipp, D. A.; Matyjaszewski, K. *Macromolecules*, **1999**, *32*, 2948.
5. Ohno, K.; Goto, A.; Fukuda, T.; Xia, J.; Matyjaszewski, K. *Macromolecules*, **1998**, *31*, 2699.
6. Goto, A.; Fukuda, T. *Macromol. Rapid Commun.* **1999**, *20*, 633.
7. Chambard, G.; Klumperman, B.; German, A. L. *Macromolecules*, **2000**, *33*, 4417.
8. Paik, H. J.; Matyjaszewski, K. *Polym. Prepr. (Am. Chem. Soc., Div. Polym. Chem.)* **2000**, *41(1)*, 470.
9. (a) Yurramendi, L.; Barandiarán, M. J.; Asúa, J. M. *Polymer* **1988**, *29*, 871. (b) de la Cal, J. C.; Leiza, J. R.; Asúa, J. M. *J. Polym. Sci. Polym. Chem.* **1991**, *29*, 155.
10. Odian, G. "Principles of Polymerization" 3rd Ed.; John Wiley and Sons; New York; **1991**; p230.
11. Kauffmann, H. F. *Makromol. Chem.* **1979**, *180*, 2649.
12. Brand, E.; Stickler, M.; Meyerhoff, G. *Makromol. Chem.* **1980**, *181*, 913.
13. Matyjaszewski, K.; Davis, K.; Patten, T.; Wei, M. *Tetrahedron*, **1997**, *53*, 15321.
14. Hindmarsh, A. C., "ODEPACK, A Systematized Collection of ODE Solvers", in *Scientific Computing*, Stepleman, R. S., *et al.* Eds., Amsterdam, **1983**, pp.55-64.
15. Marquardt, D. W. *J. Soc. Ind. Appl. Math.* **1963**, *11*, 431.
16. Moré, J. *The Levenberg-Marquardt Algorithm, Implementation and Theory in Numerical Analysis* G. A. Watson, Ed. *Lecture Notes in Mathematics* 630, Springer-Verlag, 1977.
17. Wulkow, M. *Macromol. Theory Simul.* **1996**, *5*, 393.

-
18. Kothe, T.; Marque, S.; Martschke, R.; Popov, M.; Fischer, H. *J. Chem. Soc., Perkin Trans. 2* **1998**, 1553.
 19. Griffiths, M. C.; Strauch, J.; Monteiro, M. J.; Gilbert, R. G. *Macromolecules* **1998**, 7835, 5.
 20. Kajiwara, A.; Matyjaszewski, K.; Kamachi, M. *Macromolecules* **1998**, 31, 5695.
 21. Numerical Recipes in Fortran 77: The Art of Scientific Computing, Ch.10.4, Cambridge University Press, p402.
 22. Matyjaszewski, K.; Patten, T. E.; Xia, J. *J. Am. Chem. Soc.* **1997**, 119, 674.
 23. Matyjaszewski, K.; Wei, M.; Xia, J.; McDermott, N. E. *Macromolecules* **1997**, 30, 8161.

CHAPTER 3

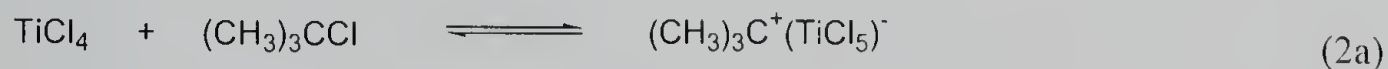
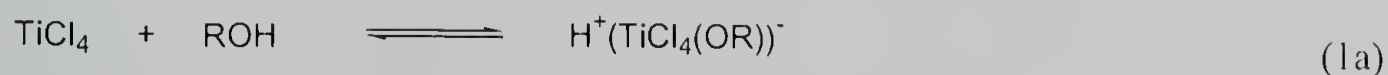
TITANIUM COMPLEXES: A POSSIBILITY AS

CATALYST FOR CONTROLLED RADICAL POLYMERIZATION

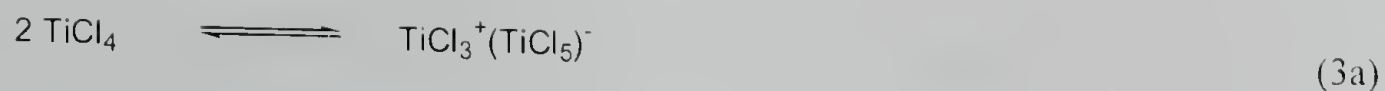
3.1 Introduction

Titanium complexes have been widely used as catalysts for a range of polymerizations. In coordination polymerizations, cocatalysts such as Group I-III metal alkyl or hydride compounds are usually used with titanium complexes to reduce them to lower oxidation states and to generate the active Ti-alkyl cations. The Lewis acid character of titanium complexes also makes it possible for them to act as cationic initiators.

Titanium halides such as titanium(III) trichloride (TiCl_3) and titanium(IV) tetrachloride (TiCl_4) have been used as initiators for cationic polymerizations. Under the right conditions and at low temperature, the high molecular weight polymers are produced in high yield. General initiation by Lewis acids requires either a proton donor such as water, alcohol, hydrogen halide, carboxylic acid (eq 1) or a carbocation precursor such as *t*-butyl chloride or triphenylmethyl chloride (eq 2)



Some Lewis acids with higher acid strengths such as TiCl_4 can initiate polymerization by a self-ionization process in addition to the cointiation process (eq 3)



An alternate self-ionization mechanism is the direct addition of initiator to monomer (eq 4).



Hasebe, *et al.* found that living cationic polymerization of styrene could be achieved by modulating the Lewis acidity of titanium(IV) complex.¹ They tested various titanium(IV) complexes ($\text{TiCl}_{4-n}\text{X}_n$) modified by the number and nature of the substituents ($\text{X} = \text{O}i\text{Pr}, \text{OPh}, \text{Cp}$) in the polymerization of styrene in conjunction with 1-phenylethyl chloride (1-PECl) as an initiator. Among them, when $\text{TiCl}_3(\text{O}i\text{Pr})$ was used in the polymerization, the prepared polystyrene had number average molecular weight that increased in direct proportion to monomer conversion and agreed well with the calculated values, assuming that one polymer chain is generated per molecules of 1-PECl. The molecular weight distributions were also narrow throughout the reactions ($\text{PDI} \sim 1.1$). In contrast, a weaker Lewis acid, CpTiCl_3 , was not effective in the styrene polymerizations, and induced slow polymerization in CH_2Cl_2 at -15°C to give high molecular weight polymers.

Titanium complexes have been also used in coordination polymerizations since Ziegler-Natta discovered the catalyst system composed of aluminum alkyl and titanium

halide for the preparation of polyethylene and stereoregular polypropylene. This work was recognized by the joint award of the Nobel Prize in Chemistry to them in 1963. An ever-increasing number of the Ziegler-Natta type catalyst systems have been developed that show high activity, high stereospecificity, and good economical performances. In the search of high activity, supported Ziegler-Natta catalysts have been developed in which the transition metal is either bonded to or occupies lattice sites in a support material. Catalysts with both high activity and high stereospecificity can be obtained from TiCl_4 ball-milled with MgCl_2 in the presence of aromatic esters. Most Ziegler-Natta catalysts are heterogeneous systems. Some early homogeneous systems have been reported but their use is limited because they usually do not show high activities or high stereochemical control.

Titanocene dichloride was used in combination with aluminum alkyl chlorides as catalysts as early as 1957. These are soluble and chemically better-defined systems, and hence, better act as models of the TiCl_3 -based heterogeneous polymerization catalysts.² One of the key advantages of homogeneous polymerization catalysts over heterogeneous ones is their well-defined active sites, which provide polymers with specific microstructures and more narrow molecular weight distributions. However, the early catalysts based on $\text{Cp}_2\text{MtX}_2/\text{AlRCl}_2$ or AlR_3 (Cp = cyclopentadienyl, Mt = metal, R = alkyl group) show quite low activity toward ethylene polymerization and failed to homopolymerize 1-olefins altogether. These early studies on titanocene or zirconocene dichloride met with only limited success, until the serendipitous discovery of the activating effect of small amounts of water³ on the system $\text{Cp}_2\text{MtX}_2/\text{AlMe}_3$ (X = Cl or

alkyl group).⁴ The subsequent controlled synthesis of methylalumoxane (MAO) by the group of Sinn and Kaminsky⁵ provided organometallic and polymer chemists with a potent cocatalyst able to activate group IV metallocenes toward the polymerization of virtually any 1-olefins as well as several cyclic olefins.⁶ However, the activity of $\text{Cp}_2\text{MtX}_2/\text{MAO}$ catalysts, although impressive toward the homo- and copolymerization of ethylene, was moderate with propylene and, more important, did not produce stereoregular polymers. Very low molecular weight, atactic oils were obtained in all cases. Between 1984 and 1986, two key discoveries were made: the effect that different alkyl-substituted Cp ligands can improve metallocene performances in olefin polymerization (the ligand effect),⁷ and the discovery that stereorigid, chiral metallocene catalysts can induce enantioselectivity in 1-olefin insertion.⁸ Since then impressive progress has been made both in practice and in mechanistic understanding.

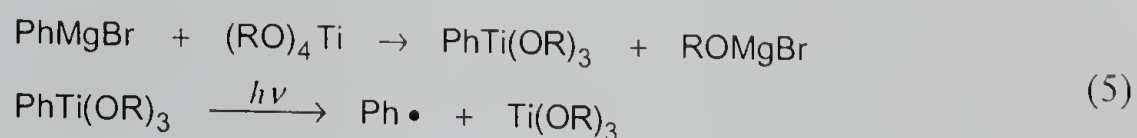
The development of other classes of coordination polymerization catalysts have renewed interest in olefin polymerization because of each catalyst's own unique reactivity and our nascent understanding of ligand/metal effects on catalyst behavior. Metallocene analogues that have received much commercial attention are the *ansa*-monocyclopentadienyl-amido or the constrained geometry catalysts (CGC) developed concurrently by Dow and Exxon. These catalysts are based on a ligand design first introduced by Bercaw⁹ for organoscandium olefin polymerization catalysts. Okuda's report in 1990 of the synthesis of a titanium CGC complex¹⁰ and reports soon after in the patent literature^{11,12,13,14} indicated that researchers at Dow and Exxon had begun what continues to be vigorous investigations into the olefin polymerization activity of these

CGC catalysts. One of the key features of these catalysts is the open nature of the catalyst active site that allows them to incorporate other olefins into polyethylene. There are a number of reports in the patent literature which detail the copolymerization of ethylene with linear α -olefins such as hexene and octene^{12,13,15,16,17,18,19} and with cyclic monomers such as norbornene.^{16,17,18,19,20} These are also among the few classes of catalysts which efficiently incorporate styrene into polyethylene.^{13,18,21} Additionally, when compared to bis-cyclopentadienyl metallocenes, CGC catalysts have increased stability toward MAO, are remarkably stable up to reaction temperatures of 160 °C, and generally give higher molecular weight polymers.²²

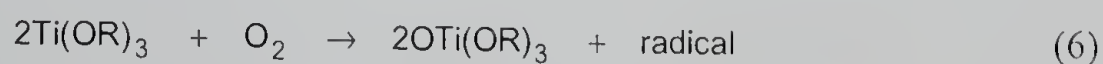
Titanium complexes have also been used to polymerize different types of vinyl monomers including styrene and vinyl chloride.²³ As an example, syndiotactic polystyrenes can be prepared using titanium complexes. Among the various alkoxy, Cp, and alkyl-substituted Cp complexes of titanium, zirconium, and hafnium investigated, e.g., by Ishihara,²⁴ Zambelli,²⁵ Chien,²⁶ Grassi,²⁷ Soga,²⁸ and McCamley,²⁹ the highest activity are achieved with mono-Cp titanocenes of the type CpTiCl₃, IndTiCl₃ (Ind = indenyl), and substituted IndTiCl₃ with MAO as a cocatalyst. Zirconium complexes are less active than titanium compounds and show both lower syndiotacticities and molecular weight for the polymers produced.

The use of titanium compounds in radical polymerization is relatively rare. Herman, *et al.* used a phenyl Grignard-titanate mixture to polymerize styrene in benzene.³⁰ While the intermediate was not isolated, the existence of the titanium-carbon

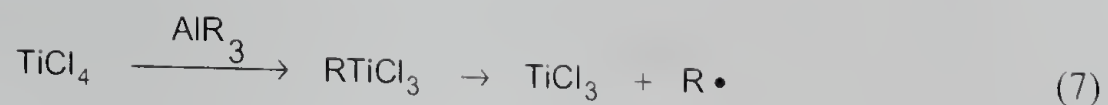
bond in this mixture was advocated, and the thermal or photonic decomposition gave free phenyl radicals and titanium products (eq 5).



Nesmeyanov, *et al.* have reported that in the presence of oxygen, the oxidation of titanium compound, $\text{Ti}(\text{OR})_3$, produced additional free radicals, yet the nature of the free radicals produced was not determined (eq 6).³¹



There also have been reports using RM-MX binary catalyst systems that can induce polymerizations of vinyl monomers. Examples include $\text{Et}_4\text{Pb}/\text{TiCl}_3$ and $\text{Et}_3\text{Bi}/\text{TiCl}_4$ for the homopolymerization of methyl methacrylate (MMA), and $\text{Et}_2\text{Zn}/\text{TiCl}_4$ for the copolymerization of MMA with styrene.³² The radical nature of the polymerization using these catalyst systems was supported by the polymers possessing the same copolymer composition as the ordinary radical produced polymers, and by the fact that the solvent polarity played no prominent role in the composition of the copolymers formed. The Ziegler system, $\text{AlEt}_3/\text{TiCl}_4$, can also initiate a 'radical' type of copolymer. The radical mechanism occurs when the monomer is added to one catalyst component before adding the other catalyst component. The formation of radical from the reduction of titanium complexes by aluminum alkyl compounds proceeds following eq 7.



In recent years, a large number of transition metal complexes have been used as catalysts for free radical polymerization, either as conventional redox initiators or in atom transfer radical polymerization (ATRP). Most of the metals are middle or late transition metals with a few exceptions. In ATRP, there have been no reports of using early transition metal complexes. Examples of metals used as ATRP catalysts include not only the first reported Cu³³ and Ru,³⁴ but also Fe,³⁵ Ni,³⁶ Pd,³⁷ Rh,³⁸ Re,³⁹ and Mo⁴⁰ (Figure 1).

IIIB	IVB	VB	VIB	VII B	VIII	VIII	VIII	IB	II B
Sc	Ti	V	Cr	Mn	Fe	Co	Ni	Cu	Zn
Y	Zr	Nb	Mo	Tc	Ru	Rh	Pd	Ag	Cd
La	Hf	Ta	W	Re	Os	Ir	Pt	Au	Hg


 Metals whose complexes have been effective in ATRP

Figure 3.1 Transition metals of which complexes have been used as ATRP catalysts.

Early transition metal complexes show high catalytic activities in many organic reactions and polymerizations, but they have limitations when used with polar functional groups in some applications. This is due to their highly oxophilic nature, which leads to deactivation by coordination with hard Lewis bases like oxygen. However, the cyclic voltammetric analysis reported in Chapter I revealed that the Ti(III)/Ti(IV) pair has a very low half-wave potential. Therefore, this redox pair should be capable of modulating the equilibrium in an atom transfer reaction, and hence, can be a candidate as a very active catalyst system for ATRP.

3.2 Controlled Polymerization of Styrene Using Titanium(IV) Complexes

Through a rather comprehensive screening of catalyst systems for ATRP, we surprisingly found that bis(cyclopentadienyl)titanium dichloride (Cp_2TiCl_2) and pentamethylcyclopentadienyltitanium trichloride (Cp^*TiCl_3) gave polystyrenes having controlled molecular weight and fairly low polydispersity without the aid of Group I-III cocatalysts. Styrene was polymerized in the presence of these titanium complexes using 1-PECl at 130 °C. The titanium complexes were completely soluble in styrene monomer, and the polymerization was performed in a homogeneous fashion. The polymerization was slow, and it took 25 h to solidify. The polymerization conditions were quite different from normally used for cationic or coordination polymerization. Cationic polymerizations, especially those initiated by Lewis acids, usually proceed at very low temperature. In coordination polymerizations, cocatalysts such as Group I-III organometallic compounds are usually used with the titanium complexes to generate Ti-alkyl complexes. We show the effect of each component on the polymerization in our system in Table 3.1.

It turned out all the components are essential to produce polystyrene having controlled molecular weight and narrow molecular weight distribution. The absence of 1-PECl (Run 2) or the titanium complex (Run 3), results in a large increase in the molecular weight and the molecular weight distribution became broader. In comparison with a normal radical polymerization using benzoyl peroxide (BPO) as a radical initiator, or the thermal polymerization of styrene, the rate of polymerization was slower, but molecular

weight of the resulting polystyrene was low, and molecular weight distribution was narrow.

Table 3.1 Polymerization of Styrene Under Various Conditions at 130 °C

Run		Time(h)	Conv(%)	Mn	PDI
1	^a Mt/1-PECl/St	2	17	8,300	1.57
2	Mt/St	2	25	89,300	1.72
3	1-PECl/St	2	16	133,300	1.78
4	BPO/St	1.5	high	46,100	1.87
5	St	7.5	high	263,000	1.66

^a Mt, Cp₂TiCl₂; 1-PECl, 1-phenylethyl chloride, St, styrene, BPO, benzoyl peroxide.

3.2.1 Kinetics of Polymerization

To investigate the characteristics of the polymerization in detail, we performed kinetic studies of the styrene polymerization using several different titanium(IV) complexes. Three commercially available titanium complexes were used, Cp₂TiCl₂, Cp*TiCl₃, and bis(pentamethylcyclopentadienyl)titanium dichloride (Cp*₂TiCl₂). Figure 3.2 shows the first order kinetic plots of monomer conversion as a function of time for the polymerization of styrene. After an initial nonlinear increase in conversion, the plot shows a linear relationship between $\ln([M]_0/[M])$ and polymerization time for all three titanium complexes, indicating approximately constant number of active species during the reaction. Number average molecular weight and PDI of the resulting polymers were lower than those of polymers prepared thermally, indicating that polymerizations were under a higher degree of control (Figure 3.3). However, molecular weight of the product

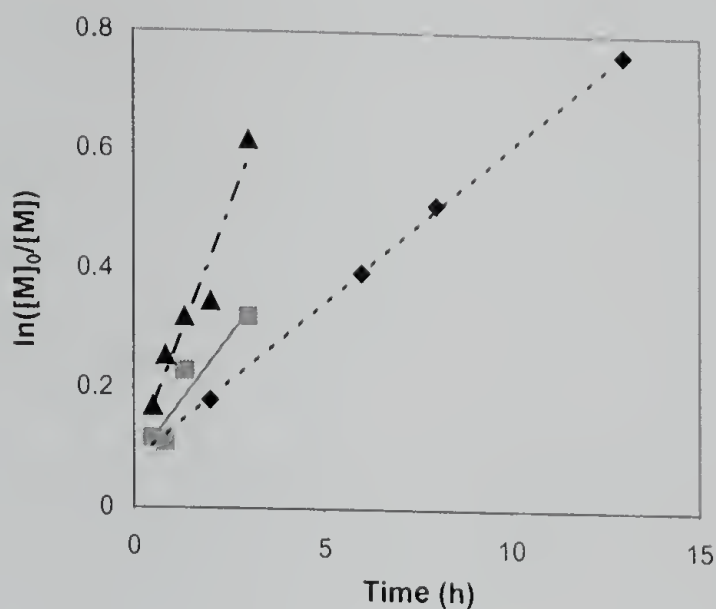


Figure 3.2 Kinetic of the polymerization of styrene using various titanium complexes at 130°C, (a) Cp_2TiCl_2 (\blacklozenge , ---); (b) Cp^*TiCl_3 (\blacksquare , —); (c) $\text{Cp}^*_2\text{TiCl}_2$ (\blacktriangle , - · -).

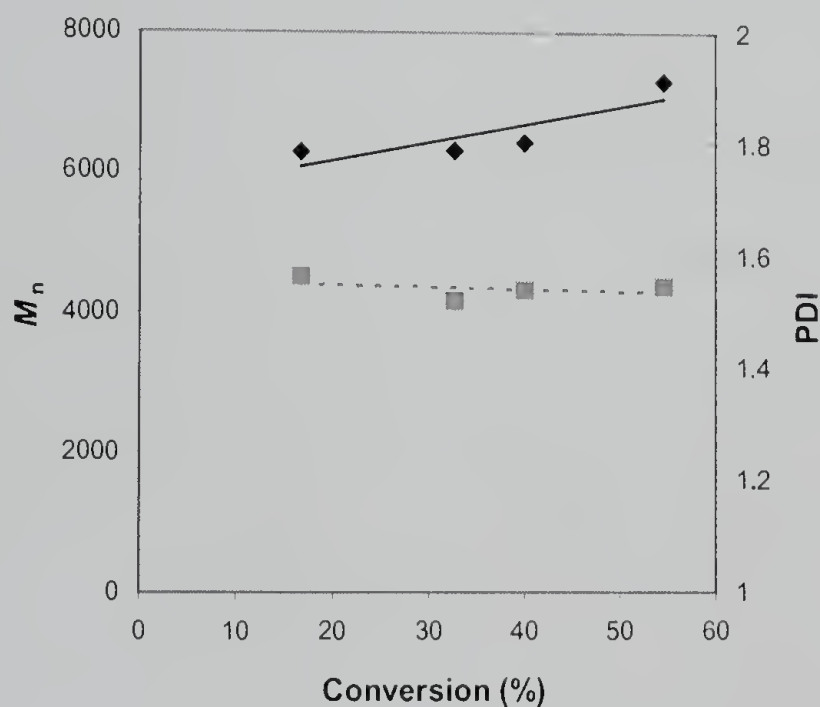


Figure 3.3 Plots of number average molecular weight (M_n , \blacklozenge , —) and polydispersity index (PDI, \blacksquare , ---) of the polymer and monomer conversion for the polymerization of styrene using Cp_2TiCl_2 at 130°C.

polymer remains almost constant throughout all conversion range after an increase at the initial stage of polymerization. This indicates that number of polymer chains is not constant, but increases throughout the polymerization by chain transfer reactions, which is normal for a conventional vinyl addition polymerization.

3.2.2 Chain Extension Reaction

One of the important applications of living polymerization is the preparation of block copolymers. All the polymer chain ends should remain active so that on further addition of monomer, the extended chain or block copolymer is formed. Actually, this is a good working definition of living polymerization. The control over molecular weight and molecular weight distribution can be achieved even if the polymerization is not perfectly living just as long as the polymerization satisfies some pre-requisitions, which we will discuss in Chapter 4 in more detail. However, successful preparation of block copolymers without substantial formation of either homopolymer is only possible in a living system. To check this living characteristic of the polymer chain ends in our system, chain extension reactions were performed. Polystyrene was prepared with 1-PECl and Cp_2TiCl_2 in bulk at 130 °C. The prepared polystyrene was isolated by precipitation, and purified from the metal catalyst by passing it through an alumina column ($M_n = 8,500$; PDI = 1.72). The purified polystyrene was dissolved in additional styrene monomer containing Cp_2TiCl_2 , and heated to 130 °C for 20 h. Figure 3.4 shows the gel permeation chromatogram of the resulting polymer. The chromatographic analysis shows that molecular weight distribution of the product polymer was unimodal and the molecular weight shifts to the higher molecular weight region ($M_n = 53,300$; PDI = 1.75). This

indicates that most of initial polymer was reactivated and available to react with more monomer.

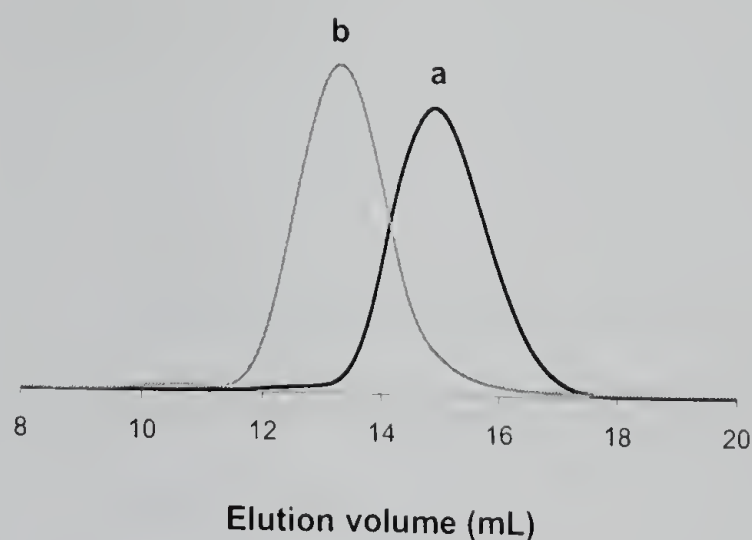


Figure 3.4 GPC traces of (a) initial polystyrene before the chain extension reaction; (b) final polystyrene after the reaction using Cp_2TiCl_2 .

3.3 Verifying the Mechanism of the Polymerization using Titanium Complexes

The kinetic studies of the styrene polymerization showed some unusual characteristics. The polymerization showed “living” characteristics in both the kinetic plot of $\ln([M]_0/[M])$ vs. time and the chain extension reactions. On the other hand, the molecular weight evolution as a function of conversion implied uncontrolled polymerization. These characteristics are different from the normal cationic polymerizations, which are catalyzed by titanium(IV) compounds. Likewise, the data and conditions used are inconsistent with a conventional coordination mechanism that is another well-known polymerization mechanism using titanium complexes, in combination with Group I-III organometallic cocatalysts. Therefore, before undergoing further development of this system, it was incumbent upon us elucidate the basic

mechanism of the polymerization. Various methodologies were used, including the use of radical inhibitors, radical chain transfer agents, copolymerizations with electron-rich monomers, polymerizations of electron-deficient monomers, and measurements of the stereoregularity of the product polymers.

3.3.1 Effects of the Radical Inhibitors

To test for the possibility of a radical mechanism, we used radical inhibitors such as TEMPO (2,2,6,6-tetramethyl-1-piperidinyloxy) or galvinoxyl (2,6-di-*t*-butyl- α -(3,5-di-*t*-butyl-4-oxo-2,5-cyclohexadien-1-ylidene)-*p*-tolylloxy). In the case of a radical polymerization, these inhibitor radicals will react with the propagating radicals, and completely halt the reaction until they are consumed.

In the kinetic studies of our polymerization, we found that the concentration of active species is almost unchanged throughout the polymerization. From the slope of the plots of $\ln([M]_0/[M])$ and polymerization time for three titanium complexes, Cp_2TiCl_2 , Cp^*TiCl_3 , and $\text{Cp}^*_2\text{TiCl}_2$, we calculated the apparent concentration of active species using the following eqs.

$$R_p = -\frac{d[M]}{dt} = k_p [R^*][M] \quad (8)$$

$$\ln\left(\frac{[M]_0}{[M]}\right) = k_p [R^*]t = \text{slope} \times t \quad (9)$$

Although this is a rough measure of the concentration of active species, we can get a general idea about the magnitude of the concentration of active species. Assuming the polymerization was operating through a radical mechanism, we could calculate the concentration of active radicals using the literature value of 1.6×10^3 for k_p . The determined concentration of radicals was 9.3×10^{-9} M for Cp_2TiCl_2 , 1.5×10^{-8} M for Cp^*TiCl_3 , and 2.8×10^{-8} M for $\text{Cp}^*_2\text{TiCl}_2$. Therefore, very small amounts of inhibitor would be enough to quench the polymerization if it occurs through a radical mechanism. Table 3.2 shows the effects of the radical inhibitor on the polymerization. When TEMPO was used, the reaction rate was decreased for both the Cp_2TiCl_2 and Cp^*TiCl_3 catalyzed reactions, but the polymerization was not completely inhibited by adding TEMPO. The molecular weight of the polymers also decreased, and the polydispersity remained at a low value. TEMPO is usually a very good inhibitor for radical polymerizations. However, at the high temperature of 130 °C, the C-O bond between terminated polymer chain and TEMPO unit can be cleaved homolytically to regenerate radical species. In fact, the nitroxide-mediated stable free radical polymerization technique uses this feature to control the concentration of active radical species. Therefore, even if the polymerizations using titanium complexes went through a radical mechanism, they would not be inhibited by TEMPO, but their reaction rates would be suppressed and this is what was observed.

In the next set of experiments, galvinoxyl was used as a radical inhibitor. Because of the strong C-O bond between the terminal polymer chain and the galvinoxyl, the polymer chain-galvinoxyl adduct doesn't undergo reinitiation by homolytic cleavage at

130 °C. The polymerization using Cp_2TiCl_2 and Cp^*TiCl_3 were completely inhibited with galvinoxyl, and no polymer was formed even after 100 h at 130 °C. As a comparison, we also used the common cationic initiators, TiCl_3 and TiCl_4 , for the polymerization of styrene. As expected, polymers were still formed in the presence of galvinoxyl, although the polymerization rates were decreased. These results also support a radical mechanism for the polymerization using Cp_2TiCl_2 and Cp^*TiCl_3 .

Table 3.2 Effect of Radical Scavenger on the Polymerization of Styrene Using Titanium Complexes

	styrene only	styrene + TEMPO	styrene +galvinoxyl
Cp_2TiCl_2	130 °C, 25h, 85% (10,400; 1.307)	130 °C, 100h, 62% (3,140; 1.343)	100 °C, 100h no polymer
Cp^*TiCl_3	130 °C, 15h, 64% (6,510; 1.350)	130 °C, 100h, 48% (2,180; 1.362)	100 °C, 100h no polymer
TiCl_3	130 °C, 2h, 58% (2,130; 1.570)	130 °C, 100h, 64% (3,080; 1.455)	100 °C, 20h, 62% (3,650; 2.052)
TiCl_4	25 °C, 10min, 83% (5,430; 1.510)	-	130 °C, 20h, 36% (3,320; 3.712)

3.3.2 Effects of the Radical Chain Transfer Agents

Another possible mechanism of polymerization using titanium complexes is a coordination mechanism. Titanium complexes have been widely used in the polymerization of olefins by a coordination mechanism since the early experiments of Ziegler and Natta. Initially, the mechanism of olefin polymerization using Ziegler-Natta catalysts was unknown at though to be one of several possibilities, which included ionic, radical, or a coordination mechanism. Among them, a radical mechanism was ruled out

from several experimental results. The copolymerization studies showed different reactivity ratios of the Ziegler-Natta system with those of copolymerization using normal radical initiator. Another experiment was using radical chain transfer agents. Radical chain transfer agents had no effect on polymer molecular weight for the coordination polymerization. Based on this idea, we used 1-octanethiol as a radical chain transfer agent to discriminate between a radical and a coordination mechanism, because thiols are known to be one of the most effective chain transfer agent for radical polymerization of styrene.

In our experiments, one equivalent of 1-octanethiol to the titanium concentration was used first. In this case, the effect of thiol radical chain transfer agent was very small, and within experimental error, the polymer molecular weight didn't changed. Table 3.3 shows the results when 5 equivalent 1-octanethiol was used in the polymerization of styrene.

Two different compounds were used in the polymerization of styrene along with the titanium complexes; an ATRP initiator, 1-PECl, and a conventional radical initiator, α,α' -Azobis(isobutyronitrile) (AIBN). Number average molecular weight of product polystyrene was similar for both cases of initiators. However, the molecular weight distribution of polystyrene prepared using AIBN was much higher than that of the polymer prepared using 1-PECl. In the next set of experiments, we used 1-octanethiol in the polymerization under exactly same conditions. When Cp_2TiCl_2 was used in the polymerization along with the chain transfer agent, the molecular weight of the product

Table 3.3 Effect of Radical Chain Transfer Agent (1-octanethiol, RSH) on the Polymerization of Styrene Using Titanium Complexes (**a**, Cp₂TiCl₂; **b**, Cp*TiCl₃) at 130 °C

	Time	Conv(%)	<i>M_n</i>	PDI
a/I-PECl/st	24 h	60	10,300	1.673
b/1-PECl/st	75 min	15		1.833
a/AIBN/st	75 min	65	12,490	5.447
b/AIBN/st	75 min	55	21,000	5.353
a/I-PECl/RSH/st	24 h	30	2,330	2.697
b/1-PECl/RSH/st	75 min	no polymer		
a/AIBN/RSH/st	75 min	30	3,120	2.267
b/AIBN/RSH/st	75 min	no polymer		

polystyrene decreased along with an increased value of the polydispersity index. These results support the view that there is an active radical chain transfer reaction in the polymerization. Interestingly, we could not obtain any polymer from polymerizations using Cp*TiCl₃ as the catalyst. Although these catalysts are structurally similar, there are some important differences in their behaviors.

3.3.3 Copolymerization of Styrene and Ethyl Vinyl Ether

The electronic character of the vinyl substituents is very important in ionic polymerizations. Likewise, the reactivity of the monomers in copolymerization is different according to the polymerization mechanism. For example, vinyl ether monomers have high reactivity in cationic polymerization mechanism. However, they have low reactivity in radical mechanism, better in select radical copolymerizations, and

do not polymerize by anionic mechanism. Hence, testing alternative monomers with various initiator systems can provide some important clues about polymerization mechanism.

Styrene and ethyl vinyl ether have quite different reactivities in radical and cationic polymerizations, even though both monomers can be polymerized to varying degrees by both polymerization mechanisms. In radical polymerization, the reactivity ratios of these two monomers in copolymerization are $r_{\text{styrene}} = 90$ and $r_{\text{ethyl vinyl ether}} = 0$, whereas the reactivity of ethyl vinyl ether in cationic polymerizations is higher than that of styrene. The copolymerization results are shown in Table 3.4. When Cp_2TiCl_2 was used, the styrene content in copolymer was as high as 83%. However, the copolymer prepared using Cp^*TiCl_3 had a styrene content of 33%. This is close to the values when cationic initiators are used in the copolymerization. These results also support the radical mechanism for the polymerization using Cp_2TiCl_2 .

Table 3.4 Copolymerization of Styrene and Ethyl Vinyl Ether Using Various Titanium Complexes at 100 °C

	Time (h)	Conv(%)	M_n	PDI	styrene content in copolymer (%)
Cp_2TiCl_2	100	16	7,760	1.704	83
Cp^*TiCl_3	100	8	73,950	3.072 (multiple peak)	33
TiCl_3	3	75	22,220	1.639 (multiple peak)	12
TiCl_4	100	>95	6,830	1.581 (multiple peak)	28
BPO	3	69	10,350	1.945	

3.3.4 Polymerization of Methyl Methacrylate

We tried to polymerize MMA using titanium complexes to rule out the cationic mechanism (Table 3.5). Because electron-withdrawing group of MMA cannot stabilize the cationic center in the propagating intermediate, this monomer does not polymerize by a cationic mechanism. The polymerization of MMA using titanium complexes as catalysts proceeded in high yields. Moreover, the rate of polymerization was faster than that of the styrene polymerizations. Compared with the polymerization using conventional radical initiators, the rate was slower and the molecular weight of resulting polymer was very high. However, molecular weight distribution of product polymer was narrower. The microstructure of polymer was examined by $^1\text{H-NMR}$ (Figure 3.5). The fraction of triads was calculated by the integration of 0.7-1.3 ppm regions for α -methyl resonance. The stereoregularity of poly(methyl methacrylate) formed using titanium complexes was very similar to that of polymers prepared by conventional radical methods. These data all indicate that the polymerization proceeded by a radical mechanism.

Table 3.5 Polymerization of Methyl Methacrylate (MMA) Using Titanium Complexes (**a**, Cp_2TiCl_2 ; **b**, Cp^*TiCl_3)

	Temp ($^{\circ}\text{C}$)	Time (h)	Conv(%)	M_n	PDI
a /1-PECI/MMA	100	3	33.8	197,500	1.667
b /1-PECI/MMA	100	1.5	92.6	309,600	1.874
a /BPO/MMA	100	1	46	40,480	3.136
b /BPO/MMA	100	1	47	66,650	2.319
BPO/MMA	100	1	71	277,400	2.886

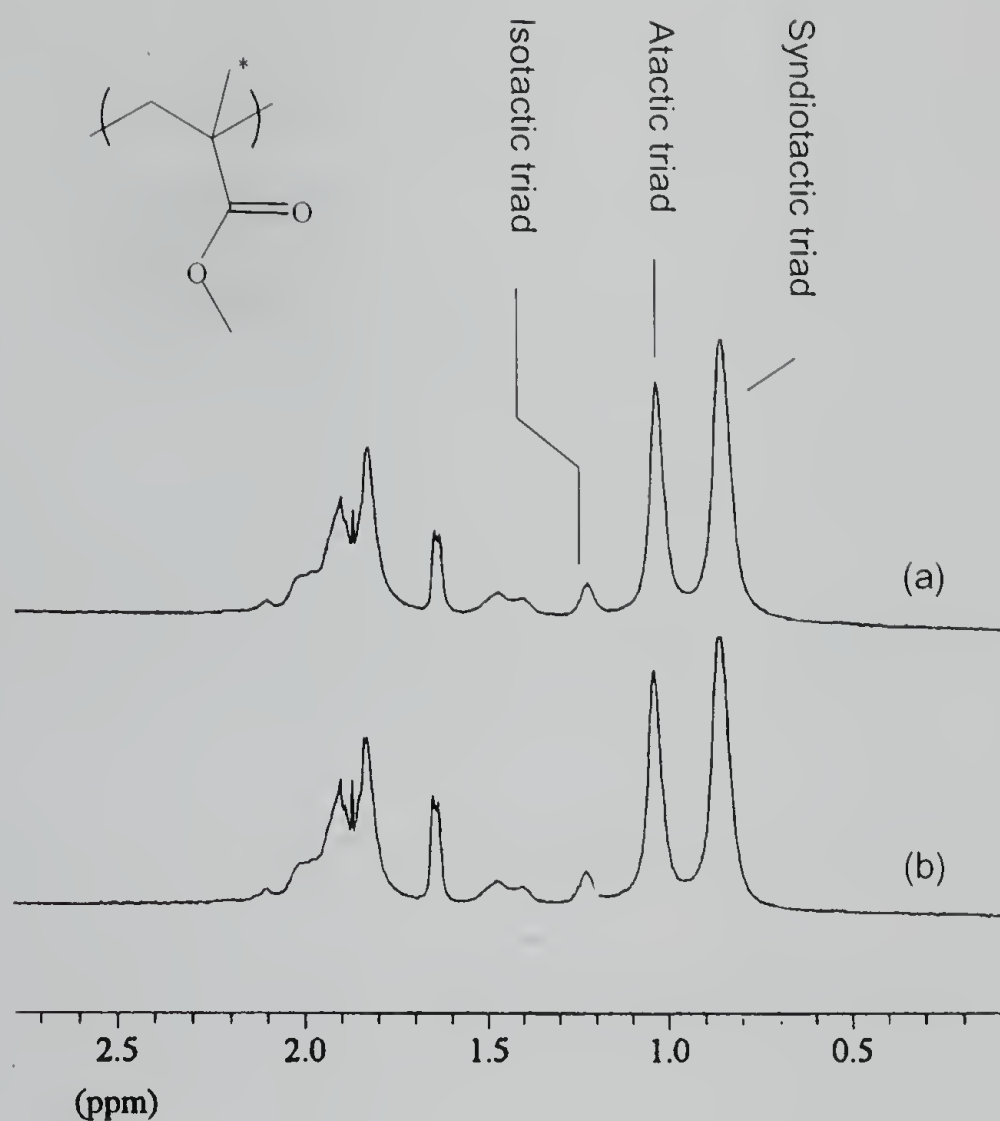


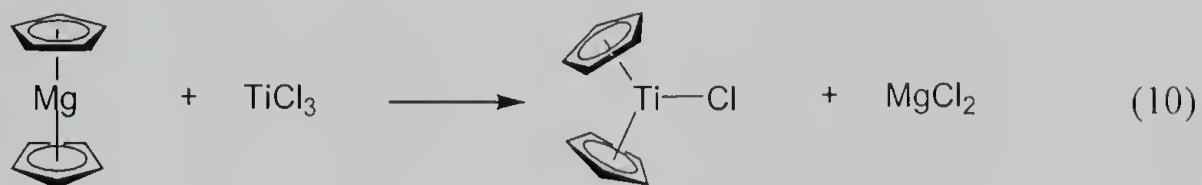
Figure 3.5 ¹H-NMR spectrum of poly(methyl methacrylate) prepared using (a) Cp_2TiCl_2 ; (b) benzoyl peroxide.

3.4 Polymerization of Styrene using Titanium(III) Complexes

The previous results gathered from the various polymerizations run to verify the mechanism, all support the radical pathway for the polymerization using Cp_2TiCl_2 . Because of their low costs and ubiquitous use in commercial polymerization processes, our goal is to use early transition metal complexes, such as titanium complexes, as ATRP catalysts. Especially interesting is the Ti(III)/Ti(IV) redox pair, which has a very low half-wave potential and could be a candidate for a very active ATRP catalyst. The

initiation of ATRP can be performed starting from metal complexes of two different oxidation states. The first one is using lower-oxidation state metal complex and alkyl halide compounds such as 1-PECl. These two components react with each other to generate a higher-oxidation state metal complex and the 1-phenylethyl radical. The other method of initiation is to use a higher-oxidation state metal complex and conventional radical initiator. In this case, the radical generated from the thermal cleavage of conventional radical initiator, quickly reacts with higher-oxidation state metal complexes to form lower-oxidation state metal complex and alkyl halide, a combination that is similar to the initial components of the first initiation method.

In our previous experiments, we used higher-oxidation state Ti(IV) complex and 1-PECl as starting materials. In this paradigm, the initial radicals should be generated from the auto-initiation reaction of monomers, which is one of the reasons for slow polymerization. To test the activity of titanium complexes as ATRP catalyst under more conventional conditions, we used lower-oxidation state $\text{Cp}_2\text{Ti(III)Cl}$ and 1-PECl as a initiation system. Cp_2TiCl was synthesized from TiCl_3 and Cp_2Mg in refluxing THF (eq 10).



The polymerization of styrene was performed with this Cp_2TiCl and 1-PECl in toluene. The polymerization mixture was prepared in drybox at room temperature. To a

heterogeneous solution of Cp_2TiCl in styrene and toluene, was added 1-PECl. The color of the solution changed from green to red immediately upon addition of the 1-PECl. This indicates that the green colored Cp_2TiCl reacts very fast with 1-PECl to generate the red-colored Cp_2TiCl_2 . After removal from the drybox, the reaction tube was immersed in oil bath thermostated at the desired temperature. Table 3.6 shows the results of polymerization of styrene at various temperatures. In general, as the temperature increases, the rate of polymerization increases and molecular weight of product polymer decreases. It is thought that these results are related to the thermal initiation reaction of the styrene monomer, i.e., as the temperature increases, more radicals are generated by the thermal Diels-Alder reaction of styrene. The increased concentration of radical then increases the rate of polymerization, and decreases the molecular weight of the product polystyrene.

Table 3.6 Polymerization of Styrene Using $\text{Cp}_2\text{Ti}^{\text{III}}\text{Cl}$ and 1-phenylethyl chloride at Various Temperatures

Run	Temp ($^{\circ}\text{C}$)	Time (h)	Conv(%)	M_n	PDI
1	30	24	90	136,080	2.094
2	70	12	21	31,010	1.733
3	90	12	69	39,360	1.82
4	110	12	80	25,760	1.815
5	130	12	86	24,950	1.723
6 ^a	130	12	91	25,680	1.984

^a without 1-phenylethyl chloride

We also performed kinetic studies of polymerization at 90 °C. The first order kinetic plot of monomer conversion as a function of time is linear after an initial fast stage of polymerization. This is similar to the case of polymerization using Cp_2TiCl_2 (Figure 3.6). The molecular weight of the product polymer as a function of conversion is also similar to that for the polymerization using Cp_2TiCl_2 , and shows a gradual increase after a big increase in the low conversion region (Figure 3.7). However, molecular weight of the product polymer was higher than that of polymer prepared using Cp_2TiCl_2 . If the polymerization follows the ATRP mechanism, radicals would be generated by chlorine transfer reaction between I-PECl and Cp_2TiCl at room temperature, which is evidenced by the color change. Therefore, the large portion of 1-phenylethyl radicals could be consumed before reaching the reaction temperature by propagation and/or termination reactions. In this case, the real components participating the polymerization at reaction temperature would be Cp_2TiCl_2 and a reduced amount of I-PECl. As we have seen in Table 3.1, I-PECl has an effect of decreasing molecular weight of product polymer. Hence, in this experiment, reduced concentration of I-PECl could increase the molecular weight of polystyrene.

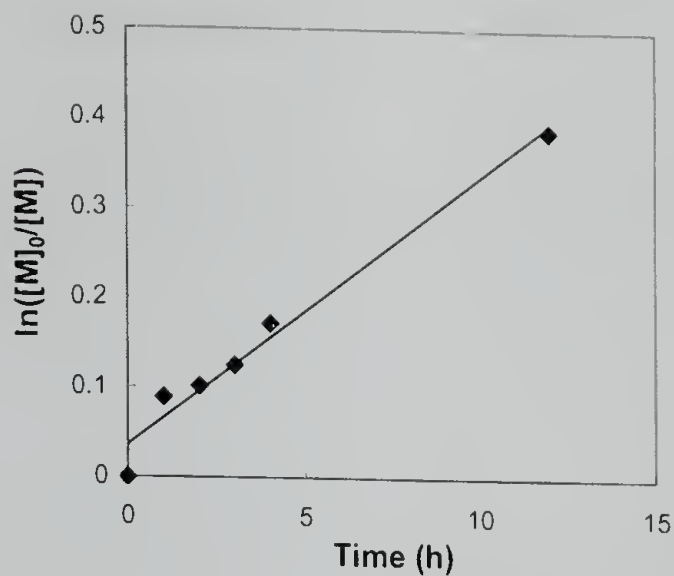


Figure 3.6 Kinetic plots of $\ln([M]_0/[M])$ vs. time for the bulk polymerization of styrene using Cp_2TiCl at 90°C .

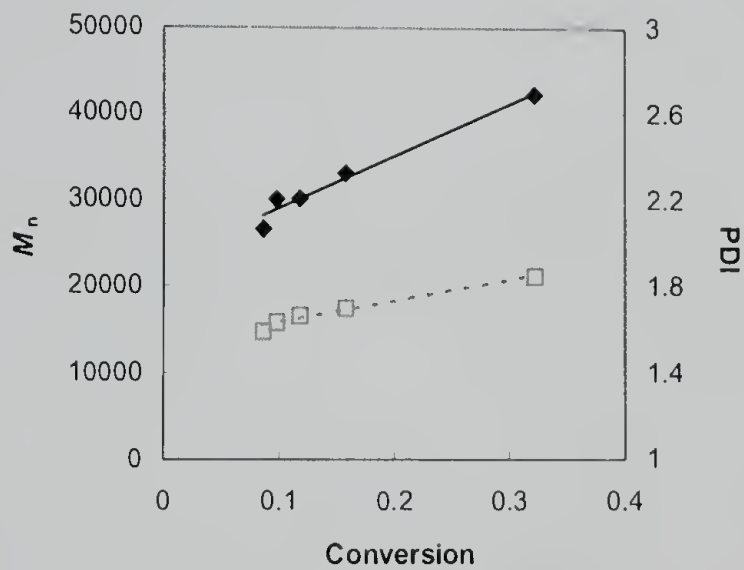


Figure 3.7 Plots of number average molecular weight (M_n , \blacklozenge , —) and polydispersity index (PDI, \square , ---) of the polymer and monomer conversion for the polymerization of styrene using Cp_2TiCl at 90°C .

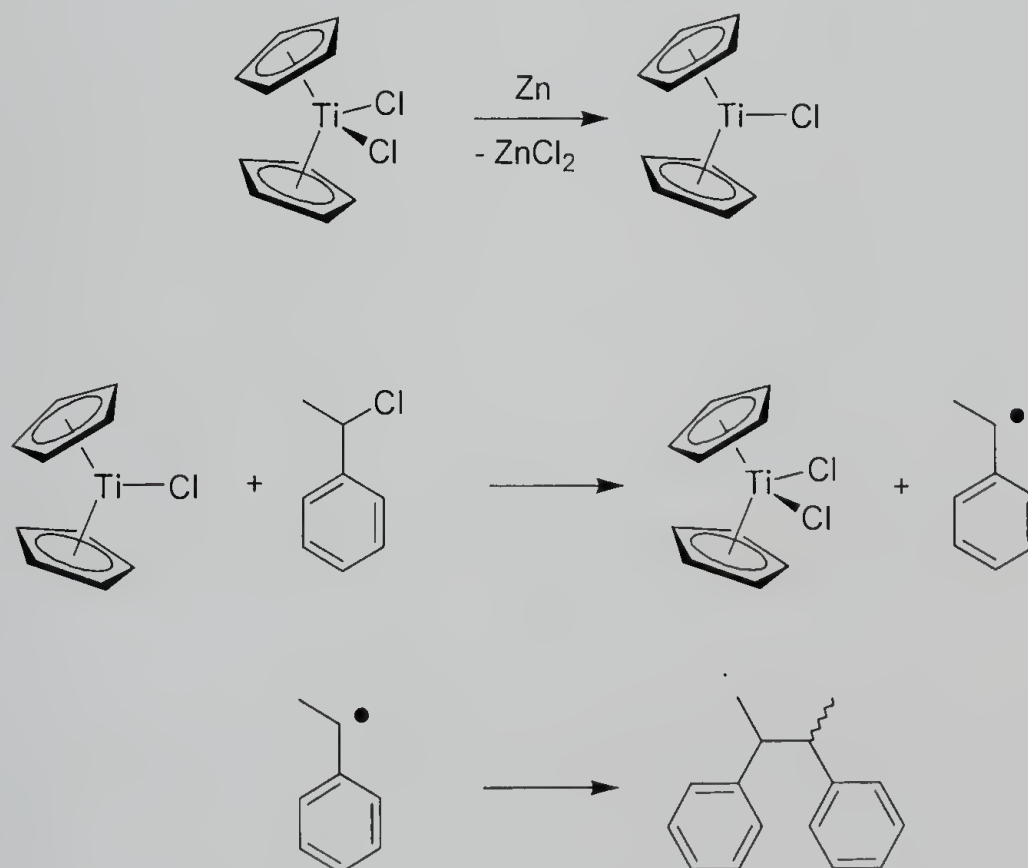
3.5 Checking Atom Transfer Reaction

From the kinetic studies using Cp_2TiCl and 1-PECl, we could not confirm that the polymerization follow an ATRP pathway. We tried to isolate intermediate species from each step to see if the polymerization using titanium complexes proceeds by ATRP mechanism.

3.5.1 Isolation of the Activation Reaction

Scheme 3.1 depicts the strategy of isolating activated products from the suspected ATRP reaction. Cp_2TiCl was prepared from Cp_2TiCl_2 and Zn metal in dehydrated toluene. After stirring at room temperature for h, the color of the solution changed from red to green, indicating Cp_2TiCl was produced. After removing the white insoluble solid, which

Scheme 3.1 Isolation of the Activation Reaction



is composed of the remaining Zn and the $ZnCl_2$ by-product, 1-PECl was added to the Cp_2TiCl solution. If atom transfer reaction takes place, chlorine atom would transfer from 1-PECl to Cp_2TiCl to generate Cp_2TiCl_2 and 1-phenylethyl radicals. These radicals would react each other to form 2,3-diphenylbutane. Figure 3.9 shows the 1H -NMR spectrum of the product of the reaction. It is found that new peaks appear at chemical shift of 2.6-2.8 ppm and 0.9-1.2 ppm corresponding methyne and methyl proton of 2,3-diphenylbutane, respectively. This 1H -NMR result and color change support the hypothesis that activation step in the atom transfer reaction is present in the polymerization of styrene using Cp_2TiCl_2 .

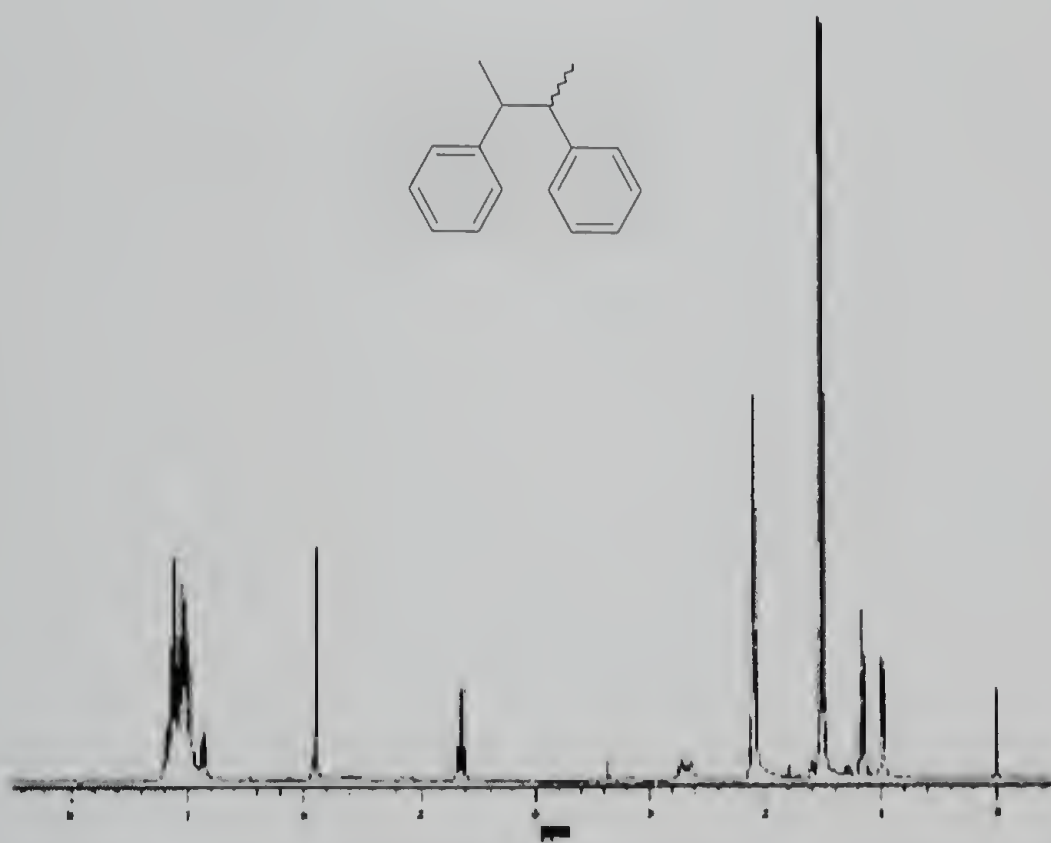
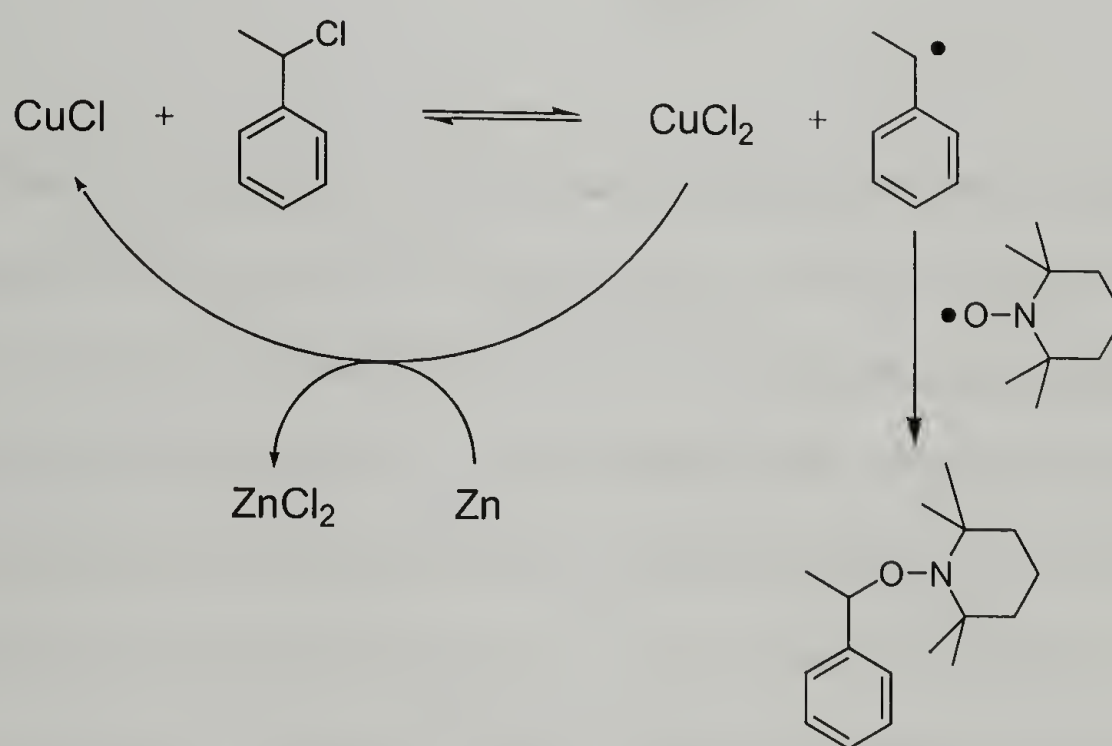


Figure 3.8 1H -NMR spectrum of Cp_2TiCl and 1-phenylethyl chloride in toluene- d_8 .

3.5.2. Isolation of the Deactivation Reaction

The isolation of products from the deactivation step of the atom transfer reaction was carried out using the trapping reactions shown in Scheme II and III. In the first step of the reaction, the 1-phenylethyl-TEMPO adduct was prepared following a literature method, from the reaction between CuCl and 1-PECl in the presence of Zn metal.⁴¹ In this reaction, we used Zn metal instead of Cu metal, and we could get the pure 1-phenylethyl-TEMPO adduct in high yields (Scheme 3.2).

Scheme 3.2 Preparation of 1-phenylethyl-TEMPO adduct



The 1-phenylethyl-TEMPO adduct was then mixed with Cp₂TiCl₂ in toluene-*d*₈, and heated at 130 °C. At high temperature, 1-phenylethyl-TEMPO adduct cleaves homolytically to generate TEMPO and the 1-phenylethyl radical. If atom transfer reaction takes place from Ti(IV), chlorine atom would transfer from Cp₂TiCl₂ to 1-phenylethyl radical to generate Cp₂TiCl and 1-PECl (Scheme 3.3).

Scheme 3.3 Isolation of the Deactivation Reaction

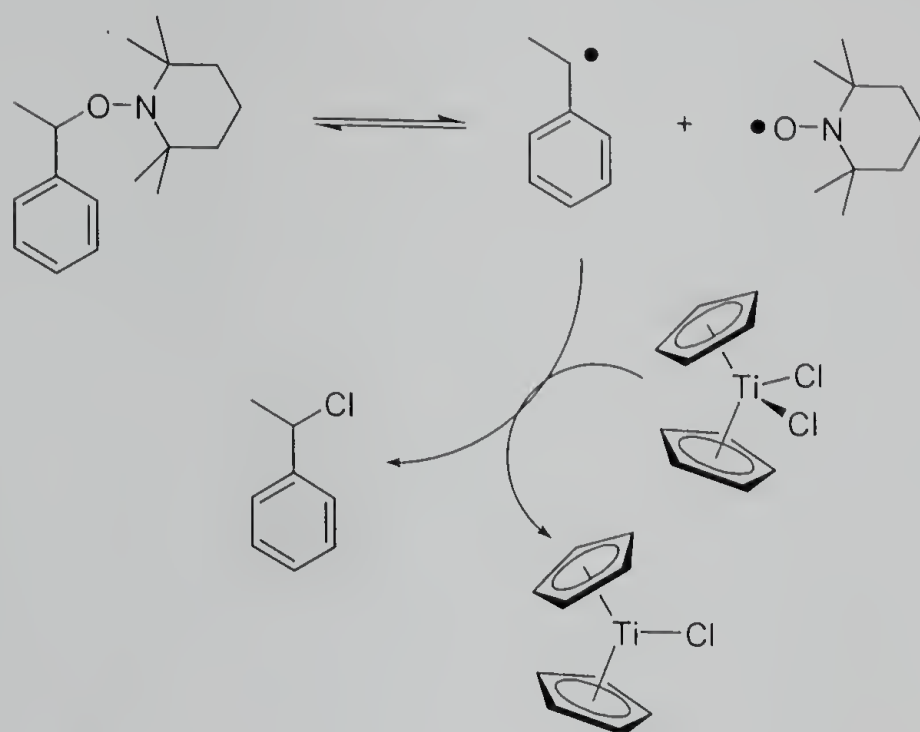


Figure 3.10 shows the $^1\text{H-NMR}$ spectrum of the reaction mixture, which reveals unexpected results. Instead of the expected peaks for 1-PECl, new peaks for styrene appear at 5.2, 5.8, and 6.8 ppm. We believe the potential pathways for the formation of styrene as shown in Schemes IV-VI. It has been reported that the 1-phenylethyl-TEMPO adduct spontaneously thermally decomposes to styrene and TEMPO by a β -hydrogen transfer reaction with a rate constant $k_{decomp} = 3 \times 10^{-5} \text{ s}^{-1}$ at 120 °C in dimethyl sulfoxide (Scheme 3.4).⁴² The 1-phenylethyl radical or 1-PECl can decompose to styrene by the chain end degradation reactions that we described as side reactions of ATRP in Chapter 2 (Scheme 3.5). The rate constants for these reactions are calculated to be $k_a = 6.62 \text{ M}^{-1} \text{ s}^{-1}$ and $k_b = 1 \times 10^{-3} \text{ M}^{-1} \text{ s}^{-1}$, respectively, at 130 °C for the $\text{CuBr}_2/\text{dNbpy}$ catalyst system. However, there has been no report for Ti(IV) complexes involved in these reactions. Scheme 3.6 depicts another potential reaction for the formation of styrene. The 1-phenylethyl radical and the paramagnetic Cp_2TiCl complex can combine to form Ti-alkyl

complexes, and this Ti-alkyl complex then undergoes β -hydrogen elimination reaction to generate styrene and the titanium hydride complex.

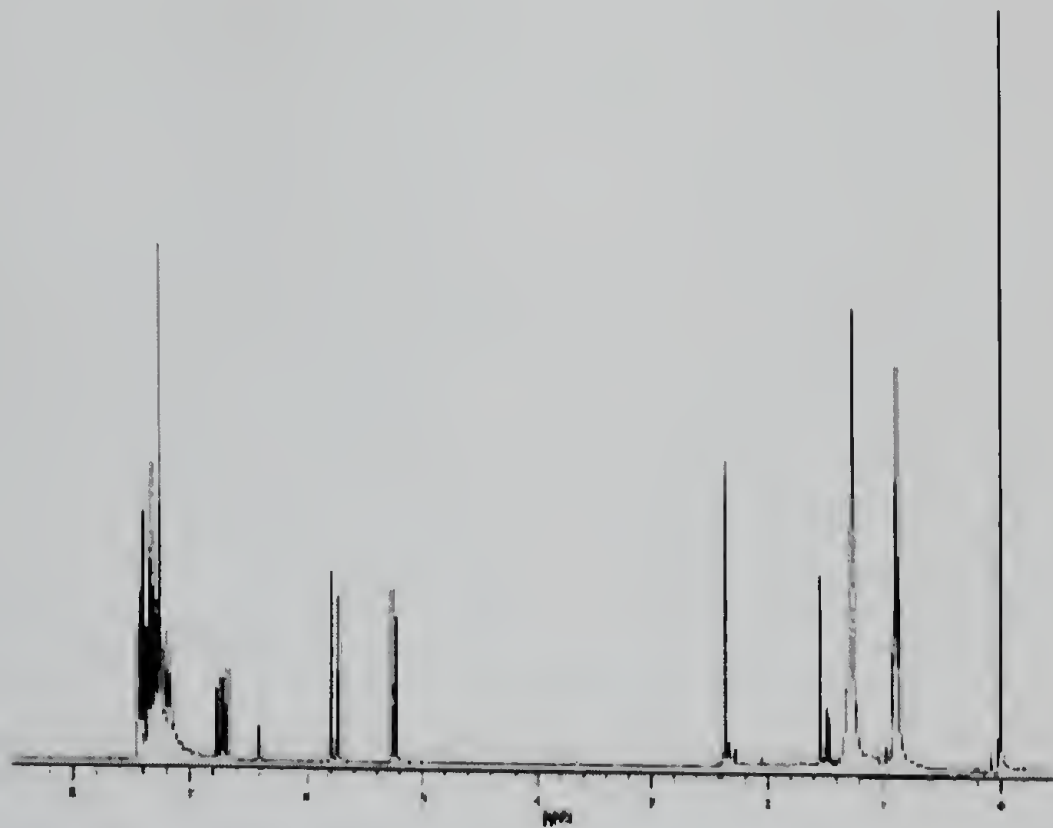
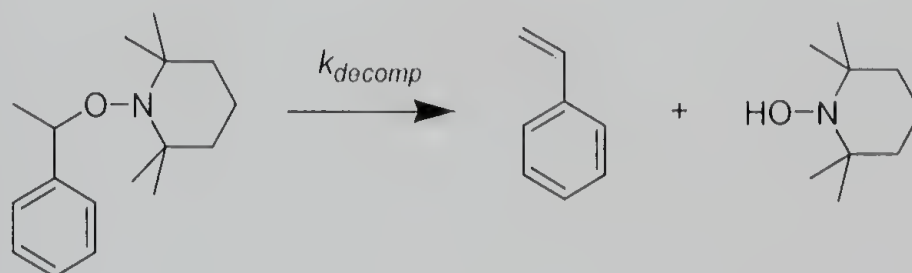
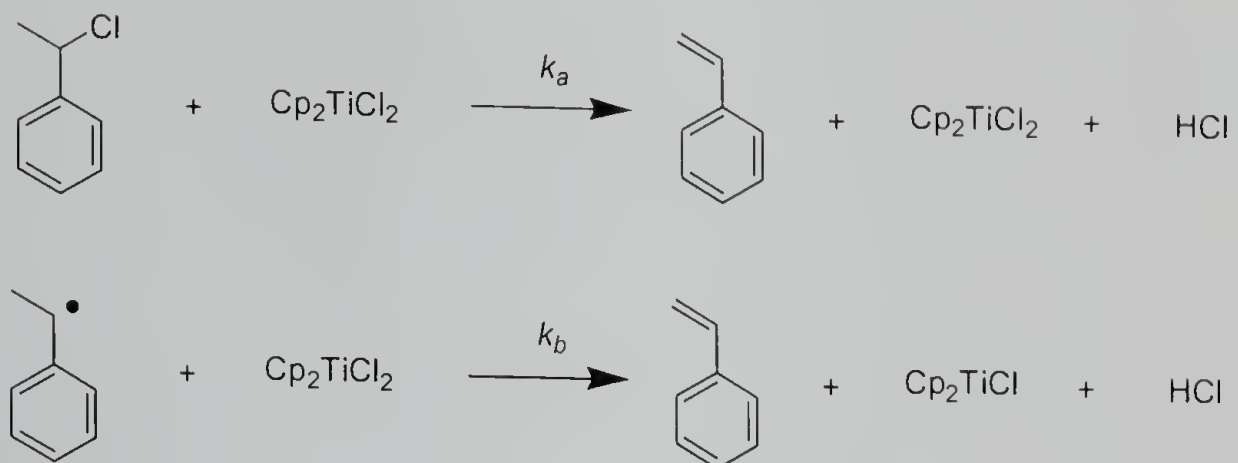


Figure 3.9 ^1H -NMR spectrum after reaction between 1-phenylethyl-TEMPO adduct and Cp_2TiCl_2 at 130 °C in toluene- d_8 .

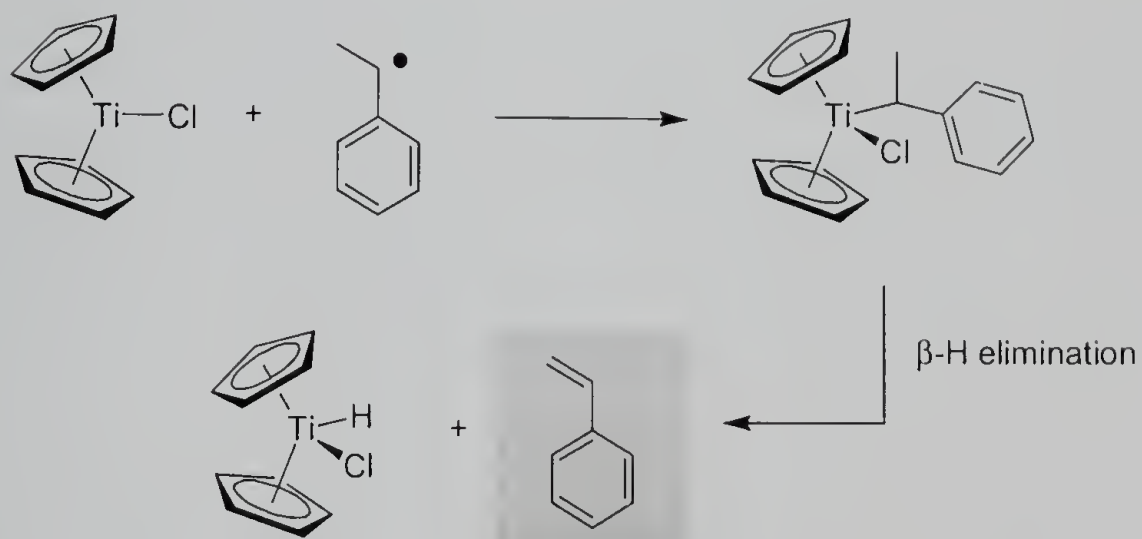
Scheme 3.4 Degradation of 1-phenylethyl-TEMPO adduct



Scheme 3.5 Degradation of polymer chain ends



Scheme 3.6 Degradation of Ti-alkyl compound



3.6 Conclusion

We used various titanium complexes in the polymerization of styrene. The properties of resulting polymer indicate that polymerization was more controlled compared with thermal polymerization. The kinetic studies indicated that lower level of termination is present and the polymer chain can be extended by adding additional monomer. Because the reaction conditions are different from the cationic polymerization or coordination polymerization that is the usual polymerization mechanism using titanium complexes, polymerizations with various conditions were performed to elucidate the mechanism of polymerization. The polymerization was completely inhibited with the use of galvinoxyl radical, and the molecular weight of resulting polymers decreased with the use of 1-octyl thiols, radical chain transfer agent. The copolymerization of styrene with ethyl vinyl ether using Cp_2TiCl_2 resulted the similar copolymer composition as when BPO was used as radical initiator. It was also possible to polymerize methyl methacrylate with these same titanium complexes. Poly(methyl methacrylate) formed using titanium complexes shows very similar stereoregularity with polymers prepared by conventional radical methods. All these results support that the polymerization mechanism involves radical mechanism. We tried to isolate intermediate species from each step to see if the polymerization using titanium complexes proceeds by ATRP mechanism. We could confirm the activation reaction from the I-PECl and Cp_2TiCl to generate active radical. However, the reversible deactivation reaction competes with other side reactions, and hard to be detected with our model system.

3.7 Experimental

3.7.1 Materials and Characterizations

NMR spectra were measured in CDCl_3 unless otherwise noted. Spectra were recorded on GE 300 spectrometer. ^1H NMR spectra were measured at 300MHz. ^1H chemical shift (δ) were referenced to a selected resonance of residual protons in the solvent employed. Coupling constants are reported in hertz. Elemental analyses were performed by the Atlantic Microlab Inc. Gas chromatography (GC) was performed using either a HP 5890 equipped with MS detector, or a HP 6890 with a FID detector. Non-polar HP-5 or medium polar HP-INNOWAX capillary column were used for the separation. Gel permeation chromatography/light scattering (GPC/LS) were performed using either Hewlett-Packard (HP) 1050 series liquid chromatography pump equipped with a Wyatt Dawn DSP-F laser photometer, a Wyatt/Optilab interferometer and a Waters 746 data module integrator, or Jasco PU-1580 series liquid chromatography pump equipped with a Wyatt Dawn DSP-F laser photometer and a Wyatt/Optilab interferometer. Tetrahydrofuran (THF) was used as the mobile phase. Sample were prepared as 0.5 - 2% polymer (w/v) solution in THF and passed through 0.45 μm filters prior to injection. Residual metal complexes were removed by passing the polymer solution through active alumina column before analysis. Separation were effected by 10^5 \AA , 10^4 \AA , 10^3 \AA , and $5 \times 10^5 \text{ \AA}$ Permagel columns (purchased from Pacific Column Co.) run in series, or a multiple series of Polymer laboratory Mixed C columns at a flow rate of 1 mL/min at 25 $^\circ\text{C}$.

Materials including bis(cyclopentadienyl)titanium dichloride (Cp_2TiCl_2), pentamethyl-cyclopentadienyltitanium trichloride (Cp^*TiCl_3), bis(pentamethylcyclopentadienyl)titanium dichloride ($\text{Cp}^*_2\text{TiCl}_2$), titanium trichloride (TiCl_3), titanium tetrachloride (TiCl_4), copper(I) chloride (CuCl), copper(II) bromide (CuBr_2), pentamethyldiethylene-triamine (PMDETA), bis(cyclopentadienyl)magnesium (Cp_2Mg), zinc metal, TEMPO, galvinoxyl, and 1-octanethiol were obtained from commercial suppliers and used without further purification. Styrene, ethyl vinyl ether and methyl methacrylate (MMA) were dried over CaH_2 overnight, and distilled twice under reduced pressure from CaH_2 prior to use. Benzoyl peroxide (BPO) was purified by dissolving in CHCl_3 at room temperature and adding an equal amount of methanol. α,α' -Azobis(isobutyronitrile) (AIBN) was purified by recrystallizing from acetone. 1-Phenylethyl bromide (1-PEBr) was purchased from Aldrich Chemical and distilled twice under reduced pressure prior to use. 1-phenylethyl chloride (1-PECl)⁴³ and 4,4'-(5-nonyl)-2,2'-bipyridine (dNbpy)⁴⁴ were prepared following literature procedures. Toluene and THF were dry and oxygen-free using a process described by Pangborn, *et al.*⁴⁵

Bis(cyclopentadienyl)titanium chloride (Cp_2TiCl). A mixture of 2 g of TiCl_3 and 2 g of Cp_2Mg in 5 mL of THF was prepared in 25 mL of Schlenk flask equipped with reflux condenser and 3-way stopcork in drybox. The flask was taken out of the drybox, and attached to a vacuum line. With a slow and continuous flow of argon, the flask was heated to reflux for 1.5 h. After reaction, THF was removed by applying vacuum, and the remaining solid was purified by sublimation. The first collection of dark red oil was discarded. The solid sublimed at 170 °C was collected, and characterized by elemental

analysis as a Cp_2TiCl . (Calc'd for $(\text{C}_{10}\text{H}_{10}\text{TiCl})$: C, 56.25; H, 4.72; Cl, 16.60. Found: C, 56.27; H, 4.65; Cl, 16.72.

1-(2,2,6,6-tetramethylpiperidinyloxy)-1-phenylethane (1-PE-TEMPO). 0.68 g (3.7 mmol) of 1-PEBr was added to a Schlenk flask with 0.69 g (4.4 mmol) of TEMPO, 0.25 g (3.8 mmol) of zinc powder, 8.3 mg (0.037 mmol) of CuBr_2 and 7.7 μL (0.037 mmol) of PMDETA. Benzene (5 mL) was then added as solvent, and the solution was degassed by three freeze-pump-thaw cycles. The solution was heated to 75 °C with stirring. After 4 h, all the zinc powder was consumed and a beige precipitate was formed. The reaction solution was loaded onto an alumina column and eluted with hexanes. The eluent strength was increased to 9:1 hexanes: CH_2Cl_2 . The alkoxyamine eluted before TEMPO and was collected as a colorless fraction. The solvent was removed to yield 1-PE-TEMPO as colorless oil. After this oil was stored overnight in a freezer, white crystals formed and were collected, yielding 0.90 g (3.4 mmol) of product (94%). ^1H NMR (300 MHz): δ (ppm) 7.3-7.1 (m, 5H, ArH); 4.78 (q, 1H, ArCH CH_3O , $J = 7$ Hz,); 1.48 (d, 3H, ArCH CH_3O , $J = 7$ Hz,); 1.25, 1.14, 1.02, 0.65 (each a broad singlet, 12H, TEMPO methyls); 1.6-1.2 (m, 6H, TEMPO methylenes).

3.7.2 Polymerization

3.7.2.1 General Methods of Polymerization

Method A: In a 8 mL vial were charged all polymerization components including monomer, initiator, metal catalyst, additives, and solvent under inert atmosphere in a drybox. The vial was sealed with airtight cap having Teflon lining, and taken out of the

box. The vial was further sealed with Teflon tape, and put into a shaker thermostated at desired temperature. The polymerization proceeded in the shaker operated at 250 rpm, and after certain time, the reaction was quenched by putting in liquid nitrogen. The vial was then opened, and THF or methylene chloride was added to dissolve or dilute the polymerization mixture. Conversion was checked either by gravimetry after precipitating polymeric product from methanol following by drying overnight under vacuum, or by directly injecting this solution to GC and determining the remaining monomer content compared with the internal standard. For other characterization such as GPC and NMR, the polymer was purified as meta-free either by repeated dissolving in THF-precipitating from methanol, or by passing short column of active alumina column.

Method B: In a drybox, all polymerization components including monomer, initiator, metal catalyst, additives, and solvent were added to a 5 mL tube having a stirring bar. The reaction tube was taken out of the drybox, degassed three times using freeze-thaw method, and sealed under vacuum. The sealed tube was immersed in an oil bath thermostated at desired temperature, and polymerization proceeded with continuous stirring. After reaction, the seal was broken, and THF or methylene chloride was added to dissolve or dilute the polymerization mixture. All characterization analyses were taken following the same procedure addressed in Method A.

3.7.2.2 Polymerization of Styrene Using Titanium(IV) Complexes

3.7.2.2.1 Kinetic Studies of the Polymerization of Styrene Using Various Titanium(IV) Complexes

In a drybox, a homogeneous solution of titanium(IV) complexes (1×10^{-4} mol), 1-PECl (1×10^{-4} mol), styrene (1×10^{-2} mol) was prepared. The solution was then divided into five vials with airtight cap having Teflon lining. The vials were taken out of the box, and further sealed with Teflon tape. The polymerization proceeded in a shaker thermostated at 130 °C, and operated at 250 rpm. After certain intervals, the reaction was quenched by putting the vial in liquid nitrogen. The vial was then opened, and THF was added to dissolve or dilute the polymerization mixture. Conversion was checked by gravimetry, and number average molecular weight and polydispersity of the product polymer were determined by GPC analysis following the general procedure.

3.7.2.2.2 Chain Extension Reaction

A 5 mL reaction tube was charged with 0.14 g of styrene chloride (1.3×10^{-3} mol), 3.2 mg of Cp_2TiCl_2 (1.3×10^{-5} mol), and 0.11 g of polystyrene prepared using Cp_2TiCl_2 and 1-PECl ($M_n = 8,500$; $\text{PDI} = 1.72$; [polymer chains] = 1.3×10^{-5} mol) in a drybox. The reaction tube was taken out of the drybox, degassed three times using the freeze-thaw method, and sealed under argon. After 4 h of polymerization at 130 °C, THF was added to the mixture, and the product polystyrene was isolated by precipitation from methanol. The polymer was purified by redissolving in THF, precipitation from methanol, and dried overnight under vacuum.

3.7.2.3 Verifying the Mechanism of the Polymerization Using Titanium Complexes

3.7.2.3.1 Polymerization of Styrene with Radical Inhibitors

The polymerization proceeded at 130 °C following the Method A described in the section of general polymerization method. The polymerization mixture was composed of styrene (0.26 g; 2.5×10^{-3} mol), titanium complexes (2.5×10^{-5} mol), 1-PECl (3.5 mg; 2.5×10^{-5} mol), and TEMPO (33 mg; 2.0×10^{-4} mol) or galvinoxyl (11 mg; 1.3×10^{-4} mol).

3.7.2.3.2 Polymerization of Styrene with Radical Chain Transfer Agent

A double set of polymerization mixture composed of styrene (0.21 g; 2.0×10^{-3} mol), titanium complexes (2.0×10^{-5} mol), and 1-PECl (2.8 mg; 2.0×10^{-5} mol) or AIBN (1.6 mg; 1.0×10^{-5} mol) were prepared in 5 mL of drying tubes under argon atmosphere. The tubes were capped with rubber septum, and 1-octanethiol (59 mg; 4×10^{-4} mol) was added to one set of tubes via syringe. The tubes were then sealed under argon, and put in a shaker operating at 250 mL at 130 °C. After the polymerization, seal was broken, THF was added to the mixture, and the product polystyrenes were isolated by precipitation from methanol. The polymers were purified by redissolving in THF, precipitation from methanol, and dried overnight under vacuum.

3.7.2.3.3 Copolymerization of Styrene with Ethyl Vinyl Ether

The polymerization proceeded at 100 °C following the Method A described in the section of general polymerization method. The polymerization mixture was composed of styrene (0.13 g; 1.25×10^{-3} mol), ethyl vinyl ether (0.09 g; 1.25×10^{-3} mol), titanium

complexes (2.5×10^{-5} mol), and 1-PECl (3.5 mg; 2.5×10^{-5} mol). A control polymerization was performed at the same condition following same procedure with styrene (0.13 g; 1.25×10^{-3} mol), vinyl ethyl ether (0.09 g; 1.25×10^{-3} mol), and BPO (6:1 mg; 2.5×10^{-5} mol).

3.7.2.3.4 Polymerization of Methyl Methacrylate

The polymerization proceeded at 100 °C following the Method A described in the section of general polymerization method. The polymerization mixture was composed of MMA (0.25 g; 2.5×10^{-3} mol), titanium complexes (2.5×10^{-5} mol), and 1-PECl (3.5 mg; 2.5×10^{-5} mol).

3.7.2.4 Polymerization of Styrene Using Titanium(III) Complexes (Cp_2TiCl)

The polymerization proceeded at desired temperature following the Method B described in the section of general polymerization method. The polymerization mixture was composed of styrene (0.21 g; 2.0×10^{-3} mol), Cp_2TiCl (4.3 mg; 2.0×10^{-5} mol), 1-PECl (2.8 mg; 2.0×10^{-5} mol), decane (28.5 mg; 2.0×10^{-4} mol) as an internal standard in determination of conversion using GC, and toluene (0.17 g; 50% solution, v/v).

3.7.3 Checking Atom Transfer Reaction

3.7.3.1 Isolation of Activation Steps in ATRP

In a drybox, a solution of 5.5 mg of Cp_2TiCl (2.5×10^{-5} mol), 7.3 mg of 1-PECl (5×10^{-5} mol), and 0.6 mL of toluene- d_8 was prepared at room temperature. On adding 1-PECl, the green color of the Cp_2TiCl solution was immediately changed to red, and after

few minutes, red solid precipitated out. The solution was added to NMR tube having airtight valve. The tube was taken out of the box, and $^1\text{H-NMR}$ spectrum of the solution was taken. The NMR tube was then put in an oil bath at $130\text{ }^\circ\text{C}$. After certain interval, $^1\text{H-NMR}$ spectrum of the solution was taken to follow the reaction.

3.7.3.2 Isolation of Deactivation Steps in ATRP

In a drybox, a solution of 6.2 mg of Cp_2TiCl_2 (2.5×10^{-5} mol), 6.5 mg of 1-PE-TEMPO (2.5×10^{-5} mol), and 0.6 mL of toluene- d_8 was prepared at room temperature. The solution was added to NMR tube having airtight valve. The tube was taken out of the box, and $^1\text{H-NMR}$ spectrum of the solution was taken. The NMR tube was then put in an oil bath at $130\text{ }^\circ\text{C}$. After certain interval, $^1\text{H-NMR}$ spectrum of the solution was taken to follow the reaction.

3.8 References

1. Hasebe, T.; Kamigaito, M.; Sawamoto, M. *Macromolecules* **1996**, *29*, 6100.
2. (a) Natta, G.; Pino, P.; Mazzanti, G.; Giannini, U.; Mantica, E.; Peraldo, M. *J. Polym. Sci.* **1957**, *26*, 120. (b) Breslow, D. S.; Newburg, N. R. *J. Am. Chem. Soc.* **1957**, *79*, 5072. (c) Breslow, D. S.; Newburg, N. R. *J. Am. Chem. Soc.* **1959**, *81*, 81. (d) Long, W. P. *J. Am. Chem. Soc.* **1959**, *81*, 5312. (e) Long, W. P.; Breslow, D. S. *J. Am. Chem. Soc.* **1960**, *82*, 1953. (f) Natta, G.; Mazzanti, G. *Tetrahedron* **1960**, *8*, 86.
3. Long, W. P.; Breslow, D. S. *Liebigs Ann. Chem.* **1975**, 463.
4. Andresen, A.; Cordes, H. G.; Herwig, J.; Kaminsky, W.; Merck, A.; Mottweiler, R.; Pein, J.; Sinn, H.; Vollmer, H. J. *Angew. Chem., Int. Ed. Engl.* **1976**, *15*, 630.
5. Sinn, H.; Kaminsky, W. *Adv. Organomet. Chem.* **1980**, *18*, 99.
6. Kaminsky, W.; Arndt, M. *Adv. Polym. Sci.* **1997**, *127*, 143.
7. (a) Ewen, J. A. In *Catalytic Polymerization of Olefins, Studies in Surface Science and Catalysis*; Keii, T., Soga, K., Eds.; Elsevier: New York, 1986; p 271. (b) Giannetti, E.; Nicoletti, G.; Mazzocchi, R. *J. Polym. Sci. Polym. Chem.* **1985**, *23*, 2117.
8. (a) Ewen, J. A. *J. Am. Chem. Soc.* **1984**, *106*, 6355. (b) Kaminsky, W.; Kulper, K.; Brintzinger, H.; Wild, F. *Angew. Chem., Int. Ed. Engl.* **1985**, *24*, 507.
9. (a) Bereaw, J. E. Presented at 3rd Chemical Congress of North America, Toronto, Canada, June 1988. (b) Shapiro, P. J.; Bunel, E.; Schaefer, W. P.; Bereaw, J. E. *Organometallics* **1990**, *9*, 867.
10. Okuda, J. *Chem. Ber.* **1990**, *123*, 1649.
11. (a) Canich, J. A. M. (Exxon). U.S. Patent 5,026,798, 1991. (b) Canich, J. A. M.; Lieciardi, G. F. (Exxon). U.S. Patent 5,057,475, 1991.
12. Canich, J. A. M. (Exxon). Eur. Pat. Appl. 0 420 436 A1, 1991.
13. Stevens, J. C.; Timmers, F. J.; Wilson, D. R.; Schmidt, G. F.; Nickias, P. N.; Rosen, R. K.; Knight, G. W.; Lai, S.-y. (Dow). Eur. Pat. Appl. 0 416 815 A2, 1991.
14. Stevens, J. C.; Neithamer, D. R. (Dow). Eur. Pat. Appl. 0 418044 A2, 1991.

-
15. (a) Pannell, R. B.; Canich, J. A. M.; Hlatky, G. G. (Exxon). PCT Int. Appl. WO 94/00500, 1994. (b) Brant, P.; Canich, J. A. M. (Exxon). PCT Int. Appl. WO 93/12151, 1993. (c) Brant, P.; Canich, J. A. M.; Merrill, N. A. (Exxon). PCT Int. Appl. WO 93/21242, 1993. (d) Brant, P.; Canich, J. A. M.; Dias, A. J.; Bamberger, R. L.; Licciardi, G. F.; Henrichs, P. M. (Exxon). PCT Intl. Appl. 94/07930, 1994. (e) LaPointe, R. E.; Rosen, R. K.; Nickias, P. N. (Dow). Eur. Pat. Appl. 0 495 375 A2, 1992. (f) Lai, S. Y.; Wilson, J. R.; Knight, G. W.; Stevens, J. C. (Dow). PCT Int. Appl. WO 93/08221, 1993. (g) Rosen, R. K.; Nickias, P. N.; Devore, D. D.; Stevens, J. C.; Timmers, F. J. (Dow). U.S. Patent 5,374,696, 1994. (h) Nickias, P. N.; McAdon, M. H.; Patton, J. T. (Dow). PCT Int. Appl. WO 97/15583, 1997.
16. Canich, J. A. M. (Exxon). U.S. Patent 5,096,867, 1992.
17. Canich, J. A. M. (Exxon). PCT Int. Appl. WO 96/00244, 1996.
18. LaPointe, R. E.; Stevens, J. C.; Nickias, P. N.; McAdon, M. H. (Dow). Eur. Pat. Appl. O 520 732 A1, 1992.
19. Devore, D. D.; Crawford, L. H.; Stevens, J. C.; Timmers, F. J.; Mussell, R. D.; Wilson, D. R.; Rosen, R. K. (Dow). PCT Int. Appl. WO 95/00526, 1995.
20. (a) Harrington, B. A. (Exxon). PCT Int. Appl. WO 96/40806, 1996. (b) Harrington, B. A.; Hlatkey, G. G.; Canich, J. A. M.; Merrill, N. A. (Exxon). U.S. Patent 5,635,573, 1997.
21. (a) Devore, D. D. (Dow). Eur. Pat. Appl. 0 514 828 A1, 1992. (b) Sernetz, F. G.; Muelhaupt, R.; Waymouth, R. M. *Macromol. Chem. Phys.* **1996**, *197*, 1071-83. (c) Xu, G. *Macromolecules* **1998**, *31*, 2395-2402.
22. Stevens, J. C. *Stud. Surf. Sci. Catal.* **1996**, *101*, 11.
23. Endo, K.; Saitoh, M. *Polymer J.* **2000**, *32*, 300.
24. Ishihara, N.; Kuramoto, M.; Uoi, M. *Macromolecules* **1988**, *21*, 3356.
25. (a) Zambelli, A.; Oliva, L.; Pellicchia, C. *Macromolecules* **1989**, *22*, 2129. (b) Pellicchia, C.; Longo, P.; Proto, A.; Zambelli, A. *Makromol. Chem., Rapid Commun.* **1992**, *13*, 265.
26. (a) Foster, P. F.; Chien, J. C. W.; Rausch, M. D. *Organometallics* **1996**, *15*, 2404. (b) Ready, T. E.; Chien, J. C. W.; Rausch, M. D. *J. Organomet. Chem.* **1996**, *519*, 21.

-
27. (a) Zambelli, A.; Longo, P.; Pellicchia, C.; Grassi, A. *Macromolecules* **1987**, *20*, 2035. (b) Grassi, A.; Saccheo, S.; Zambelli, A.; Laschi, F. *Macromolecules* **1998**, *31*, 5591.
28. Soga, K.; Yu, C. H.; Shiono, T. *Makromol. Chem., Rapid Commun.* **1988**, *9*, 351.
29. Duncalf, D. J.; Wade, H. J.; Waterson, C.; Derrick, P. J.; Haddleton, D. M.; McCamley, A. *Macromolecules* **1996**, *29*, 6399.
30. Herman, D. F.; Nelson, W. K. *J. Am. Chem. Soc.* **1953**, *75*, 3877.
31. Nesmeyanov, A. N.; Nogina, O. V.; Freidlina, R. K. *Dokl. Akad. Nauk SSSR* **1954**, *95*, 813.
32. Inoue, S.; Tsuruta, T.; Furukawa, J. *Makromol. Chem.* **1961**, *49*, 13.
33. (a) Wang, J.-S.; Matyjaszewski, K. *J. Am. Chem. Soc.* **1995**, *117*, 5614. (b) Percec, V.; Barboiu, B. *Macromolecules* **1995**, *28*, 7970. (c) Haddleton, D. M.; Jasieczek, C. B.; Hannon, M. J.; Shooter, A. J. *Macromolecules* **1997**, *30*, 2190.
34. (a) Kato, M.; Kamigaito, M.; Sawamoto, M.; Higashimura, T. *Macromolecules* **1995**, *28*, 1721. (b) Takahashi, H.; Ando, T.; Kamigaito, M.; Sawamoto, M. *Macromolecules* **1999**, *32*, 6461.
35. (a) Ando, T.; Kamigaito, M.; Sawamoto, M. *Macromolecules* **1997**, *30*, 4507. (b) Matyjaszewski, K.; Wei, M.; Xia, J.; McDermott, N. E. *Macromolecules* **1997**, *30*, 8161. (c) Teodorescu, M.; Gaynor, S. G.; Matyjaszewski, K. *Macromolecules* **2000**, *33*, 2335. (d) Kotani, Y.; Kamigaito, M.; Sawamoto, M. *Macromolecules* **2000**, *33*, 3543.
36. (a) Granel, C.; Dubois, Ph.; Jérôme, R.; Teyssié, Ph. *Macromolecules* **1996**, *29*, 8576. (b) Uegaki, H.; Kotani, Y.; Kamigaito, M.; Sawamoto, M. *Macromolecules* **1997**, *30*, 2249. (c) Moineau, G.; Minet, M.; Dubois, Ph.; Teyssié, Ph.; Senninger, T.; Jérôme, R. *Macromolecules* **1999**, *32*, 27.
37. Lecomte, Ph.; Draiper, I.; Dubois, Ph.; Teyssié, Ph.; Jérôme, R. *Macromolecules* **1997**, *30*, 7631.
38. (a) Percec, V.; Barboiu, B.; Neumann, A.; Ronda, J. C.; Zhao, M. *Macromolecules* **1996**, *29*, 3665. (b) Moineau, G.; Granel, C.; Dubois, Ph.; Jérôme, R.; Teyssié, Ph. *Macromolecules* **1998**, *31*, 542. (c) Petrucci, M. G. L.; Lebuis, A.-M.; Kakkar, A. K. *Organometallics* **1998**, *17*, 4966.
39. Kotani, Y.; Kamigaito, M.; Sawamoto, M. *Macromolecules* **1999**, *32*, 2420.

-
40. Brandts, J. A. M.; van de Geijn, P.; van Faassen, E. E.; Boersma, J.; van Koten, G. J. *Organomet. Chem.* **1999**, *584(2)*, 246.
41. Matyjaszewski, K.; Woodworth, B. E.; Zhang, X.; Gaynor, S. G.; Metzner, Z. *Macromolecules* **1998**, *31*, 5955.
42. Li, I.; Howell, B. A.; Matyjaszewski, K.; Shigemoto, T.; Smith, P. B.; Priddy, D. B. *Macromolecules* **1995**, *28*, 6692.
43. Landini, D.; Rolla, F. *J. Org. Chem.* **1980**, *45*, 3527.
44. Matyjaszewski, K.; Patten, T. E.; Xia, J. *J. Am. Chem. Soc.* **1997**, *119*, 674.
45. Pangborn, A. B.; Giardello, M. A.; Grubbs, R. H.; Rosen, R. K.; Timmers, F. J. *Organometallics* **1996**, 1518.

CHAPTER 4

PREPARATION OF POLYMERS HAVING VARIOUS ARCHITECTURES USING CONTROLLED RADICAL POLYMERIZATION TECHNIQUES

4.1 Introduction

Driven by developing technologies, the demand for new materials has been growing continuously and significantly in modern society. The advantage of polymers over other materials such as metals and ceramics is the ability to tailor their chemical or physical properties by modifying their functionality and architecture. Incorporating functional groups is one direction researchers have used to modify properties. Functional polymers are those polymers whose properties and characteristics are based on functional groups.¹ Typical functionalities include chemically reactive, biologically active, electroactive, photoactive, ionic, polar, and optically active groups.² With the many options available, functionalized polymers are finding utility as reagents in organic synthesis, catalysis, trace analysis, sensory materials, packing material for chromatographic applications, and medicinal applications.³ Another approach to tailoring polymer properties is the synthesis of materials with novel architectures. Changing the architecture of a polymer can endow the polymers with unique physical properties.^{1,4} Indeed, an astonishing number of polymer architectures have already been synthesized (Figures 4.1 and 4.2).^{4,5} These architectures include the random coil conformation of most synthetic polymers in solution (**i**), helices (**ii**), rigid rods (**iii**), dendrimers (**iv**), hyperbranched (**v**), rings (**vi**), ribbons (or ladders, **vii**), stars (with up to 200 arms, **viii**), and combs (or grafts, **ix**). Combination of the above architectures are being developed to yield tadpole shaped polymers (dendrimers and random coil, **x**), bolo polymers (two dendrimers at the end of a random coil, **xi**), bead polymers (**xii**), cyclic ribbons (**xiii**), linked rings (or cyclophanes, **xiv**), cyclopolymers (**xv**), threaded rings (or rotaxanes, **xvi**), and broken worms (**xvii**). A polymer composed of two or more monomers allows the preparation of di-block

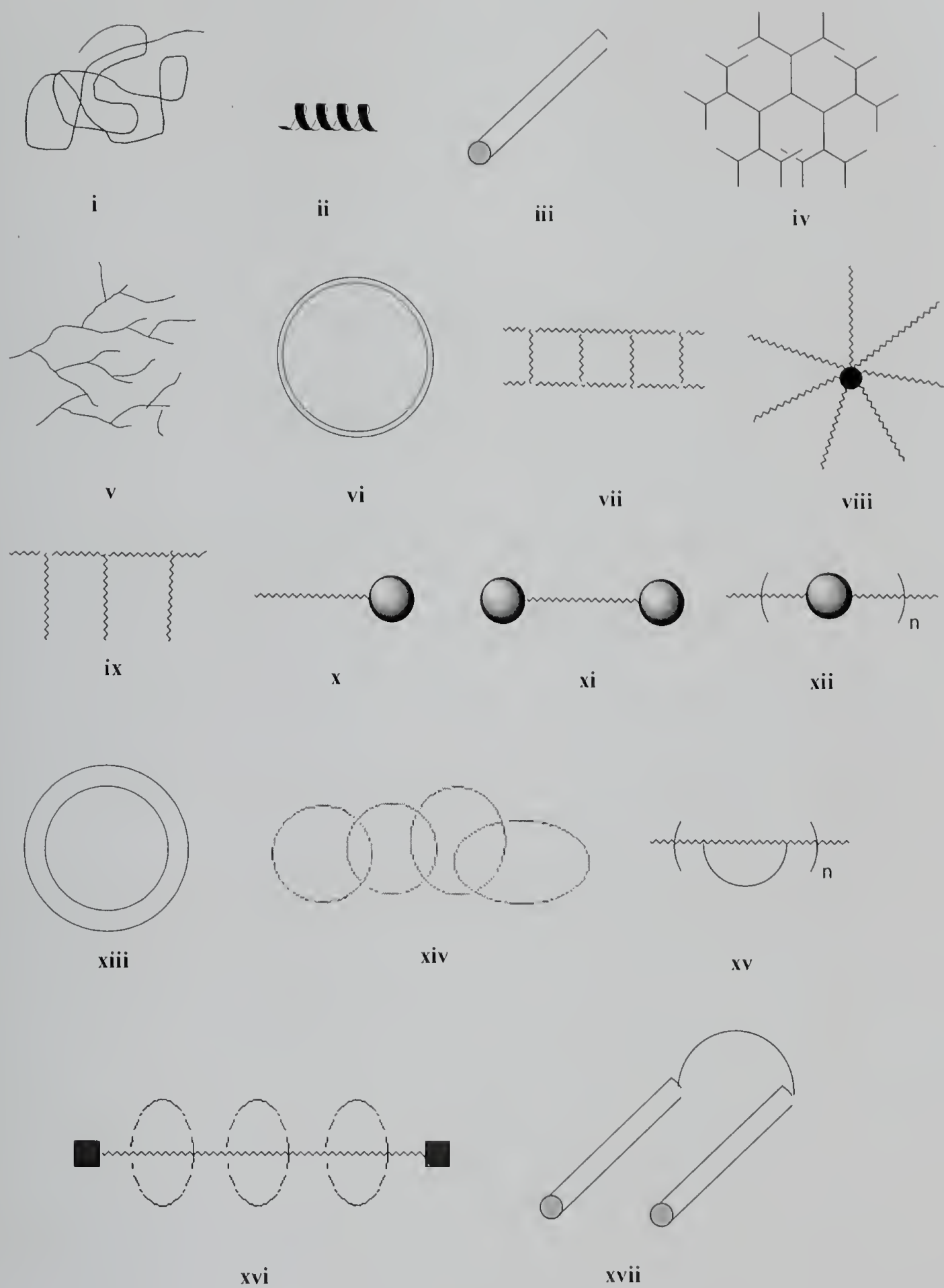


Figure 4.1 Polymer architectures that have been prepared to date.

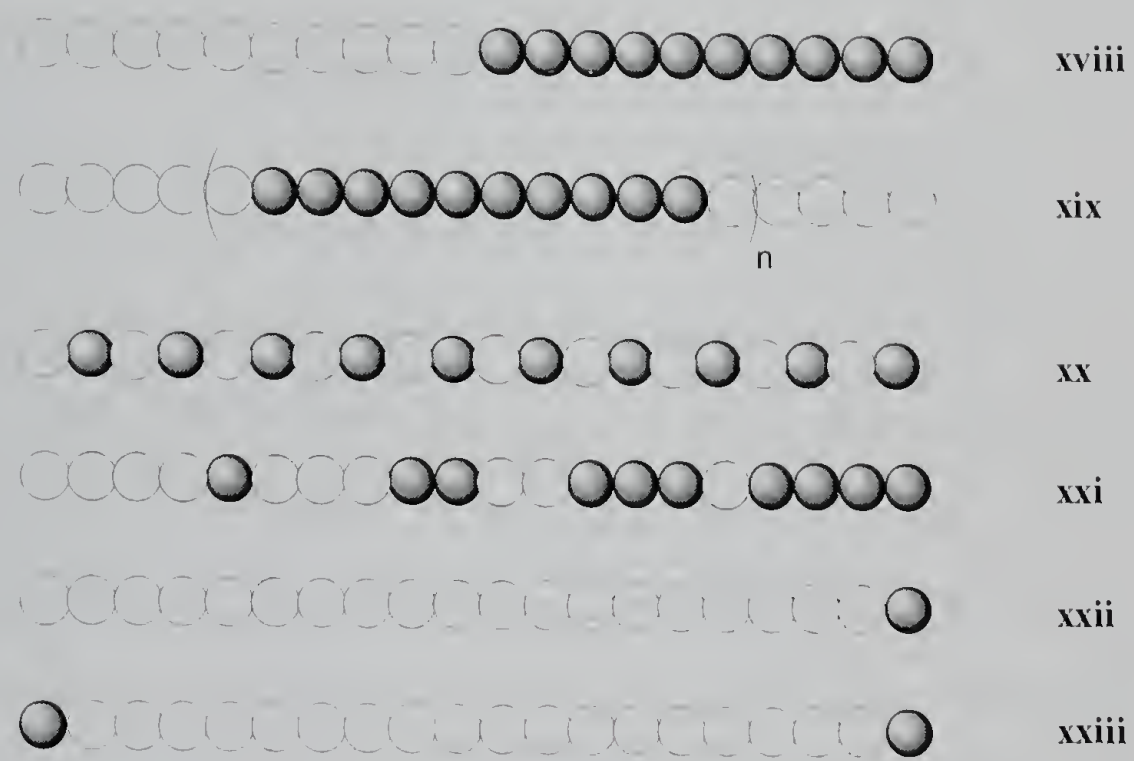


Figure 4.2 Polymer architectures involving two monomers, A (○) and B (●).

copolymers (xviii), tri-block copolymers ($n = 1$, xix), random block copolymers ($n > 1$, xix), alternating copolymers (xx), and end-functionalized polymers (xxi, xxii). Some of these architectures have already found applications as high-temperature plastics (vii), strengthening agents (viii), elastomer (ix), adhesives (ix), compatibilizers for polymer blending (xviii), dispersing agents (xviii, xxi), thermoplastic elastomers (xix), and crosslinking agents (xxii).

In order to fashion polymers with these architectures described above to be realized, there must be simultaneous improvements in polymer synthetic methods. Living polymerizations have been used extensively to this end.⁶ Living polymerization was first defined by Szwarc⁷ as a chain growth process without chain breaking reactions (transfer and termination). Such a polymerization provides endgroup control and enables the synthesis of macromolecules with important architectures such as block copolymers by the sequential monomer addition. However, all living polymerizations do not necessarily provide the necessary control of the molecular weight and a narrow molecular weight distribution of the product polymer. Some control over the polymer structure can be achieved even in the presence of transfer and termination reactions as long as their rates are low enough not too significant. In addition to slow transfer and termination steps, controlled polymerization requires fast initiation compared to propagation reaction, fast exchange between various active species compared to propagation reaction of the fastest species, and slower depropagation than propagation rates. With these pre-requisition met, it is possible to achieve control over the molecular weight of the polymer and provide a unimodal, narrow molecular weight distribution. Under these conditions, it becomes possible to prepare polymers having the novel architectures shown in Figure 4.1.

Until this point, most well-defined polymers have been prepared using ionic polymerization methods. Unfortunately, these reactions have to be carried out under very strict conditions, which include exclusion of oxygen and moisture, and at low temperatures. Moreover, there is a limitation on the monomers that can be polymerized by ionic (either anionic or cationic) polymerization methods. Because the active centers have an ionic charge, these polymerizations are successful only with monomers that have substituent groups that can stabilize the active center. For example, vinyl monomers having electron-donating groups such as α -olefins and vinyl ethers cannot be polymerized via anionic mechanism. Likewise, vinyl monomers having electron-withdrawing groups such as vinyl halides and acrylates do not polymerize with cationic initiators. With a lesser dependence on electronic substituents, radical polymerizations thus have advantages over ionic polymerizations. A large variety of monomers can be polymerized or copolymerized radically, and reaction conditions are not particularly demanding e.g., these reactions tolerate water, acids and bases, and in some cases, oxygen.

Even though “living”/controlled free radical polymerizations are not perfect living systems, they are more than adequate to a sufficient level of control to afford the synthesis of various architectures. This is due to the facts that irreversible termination reactions are minimized by maintaining a dynamic equilibrium between active radicals and a large concentration of the dormant species, and that the initiation step is fast and quantitative. As a result, there have been an enormous number of reports of using controlled radical polymerization methods to prepare polymers with specific architectures. Examples include block copolymers,⁸ branched⁹ and hyperbranched polymers,^{9b,10} star polymers,^{9a,11} and dendritic polymers.¹² We too, have been interested

in the development of strategies to prepare polymers having various architectures using controlled radical polymerization techniques.

Of the various non-linear polymer architectures, branched and hyperbranched polymers hold particular attraction in academics and industry due to their unusual and/or improved properties for some applications. For example, these polymers have been shown to be useful as rheology control agents, compatibilizers for polymer blends, and emulsifiers.¹³ For these reasons, we developed strategies to prepare branched and hyperbranched polymers using controlled free radical polymerization techniques.

4.2 Preparation of Branched (or Comb) Polymers by the Sequential Use of Conventional Radical Polymerization and ATRP

The first goal was to prepare branched polymers using a combination of conventional free radical polymerization and atom transfer radical polymerization (ATRP) techniques. One of the unique features of ATRP is the structure of the initiator, which differs substantially from initiators used for the conventional radical polymerization. Typical ATRP initiators have relatively simple chemical structures, such as activated alkyl halides or sulfonyl chlorides. These groups can be easily incorporated into the monomers without significantly affecting the reactivity of vinyl groups in the radical polymerization. For the polymerization of styrene, benzyl halides are widely used as initiating groups because they have the same structure as the dormant species present during the polymerization. Although it is known that polystyrene initiated by 1-phenylethyl chloride (1-PECl) has a lower polydispersity index (PDI) value than that from

a benzyl chloride initiator,¹⁴ we elected to use benzyl chloride initiating groups because they are much easier to incorporate into styrene monomers.

Our approach to branched or comb polymers was to prepare the backbone by conventional polymerization of benzyl chloride substituted monomers followed by grafting of the arms using ATRP techniques. The backbone polymers were prepared by the conventional free radical polymerization technique using α,α' -azobis(isobutyronitrile) (AIBN) as an initiator. Styrene and vinylbenzyl chloride (50/50) were copolymerized in benzene at 60 °C. The resulting copolymer had $M_n = 36,600$, and PDI = 1.82. ¹H-NMR spectrum shows that the content of vinylbenzyl chloride in the copolymer is about 50%, which is equal to the initial monomer feed ratio. This copolymer could then be used to prepare graft copolymers by the controlled growth of grafted chains from the benzyl chloride groups of the backbone by ATRP technique. Polystyrene branches were prepared using CuCl/4,4'-diphenoxybipyridine (pby) as a catalyst system. GPC chromatographic analysis shows the molecular weight of the product branched copolymer increased unimodally (Figure 4.3). This indicates termination reactions by coupling two active radicals were minimized, and the occurrence of crosslinked product by inter-chain coupling reaction was absent. However, at high conversions, coupling products were observed. This observation is consistent with the fact that ATRP is not perfectly free from the termination reactions, and the density of the initiating sites along the backbone polymer chain is high.

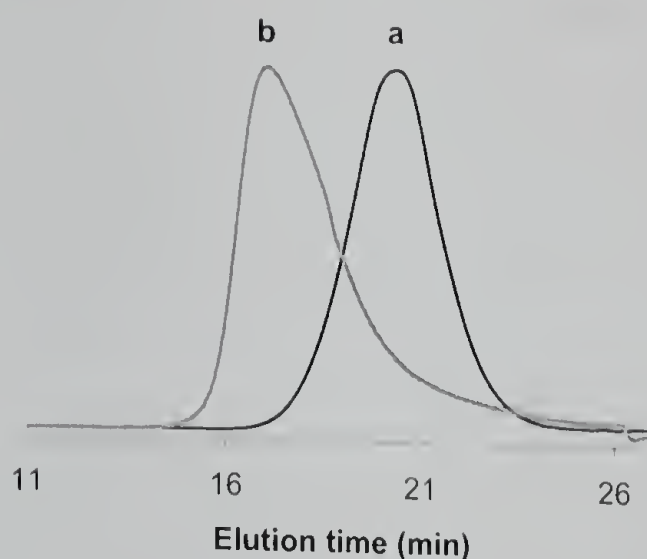


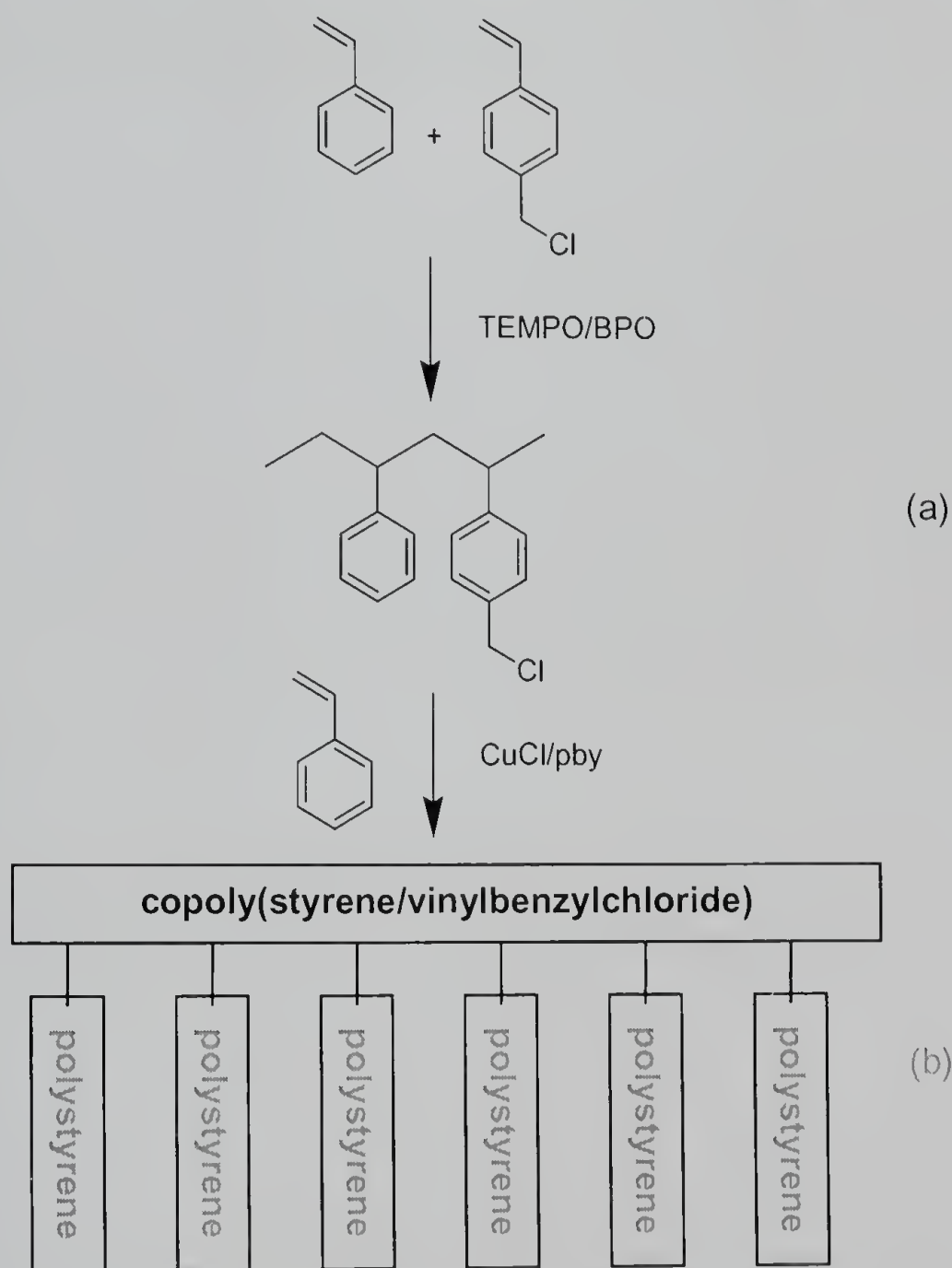
Figure 4.3 GPC chromatograms of (a) backbone polymer prepared by conventional free radical polymerization method and (b) branched polymer prepared by ATRP.

4.3 Branched Polymers by the Sequential Use of Two Different Controlled Free Radical Polymerization Methods

Well-defined branched polymers also can be prepared by the sequential use of nitroxide-mediated stable free radical polymerization (SFRP) and ATRP methods. The previous approach controls the structure of the branches, but there was no control during the preparation of the backbone polymer. This could be overcome by applying another controlled radical polymerization technique to the preparation of the polymer backbone (Scheme 4.1). Vinylbenzyl chloride could be copolymerized with styrene by the nitroxide-mediated SFRP method using benzoyl peroxide (BPO)/TEMPO. The polymerization was well controlled and the prepared polymer had controlled molecular weight and low polydispersity ($M_n = 12,600$; PDI = 1.17). The chloromethyl groups of this copolymer were again used as initiating sites for the graft copolymerization of second monomer by ATRP method using CuCl/pby as a polymerization catalyst. GPC chromatographic analysis of the resulting graft copolymer shows that the molecular weight increases unimodally while maintaining low polydispersity ($M_n = 125,000$; PDI =

1.19), and there is no polystyrene homopolymer formed by thermal initiation (Figure 4.4). Using this SFRP/ATRP sequential method, the structures of both backbone and branch polymers could be well controlled.

Scheme 4.1 Preparation of Branched Polymers by the Sequential Use of Two Different Controlled Free Radical Polymerization Methods



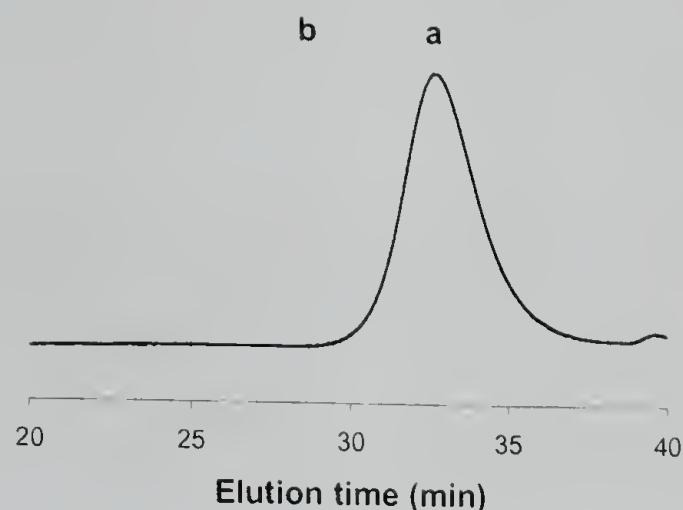


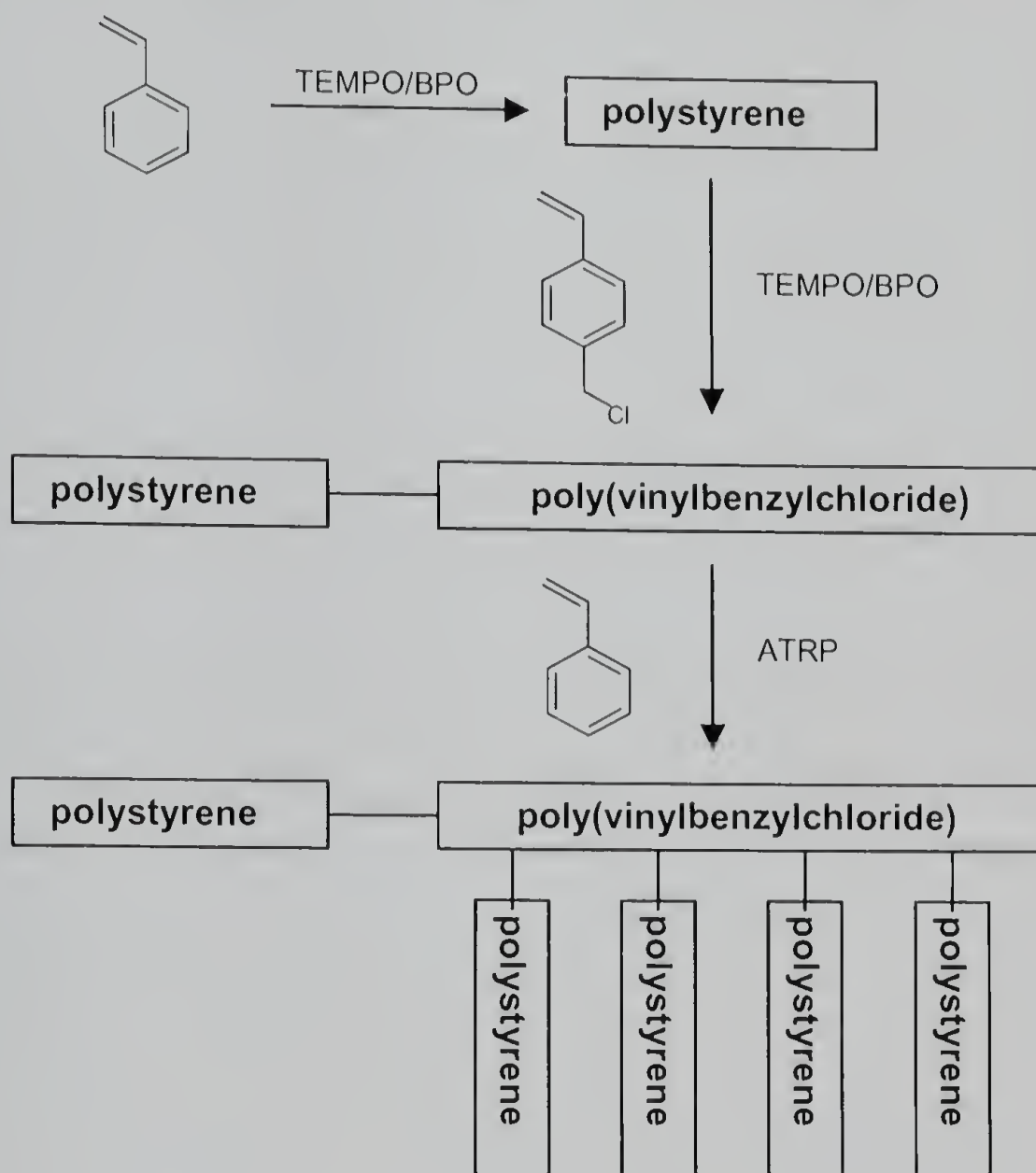
Figure 4.4 GPC chromatograms of (a) backbone polymer prepared by nitroxide-mediated SFRP method and (b) branched polymer by ATRP.

The sequential use of two different controlled free radical polymerizations provides various controls over the branched polymer structure. Not only are we able to control the molecular weight and polydispersity of the branched polymers, but we also have the ability to vary the structure of the branched polymer by changing composition of monomers of backbone polymer, copolymerization method (block or random), and the monomer used for the branches. As an example, we prepared linear-branched block copolymer using this approach.

Block copolymers of styrene and vinylbenzyl chloride were prepared and used as backbone polymers. In the first step, polystyrene was prepared by the nitroxide-mediated SFRP method using the BPO/TEMPO bimolecular initiating system. This polymer bearing terminal nitroxide groups isolated and later reinitiated by heating at 130 °C in the presence of the vinylbenzyl chloride monomer. The benzylchloride groups along the

second block segment were then used as branch-initiating sites by ATRP to give a linear-branched block copolymer (Scheme 4.2).

Scheme 4.2 Preparation of Linear-Branched Block Copolymer by the Sequential Use of Two Different Controlled Free Radical Polymerization Methods



In this example, the density of the benzylchloride groups along the backbone was very high because the second block was a homopolymer of vinylbenzyl chloride. The possibility of uncontrolled intra- and inter-molecular coupling reactions is likewise very high, and the reaction mixtures easily gelled even at slightly extended reaction times. To

avoid the undesired gellation, we stopped the graft polymerizations at low conversions. Figure 4.5 shows the GPC chromatograms for the polymers in each step. The molecular weight of the backbone poly(styrene-*b*-(vinylbenzyl chloride)) ($M_n = 8,800$; PDI = 1.18) was clearly extended during the blocking process from the initial polystyrene ($M_n = 4,500$; PDI = 1.19), and the molecular weights of both segments were well-matched with

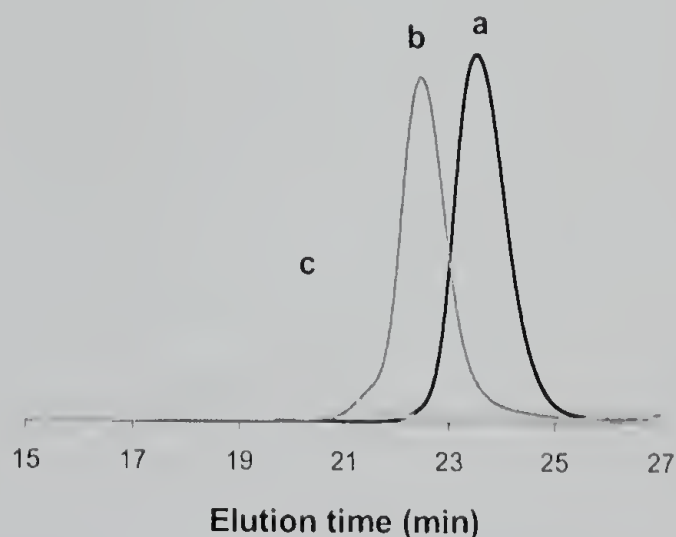


Figure 4.5 GPC chromatograms of linear-branched block copolymers prepared by the sequential use of two different controlled free radical polymerization methods: (a) initial polystyrene by nitroxide-mediated SFRP method (---); (b) linear block copoly(styrene-*b*-vinylbenzyl chloride) (- -); and (c) linear-branched block copolymers ().

the values calculated from the initiator/monomer ratios and the yields of the polymerization. The polydispersity of the polymers were fairly low at less than 1.2. The molecular weight of the branched polymer during the grafting process also increased to higher molecular weight, and there was no residual peak for the remaining backbone copolymer. However, the GPC chromatogram of the branched polymer was not unimodal, and was composed of a main peak at lower molecular weight and a higher molecular weight shoulder. We attribute this shoulder to the product resulting from the coupling of individual chains. The backbone block copolymer was grown in controlled fashion as

evidenced by a well-shaped main peak, but even at low conversion, the intermolecular termination reaction took place to form the higher molecular weight shoulder.

4.4 Hyperbranched Polymers by the Sequential Use of Two Different Controlled Free Radical Polymerization Methods

By combining these different radical polymerization techniques, it is possible to prepare various polymer structures. In addition to the branched polymers shown in the previous section, we prepared both hyperbranched and star-like polymers. Hyperbranched polymers were prepared using an “inverse” synthetic approach. In this case, the ATRP method was first used to prepare hyperbranched polymers from an AB₂ type monomer through a process that is sometimes called a self-condensing vinyl polymerization.¹⁵ Vinylbenzyl chloride has two different functional groups that are reactive under ATRP conditions: a vinyl group that is a normal polymerizable group in radical process, and the benzyl chloride group that can generate radical by the activation reaction in ATRP. Therefore, homopolymerization of this monomer using ATRP produces hyperbranched polymers. Specifically, we used this approach to prepare hyperbranched polymers from vinylbenzyl chloride using CuCl/bipyridine (bpy) as a catalyst system at 130 °C. The product polymer was analyzed by GPC and found to have $M_n = 1,400$ and PDI = 1.98 based on linear polystyrene standards. Because of the compact structure of the hyperbranched polymer, the real molecular weight is expected to be higher. Evidence of the hyperbranched structure is presented in Figure 4.6, which shows the plot of molecular weight vs. radius of gyration of the polymer measured by GPC/light scattering (LS). The slope of this plot corresponds to 1/3 for a solid sphere, 1/2 for a random coil, and 1 for a rigid-rod polymer. Compared with linear polystyrene, the product polymer has smaller

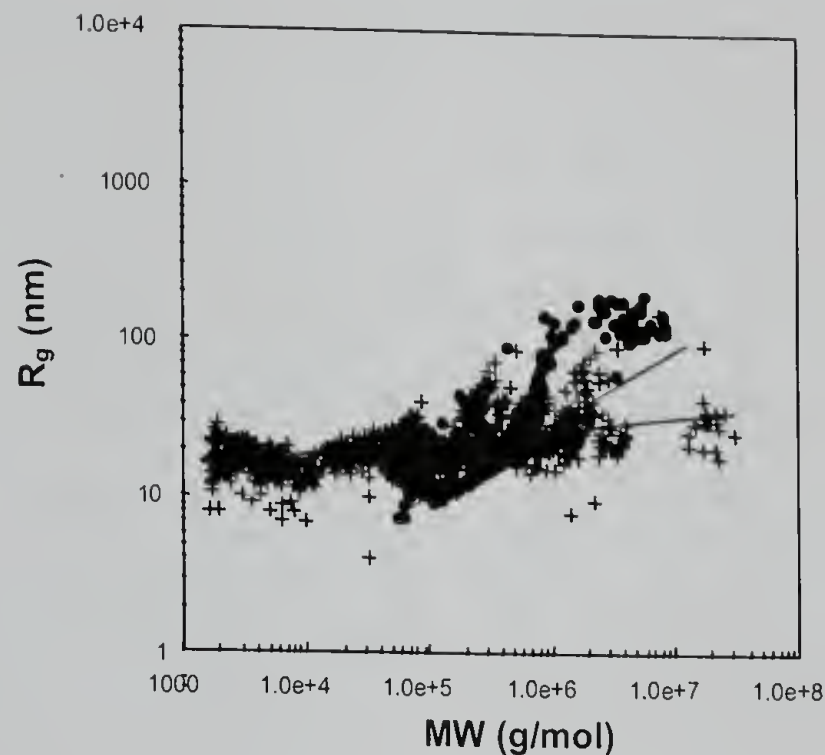


Figure 4.6 Plots of of molecular weight (MW) vs. radius of gyration (R_g) of the polymer measured by GPC-LS, linear polystyrene (\diamond , slope = 0.472) and hyperbranched poly(vinylmethyl chloride) (+, slope = 0.082).

values for the slope that indicate a more compact structure, which is consistent with a hyperbranched structure. The hyperbranched polymer has a single terminal vinyl group that emanates from the initiating point. The $^1\text{H-NMR}$ spectrum of the polymer shows the vinyl protons in from the initiating point. The $^1\text{H-NMR}$ spectrum of the polymer shows the vinyl protons in the hyperbranched polymers (Figure 4.7). From the ratio of the area of the vinyl protons to aromatic and aliphatic protons, we calculate the number average molecular weight of the hyperbranched polymer to be 2,100, which, as expected, is higher than the value calculated based on GPC results. The number of chloromethyl groups in the polymer chains was also calculated from the ratio of vinyl protons and methylene protons of chloromethyl groups in the $^1\text{H-NMR}$ spectrum: This calculation shows that the number of chloromethyl groups present in a hyperbranched chain on average is 11.2.

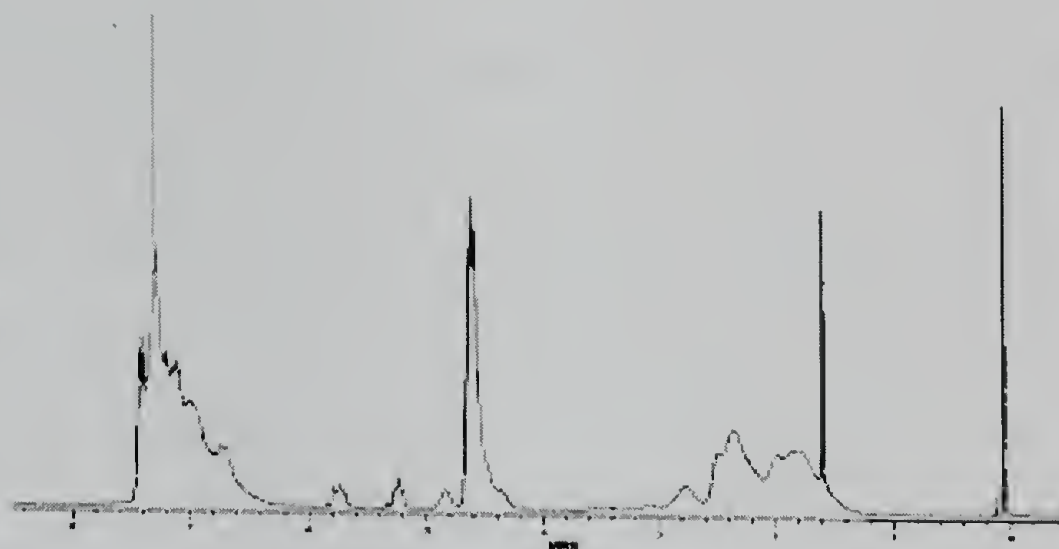


Figure 4.7 ^1H -NMR spectrum of hyperbranched poly(vinylbenzyl chloride).

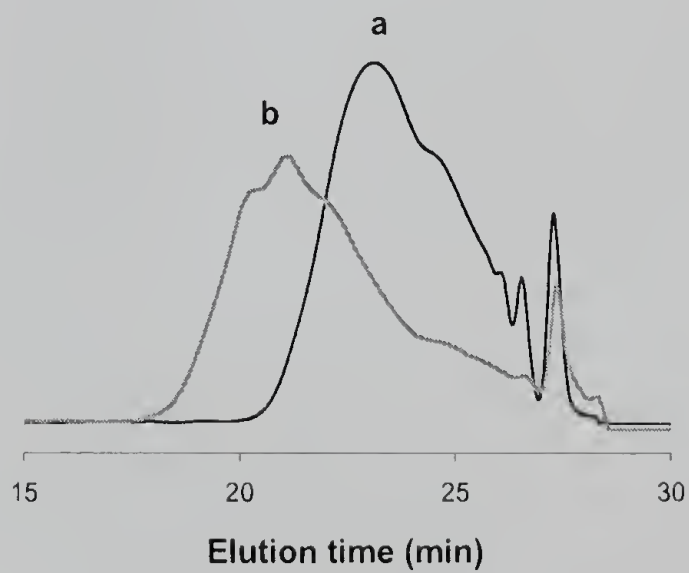
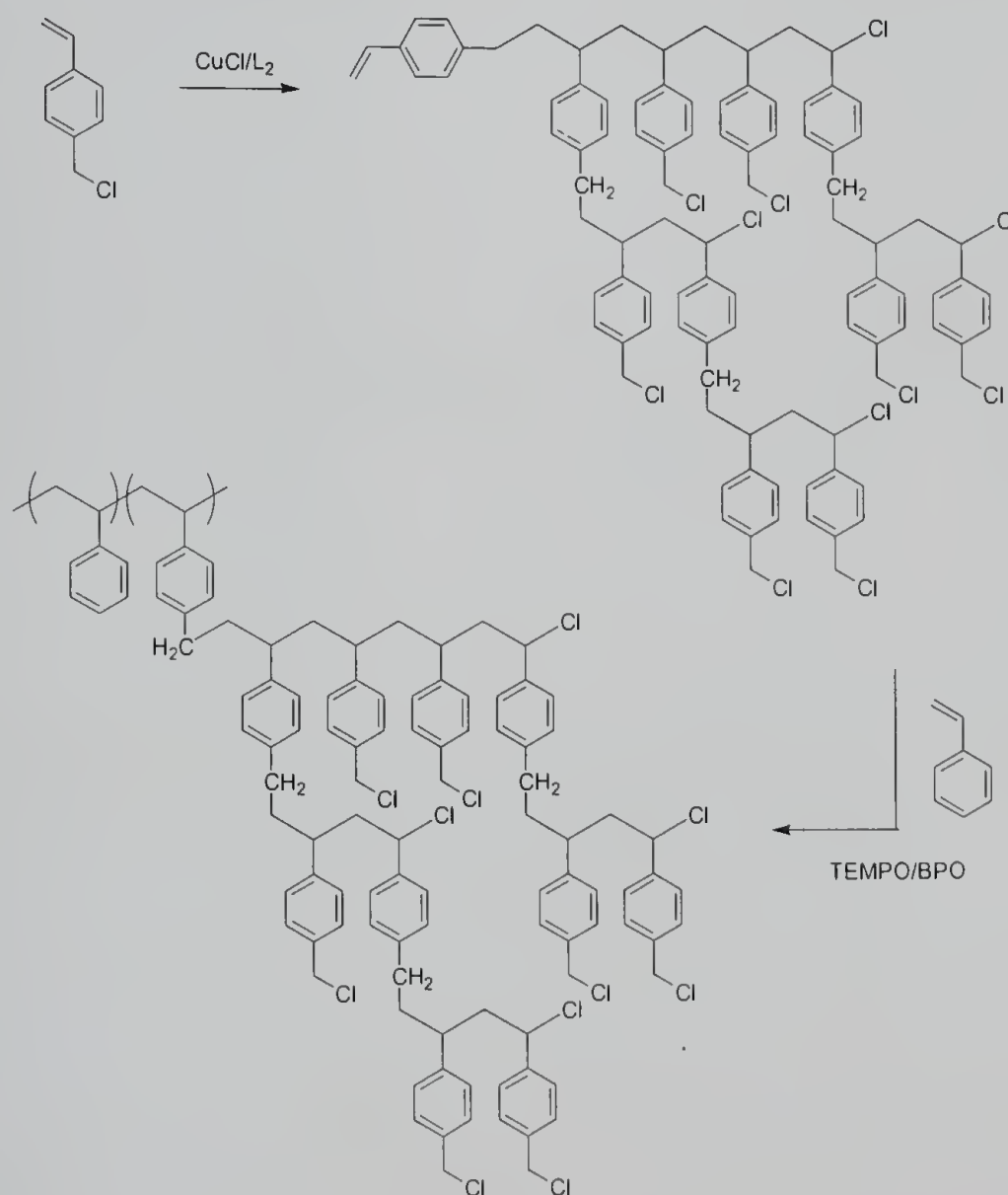


Figure 4.8 GPC chromatograms of (a) poly(vinylbenzyl chloride) and (b) styrene-poly(vinylbenzyl chloride) copolymer.

The vinyl groups at one end of the hyperbranched polystyrenes make it possible for these polymers to act as macromonomers, which could be copolymerized with styrene using the nitroxide-mediated SFRP method to control the branching density of polymers (Scheme 4.3). The reaction of the hyperbranched macromonomers with additional styrene and BPO/TEMPO at 130 °C resulted a copolymer having $M_n = 39,800$ and $PDI = 1.66$. The GPC chromatogram of the resulting copolymer shows a unimodal distribution (Figure 4.8).

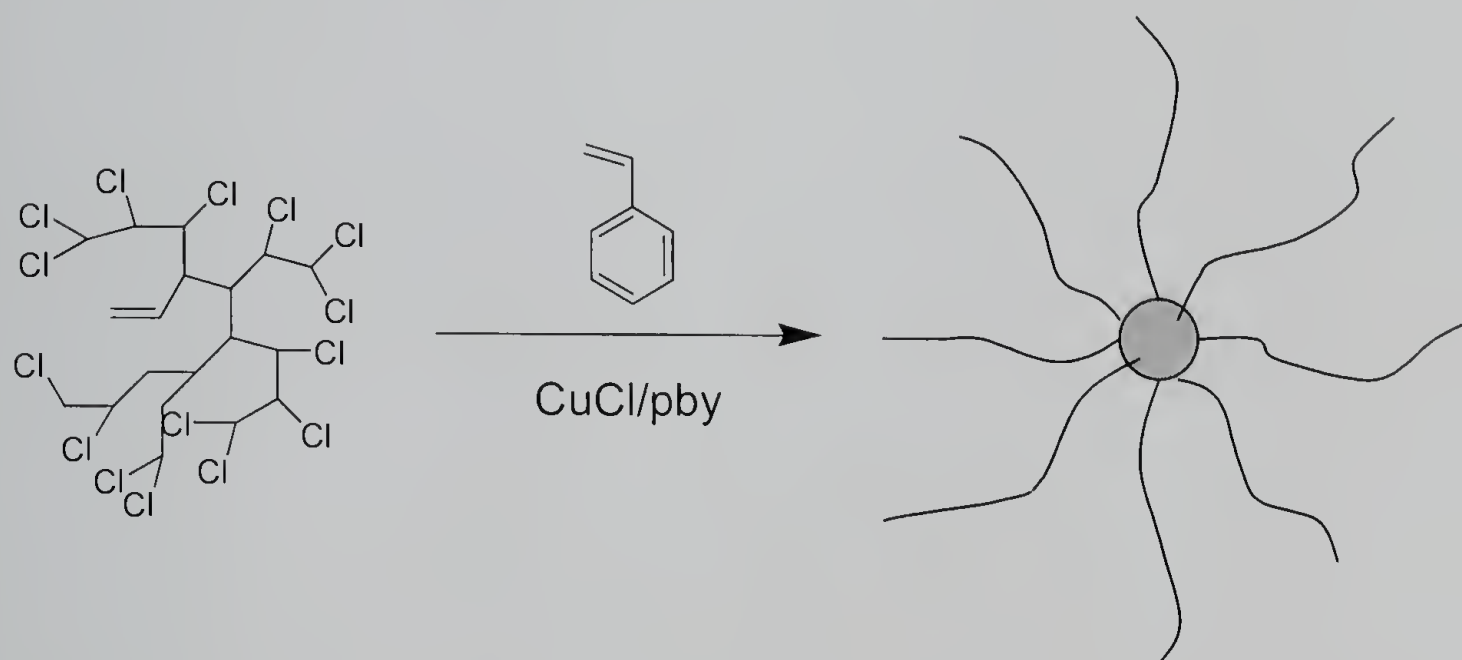
Scheme 4.3 Preparation of Hyperbranched Polymers by the Sequential Use of Two Different Controlled Free Radical Polymerization Methods



4.5 Star-like Polymers by Two-Step Reaction Using ATRP Methods

Slight modification of the polymerization method has the potential to generate new structures of polymers. From the same hyperbranched macromonomer and the same secondary monomer (styrene), we prepared star-like polymers. Instead of using nitroxide-mediated SFRP methods (BPO/TEMPO) in the second step, we used CuCl/pby as an ATRP catalyst system. Under this conditions, the chloromethyl groups of initial hyperbranched polymer act as initiating sites of ATRP in the second step.

Scheme 4.4 Preparation of Star-Like Polymers by Two-Step Reaction Using ATRP Methods



Although the initial hyperbranched polymer doesn't have a perfect globular structure, the relatively compact structure can be considered as a legitimate core, and the polystyrene branches grow from it to form star-like structure (Scheme 4.4). In this procedure, the vinyl group presented on the hyperbranched polymer could also be incorporated in a chain with another core to produce complex structure. However, the concentration of the vinyl groups is much smaller than that of styrene monomer,

especially in a bulk process so this is a low probability process. To further minimize this probability, the second polymerization was stopped at low conversion, thus promoting the formation of stars. Figure 4.9 shows the GPC chromatogram of the initial hyperbranched polymer and the final star-like polymer. The hyperbranched polymer having $M_n = 1,400$ and $PDI = 1.27$, was extended while maintaining its unimodality to $M_n = 23,500$ and $PDI = 1.92$. The number of arms would be equal to the number of chloromethyl groups in the initial hyperbranched polymer assuming that all benzyl chloride groups were activated in the ATRP process. From the $^1\text{H-NMR}$ spectrum, the number of arms present in a star-like polymer chain on average is calculated to be 6.1.

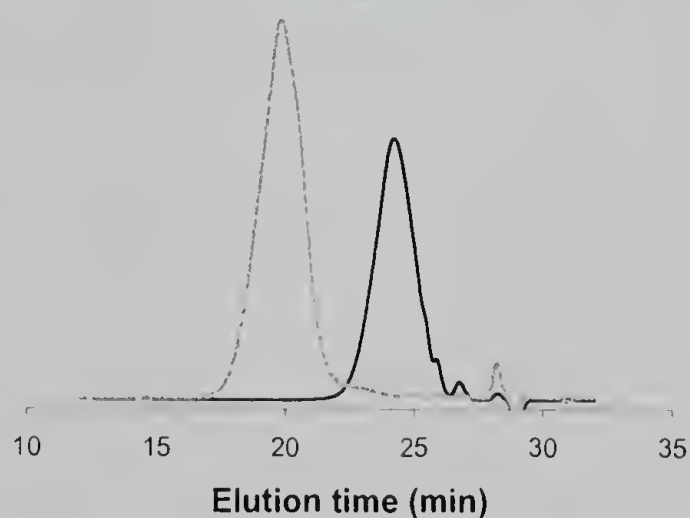


Figure 4.9 GPC chromatograms of poly(vinylbenzyl chloride) (—) and the star-like polymer (---).

4.6 Branched Polymers Using Protection-Deprotection Chemistry

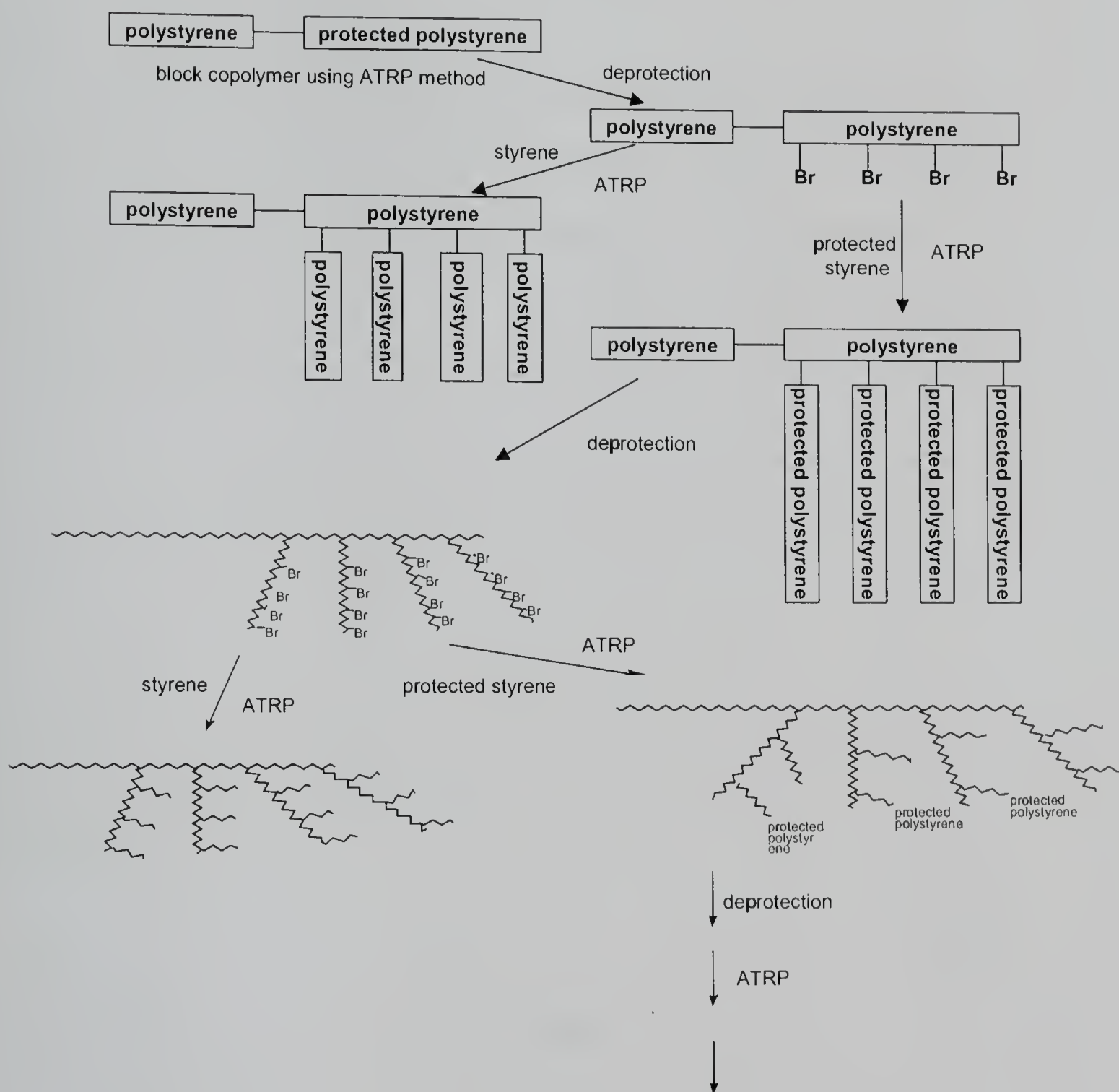
The previous methods are simple, however, there is a limitation on the monomers that can be polymerized these method because only styrenic monomers are known to be polymerized in controlled manner by the nitroxide-mediated SFRP polymerization. On

the other hand, the ATRP method is versatile and a variety of monomers can be polymerized in a controlled manner. Therefore, we tried to develop a new method to prepare branched polymers using exclusively ATRP methods. In the previous method, the benzyl chloride groups that are used as initiating sites for the graft polymerization step are compatible with the nitroxide-mediated SFRP method, and neither affect the formation of the backbone nor react to deactivate the side-chain initiators. However, these groups cannot be used directly in the preparation of backbone polymer by ATRP method because of their premature initiation during the polymerization to form a hyperbranched structure. To solve this problem, a protection-deprotection strategy was adapted. The graft initiating sites were protected by suitable groups during the preparation of the parent backbone polymer. The latent initiating sites for the graft polymerization were then deprotected using simple chemical transformation (Scheme 4.5).

This protection-deprotection strategy is very useful because it allows an ever-greater range of complex structural variations in the polymers prepared. Firstly, two or more different protected groups can be incorporated into the polymer backbones. These different protecting groups could be transformed into initiating sites under different deprotection reaction conditions. This makes it possible to attach various different kinds of branches to the same backbone, or in some cases, to prepare highly functional polymers by selective deprotection-grafting steps. An example of this would be the preparation of dendrigraft polymers. If just simple monomers such as styrene and MMA are used in the grafting steps, branched polymers can be prepared. Instead, however, if another protected monomer is copolymerized with the simple monomer and the same deprotection-grafting steps are applied, a second generation of branches (branches on

branches) can be introduced in the polymer structure. In analogy with the divergent growth approach to dendritic macromolecules, this stepwise deprotection-grafting strategy can be continued to give larger and larger “comb-burst” macromolecules. The .

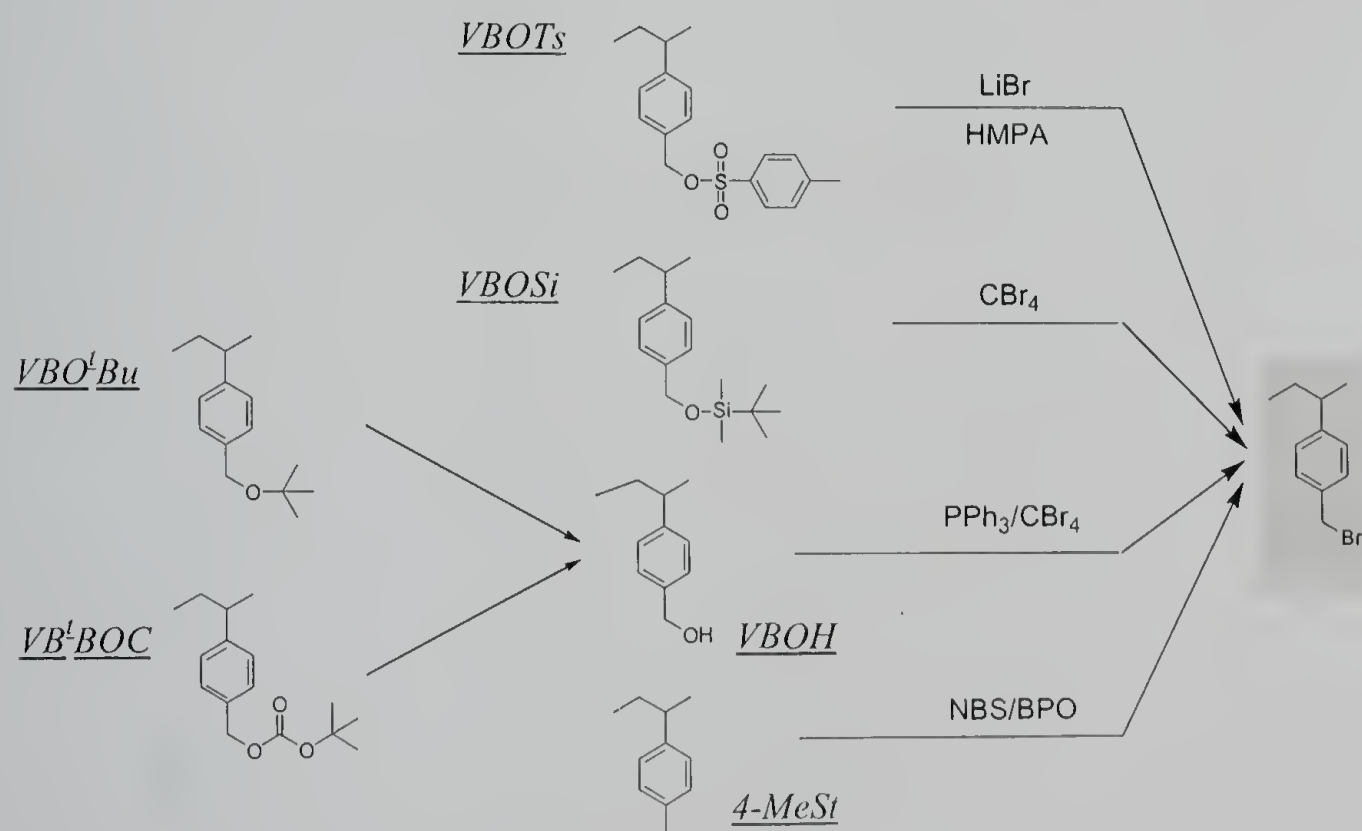
Scheme 4.5 Preparation of Branched and Hyperbranched Polymers Using Protection-Deprotection Chemistry



mild reaction conditions would permit a wide variety of monomer units and functional groups to be introduced at various stages of the synthesis, or at various 'levels' throughout the structure. Ideally, the deprotection-grafting step can be repeated to form very complex structures. However, because there always is the possibility of coupling reactions between active radicals, the reaction has a limitation and caution should be exercised in order to avoid uncontrolled crosslinking reactions.

Several structures were prepared and tested as protected monomers. Scheme 4.6 shows the monomer structures for protected styrene and the deprotection chemistry that we used. Several factors were considered in making these selections including ease of synthesis of protected monomer, simple and clean deprotection reactions, and inertness of the protecting group under the normal ATRP condition.

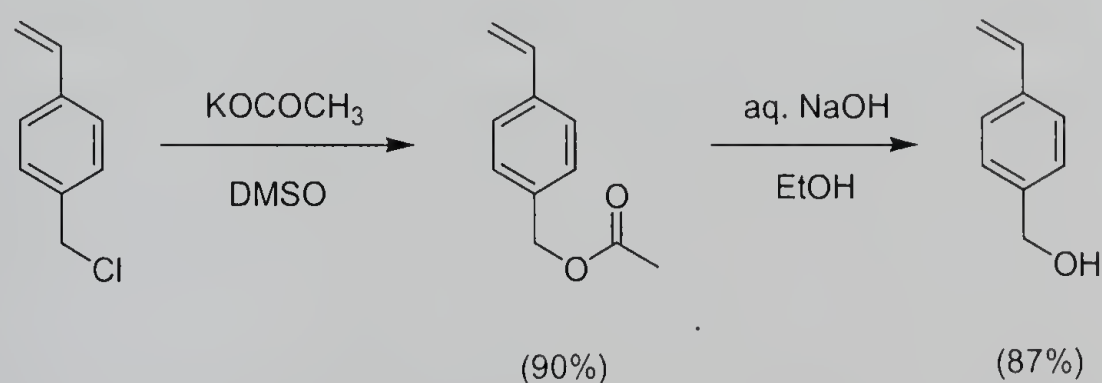
Scheme 4.6 Candidate Structures for Protected Styrene



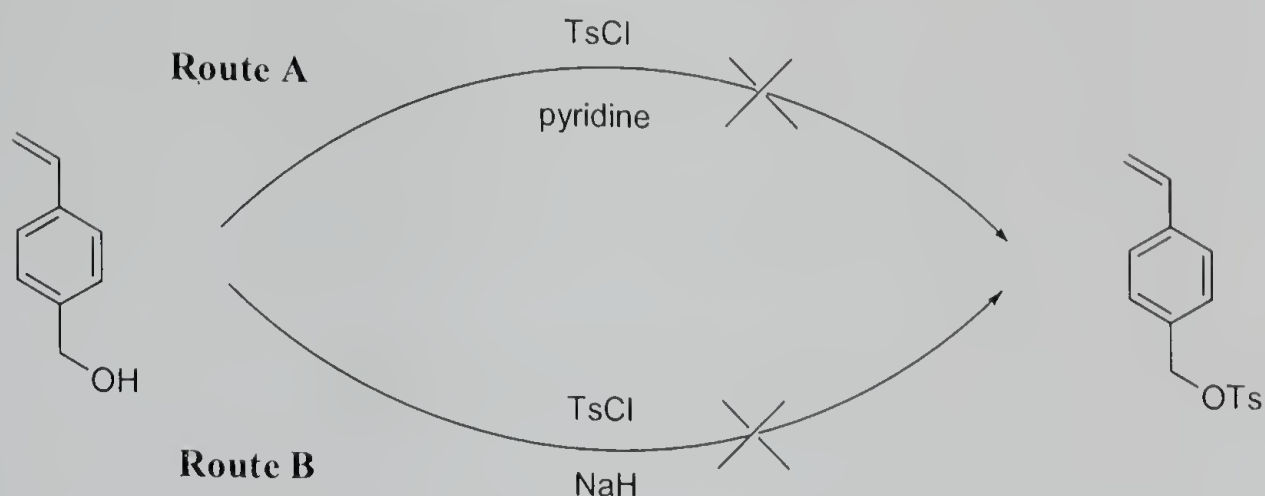
4.6.1 Vinylbenzyltosylate (VBOTs)

We first tried *p*-toluenesulfonyl (tosyl-) moieties as protecting groups of the benzyl chloride groups. The tosyl group is a well-known protecting group, and can be deprotected back to a benzyl chloride group by a simple one-step reaction (Scheme 4.6). We tried to prepare VBOTs by the synthetic route depicting in Scheme VII and VIII. The synthesis of vinylbenzylalcohol (VBOH) was straightforward, and it was prepared in high yields in two steps (Scheme 4.7). However, the efforts to synthesize VBOTs were unsuccessful. We used pyridine as a base to scavenge the HCl by-product in the first trial, but only recollected the reactant VBOH. It was thought that the benzyl tosylate is so unstable, it reacted immediately with trace amounts of water present in pyridine to hydrolyzed back to VBOH. Moreover, any acidic by-product could accelerate the hydrolysis reaction. In second attempt, the benzyl alcohol was deprotected using sodium hydride and the resulting alkoxide was allowed to react with tosyl chloride to minimize the possibility of hydrolysis. However, we obtained a very complex mixture of unidentified products upon analysis using both GC and NMR techniques (Scheme 4.8).

Scheme 4.7 Preparation of VBOH



Scheme 4.8 Attempts to Prepare VBOTs



4.6.2 Vinylbenzyl dimethyl-*t*-butylsilyl ether (VBOSi)

Next we targeted vinylbenzyl dimethyl-*t*-butylsilyl ether (VBOSi). The *t*-butyldimethylsilyl (TBDMS) group was first introduced into organic synthesis by Stork, *et al.*¹⁶ and Corey, *et al.*¹⁷, and is one of the most popular and useful protecting groups for hydroxyl groups. The stability of hindered TBDMS under various reaction conditions allows one to carry it unchanged through several synthetic steps,¹⁸ which cannot be done with the less stable trimethylsilyl protection group. Mattes, *et al.* found that when treated with CBr_4 and PPh_3 in dichloromethane or acetonitrile, benzyl silyl ether transformed to benzyl bromide in 50 – 80 % of yield.¹⁹ Similar bromination of silyl ether group using triphenylphosphine-dibromide was also reported by Aizpurua, *et al.*²⁰ These results were encouraging and prompted us to investigate the polymerization of VBOSi using ATRP method.

VBOSi was prepared in pure form by the reaction of VBOH and *t*-butyldimethylsilyl chloride in the presence of imidazole as an acid scavenger in

dimethylformate (Scheme 4.9). The GC chromatogram and NMR spectrum data confirmed the clean synthesis of VBOSi (Figure 4.10 and 4.11). Two peaks in GC spectrum correspond to the 3- and 4-substitution on the phenyl groups, which was the original isomeric mixture of the starting material, vinylbenzyl chloride.

Scheme 4.9 Preparation of VBOSi

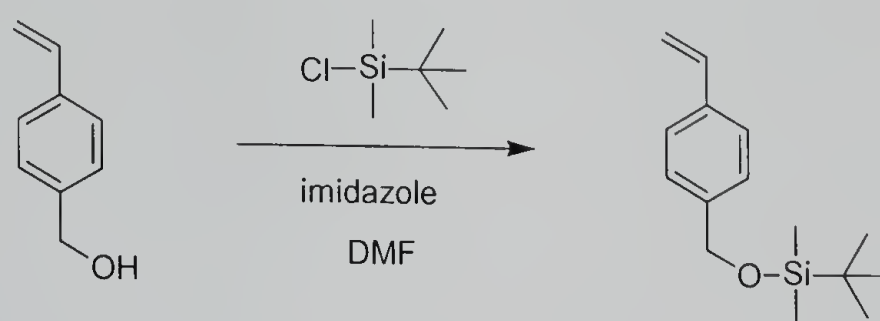


Table 4.1 shows the results of polymerization of VBOSi under various reaction conditions. In Run 1-4, CuX/pby was used as a polymerization catalyst. For the bulk polymerizations, the solubility of the catalyst system in the VBOSi monomer was so low that the color of the reaction mixture didn't change after mixing (the color of the copper(I) form of the CuX/pby is dark red and the oxidized form is dark green), which implies that the real concentration of the catalyst system participating in the reaction would be very low. In spite of this, the reaction using CuCl/pby at 130 °C was very fast, and the mixture was completely solidified after 3 h (Run 1). However, the solid product could not be dissolved in THF, and only formed a gel. Reactions using CuBr at 110 °C was very slow, and the viscosity of the polymerization mixture stayed low even after a few days. The reaction was stopped after 10 days, and work-up afforded poly(VBOSi) having an uncontrolled structure (Run 2) as evidenced by its lack of solubility. To

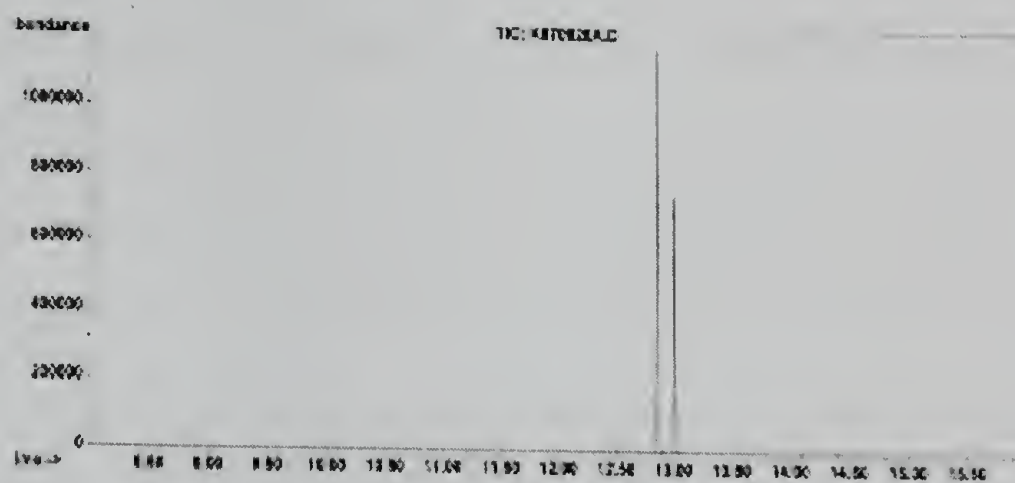


Figure 4.10 GC chromatogram of VBOSi.

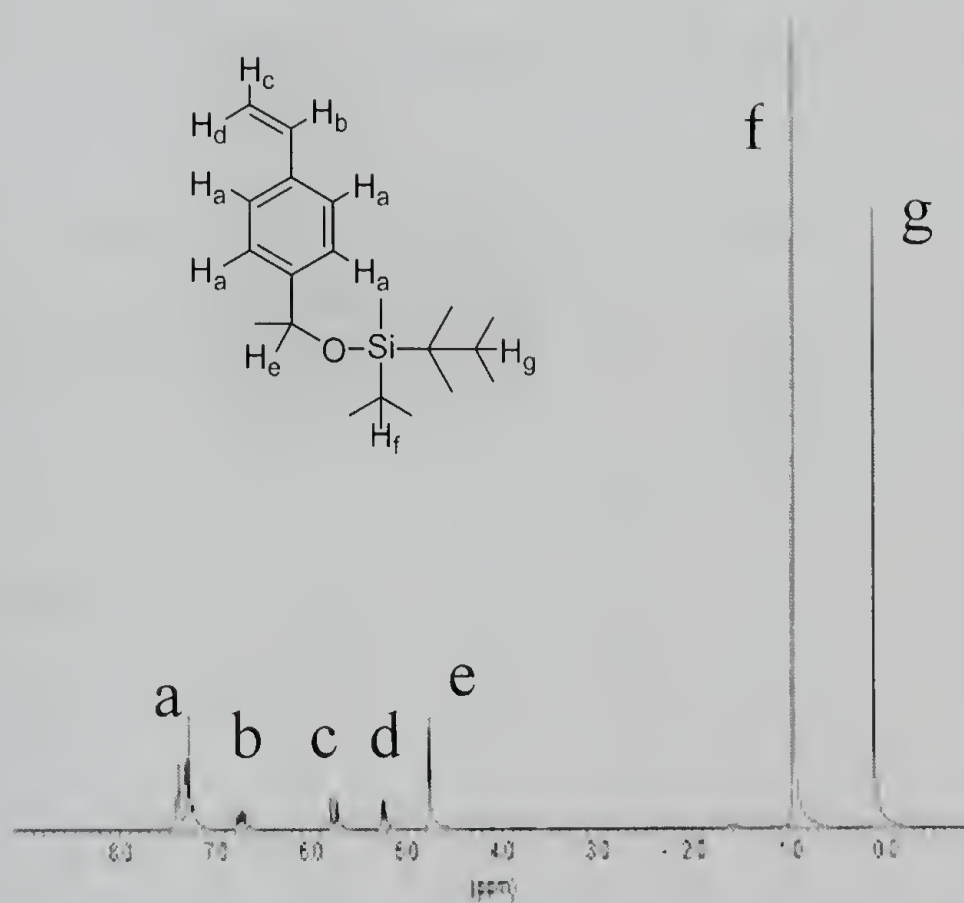


Figure 4.11 ^1H -NMR spectrum of VBOSi.

increase the solubility of metal catalyst, we performed solution polymerization and copolymerization with styrene. When diphenylether was used as a solvent (50 %, v/v), the catalyst was more soluble in the reaction mixture (as evidenced by the color change of the solution to reddish brown), but it still remained heterogeneous. The dilution caused the polymerization rate to decrease and a reach 70 % of conversion was reached after 3 days. The characterizations of the product polymer show that the molecular weight was much higher than the theoretical value and polydispersity was also high (Run 3). The 1/1 copolymerization with styrene made the reaction mixture more homogeneous. The color of the reaction mixture turned to greenish gray after 10 h, which indicates the formation of CuCl₂ by the atom transfer reaction. However, the properties of the resulting copolymer were still below a satisfactory limit (Run 4). In Run 5 and 6, we used 4,4'-di(4-ethylphenoxy)-2,2'-bipyridine (epy) and 4,4'-di(4-methoxy-phenoxy)-2,2'-bipyridine (mpy) as ligands because the copper complex with these ligands showed better solubility

Table 4.1 Polymerization of VBOSi Under Various Conditions

Run	Catalyst system	condition	T(°C)	Time(h)	Conv(%)	<i>M_n</i>	PDI
1	CuCl/pby	Bulk	130	3	gelled		
2	CuBr/pby	Bulk	110	1.5	93	34,300	1.84
3	CuCl/pby	solution ^a	110	1	47	66,700	2.32
4	CuCl/pby	Copolymerization w/ styrene (1/1)	110	1	71	52,000	1.62
5	CuCl/epy	Bulk	110	24	gelled		
6	CuCl/mpy	Bulk	110	1	46	74,500	1.62
7	CuCl/pby	BzOSi	130			10,500	1.11
8	CuCl/mpy	BzOSi	130	1	71	17,800	1.35

^a in diphenylether (50%, v/v)

in the polymerization of styrene.²¹ We used solution polymerization and the lower temperature to minimize the undesirable cross-linking reactions. The reactions were more homogeneous, but the one using epy produced gelled product after 2 days of polymerization. The product of the reaction using mpy did not gel, but the molecular weight was much higher than theoretical value and PDI was also high.

TBDMS groups can affect the polymerization in several aspects: 1) they can change the polarity of the reaction mixture, and affect the activity of metal complexes. However, bulk styrene is a good medium for ATRP, and the TBDMS should be likewise nonpolar. Hence, polarity is not thought to be an important factor in this case. 2) They can affect the reactivity of monomer. Even though the effect is small, the substituent group at 4-position of styrene monomer can affect the reactivity of the monomer in a radical polymerization. Matyjaszewski, *et al.* polymerized various 4-substituted styrene using ATRP method, and found that there is a correlation between the electron perturbation of substituents and the rate of polymerization of these monomers.²² However, the TBDMS group is far removed from the vinyl making this an unlikely contribution. 3) The functional groups can participate in the side reactions to deactivate or poison the metal complexes resulting loss of activity. To find out the reason behind the controllability, we added a compound bearing the same functionality as the VBOSi monomer, benzyldimethyl-*t*-butylsilylether (BzOSi), into a styrene polymerization reaction. Two ligands were used in the polymerization, pby and mpy. In both cases, while the reaction rates were very slow because the additive acts as a diluent and reduces the concentration of monomer and metal complexes, the resulting polymers had low polydispersity of 1.1-1.4. The molecular weight of the polymers was higher than predicted, but were reasonable

values for a controlled system. These results indicate that TBDMS groups do not affect the control of polymerization by ATRP, which support the possibility of effect of protection groups to monomer activity as the reason of poor control in polymerization. However, the metal deactivation may still be present as evidenced by the slow reaction and higher molecular weight than predicted one. Another possible explanation of poor control is the premature deprotection reaction of the TBDMS groups. If the protection groups are cleaved during the polymerization, they generate active centers that may cause metal poisoning and inter-/intra-molecular cross-linking reactions. These side reactions could increase the molecular weight and polydispersity for the polymerization of VBOSi, but these effects would be small for the polymerization of styrene having BzOSi.

4.6.3 Vinylbenzylalcohol (VBOH)

In the preparation of VBOTs and VBOSi derivatives, VBOH was used as an intermediate. Because the benzyl alcohol group can be transformed to halogen group in some straightforward, VBOH itself was thought to be the very good candidate as a protected monomer. Furthermore, it was known that ATRP could be carried out in an aqueous medium, which indicated these systems tolerate the -OH functional group. VBOH was polymerized with the CuCl/pby catalyst in bulk. The product, however, gelled after 8 h reaction at 130 °C. A small portion of this sample was soluble in THF, and this was characterized by GPC. The chromatogram was composed of mixture of multiple peaks as shown in Figure 4.12. We used the same strategy of adding a diluent possessing the functional group to a styrene polymerization in order to probe the reasons for the poor control in this polymerization. The polymerization of styrene in the presence of benzyl alcohol generated polymers having broad molecular weight distributions (Figure 4.13).

This indicates that the benzyl alcohol moiety significantly affect the polymerization by ATRP method, and should be masked with other groups to be used in protection-deprotection strategy.

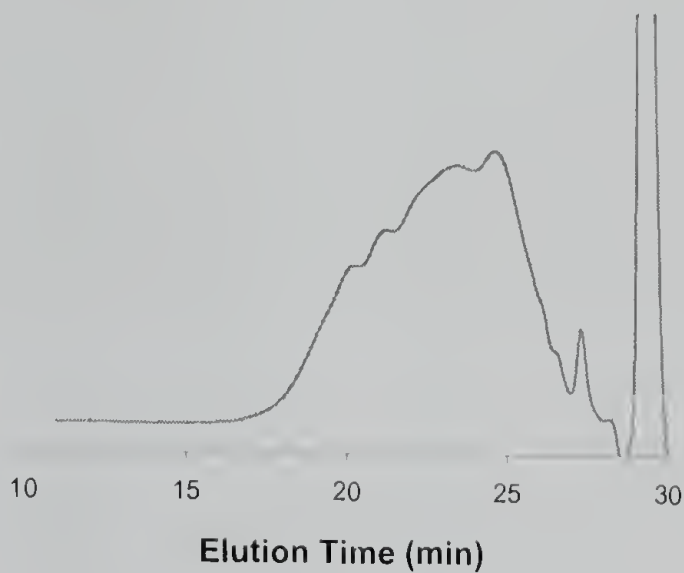


Figure 4.12 GPC chromatogram of poly(vinylbenzyl alcohol).

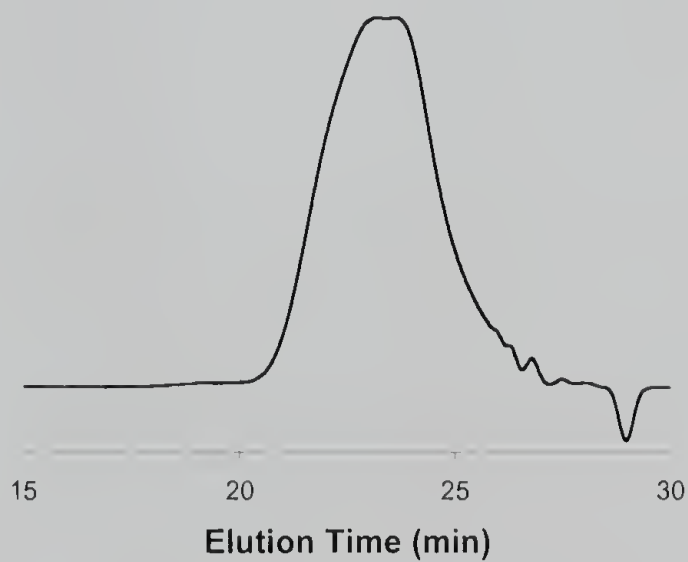
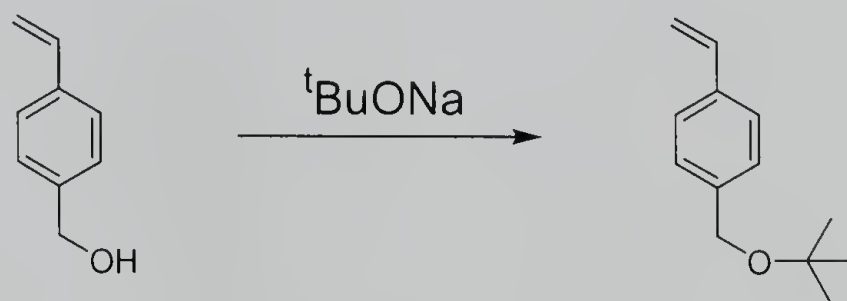


Figure 4.13 GPC chromatogram of polystyrene prepared in the presence of benzyl alcohol.

4.6.4 Vinylbenzyl-*t*-butylether (VBO*t*-Bu)

As another protecting group for the hydroxyl functionality, *t*-butyl ether was used. With this protecting group, we would have two choices of deprotection procedures. The *t*-butyl ether group can be deprotected to a hydroxyl, and then transformed to benzyl bromide to be used as the initiating site in a grafting polymerization. The *t*-butyl ether group also can be directly brominated using triphenyldibromide.²³ Vinylbenzyl-*t*-butylether (VBO*t*-Bu) was prepared from the reaction with VBOH (Scheme 4.10) and sodium *t*-butoxide, and analyses using GC and NMR confirmed purity of the product (Figure 4.14 and 4.15).

Scheme 4.10 Preparation of VBO*t*-Bu



The VBO*t*-Bu was polymerized using CuCl/pby as a catalyst in diphenylether (50 %, v/v). The polymerization mixture was not completely homogeneous, and had a pale greenish color at 130 °C and dark reddish brown at 110 °C. After 4 days polymerization at 130 °C, the reaction mixture still had a low viscosity indicating low conversion. The resulting polymer had a low molecular weight, and the polydispersity of the polymer was very high at about 2.9. The polymerization at 110 °C also showed low conversion, but the molecular weight of resulting polymer was higher than that of 130 °C polymerization

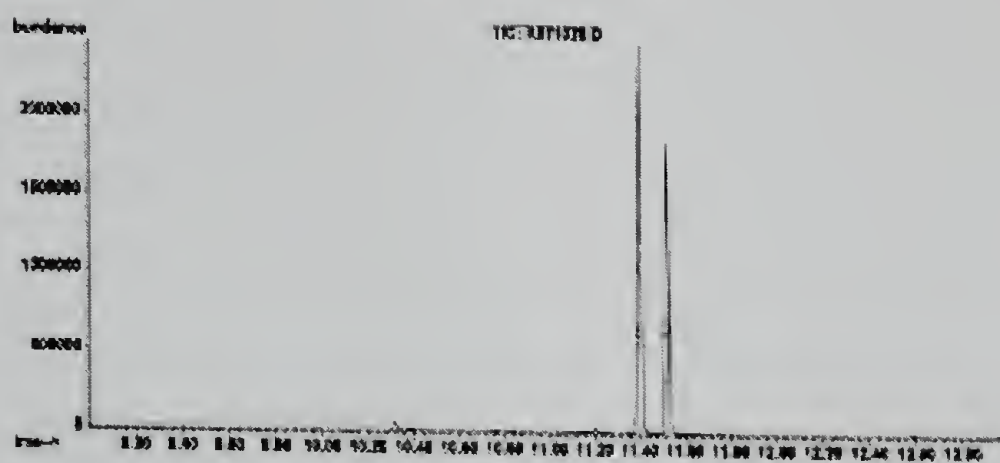


Figure 4.14 GC chromatogram of VBO*t*-Bu.

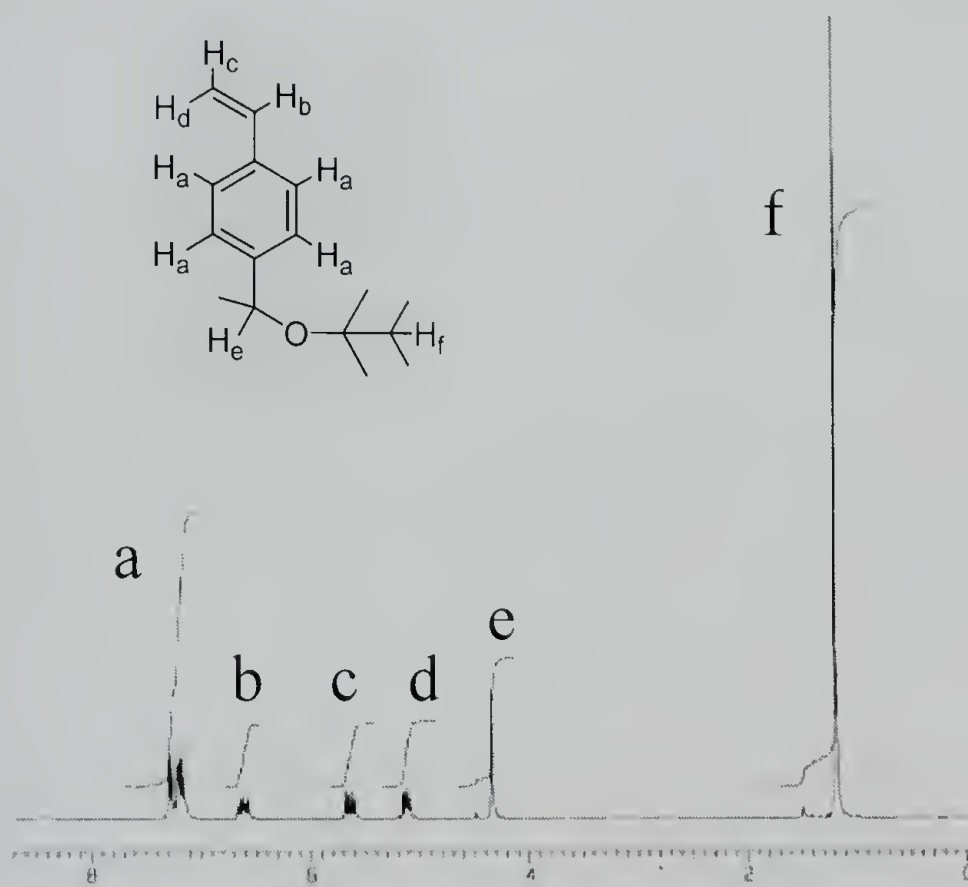


Figure 4.15 ^1H -NMR spectrum of VBO*t*-Bu.

product. Polydispersity of product polymer was lower for the reaction at 110 °C, and the chromatogram indicates mixture of multiple peaks for both cases (Figure 4.16).

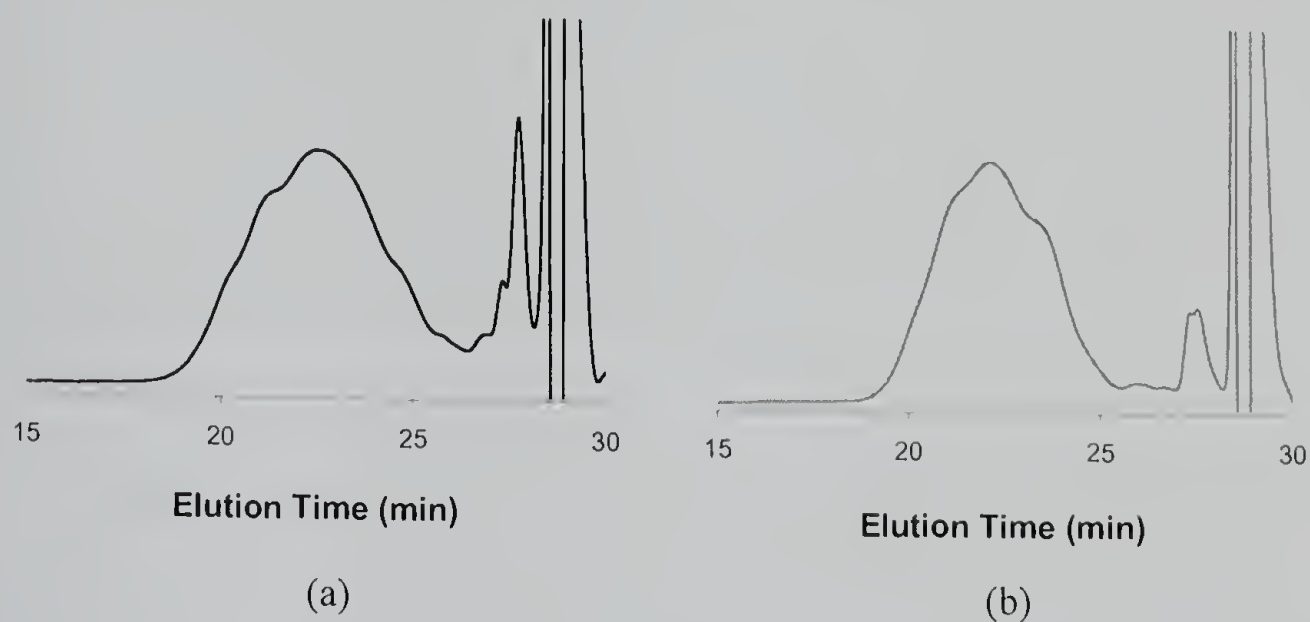


Figure 4.16 GPC chromatogram of poly(vinylbenzyl-*t*-butylether) polymerized at (a) 130 °C and (b) 110 °C.

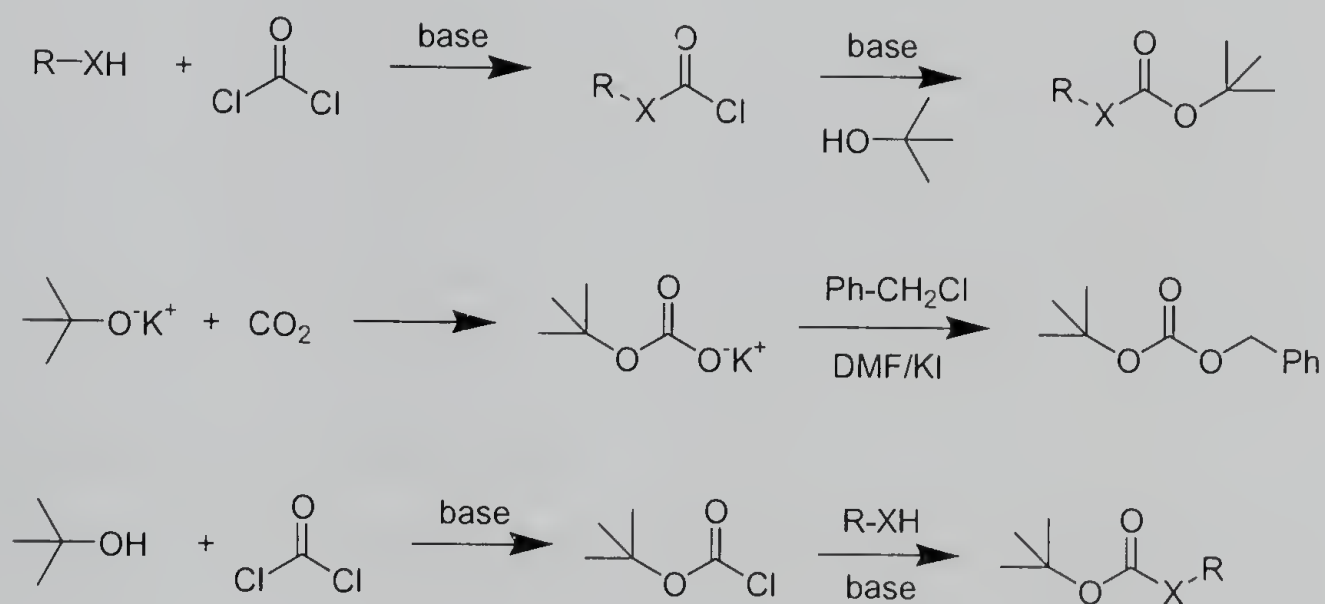
4.6.5 Vinylbenzyl-*t*-butyloxycarbonate(VB-*t*-BOC)

t-Butyloxycarbonate (*t*-BOC) group is one of the most widely used protecting groups of amino functionalities, and is especially used in peptide synthesis.²⁴ The use of this protecting group for either hydroxyl or thiol functionalities has been rare. Fréchet, *et al.*, reported using the *t*-BOC group to protect the phenols of poly(*p*-hydroxystyrene). The *t*-BOC group is resistant to both the conditions of the Wittig reaction and of cationic polymerization in liquid sulfur dioxide. In addition, the unique ability of the *t*-BOC group to be removed by thermolysis or by the action of a catalytic amount of strong acid was the basis for its use with poly(*p*-*t*-BOC-hydroxystyrene) in a photoimaging system exhibiting the phenomenon of chemical amplification.²⁵

4.6.5.1 Synthesis of VBT-BOC

Because of its use in peptide synthesis, the preparation of *t*-BOC derivatives of amines has been studied extensively. However, there have been only a few reports on the *t*-butyloxycarbonylation of hydroxyls and thiols,²⁶ and most of the examples are characterized by generally low yields and/or the use of extremely toxic or unstable reagents (Scheme 4.11). Rather recently, Houlihan, *et al.* used di-*t*-butyl dicarbonate as an *t*-butyloxycarbonylation reagent in the reaction of phenols, alcohols, enols, and thiols under phase transfer condition, and acquired *t*-BOC protected products in high yields.²⁷

Scheme 4.11 Literature Methods of *t*-butyloxycarbonylation of Hydroxyls and Thiols



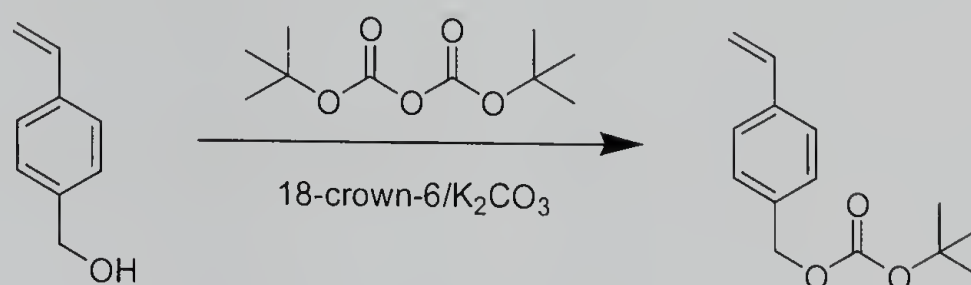
where, R = alkyl or aryl

X = O or S

Following Houlihan's method, we protected the benzyl alcohol moieties of vinylbenzyl alcohol with *t*-BOC groups using di-*t*-butyl dicarbonate as a *t*-butyloxycarbonylation reagent (Scheme 4.12). The reaction was slow even with the use of

a catalytic amount of 18-crown-6 and an equivalent amount of powdered anhydrous potassium carbonate, but after 2 days, the reaction was complete as evidenced by TLC chromatogram. The infrared spectrum of the resulting carbonate showed a strong carbonyl band near 1740 cm^{-1} , and integration of NMR spectrum matched well with the expected resonances of VBt-BOC (Figure 4.17). The GC spectrum showed almost pure VBt-BOC with trace amounts of the initial VBOH, and the mass spectrum included a characteristic pattern for the loss of *t*-BOC (m/e 100) and a peak at m/e 57 (Figure 4.18).

Scheme 4.12 Preparation of VBt-BOC



4.6.5.2 Homopolymerization of VBt-BOC

We polymerized VBt-BOC under a variety of conditions to test the reactivity of the monomer (Table 4.2). In the first set of experiments, the pby ligand was used along with copper halide to catalyze the polymerization (Run 1, 2). The reaction was performed under solution polymerization conditions using diphenylether as a solvent to minimize the crosslinking reaction in case of any premature deprotection of *t*-BOC groups – a side reaction that was observed in the polymerization of VBOSi. The polymerization at 130 °C using CuCl was fast, and the molecular weight of the polymer was fairly well controlled. However, GPC chromatogram showed the polymer was not unimodal but a

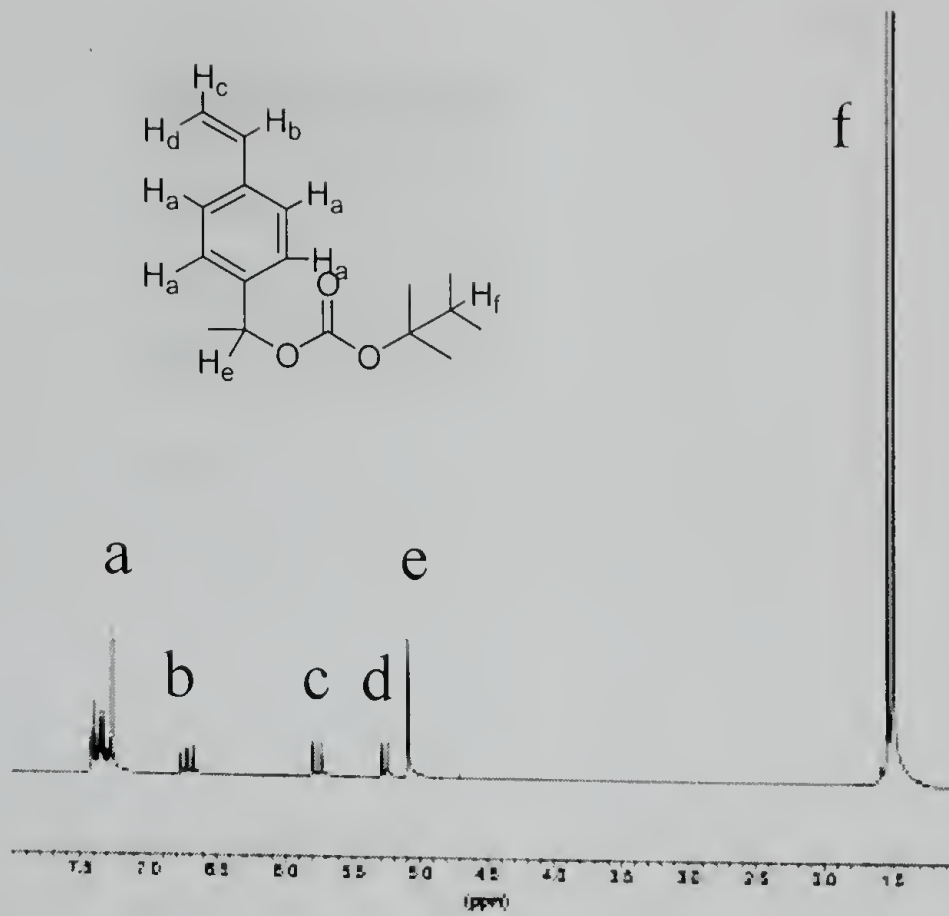


Figure 4.17 ¹H-NMR spectrum of VBt-BOC.

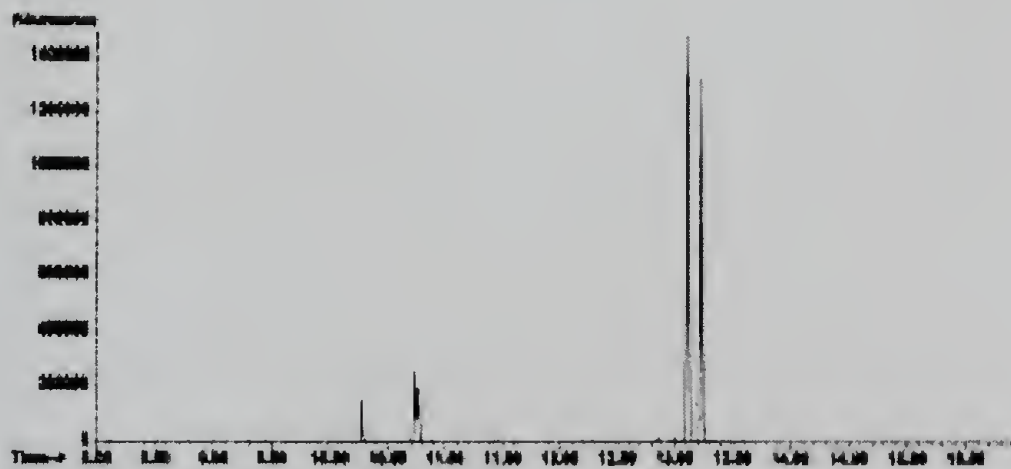


Figure 4.18 GC chromatogram of VBt-BOC.

mixture of two peaks (Figure 4.19a). The lower molecular weight peak had a narrow distribution, but was contaminated with a higher molecular weight shoulder that had exactly twice the molecular weight as the first. The polymer prepared at 110 °C using CuBr also has similar properties. The reaction was very slow and took 3 days to reach 80 % conversion, but the molecular weight matched with the theoretical value calculated from the monomer/initiator ratio and conversion. However, the molecular weight distribution curve was again composed of a lower molecular weight peak having narrow distribution and a higher molecular weight shoulder at twice molecular weight (Figure 4.19b).

Table 4.2 Polymerization of VBt-BOC Under Various Conditions

Run	Catalyst system	condition	T(°C)	Time(h)	Conv(%)	M_n	PDI
1	CuCl/pby	solution ^a	130	6		10,500	1.85
2	CuCl/pby	solution ^a	110	3 days	80	8,900	1.33
3	CuCl/epy	solution ^a	110	12 days	gelled		
4	CuCl/mpy	solution ^a	110	15 days	gelled		
5	BPO/TEMPO	bulk	130	23	55	11,400	1.14
6	CuCl/mpy	Bzt-BOC	130	30	low	8,600	1.15
7	CuCl/pby	Copolymerization w/ styrene (1/1)	110	10	95	11,300	1.36

^a in diphenylether (50%, v/v)

In the next set of experiments, we catalyzed the polymerization with CuCl complexes possessing two different ligands (Run 3 and 4). As was discussed in the

polymerization of VBOSi, copper complexes with epy and mpy ligands were reported to provide better control over other ligands in the polymerization of styrene. Using these

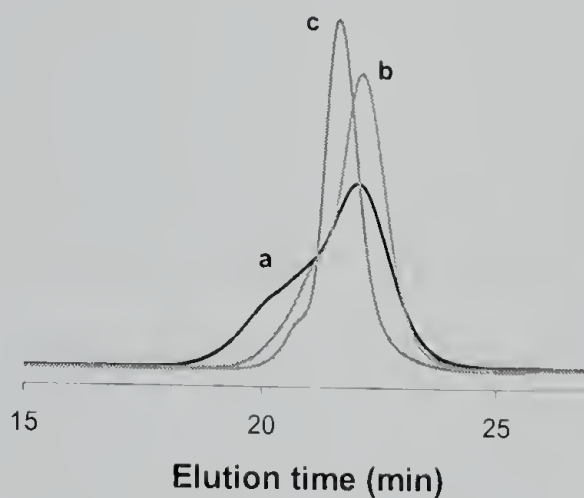


Figure 4.19 GPC chromatogram of poly(VBt-BOC) prepared using CuCl/pby as a catalyst at 130 °C, (a) Run 1, (b) Run 2, (c) Run 5 in Table 4.2.

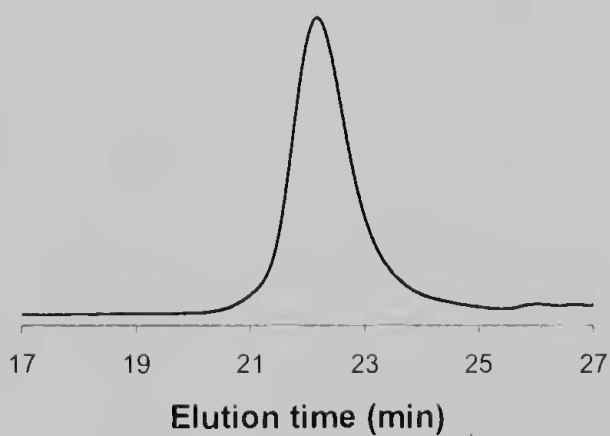


Figure 4.20 GPC chromatogram of polystyrene prepared in the presence of Bzt-BOC (Run 7).

complexes as catalysts, however, the polymerizations of *VBt*-BOC was very slow, and took more than 10 days to reach high conversion, and ultimately gelled in THF. In Run 5, we polymerized *VBt*-BOC by an alternative controlled radical polymerization technique, the nitroxide-mediated SFRP method. Poly(*VBt*-BOC) prepared using BPO/TEMPO had a low PDI value of 1.14, even under the more extreme conditions of higher temperature (130 °C) and in the absence of solvent. Moreover, the portion of the higher molecular weight shoulder in the GPC chromatogram was smaller than that of polymers prepared by the ATRP method (Figure 4.19c). In the polymerizations of protected monomers by the ATRP technique, one of the persistent concerns is the reaction between the metal complex and the protecting groups. Most protecting groups and the deprotected counterparts by the premature cleavage under the polymerization condition are all polar groups. Therefore, there is always the possibility of a reaction between these polar groups and the metal complexes, leading to catalyst deactivation, and ultimately loss of control in the polymerization. Another attempt to elucidate the cause of the reduced control in the polymerization of *VBt*-BOC was performed (Run 6). Styrene was polymerized in the presence of benzy-*t*-butyloxycarbonate (*Bzt*-BOC) that possess the same functional group as *VBt*-BOC. A complex of CuCl/*mpy* was used as a catalyst for the polymerization, and the reaction was run at 130 °C. The polymerization rate was very slow, even taking the dilution factor caused by *Bzt*-BOC into consideration, but the prepared polymer had the same narrow molecular weight distribution as that of polystyrene prepared without *Bzt*-BOC. The GPC chromatogram of the resulting polystyrene shows no high molecular weight shoulder (Figure 4.20). If in the polymerization using *Bzt*-BOC, premature deprotection occurred followed by coupling reactions, it would produce only the dimeric compound, and not produce the twice molecular weight polymers by the inter-chain

combination reaction as in the polymerization of VB*t*-BOC. However, it appears that the metal complexes can be poisoned by reaction with the functional groups, which reduce the rate of polymerization.

In the preparation of branched polymers, the VB*t*-BOC monomer could not be homopolymerized because the branching density of homopoly(VB*t*-BOC) is very high, and this high density of active radicals causes undesirable intra- and/or inter-chain coupling reactions. To avoid this, copolymerization with styrene was used to control the branching density. Run 7 shows the results of the copolymerization of VB*t*-BOC and styrene. A 50/50 mixture of VB*t*-BOC and styrene was polymerized with CuCl/pby in bulk at 110 °C. The polymerization was completed (conversion > 95%) after 10 hours, and the resulting copolymer had a controlled molecular weight ($M_n = 11,300$) and relatively narrow polydispersity (PDI = 1.36). The higher molecular weight shoulder was still present, but not as significant as for the homopolymerization of VB*t*-BOC.

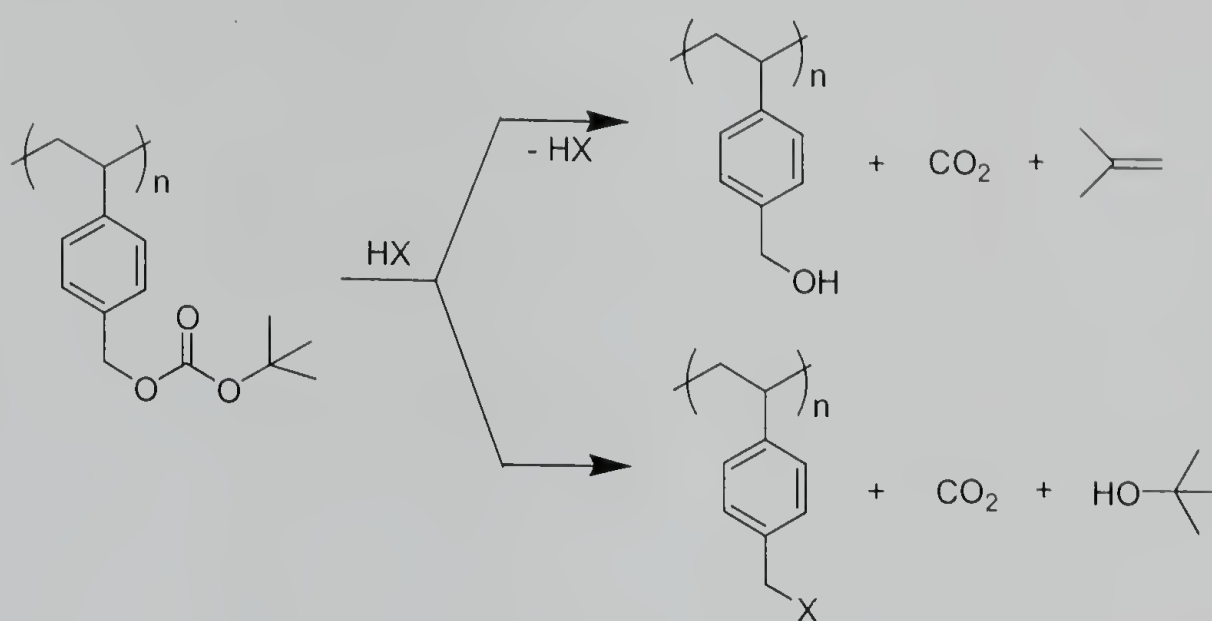
4.6.5.3 Deprotection Reaction of Poly(VB*t*-BOC)

Various methods have been reported to be effective for the cleavage of *t*-BOC groups, especially when they are used as protecting groups of amino groups.²⁸ The methods include thermal cleavage,²⁹ acid catalyzed reactions,³⁰ and organosilicon reagents mediated ones.³¹ Among them, the organosilicon reagents such as trimethylsilyl iodide (TMSI) and trimethylsilyl perchlorate are considered extremely useful for use in peptide synthesis. This is because, not only are the *t*-BOC groups cleaved but also are the ester and ether protecting groups that are commonly used. Moreover, the deprotection reactions using organosilicon derivatives are carried out under neutral conditions and at

room temperature or slightly above. An important difference between TMSI deprotection and acid-catalyzed deprotection procedures commonly used in peptide synthesis is that in the case of former, the key blocking groups, *i.e.*, *t*-butyl, benzyl, or alkyl, are removed by S_N2 attack of iodide at the alkyl group without the formation of a carbonium ion. Therefore, TMSI deprotection of peptide can be free from side reactions, which include the *t*-butylation and/or benzylation of the aromatic species in a peptide chain by the *t*-butyl and/or benzyl carbonium ions. Hence, purer products can be produced. However, TMSI deprotection is too facial and suffers from poor selectivity when benzyl protecting groups are present.³² Kaiser, *et al.* found that the use of trimethylsilyl chloride (TMSCl) along with 1-3 equivalents of phenol in CH₂Cl₂ provides selectivity in the cleavage of *t*-BOC vis-a-vis the benzyl group.^{31c} The mechanism of deprotection in this case was proposed to involve a cleavage reagent responsible was a TMSCl-phenol complex, which provides an acidic proton.

The selectivity of the cleavage between *t*-BOC and benzyl group provided by TMSCl-phenol system was of interest because of the structure of our VB*t*-BOC monomer. In our study, the *t*-BOC group is used to protect benzylic hydroxyl functionality, but during the deprotection reaction under acidic conditions, both *t*-BOC and benzyl groups can be cleaved (Scheme 4.13). The selective cleavage of the *t*-BOC group by TMSCl-phenol was expected to produce well-defined deprotection, and give more control in the structure of product polymer. Following the literature procedure for cleavage of amine protected *t*-BOC groups, we tried to deprotect poly(VB *t*-BOC) with TMSCl and phenol in methylene chloride. However, even after 2 days at 40 °C as to 1 h

Scheme 4.13 Deprotection of Poly(VB*t*-BOC)



at room temperature for amine deprotection, no reaction took place. The ¹H-NMR spectra were identical before and after the reaction. Another deprotection reaction attempt HCl gas was tried, but the product gelled and was no longer soluble in THF or chloroform.

Trifluoroacetic acid has also been used to remove the *t*-BOC protecting group from amines. The poly(VB*t*-BOC) samples were dissolved in CH₂Cl₂, and treated with trifluoroacetic acid for 24 h at room temperature. The product polymer was isolated by precipitating into petroleum ether, and characterized by GPC and ¹H-NMR analyses. The GPC chromatogram shows no change in the molecular weight distribution curve, which indicates that either chain cleavage or crosslinking reaction did not take place during the deprotection reaction. Figure 4.21 is the ¹H-NMR spectra of parent protected polymer (a) and deprotected polymer (b). The peak at 1.5 ppm corresponding to the *t*-butyl proton from VB*t*-BOC disappeared, and the peak at 4.9 ppm corresponding to the benzylic

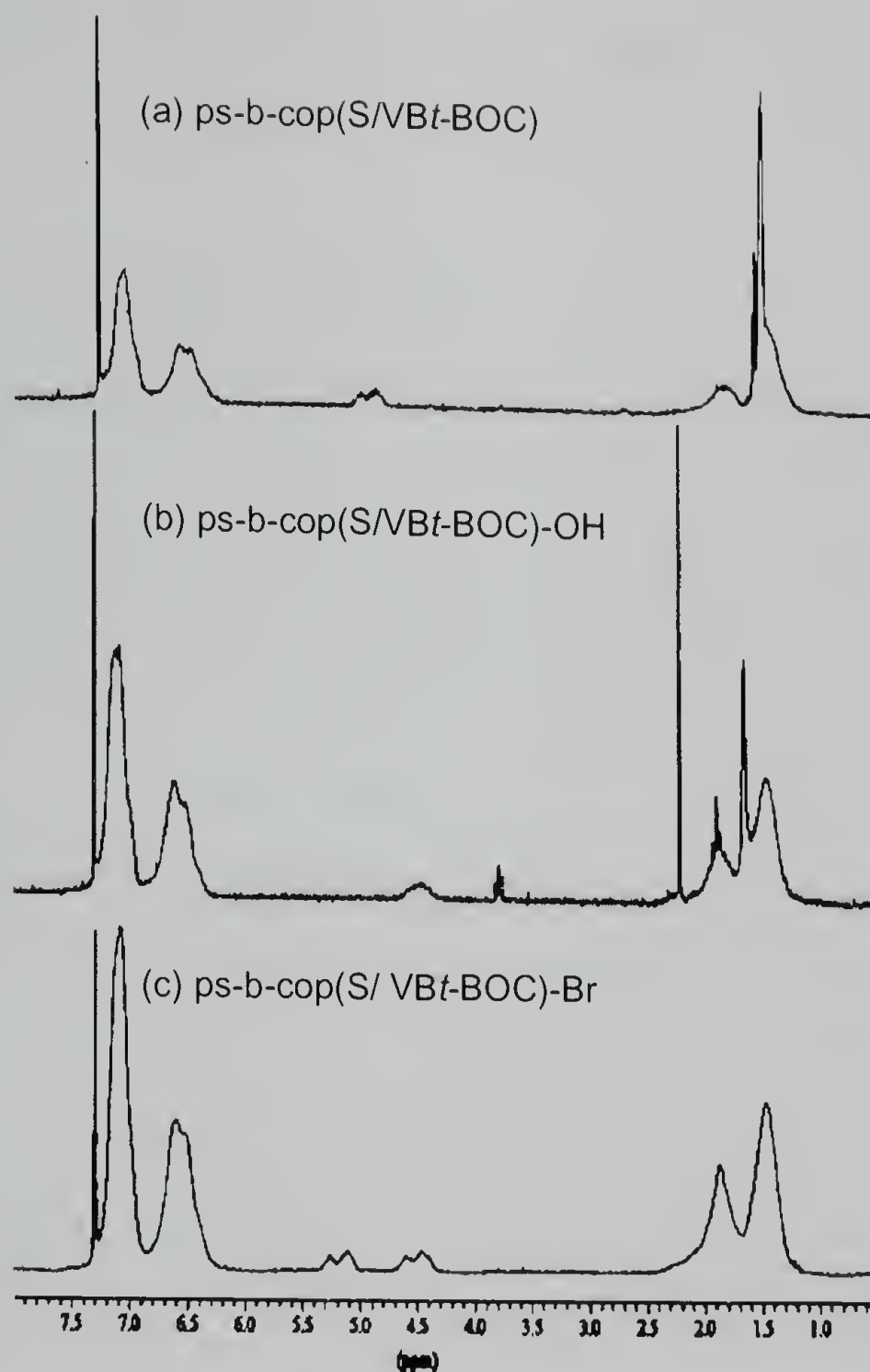


Figure 4.21 Deprotection reaction of *t*-BOC group.

proton from VBt-BOC is shifted upfield to 4.5 ppm corresponding to the benzylic proton from VBOH. The benzyl alcohol moieties were then transformed into the corresponding benzyl bromides by the reaction with triphenylphosphine and carbon tetrabromide in THF at room temperature for 1.5 h. The $^1\text{H-NMR}$ spectra of the final polymer (c) shows that new peak at 5.2 ppm corresponding to the benzylic proton from benzyl bromide moieties

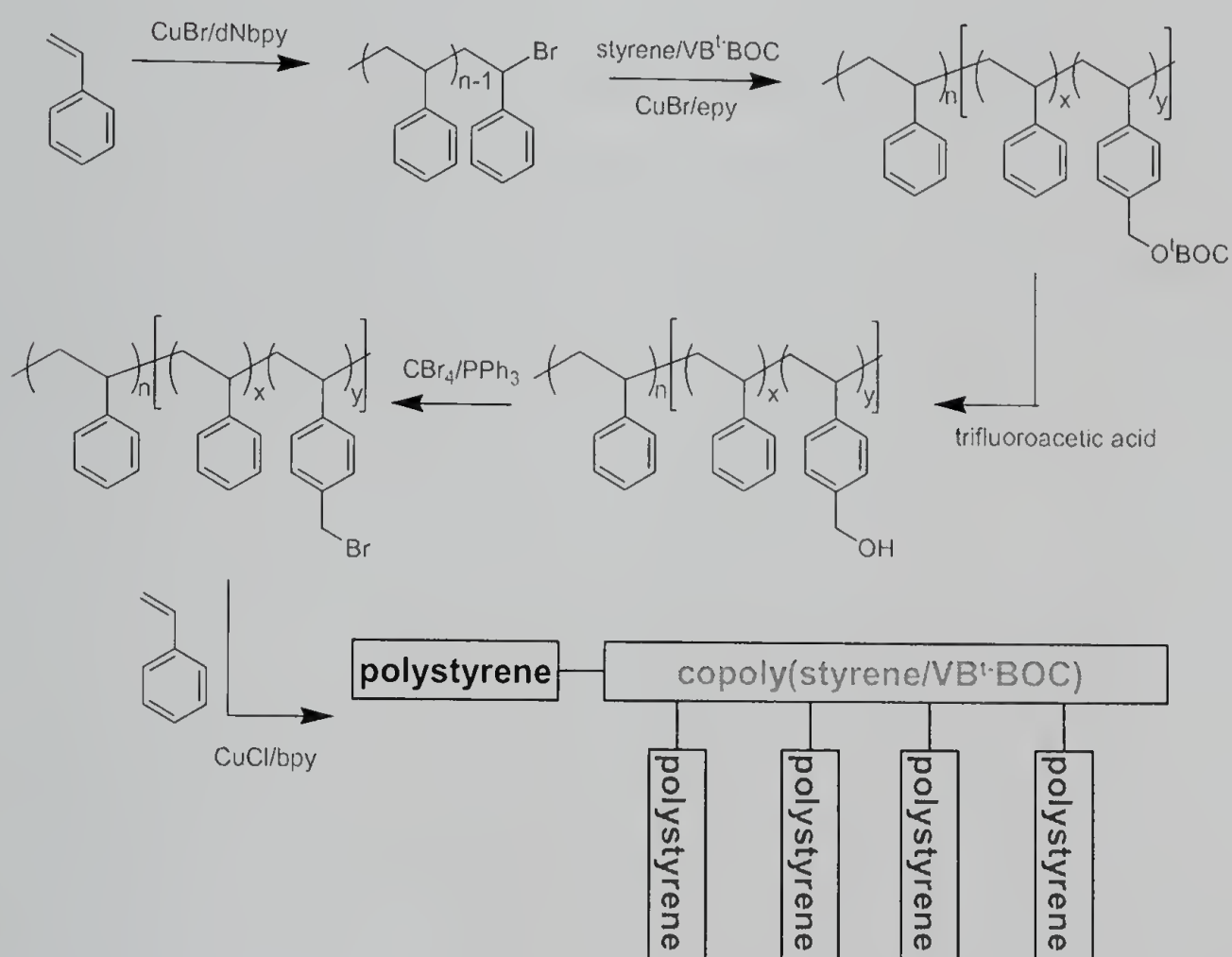
appears, and from the integration of these peaks, the conversion of the bromination of benzyl alcohol groups is calculated to be about 50%.

4.6.5.4 Preparation of Linear-Branched Block Copolymer

As was discussed previously, linear-branched block copolymer structure is an interesting architecture for polymers due to their unique physical properties. In addition, on preparation of this architecture, we can check the synthetic possibilities of some polymer structures, which include block copolymer and branched polymers at the same time. We prepared a block copolymer that was composed of two block segments: a linear polystyrene block and random copolymer of styrene and VB*t*-BOC. The VB*t*-BOC moieties along the second block were deprotected to generate benzyl bromide functionalities, and graft polymerization was then initiated from the unmasked benzyl bromides using the ATRP technique (Scheme 4.14). The initial polystyrene block segment was prepared using CuCl/epy as a catalyst. Upon workup after 4 h reaction at 130 °C, a good yield (> 90%) of polymer was obtained. Figure 4.22a shows the GPC chromatogram of the product polystyrene. The molecular weight of polystyrene is close to the expected value based on the polymerization conversion and the initial ratio of monomer to initiator, and the molecular weight distribution was narrow ($M_n = 2,000$ (th 2,000); PDI = 1.14). The isolated polystyrene segment was dissolved in an additional monomer mixture of styrene and VB*t*-BOC (75/25), and using the CuCl/epy catalyst, the second segment of the block copolymer was prepared by ATRP at 110 °C. Again high yields were attained and the product block copolymer had a molecular weight close to the theoretical value, and a relatively narrow molecular weight distribution ($M_n = 22,000$ (th 22,000); PDI = 1.29; Figure 4.22b). Deprotection of *t*-BOC groups, to generate the benzyl

bromide groups that are used as initiating sites for the graft polymerization, was performed in two steps. The *t*-BOC group was first cleaved by the reaction with trifluoroacetic acid at room temperature for 24 h. The resulting benzyl alcohol moieties were then transformed into the corresponding benzyl bromides by the reaction with triphenylphosphine and carbon tetrabromide in THF at room temperature for 1.5 h. From the ¹H-NMR analysis, it was determined that there were on average 10.3 benzyl bromide groups per polymer chain.

Scheme 4.14 Preparation of Linear-Branched Block Copolymer Using VB*t*-BOC



From this deprotected block copolymer, both polystyrene and PMMA branches were successfully grown using ATRP method. The graft polymerizations were performed

using CuCl/bpy at 110 °C, and the reactions were stopped at low conversion to minimize side reactions. Figure 4.22c shows the GPC chromatogram of the grafted polymers. The molecular weight of grafted polymers increased to higher values for most part, but there is a residual peak for the backbone polymer. This seems to indicate that the deprotection reactions are not homogeneous and there are chains within the sample that have few, if any, benzyl bromide groups. The GPC chromatograms also show that there is a high molecular weight shoulder present, which is presumably the result of the inter-chain coupling reactions. These are especially pronounced for PMMA branched polymers where the amount of grafting was higher. From these data, we conclude that the use of Vbt-BOC in the preparation of branched polymer by protection-deprotection strategy provides a viable way of preparing novel architectures of polymers. However, in the long-term, better deprotection methods could be developed that would allow for greater control over the polymer structure. Additionally, development of other protected monomers having clean and simple deprotection pathway would also be very useful.

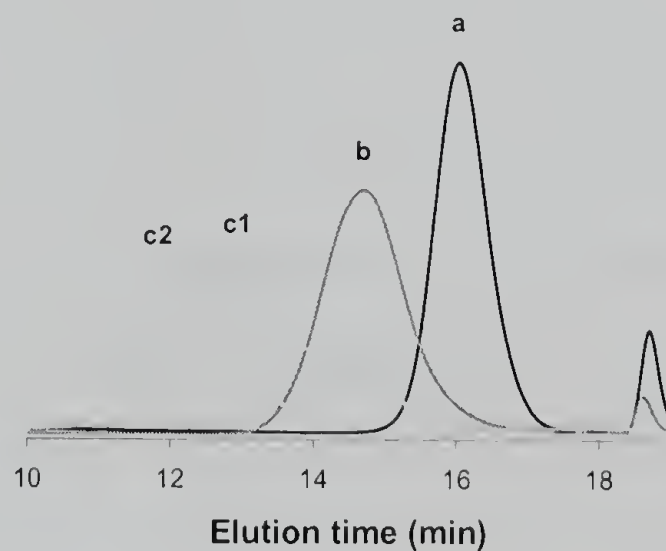


Figure 4.22 GPC chromatograms of linear-branched block copolymer, (a) initial polystyrene, (b) copoly[styrene-*b*-(styrene/Vbt-BOC)] backbone, (c1) linear-branched block copolymer having polystyrene branches, (c2) linear-branched block copolymer having PMMA branches.

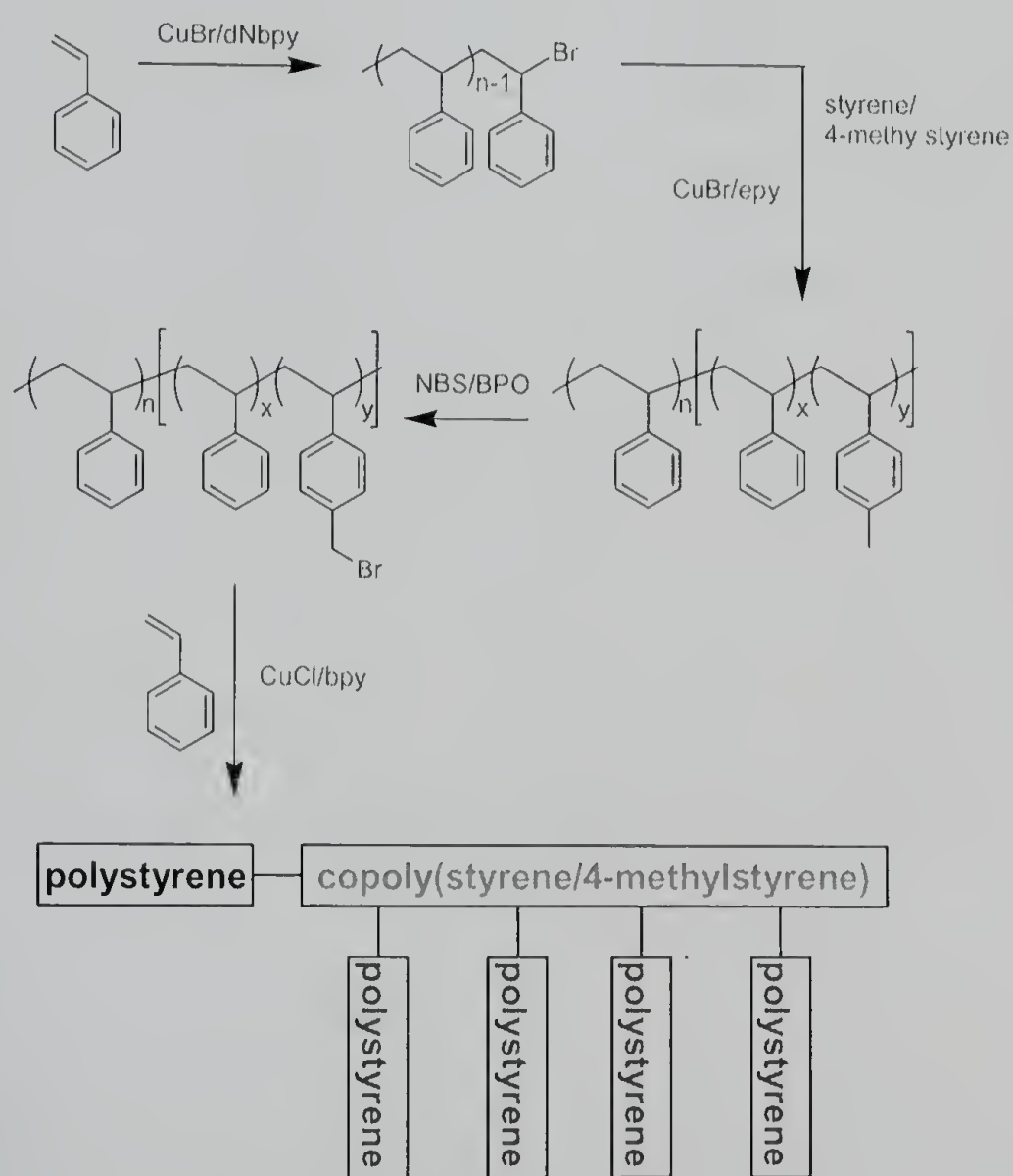
4.6.6 4-Methylstyrene

In addition to the vinylbenzyl alcohol based protected monomers, an alternative, and potentially simplifies, protection method was investigated. There have been several reports of halogenation of poly(4-methylstyrene) to introduce chloromethyl- or bromomethyl groups on to the rings. The homogeneous solution-phase free-radical initiated partial chlorination of poly(4-methylstyrene) resulted in main-chain chlorination and di- and tri- as well as monochlorination of the methyl groups.³³ Furthermore, under some conditions of homogeneous chlorination, the reaction is accompanied by either chain cleavage or crosslinking of the polymer. Mohanraj, *et al.* have reported the selective chlorination of the methyl group of poly(4-methylstyrene) in chlorinated aliphatic hydrocarbons at ambient temperatures using aqueous sodium hypochlorite and a phase-transfer catalyst such as benzyltriethylammonium chloride.³⁴ However, this method is only effective for the partial chlorination, and at higher conversion, undesired side reactions including multi-chlorination, chain cleavage, or crosslinking of the parent polymer take place.³⁵ Bromination reactions are, on the other hand, highly selective toward formation of the monobromination of the methyl groups. Chung, *et al.* reported the radical bromination of α -olefin/4-methylstyrene copolymers.³⁶ Bromination by the reaction of copoly(α -olefin/4-methylstyrene) using N-bromosuccinimide (NBS) and benzoyl peroxide (BPO) in anhydrous carbon tetrachloride is highly specific and yields a product with almost exclusive substitution on the *para*-methyl group to yield the benzylic bromide functionality.

This selectivity of the bromination reaction motivated us to use 4-methylstyrene as a protected monomer for the preparation of branched polymers. The same synthetic

strategy used to prepare the linear-branched block copolymer was applied here. A block copolymers with polystyrene segments and random copoly(styrene/4-methylstyrene) segments were prepared by the ATRP technique. The methyl group along the second block segment of copoly(styrene/4-methylstyrene) were then brominated, and the resulting benzyl bromide functionalities were used as initiating sites for the graft polymerization by ATRP to give linear-branched block copolymer (Scheme 4.15). In the first step, polystyrene was prepared by ATRP technique using the CuBr/4,4'-di-5-nonyl-2,2'-bipyridine (dNbpy) catalyst system. The resulting polystyrene was isolated and

Scheme 4.15 Preparation of Linear-Branched Block Copolymer Using 4-Methylstyrene



characterized by GPC chromatographic analysis and found to have a controlled structure ($M_n = 2,900$; PDI = 1.08; Figure 4.23a). This polymer was then reinitiated with an additional monomer feed of styrene/4-methyl styrene (mol ratio = 75/25) and the CuBr/epy catalyst system at 110 °C to form the second segment of the block copolymer ($M_n = 5,100$; PDI = 1.10; Figure 4.23b). The second block segment was composed of 75/25 ratio of styrene and 4-methylstyrene to control the density of branches in order to minimize the inter-chain coupling reaction during the grafting step. The methyl groups of 4-methylstyrene moieties were brominated using NBS/BPO to afford the benzyl bromide functionalities. The reaction was monitored using $^1\text{H-NMR}$ analysis. The methyl proton resonance at 2.3 ppm decreased, and a new peak appeared at 4.4 ppm, which corresponds to the chemical shift of the methylene protons in benzyl bromide group. Additionally, the $^{13}\text{C-NMR}$ spectrum showed a new signal at 34 ppm, which is also diagnostic for the methylene carbon in benzyl bromide group. Molecular weight measurements showed that the number-average molecular weight and molecular weight distribution of the new copolymer were the same within experimental error as those of the starting copolymer. These data support the conclusion that, within detectable limits, the methyl groups of the starting backbone copolymer had been converted to bromo-methyl groups without undergoing either chain cleavage or crosslinking reactions. From the ratio of the area of the peak for bromomethyl proton to the peaks for aromatic and aliphatic protons, we calculate that on average 5.7 benzyl bromide groups are present in a polymer chain.

The benzylbromide groups were then used as branch-initiating sites for ATRP grafting. Two different branches were prepared using CuBr/bpy as a catalyst at 110 °C. In both cases, the grafting reactions were quenched at low conversion to avoid any undesired

side reactions including inter-chain coupling reactions. The graft polymerization of styrene reached 20% of conversion after 2 h. Figure 4.23c shows GPC chromatogram of the product polymer. The molecular weight of the backbone block copolymer was clearly extended to higher molecular weight after the grafting process ($M_n = 44,900$). However, it is higher than the theoretical value ($M_{n,theory} = 29,300$) that is calculated as follows;

$$M_{n,theory} = M_{n,backbone} + n_{branch} \times \frac{[M]_0}{[I]_0} \times MW_{monomer} \times conversion \quad (1)$$

where, $M_{n,backbone}$ is the number average molecular weight of backbone polymer, n_{branch} is the number of initiating sites (benzyl bromide groups) in a backbone polymer chain, $[M]_0$ is the initial concentration of the grafting monomer, $[I]_0$ is the initial concentration of initiating sites, and $MW_{monomer}$ is the molecular weight of the grafting monomer.

The molecular weight distribution of the product polymer is unimodal, but was significantly broadened during the grafting process (PDI = 1.66). The higher molecular weight and broad molecular weight distribution indicate that a wide range of branch lengths or numbers of grafts per backbone must exist in the grafted polymer. One possible explanation is that the bromination reaction of the methyl groups by NBS/BPO was not perfectly selective to form benzyl bromide groups. Although this type of bromination is highly specific to give the benzyl bromide functionality, with an excess amount of NBS relative to the 4-methylstyrene moieties, bromination on other sites including the backbone methyne proton can take place. These unexpected brominated groups also could be active as initiating sites for the grafting process, but with different initiation reaction

rates. As a result, the molecular weight distribution of the grafted polymer would be broadened.

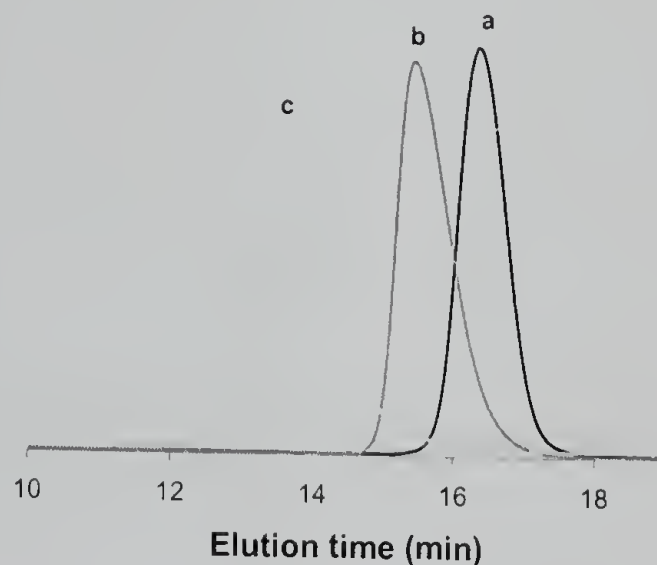


Figure 4.23 GPC chromatograms of linear-branched block copolymer, (a) initial polystyrene, (b) copoly[styrene-*b*-(styrene/4-methylstyrene)] backbone, (c) linear-branched block copolymer having polystyrene branches.

Grafted polymers with PMMA branches were also prepared under the same reaction conditions. This reaction was very fast, and after 15 min, the reaction mixture was completely solidified. Upon workup the conversion of the grafting monomer was calculated to be 38%. Figure 4.24 is the GPC chromatogram of the product polymer. The characteristics of the product polymer are similar to those samples with polystyrene branches. The molecular weight of the grafted polymer is extended from the starting backbone copolymer without any trace of residual backbone polymer. However, number average molecular weight of the polymer is higher than the theoretical value, and molecular weight distribution is broad ($M_n = 68,700$; PDI = 1.62).

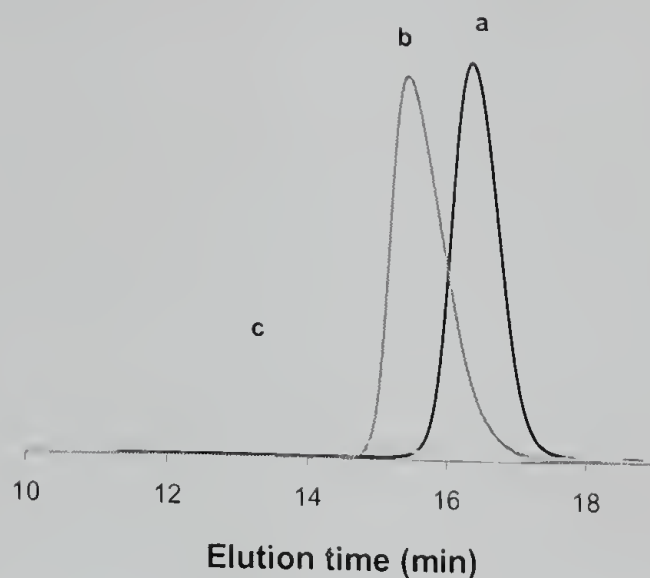
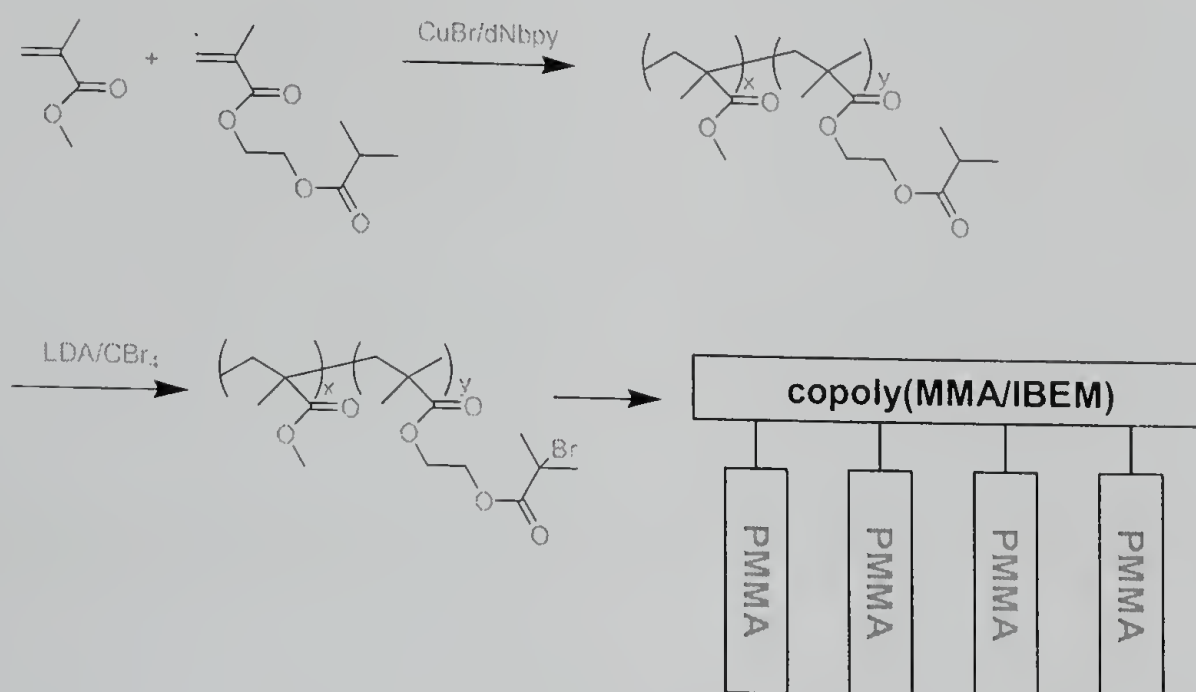


Figure 4.24 GPC chromatograms of linear-branched block copolymer, (a) initial polystyrene, (b) copoly[styrene-*b*-(styrene/4-methylstyrene)] backbone, (c) linear-branched block copolymer having PMMA branches.

4.6.7 2-Isobutyryloxyethyl Methacrylate (IBEM)

One of the advantages of using protection-deprotection strategies is that not only styrenic monomers, but also other different types of monomers including acrylates can be incorporated into the backbone. In this section, we prepared branched PMMA using a protection-deprotection method as an example. Previously, branched PMMA with controlled architecture could only be prepared by anionic polymerization or group transfer polymerization methods,³⁷ which have very demanding reaction conditions. In this case, 2-(isobutyryloxy)ethyl methacrylate (IBEM) was used as a protected monomer. By applying the same method as used for the preparation of the branched polystyrene, we could prepare structurally controlled branched PMMA that could not be prepared by the sequential use of nitroxide-mediated polymerization and ATRP (Scheme 4.16).

Scheme 4.16 Preparation of Branched PMMA Using IBEM



The IBEM monomer, prepared from 2-hydroxyethyl methacrylate and isobutyryl chloride in the presence of pyridine in dry benzene, was copolymerized with methyl methacrylate (10/90) under ATRP condition. The polymerization was run in diphenylether at 90 °C using CuBr/dNbpy as a catalyst. After 10 h of polymerization, the conversion reached 80%, and the product copolymer had $M_n = 24,600$ and PDI = 1.17 (Figure 4.25a). The composition of copolymer was calculated using ¹H-NMR analysis, and it was found to correspond to the initial monomer feed ratio, 10/90 (IBEM/MMA).

The initiating sites for the graft polymerization were generated on the IBEM component of copolymer. The copolymer was treated with lithium diisopropylamine (LDA) at 0 °C in THF, and the Li enolates was then halogenated by carbon tetrabromide. The halogenation reaction was monitored using ¹H-NMR analysis (Figure 4.26). The peak at 2.5 ppm corresponding to the methyne proton (H_d) from IBEM disappeared, and

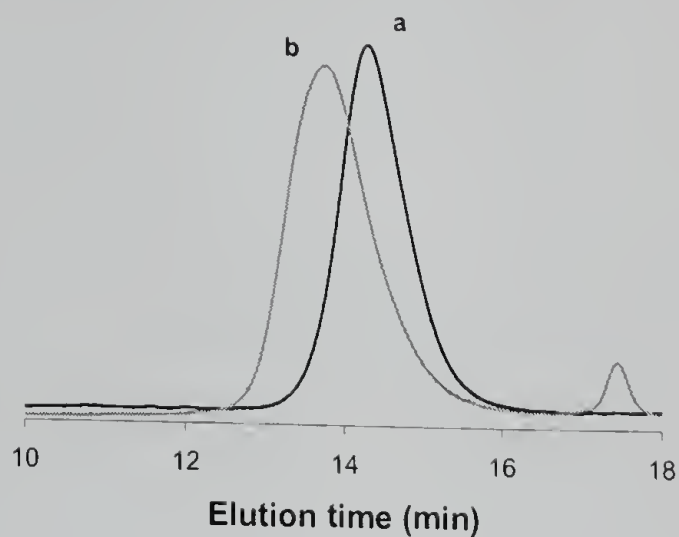


Figure 4.25 GPC chromatograms of branched PMMA. (a) backbone copoly(MMA/IBEM), (b) branched PMMA.

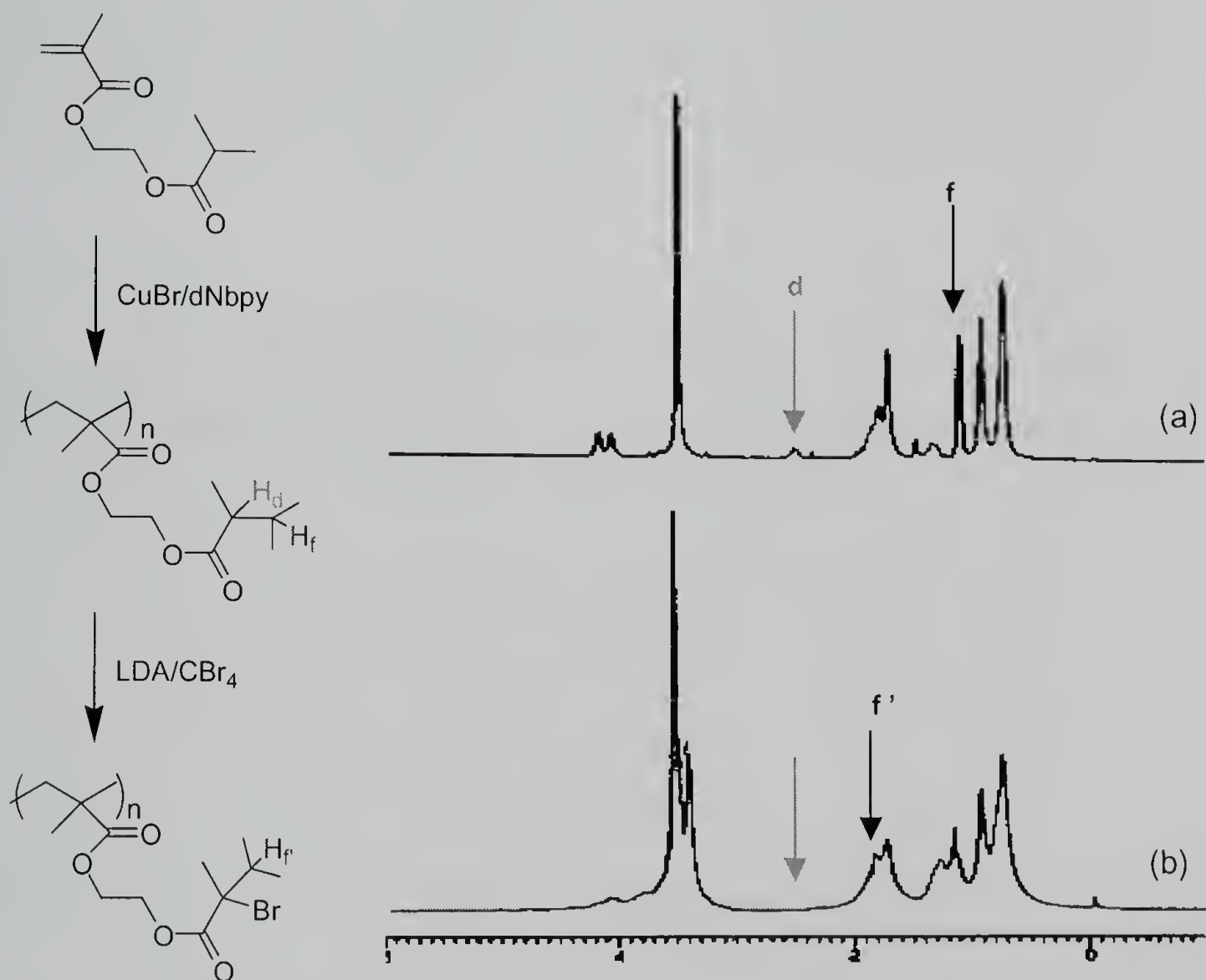


Figure 4.26 $^1\text{H-NMR}$ spectrums for, (a) copoly(MMA/IBEM), (b) brominated copolymer.

the peak at 1.1 ppm corresponding to the methyl proton (H_f) is shifted downfield to 1.9 ppm (H_f).

The backbone copolymer possessing halogenated pendant groups was then used to prepare a graft copolymer by ATRP techniques. PMMA branches were prepared using CuBr/dNbpy as a catalyst system. The product polymer was characterized by GPC to establish the graft nature (Figure 4.25b). The molecular weight is smaller than the expected value even considering the fact that the true value of the molecular weight for the branched polymers would be higher than the relative molecular weight calculated from GPC analysis. However, the molecular weight distribution of the product polymer is narrow and unimodal indicating controlled reaction during the graft polymerization.

4.7 Conclusion

Several strategies have been developed to prepare polymers having higher order structure including branched, hyperbranched, star, and dendrigrafts. The combination of nitroxide mediated SFRP and ATRP techniques successfully provided relatively simple routes to form branched and hyperbranched polymers in controlled structures. However, there was limitation of backbone polymer because only styrenic monomers can be polymerized in controlled way by SFRP, which is the method to prepare backbone polymer. To overcome this limitation by using the ATRP method only, a new strategy using protection-deprotection chemistry was employed. Alkyl halide groups that can be used as initiating sites in ATRP process were protected by suitable groups, and monomers containing these protected groups were polymerized by ATRP to form backbone polymer. The deprotection chemistry was then employed to regenerate initiating sites for the

branch formation. Among the various protected monomers tested, we could prepare branched polystyrene having controlled structure using VBT-BOC and 4-methyl styrene. We demonstrated the preparation of block copolymer of linear and branched polystyrene using this strategy, and the molecular weight distributions of the resulting polymers were narrow and unimodal. Branched PMMA was also prepared using the same method using IBEM as a protected monomer. After copolymerization of MMA and IBEM, alkyl bromide moieties were introduced to the IBEM and PMMA branches were prepared by ATRP method. The resulting branched PMMA had unimodal molecular weight distribution and low polydispersity.

4.8 Experimental

4.8.1 Characterizations

IR spectra were determined with either a Perkin-Elmer 1600 series FTIR or Jasco FT/IR-410 spectrometer as thin films coated on NaCl plates. ^1H and ^{13}C NMR spectra were measured in CDCl_3 unless otherwise noted. Spectra were recorded on either a Varian 200, Bruker 200, 300, or GE 300 spectrometer. ^1H NMR spectra were measured at 200 or 300 MHz. Proton decoupled ^{13}C NMR spectra were recorded at 75 MHz. ^1H chemical shift (δ) were referenced to a selected resonance of residual protons in the solvent employed. ^{13}C chemical shift (δ) were referenced to the carbon resonance of the solvent employed. Gas chromatography (GC) was performed using either HP 5890 equipped with MS detector, or HP 6890 with FID detector. Non-polar HP-5 or medium polar HP-INNOWAX capillary column were used for the separation. Gel permeation chromatography/light scattering (GPC/LS) were performed using either Hewlett-Packard (HP) 1050 series liquid chromatography pump equipped with a Wyatt Dawn DSP-F laser photometer, a Wyatt/Optilab interferometer and a Waters 746 data module integrator, or a Jasco PU-1580 series liquid chromatography pump equipped with a Wyatt Dawn DSP-F laser photometer and a Wyatt/Optilab interferometer. Tetrahydrofuran (THF) was used as the mobile phase. Sample were prepared as 0.5 - 2% polymer (w/v) solution in THF and passed through 0.45 μm filters prior to injection. Residual metal complexes were removed by passing the polymer solution through active alumina column. Separation were effected by 10^5 \AA , 10^4 \AA , 10^3 \AA , and $5 \times 10^5 \text{ \AA}$ Permagel columns (purchased from Pacific Column Co.) run in series, or a multiple series of Polymer laboratory Mixed C columns.

4.8.2 Materials

Materials were obtained from commercial suppliers and used without further purification unless otherwise noted. Styrene, methyl methacrylate (MMA), vinylbenzyl chloride, 4-methyl styrene (4-MeSt) and benzyl chloride were dried over CaH_2 overnight, and distilled twice under reduced pressure from CaH_2 prior to use. *p*-Toluenesulfonyl (tosyl) chloride was purified by recrystallizing from benzene. Benzoyl peroxide (BPO) was purified by dissolving in CHCl_3 at room temperature and adding an equal amount of methanol. α,α' -Azobis(isobutyronitrile) (AIBN) was purified by recrystallizing from acetone. Imidazole was purified by sublimation two times before use. Bipyridine (bpy) was purchased from Aldrich, and purified by recrystallization from ethyl alcohol. 4,4'-di-5-nonyl-2,2'-bipyridine (dNbpy)³⁸ and 4,4'-di-phenoxy-2,2'-bipyridine (pby)³⁹ were prepared following literature procedures. 4,4'-di-(*p*-ethylphenoxy)-2,2'-bipyridine (epy) and 4,4'-di-(*p*-methoxyphenoxy)-2,2'-bipyridine (mpy) were prepared following the methods described in Chapter 1.

4.8.2.1 Preparation of Protected Monomers

Vinylbenzylacetate. To a 250 mL round-bottom flask containing 16 g (160 mmol) of potassium carbonate was added 50 mL of dimethyl sulfoxide and 22 g (140 mmol) of vinylbenzyl chloride. The yellowish heterogeneous mixture was stirred at 40 °C for 5 days, and then the reaction mixture was filtered and washed with 300 mL of water. The oily component was extracted with 20 mL of chloroform (three times), and the remaining water was removed drying over Na_2SO_4 . The mixture was filtered and evaporated to remove most of chloroform. The remaining liquid was then distilled under vacuum to afford 22.4 g (90%) of vinylbenzylacetate as a colorless liquid, bp 58 °C (60

mtorr), which was stored in the freezer until use. IR (neat): 3008 (m), 2955 (m), 1739 (s), 1378 (m), 1226 (s), 1028 (s), 991 (m), 912 (m) cm^{-1} . ^1H NMR (300 MHz): δ (ppm) 7.22 (m, 4H), 6.67 (q, 1H), 5.62 (d, 1H), 5.13 (d, 1H), 4.95 (s, 2H), 1.97 (s, 3H). MS (EI): m/z 176 (M^+), 134, 115, 105, 91, 77.

Vinylbenzylalcohol (VBOH). To a 100 mL round bottom flask equipped with reflux condenser was added 22 g (120 mmol) of vinylbenzyl acetate, 12 g of sodium hydroxide in 12 mL of water, and 70 mL of ethyl alcohol. The reaction mixture was refluxed for 1.5 hr, and diluted with 300 mL of water. The product mixture was extracted with 4 \times 20 mL of chloroform, and then dried over Na_2SO_4 . The solution was filtered and evaporated to remove most of chloroform. The distillation under reduced pressure afforded 14.5 g (87%) of vinylbenzylalcohol as a colorless liquid, bp 58 °C (60 mtorr), which was stored in the freezer until next use. IR (neat): 3328 (br, s), 3006 (m), 2872 (m), 1629 (m), 1406 (s), 1211 (m), 1157 (m), 1013 (s), 990 (s), 908 (m) cm^{-1} . ^1H NMR (300 MHz): δ (ppm) 7.37 (m, 4H), 6.72 (q, 1H), 5.78 (d, 1H), 5.27 (d, 1H), 4.67 (s, 2H), 1.81 (s, 1H). MS (EI): m/z 134 (M^+), 115, 105, 91, 77.

Attempts to prepare vinylbenzyltosylate (VBOTs). Method A: A 2-neck 100 mL round bottom flask equipped with magnetic bar and nitrogen flow was charged with 4.0 g of vinylbenzyl alcohol (3×10^{-2} mol) and 4.0 mL of pyridine (5×10^{-2} mol). The flask was cooled to 0 °C using an ice bath, and 5.7 g of tosyl chloride (3×10^{-2} mol) dissolved in 20 mL of methylene chloride was added dropwise over 1.5 h. Temperature was then increased to room temperature and the reaction was continued for 24 h. After

the reaction, 16 mL of sulfuric acid was added to the mixture, and the mixture was washed with water to remove pyridine-hydrogen chloride salt. After phase separation, the organic layer was dried over Na_2SO_4 . The mixture was filtered, evaporated, and distillation under reduced pressure gave liquid compound (33 °C / 45 mtorr), which was characterized as starting vinylbenzylalcohol.

Method B: A 3-neck 200 mL round bottom flask equipped with two addition funnels, refluxing condenser, and nitrogen flow was charged with 4.0 g of vinylbenzyl alcohol (3×10^{-2} mol) and 20 mL of diethyl ether. The mixture was refluxed by heating, and 0.72 g of sodium hydride in 40 mL of diethyl ether was added dropwise over 1 h. After additional 15 h, the mixture was cooled to -10 °C, and 6.4 g of tosyl chloride (3.3×10^{-2} mol) in 30 mL of diethyl ether was added dropwise for 30 min. The temperature was slowly increased to room temperature, and the mixture was stirred for additional 1 h at room temperature. White solid was precipitated from yellow liquid, and the yellow liquid was characterized by GC and NMR as to be a mixture of reactant, product, and unidentified compounds.

Vinylbenzyl-*t*-butyldimethylsilylether (VBOSi). To a 25 mL flask with magnetic stirring bar were added 6.7 g of vinylbenzylalcohol (5×10^{-2} mol), 9.0 g of *t*-butyldimethylsilyl chloride (6×10^{-2} mol), 8.5 g of imidazole (1.25×10^{-1} mol), and 13 mL of dimethylformamide. After stirring for 24 h at 35 °C, water was added to the reaction mixture, and the organic layer was extracted with chloroform (4 times). The extracted chloroform solution was dried over Na_2SO_4 . Filtration and evaporation under reduced pressure afforded vinylbenzyl-*t*-butyldimethylsilylether as a colorless liquid. ^1H

NMR (300 MHz): δ (ppm) 7.29 (m, 4H), 6.72 (m, 1H), 5.74 (m, 1H), 5.22 (m, 1H), 4.74 (s, 2H), 0.95 (s, 9H), 0.11 (s, 6H). MS (EI): m/z 248 (M^+), 191, 161, 117, 91, 75, 57.

Benzyl-*t*-butyldimethylsilylether (BzOSi). Benzyl-*t*-butyldimethylsilylether was prepared similarly to vinylbenzyl *tert*-butyldimethylsilylether from benzyl alcohol. The reaction was run for 2 days at room temperature. After work-up, the resulting liquid was distilled twice at reduced pressure (30 °C/400 mtorr) to afford benzyl-*t*-butyldimethylsilylether as a colorless liquid. ^1H NMR (300 MHz): δ (ppm) 7.16 (m, 5H), 4.65 (s, 2H), 0.80 (s, 9H), 0.00 (s, 6H). MS (EI): m/z 165, 135, 91, 75, 65, 57.

Vinylbenzyl-*t*-butylether (VBO*t*-Bu). A 100 mL flask was charged with 4.8 g of sodium *t*-butoxide (5×10^{-2} mol), 9.2 g of vinylbenzyl chloride (6×10^{-2} mol), and 30 mL of dimethylformamide. The reaction mixture was heated overnight and methylene chloride was added to give precipitate. After filtering, the solution was washed with water, and dried over Na_2SO_4 . Methylene chloride was removed using a rotary evaporator, and distillation under reduced pressure afforded vinylbenzyl-*t*-butylether as a colorless liquid (40 °C/60 mtorr) ^1H NMR (300 MHz): δ (ppm) 7.22 (m, 4H), 6.61 (m, 1H), 5.65 (m, 1H), 5.13 (m, 1H), 4.37 (s, 2H), 1.22 (s, 9H). MS (EI): m/z 190 (M^+), 134, 117, 105, 91, 77, 57.

Vinylbenzyl-*t*-butyloxycarbonate (VB*t*-BOC). A solution of 2.3 g of vinylbenzyl alcohol (2.3×10^{-2} mol) in 5 mL of THF containing a catalytic amount of 18-crown-6 was treated with 3.0 g of powdered potassium carbonate and 4.4 g of di-*t*-butyl

dicarbonate (2×10^{-2} mol). The mixture was stirred for 48 h at room temperature, then 10 mL of water were added. The organic layer was extracted with 4×5 mL of chloroform, and dried over Na_2SO_4 . After filtration, chloroform was removed by evaporation under reduced pressure. Distillation under reduced pressure afforded vinylbenzyl-*t*-butyloxycarbonate as a colorless liquid (32 °C/75 mtorr). IR (neat): 2981 (m), 1740 (s), 1370 (s), 1277 (m), 1161 (s), 1119 (s), 1072 (s), 856 (m) cm^{-1} . ^1H NMR (300 MHz): δ (ppm) 7.35 (m, 4H), 6.71 (m, 1H), 5.74 (d, 1H), 5.26 (d, 1H), 5.08 (s, 2H), 1.50 (s, 9H). MS (EI): m/z 234 (M^+), 178, 134, 117, 105, 91, 77, 57.

Benzyl-*t*-butyloxycarbonate (Bzt-BOC). Benzyl-*t*-butyloxycarbonate was prepared similarly to vinylbenzyl-*t*-butyloxycarbonate from benzyl alcohol. Distillation under reduced pressure afforded vinylbenzy- *t*-butyloxycarbonate as a colorless liquid (46 °C/240 mtorr). ^1H NMR (300 MHz): δ (ppm) 7.30 (m, 5H), 5.04 (s, 2H), 1.42 (s, 9H). MS (EI): m/z 208 (M^+), 153, 146, 107, 91, 77, 57.

2-(Isobutyryloxy)ethyl methacrylate (IBEM). To a solution of 2-hydroxyethyl methacrylate (13 g, 0.1 mol) in dry benzene (50 mL), pyridine (8 mL, 0.1 mol) was added with stirring and the mixture was cooled to 0 °C. A 10% excess of isobutyryl chloride (11.6 g, 0.11 mol) was added through the dropping funnel at a slow rate, so that the temperature was kept as low as possible. A white solid started to precipitate immediately. After addition was complete, the mixture was allowed to stir at 0 °C for 3 h. Benzene (30 mL) was then introduced into the reaction mixture in order to facilitate filtration of the pyridine hydrochloride by-product. The solution was collected and the solvent removed

on a rotary evaporator. The pale yellow oil that remained was distilled at reduced pressure to afford 2-(isobutyryloxy)ethyl methacrylate (90%) as a colorless liquid (64 °C/60 mtorr). IR (neat): cm^{-1} . ^1H NMR (300 MHz): δ (ppm) 6.12 (s, 1H), 5.58 (s, 1H), 4.33 (m, 4H), 2.56 (m, 1H), 1.93 (s, 3H), 1.16 (d, 6H).

4.8.3 Deprotection Reactions

4.8.3.1 Deprotection of *t*-Butyloxycarbonate group

0.2 g of the copolymer of polystyrene-block-copoly(styrene/VB¹BOC) (styrene/VB¹BOC = 83/17; M_n = 17,850; PDI = 1.285) was dissolved in 5 mL of methylene chloride, and treated with 0.5 mL of trifluoroacetic acid. The mixture was stirred for 24 h, and the polymer was precipitated by pouring into petroleum ether. After filtration, the resulting polymer was dried overnight under reduced pressure (yield, 0.18 g). 0.17g of the polymer was redissolved in 5 mL of THF, and treated with 79 mg of triphenylphosphine and 0.1 g of carbon tetrabromide. The mixture was stirred for 1.5 h at room temperature, and polymer was isolated by precipitating from methanol. Filtration and drying overnight under reduced pressure afforded 0.14 g of brominated polymer.

4.8.3.2 Bromination of Poly(4-methyl styrene)

The polymer was allowed to react with NBS (NBS/methyl group molar ratio = 2 : 1) in anhydrous carbon tetrachloride solution in the dark, under a nitrogen atmosphere, in the presence of 2% by weight BPO, at the boiling point of the solvent for 2 h. The solutions were filtered to eliminate the insoluble succinimide produced and purified by passing through an Al_2O_3 column. The polymer was precipitated by methanol and dried under vacuum.

4.8.3.3 Bromination of Poly(IBEM)

A 2 M solution of *n*-BuLi in hexane (1.1 mL, 2.2×10^{-4} mol) was added to a solution of diisopropylamine (0.22 g, 2.2×10^{-4} mol) in 1 mL of THF at 0 °C under an argon atmosphere. The mixture was stirred for 15 min at 0 °C and cooled to -78 °C. With a continuous stirring, a solution of copoly(MMA/IBEM) (0.22 g, 2×10^{-4} mol) in 3 mL of THF was added dropwise to this solution. The mixture was stirred for 20 min, and carbon tetrabromide (0.07 g, 2×10^{-4} mol) in 1 mL of THF was added dropwise. The mixture was allowed to warm to room temperature and then was stirred for 3 h. Cold HCl (2 mL, 1M) was added, and then the solid was filtered. The organic layer was separated and the solvent was evaporated to dry. The combined crude solid was dissolved in THF and the polymer was precipitated by hexane and dried under vacuum.

4.8.4 Polymerization

4.8.4.1 Preparation of Branched Polymers Using Conventional Radical Polymerization and ATRP Method

In a 25 mL flask, 3.1 g of styrene (0.03 mol), 4.6 g of vinylbenzyl chloride (0.03 mol), and 4 mL of benzene were degassed by stirring and bubbling dry nitrogen for 15 min. The mixture was heated at 60 °C, and AIBN dissolved in 4 mL of degassed benzene was added to it. After 1 h of polymerization, THF was added to dissolve the reaction mixture, and polymer was isolated by precipitation from methanol. The copolymer was filtered and dried overnight under vacuum. A 5 mL reaction tube was charged with 0.86 g of styrene (8.2×10^{-3} mol), 5.5 mg of copper(I) chloride (5.6×10^{-5} mol), 57 mg of pby (1.7×10^{-4} mol), and 0.02g of copoly(styrene/vinylbenzyl chloride) in a drybox. The reaction tube was removed from the drybox, degassed three times using a freeze-thaw

method, and sealed under vacuum. The reaction mixture was not homogeneous at room temperature, but became so at the reaction temperature of 130 °C. After 6 h of polymerization, the mixture was dissolved in THF, and the branched polymer was isolated by precipitation from methanol, filtering, and dried under vacuum.

4.8.4.2 Preparation of Branched Polymers by the Sequential Use of Two Different Controlled Free Radical Polymerization Methods

To a 25 mL Schlenk flask were added 0.78 g of styrene (7.5×10^{-3} mol), 1.14 g of vinylbenzyl chloride (7.5×10^{-3} mol), 18 mg of benzoyl peroxide (7.5×10^{-5} mol), and 15 mg of TEMPO (9.8×10^{-3} mol) under nitrogen atmosphere. The flask was degassed several times using a freeze-thaw method, and immersed into the oil bath. The reaction flask was heated at 95 °C for 3.5 h to ensure the decomposition of BPO, and then heated at 125 °C for 12 h. After reaction, the solidified mixture was dissolved in THF, and the polymer was precipitated from methanol. The resulting copoly(styrene/vinylbenzyl chloride) were dried overnight under vacuum. The small portion of this sample (0.02 g) was dissolved in 0.86 g of styrene, and added to a 5 mL reaction tube containing 5.5 mg of copper(I) chloride and 57 mg of pby in a drybox. The reaction tube was removed from the drybox, degassed three times using the freeze-thaw method, and sealed under vacuum. The reaction mixture was not homogeneous at room temperature, but became so at reaction temperature of 130 °C. After 4 h of polymerization, the mixture was dissolved in THF, and the branched polymer was isolated by precipitation from methanol, filtering, and dried under vacuum.

4.8.4.3 Preparation of Hyperbranched Polymers by the Sequential Use of Two Different Controlled Free Radical Polymerization Methods

A 5 mL reaction tube was charged with 0.98 g of vinylbenzyl chloride (6.4×10^{-3} mol), 6.4 mg of copper(I) chloride (6.4×10^{-5} mol), and 30 mg of bpy (1.9×10^{-4} mol) in a drybox. The reaction tube was removed from the drybox, degassed three times using the freeze-thaw method, and sealed under argon. After 2 h of polymerization at 130 °C, THF was added to the mixture, and the hyperbranched poly(vinylbenzyl chloride) was isolated by precipitation from methanol. The polymer was purified by redissolving in THF, precipitation from methanol, and dried overnight under vacuum. To a 5 mL reaction tube were added 0.4 g of hyperbranched poly(vinylbenzyl chloride), 0.78 g of styrene, 18 mg of BPO, and 15 mg of TEMPO under nitrogen. The reaction tube was degassed several times using the freeze-thaw method, and sealed under vacuum. The reaction flask was heated at 95 °C for 3.5 h to ensure the decomposition of BPO, and then heated at 130 °C for 24 h. After reaction, the solidified mixture was dissolved in THF, and the polymer was precipitated from methanol.

4.8.4.4 Preparation of Star Polymers by the Sequential Use of Two Different Controlled Free Radical Polymerization Methods

In a drybox, 5 mg of hyperbranched poly(vinylbenzyl chloride) (3.3×10^{-5} mol of benzyl chloride) prepared with the same method was dissolved in 0.35 g of additional styrene (3.3×10^{-3} mol) having 3.3 mg of CuCl (3.33×10^{-5} mol) and 10 mg of bpy (6.6×10^{-5} mol) in a 5 mL of drying tube. The tube was capped, and removed from the drybox. After degassing by three times by the freeze-thaw method, the tube was sealed under vacuum, and placed in an oil bath thermostated at 130 °C. The polymerization was

continued for 2 h, and quenched by immersing in LN₂. The seal was broken, and THF was added to dissolve the solid product. The polymer was purified by precipitation in methanol and dried overnight under vacuum yield 0.25 g of product polymer (70%).

4.8.4.5 Branched Polymers Using Protection-Deprotection Chemistry

4.8.4.5.1 General Procedure

A mixture of monomer, initiator, metal halide, ligand, and solvent was prepared in a 5 mL of drying tube in a drybox under an inert atmosphere. The tube was removed from the drybox. After degassing by three times by the freeze-thaw method, the tube was sealed under vacuum, and placed in an oil bath thermostated at the desired temperature. The polymerization was quenched by immersing in LN₂. The seal was broken, and THF was added to dissolve the solid product. The polymer was purified by precipitation in methanol and dried overnight under vacuum. The conversion was determined by gravimetry, and the resulting polymers were characterized by ¹H-NMR and GPC after removing the residual metal catalysis by passing the polymer solution through active alumina column.

4.8.4.5.2 Polymerization of Styrenes in the Presence of Additives Bearing the Same Functionalities as the Protecting Groups

The same concentration of additives as styrene was used to introduce the same amount of functional groups as the polymerization of protected styrenes. The polymerization mixture was composed of 0.52 g of styrene (5×10^{-3} mol), 5.8 μ L of benzyl chloride (5×10^{-5} mol), 4.9 mg of copper(I) chloride (5×10^{-5} mol), ligand (pby or mpy; 1×10^{-4} mol), and additive (BzOSi, benzyl alcohol, or Bzt-BOC; 5×10^{-3} mol).

4.8.4.5.3 Preparation of Linear-Branched Block Copolymer

From VBt-BOC; The initial polystyrene block segment was prepared from 0.31 g of styrene (3×10^{-3} mol), 8.7 mg of benzyl chloride (6.9×10^{-5} mol), 6.9 mg of copper(I) chloride (6.9×10^{-5} mol), and 56 mg of epy (1×10^{-4} mol). After 4 h reaction at 130 °C, polymerization was quenched by immersing in LN₂, and polystyrene was purified from metal catalysts by repeated dissolving in THF / precipitating from methanol. The small portion of this sample (0.12 g) was dissolved in 0.26 g of styrene and 0.18 g of VBt-BOC, and added to a 5 mL reaction tube containing 3.0 mg of copper(I) chloride and 24 mg of epy in a drybox. The polymerization was run following general procedure at 110 °C for 20 h, and the product copolymer of polystyrene-*b*-copoly(styrene/VB^tBOC) was isolated. After two steps of deprotection reactions described in section 3.1, the polymer (0.016 g; [-Br] cal'd as 1×10^{-5} mol) was dissolved in additional monomer (styrene or MMA; 2×10^{-3} mol) containing 1.0 mg of copper(I) chloride (1×10^{-5} mol) and 4.7 mg of bpy (3×10^{-5} mol) in a drybox. The polymerization was run following general procedure at 110 °C for 2.5 h (styrene) or 1 h (MMA), and the product copolymer of polystyrene-*b*-copoly(styrene/VB^tBOC) was isolated by precipitation from methanol, filtering, and dried under vacuum.

From 4-MeSt; The initial polystyrene block segment was prepared from 0.20 g of styrene (2×10^{-3} mol), 19 mg of 1-phenylethyl chloride (1×10^{-4} mol), 14 mg of copper(I) bromide (1×10^{-4} mol), and 82 mg of dNbpy (2×10^{-4} mol). After 5 h reaction at 110 °C, polymerization was quenched by immersing in LN₂, and polystyrene was purified from metal catalysts by repeated dissolving in THF / precipitating from methanol. The small

portion of this sample (0.1 g) was dissolved in 0.13 g of styrene and 0.044 g of 4-MeSt, and added to a 5 mL reaction tube containing 3.9 mg of copper(I) bromide and 23 mg of epy in a drybox. The polymerization was run following general procedure at 110 °C for 20 h, and the product copolymer of polystyrene-*b*-copoly(styrene/4-MeSt) was isolated. After the deprotection reaction described in section 3.2, the polymer (0.01 g; [-Br] cal'd as 1×10^{-5} mol) was dissolved in additional monomer (styrene or MMA; 2×10^{-3} mol) containing 1.0 mg of copper(I) chloride (1×10^{-5} mol) and 4.7 mg of bpy (3×10^{-5} mol) in a drybox. The polymerization was run following general procedure at 110 °C for 2 h (styrene) or 15 min (MMA), and the product copolymer of polystyrene-*b*-copoly(styrene/VB^tBOC) was isolated by precipitation from methanol, filtering, and dried under vacuum.

4.8.4.5.4 Preparation of Branched PMMA

The backbone copolymer of MMA and IBEM was prepared from 0.27 g of MMA (2.7×10^{-3} mol), 0.06 g of IBEM (3×10^{-4} mol), 5.7 mg of tosyl chloride (3×10^{-5} mol), 4.3 mg of copper(I) bromide (3×10^{-5} mol), 25 mg of dNbpy (6×10^{-5} mol), and 0.37g of diphenylether (50%, v/v). After 10 h reaction at 90 °C, polymerization was quenched by immersing in LN₂, and the product copolymer was purified from metal catalysts by repeated dissolving in THF / precipitating from methanol. After the deprotection reaction described in section 3.3, the polymer (0.02 g; [-Br] cal'd as 2×10^{-5} mol) was dissolved in a mixture of additional MMA (2×10^{-3} mol), 2.9 mg of copper(I) bromide (2×10^{-5} mol), 16 mg of bpy (4×10^{-5} mol), and 0.69g of diphenylether (33%, v/v) in a drybox. The polymerization was run following general procedure at 90 °C for 24 h, and the product

branched PMMA was isolated by precipitation from methanol, filtering, and dried under vacuum.

4.9 References

1. Vogl, O.; Jaycox, G.; Hatada, K. *J. Macromol. Sci., Chem.* **1990**, *A27*, 1781 and references therein.
2. Baily, D.; Tirrell, D.; Vogl, O. *J. Macromol. Sci., Chem.* **1978**, *A12*, 661.
3. *Syntheses and Separations Using Functional Polymers*; Sherrington, D.; Hodge, P. Eds.; John Wiley & Sons: New York, 1988.
4. Webster, O. *Macromol. Symp.* **1995**, *98*, 1361.
5. Tomalia, D.; Hedstrand, D.; Ferritto, M. *Macromolecules* **1991**, *24*, 1435 and references therein.
6. Webster, O.W. *Science* **1991**, *251*, 887.
7. Szwarc, M. *Nature* **1956**, *176*, 1168.
8. Matyjaszewski, K.; Acar, M. H.; Beers, K. L.; Coca, S.; Davis, K. A.; Gaynor, S. G.; Miller, P. J.; Paik, H.-J.; Shipp, D. A.; Teodorescu, M.; Xia, J.; Zhang, X. *Polym. Prepr. (Am. Chem. Soc., Div. Polym. Chem.)* **1999**, *40(2)*, 966.
9. (a) Hawker, C. J. *Angew. Chem. Int. Ed. Engl.* **1995**, *34*, 1456. (b) Grubbs, R. B.; Hawker, C. J.; Dao, J.; Fréchet, J. M. J. *Angew. Chem. Int. Ed. Engl.* **1997**, *36*, 270. (c) Hawker, C. J.; Mecerreyes, D.; Elce, E.; Dao, J.; Hedrick, J. L.; Barakat, I.; Dubois, P.; Jérôme, R.; Volksen, W. *Macromol. Chem. Phys.* **1997**, *198*, 1553. (d) Beers, K. L.; Gaynor, S. C.; Matyjaszewski, K. *Polym. Prepr. (Am. Chem. Soc., Div. Polym. Chem.)* **1996**, *37(1)*, 571.
10. (a) Hawker, C. J.; Fréchet, J. M. J.; Grubbs, R. B.; Dao, J. *J. Am. Chem. Soc.* **1995**, *117*, 10763. (b) Gaynor, S. C.; Edelman, S.; Matyjaszewski, K. *Macromolecules* **1996**, *29*, 1079. (c) Matyjaszewski, K.; Gaynor, S. C.; Kulfan, A.; Podwika, M. *Macromolecules* **1997**, *30*, 5192. (d) Mecerreyes, D.; Trollsås, M.; Hedrick, J. L. *Macromolecules* **1999**, *32*, 8753.
11. Heise, A.; Nguyen, C.; Malek, R.; Hedrick, J. L.; Frank, C. W.; Miller, R. D. *Macromolecules* **2000**, *33*, 2346.
12. (a) Leduc, M.R.; Hawker, C.J.; Dao, J.; Fréchet, J. M. J. *J. Am. Chem. Soc.* **1996**, *118*, 1111. (b) Matyjaszewski, K.; Shigemoto, T.; Fréchet, J. M. J.; Leduc, M. R. *Macromolecules* **1996**, *29*, 4167. (c) Leduc, M. R.; Hayes, W.; Fréchet, J. M. J. *J. Polym. Sci., Part A* **1998**, *36*, 1.
13. Rempp, P. F.; Lutz, P. J. in *Comprehensive Polymer Chemistry, Vol. 7*, Aggarwal, S. V. ed. Pergamon, Oxford, **1988**, Chapter 12.

-
14. Our lab, unpublished data
 15. (a) Fréchet, J.M.J.; Henmi, M.; Gitsov, I.; Aoshima, S.; Leduc, M.R.; Grubbs, R.B. *Science* **1995**, *269*, 1080. (b) Gaynor, S.C.; Edelman, S.; Matyjaszewski, K. *Macromolecules* **1996**, *29*, 1079.
 16. Stork, G.; Hudrlik, P. F. *J. Am. Chem. Soc.* **1968**, *90*, 4462.
 17. Corey, E. J.; Venkateswarlu, A. *J. Am. Chem. Soc.* **1972**, *94*, 6190.
 18. Lalonde, M.; Chan, T. H. *Synthesis* **1985**, 817.
 19. Mattes, H.; Benezra, C. *Tetrahedron Letters* **1987**, *28*, 1697.
 20. Aizpurua, J. M.; Cossio, F. P.; Palomo, C. *J. Org. Chem.* **1986**, 4941.
 21. Our lab, unpublished data
 22. Qiu, J.; Matyjaszewski, K. *Macromolecules* **1997**, *30*, 5643.
 23. Marchand, A. P.; Weimer, W. R. Jr *Chem. Ind.* **1969**, 200.
 24. (a) Carpino, L. A. *J. Am. Chem. Soc.* **1957**, *79*, 98. (b) McKay, F. C.; Albertson, N. F. *J. Am. Chem. Soc.* **1957**, *79*, 4686. (c) Anderson, G. W.; McGregor, A. C. *J. Am. Chem. Soc.* **1957**, *79*, 6180. (d) Carpino, L. A. *Acc. Chem. Res.* **1973**, *6*, 191. (e) Bodanski, M.; Klaussner, Y.; Ondetti, M. A. *Peptide synthesis*, 2nd Ed. Wiley-Interscience, New York, 1976, p.26.
 25. Willson, C. G.; Ito, H.; Fréchet, J. M. J.; Houlihan, F. *Proceedings 28th IUPAC Macromolecular Symposium*, Amherst, Mass. **1982**, p.448.
 26. (a) Carpino, L. A.; Collins, D.; Gowecke, S.; Mayo, J.; Thatte, S. D.; Tibbets, F. *Org. Synth. Coll.* **1973**, *5*, 166. (b) Scott, J. W. *Org. Prep. Proceed. Int.* **1980**, *12*, 242. (c) Gelin, R.; Gelin, S.; Gallaud, A. *Bull. Soc. Chim. Fr.* **1973**, *12*, 3416. (d) Pozdnev, V. F.; Nishnova, I. A. *Zh. Org. Khim.* **1976**, *12*, 1407. (e) Carpino, L. A.; Carpino, B. A.; Giza, C. A.; Murray, R. W.; Santilli, A. A.; Terry, P. H. *Org. Synth.* **1964**, *44*, 22.
 27. Houlihan, F.; Bouchard, F.; Fréchet, J. M. J.; Willson, C. G. *Can. J. Chem.* **1985**, *63*, 153.
 28. Greene, T. W.; Wuts, P. G. M. *Protective Groups in Organic Synthesis*, 3rd Ed. Wiley-Interscience, New York, 1999, p.518.
 29. (a) Rawal, V. H.; Jones, R. J.; Cava, M. P. *J. Org. Chem.* **1987**, *52*, 19. (b) Wasserman, H. H.; Berger, G. D.; Cho, K. R. *Tetrahedron Lett.* **1985**, *26*, 1411.

-
30. (a) Stahl, G. L.; Walter, R.; Smith, C. W. *J. Org. Chem.* **1978**, *43*, 2285. (b) Lundt, B. F.; Johansen, N. L.; Vølund, A.; Markussen, J. *Int. J. Pept. Protein Res.* **1978**, *12*, 258. (c) Bodanszky, M.; Bodanszky, A. *Int. J. Pept. Protein Res.* **1984**, *23*, 565. (d) Masui, Y.; Chino, N.; Sakakibara, S. *Bull. Chem. Soc. Jpn.* **1980**, *53*, 464.
31. (a) Olah, G. A.; Narang, S. C. *Tetrahedron* **1982**, *38*, 2225. (b) Tsuji, T.; Kataoka, T.; Yoshioka, M.; Sando, Y.; Nishitani, Y.; Hirai, S.; Maeda, T.; Nagata, W. *Tetrahedron Lett.* **1979**, 2793. (c) Kaiser, E. Sr.; Tam, J. P.; Ubiak, T. M.; Merrifield, R. B. *Tetrahedron Lett.* **1988**, *29*, 303.
32. Lott, R. S.; Chauhan, V. S.; Stammer, C. H. *J. Chem. Soc., Chem. Commun.*, **1979**, 495.
33. (a) Tarascon, R. G.; Hartney, M. A.; Bowden, M. J. *Materials for microlithography, ACS Symp. Ser.* **1984**, 266, 361. (b) Hartney, M. A.; Tarascon, R. G.; Novembre, A. E. *J. Vac. Sci. Technol. (B)* **1985**, *3(1)*, 360.
34. Mohanraj, S.; Ford, W. T. *Macromolecules* **1986**, *19*, 2470.
35. Jones, R. G.; Matsubayashi, Y. *Polymer* **1990**, *31*, 1519.
36. Chung, T. C.; Lu, H. L. *U. S. Pat.* 5,543,484, 1996.
37. Dos Santos, C.G.; Jenkins, A.D.; Walton, D.R.M.; Stejskal, J.; Kratochvíl, P. *Coll. Czech. Chem. Commun.* **1993**, *58*, 2523.
38. Matyjaszewski, K.; Patten, T. E.; Xia, J. *J. Am. Chem. Soc.* **1997**, *119*, 674.
39. Maerker, C. *J. Am. Chem. Soc.* **1958**, *80*, 2745.

BIBLIOGRAPHY

- Abrol, S.; Kambouris, P. A.; Looney, M. G.; Solomon, D. H. *Macromol. Rapid Commun.* **1997**, *18*, 755.
- Aizpurua, J. M.; Cossio, F. P.; Palomo, C. *J. Org. Chem.* **1986**, 4941.
- Anderson, G. W.; McGregor, A. C. *J. Am. Chem. Soc.* **1957**, *79*, 6180.
- Ando, T.; Kamigaito, M.; Sawamoto, M. *Macromolecules* **1997**, *30*, 4507.
- Ando, T.; Kamigaito, M.; Sawamoto, M. *Macromolecules*, **2000**, *33*, 5825.
- Andresen, A.; Cordes, H. G.; Herwig, J.; Kaminsky, W.; Merck, A.; Mottweiler, R.; Pein, J.; Sinn, H.; Vollmer, H. J. *Angew. Chem., Int. Ed. Engl.* **1976**, *15*, 630.
- Arvanitopoulos, L. D.; Greuel, M. P.; Harwood, H. J. *Polym. Prepr. (Am. Chem. Soc., Div. Polym. Chem.)* **1994**, *35(2)*, 549.
- Ashford, E. J.; Naldi, V.; O'Dell, R.; Billingham, N. C.; Armes, S. P. *Chem. Commun.* **1999**, 1285.
- Baethge, H.; Butz, S.; Schmidt-Naake, G. *Macromol. Rapid Commun.* **1997**, *18*, 911.
- Baily, D.; Tirrell, D.; Vogl, O. *J. Macromol. Sci., Chem.* **1978**, *A12*, 661.
- Baldovi, M. V.; Mohtat, N.; Scaiano, J. C. *Macromolecules* **1996**, *29*, 5497.
- Beckwith, A. J.; Bowry, V. W.; Ingold, K. U. *J. Am. Chem. Soc.* **1992**, *114*, 4983.
- Beers, K. L.; Gaynor, S. C.; Matyjaszewski, K. *Polym. Prepr. (Am. Chem. Soc., Div. Polym. Chem.)* **1996**, *37(1)*, 571.
- Benoit, D.; Grimaldi, S.; Finet, J.; Tordo, P.; Fontanille, M.; Gnanou, Y. In *Controlled Radical Polymerization*; Matyjaszewski, K., Ed.; ACS Symp. Ser. No. 685; American Chemical Society: Washington, DC, 1998; p 225.
- Benoit, D.; Grimaldi, S.; Finet, J.; Tordo, P.; Fontanille, M.; Gnanou, Y. *Polym. Prepr. (Am. Chem. Soc., Div. Polym. Chem.)* **1997**, *38(1)*, 729.
- Benoit, D.; Harth, E.; Fox, P.; Waymouth, R. M.; Hawker, C. J. *Macromolecules*, **2000**, *33*, 363.

- Bercaw, J. E. Presented at 3rd Chemical Congress of North America, Toronto, Canada, June 1988.
- Bertin, D.; Boutevin, B. *Polym. Bull.* **1996**, *37*, 337.
- Bodanski, M.; Klaussner, Y.; Ondetti, M. A. *Peptide synthesis*, 2nd Ed. Wiley-Interscience, New York, 1976, p.26.
- Bodanszky, M.; Bodanszky, A. *Int. J. Pept. Protein Res.* **1984**, *23*, 565.
- Boeré, R. T.; Oakley, R. T.; Reed, R. W. *J. Organomet. Chem.* **1987**, *331*, 161.
- Bohrisch, J.; Wendler, U.; Jaeger, W. *Macromol. Rapid. Commun.* **1997**, 975.
- Borsig, E.; Lazar, M.; Capla, M.; Florian, S. *Angew. Makromol. Chem.* **1969**, *9*, 89.
- Bowry, V. W.; Ingold, K. U. *J. Am. Chem. Soc.* **1992**, *114*, 4992.
- Brand, E.; Stickler, M.; Meyerhoff, G. *Makromol. Chem.* **1980**, *181*, 913.
- Brandts, J. A. M.; van de Geijn, P.; van Faassen, E. E.; Boersma, J.; van Koten, G. *J. Organomet. Chem.* **1999**, *584(2)*, 246.
- Brant, P.; Canich, J. A. M. (Exxon). PCT Int. Appl. WO 93/12151, 1993.
- Brant, P.; Canich, J. A. M.; Dias, A. J.; Bamberger, R. L.; Licciardi, G. F.; Henrichs, P. M. (Exxon). PCT Intl. Appl. 94/07930, 1994.
- Brant, P.; Canich, J. A. M.; Merrill, N. A. (Exxon). PCT Int. Appl. WO 93/21242, 1993.
- Braslau, R.; Burrill, L. C.; Siano, M.; Naik, N.; Howden, R. K.; Mahal, L. K. *Macromolecules* **1997**, *30*, 7348.
- Braun, D. *Macromol. Symp.* **1996**, *111*, 63.
- Breslow, D. S.; Newburg, N. R. *J. Am. Chem. Soc.* **1957**, *79*, 5072.
- Breslow, D. S.; Newburg, N. R. *J. Am. Chem. Soc.* **1959**, *81*, 81.
- Briceño, G.; Chang, H.; Sun, X.; Schultz, P. G. *Science* **1995**, *270*, 273.
- Brocchini, S.; James, K.; Tangpasuthadol, V.; Kohn, J. *J. Am. Chem. Soc.* **1997**, *119*, 4553.
- Burczyk, A. F.; O'Driscoll, K. F.; Rempel, G. L. *J. Polym. Sci., Polym. Chem. Ed.* **1984**, *22*, 3255.

- Burguiere, C.; Dourges, M. A.; Charleux, B.; Vairon, J. P. *Macromolecules* **1999**, *32*, 3883.
- Calata, J. M.; Bubel, F.; Hammouch, S. O. *Macromolecules* **1995**, *28*, 8441.
- Canich, J. A. M. (Exxon). Eur. Pat. Appl. 0 420 436 A1, 1991.
- Canich, J. A. M. (Exxon). PCT Int. Appl. WO 96/00244, 1996.
- Canich, J. A. M. (Exxon). U.S. Patent 5,026,798, 1991.
- Canich, J. A. M. (Exxon). U.S. Patent 5,096,867, 1992.
- Canich, J. A. M.; Licciardi, G. F. (Exxon). U.S. Patent 5,057,475, 1991.
- Carpino, L. A. *Acc. Chem. Res.* **1973**, *6*, 191.
- Carpino, L. A. *J. Am. Chem. Soc.* **1957**, *79*, 98.
- Carpino, L. A.; Carpino, B. A.; Giza, C. A.; Murray, R. W.; Santilli, A. A.; Terry, P. H. *Org. Synth.* **1964**, *44*, 22.
- Carpino, L. A.; Collins, D.; Gowecke, S.; Mayo, J.; Thatte, S. D.; Tibbets, F. *Org. Synth. Coll.* **1973**, *5*, 166.
- Chambard, G.; Klumperman, B.; German, A. L. *Macromolecules*, **2000**, *33*, 4417.
- Chateauneuf, J.; Luszyk, J.; Ingold, K. U. *J. Org. Chem.* **1988**, *53*, 1629.
- Chiefari, J.; Chong, Y. K.; Ercole, F.; Krstina, J.; Jeffery, J.; Le, T. P. T.; Mayadunne, R. T. A.; Meijs, G. F.; Moad, C. L.; Moad, G.; Rizzardo, E.; Thang, S. H. *Macromolecules* **1998**, *31*, 5559.
- Chong, Y. K.; Le, T. P. T.; Moad, G.; Rizzardo, E.; Thang, S. H. *Macromolecules* **1999**, *32*, 2071.
- Chung, T. C.; Lu, H. L. *U. S. Pat.* 5,543,484, 1996.
- Ciampolini, M.; Nardi, N. *Inorg. Chem.* **1966**, *5*, 41.
- Colombani, D. *Prog. Polym. Sci.* **1997**, *22*, 1649.
- Connolly, T. J.; Maldoví, M. V.; Mohtat, N.; Scaiano, J. C. *Tetra. Lett.* **1996**, *37*, 4919.
- Corey, E. J.; Venkateswarlu, A. *J. Am. Chem. Soc.* **1972**, *94*, 6190.

- Crivello, J. V.; Lee, J. L.; Conlon, D. A. *J. Polym. Sci., Polym. Chem.* **1986**, *24*, 1251.
- Curran, D. P. *Comprehensive Organic Synthesis*; Trost, B. M., Fleming, I., Eds.; Pergamon: Oxford, UK, 1991; Vol. 4, p175.
- Curran, D. P. *Synthesis* **1988**, 489.
- Danielson, E.; Golden, J.; McFarland, E. W.; Reaves, C. M.; Weinberg, W. H.; Wu, X. D. *Nature* **1997**, *389*, 944.
- Davis, A. G.; Griller, D.; Roberts, B. P. *J. Chem. Soc. Perkin Trans. II* **1972**, 2229.
- de la Cal, J. C.; Leiza, J. R.; Asúa, J. M. *J. Polym. Sci. Polym. Chem.* **1991**, *29*, 155.
- Devonport, W.; Michalak, L.; Malmström, E.; Mate, M.; Kurdi, B.; Hawker, C. J.; Barclay, G. G.; Sinta, R. *Macromolecules* **1997**, *30*, 1929.
- Devore, D. D. (Dow). Eur. Pat. Appl. 0 514 828 A1, 1992.
- Devore, D. D.; Crawford, L. H.; Stevens, J. C.; Timmers, F. J.; Mussell, R. D.; Wilson, D. R.; Rosen, R. K. (Dow). PCT Int. Appl. WO 95/00526, 1995.
- Diar, *Inorg. Chem.* **1995**, *34*, 6100.
- Dos Santos, C.G.; Jenkins, A.D.; Walton, D.R.M.; Stejskal, J.; Kratochvíl, P. *Coll. Czech. Chem. Commun.* **1993**, *58*, 2523.
- Duncalf, D. J.; Wade, H. J.; Waterson, C.; Derrick, P. J.; Haddleton, D. M.; McCamley, A. *Macromolecules* **1996**, *29*, 6399.
- Endo, K.; Saitoh, M. *Polymer J.* **2000**, *32*, 300.
- Ewen, J. A. In *Catalytic Polymerization of Olefins, Studies in Surface Science and Catalysis*; Keii, T., Soga, K., Eds.; Elsevier: New York, 1986; p 271.
- Ewen, J. A. *J. Am. Chem. Soc.* **1984**, *106*, 6355.
- Fischer, A.; Brembilla, A.; Lochon, P. *Macromolecules* **1999**, *32*, 6069.
- Fischer, H. *J. Am. Chem. Soc.* **1986**, *108*, 3925.
- Fischer, H. *J. Polym. Sci., Part A* **1999**, *37*, 1885.
- Fischer, H. *Macromolecules* **1997**, *30*, 5666.
- Fischer, J. *J. Am. Chem. Soc.* **1986**, *108*, 3925.

- Foster, P. F.; Chien, J. C. W.; Rausch, M. D. *Organometallics* **1996**, *15*, 2404.
- Fréchet, J.M.J.; Henmi, M.; Gitsov, I.; Aoshima, S.; Leduc, M.R.; Grubbs, R.B. *Science* **1995**, *269*, 1080.
- Fukuda, T.; Terauchi, T.; Goto, A.; Ohno, K.; Tsujii, Y.; Miyamoto, T. *Macromolecules* **1996**, *29*, 6393.
- Fukuda, T.; Terauchi, T.; Goto, A.; Tsujii, Y.; Miyamoto, T. *Macromolecules* **1996**, *29*, 3050.
- Furka, A.; Sebestyen, F.; Asgedom, M.; Dibo, G. *Abstr. 14th Int. Congr. Biochem., Prague, 1988: Abstr. 10th Int. Symp. Med. Chem., Budapest, 1988.*
- Furka, A.; Sebestyen, F.; Asgedom, M.; Dibo, G. *Int. J. Pept. Protein Res.* **1991**, *37*, 487.
- Ganachaud, F.; Monteiro, M. J.; Gilbert, R. G.; Dourges, M.-A.; Thang, S. H.; Rizzardo, E. *Macromolecules* **2000**, *33*, 6738.
- Gandini, A.; Plesch, P. H. *J. Chem. Soc.* **1965**, 4826.
- Gao, B.; Chen, X.; Ivan, B.; Kops, J.; Batsberg, W. *Macromol. Rapid Commun.* **1997**, *18*, 1095.
- Gaynor, S.; Qiu, J.; Matyjaszewski, K. *Macromolecules* **1998**, *31*, 5951.
- Gaynor, S.; Balchandani, P.; Kulfan, A.; Podwika, M.; Matyjaszewski, K. *Polym. Prepr. (Am. Chem. Soc., Div. Polym. Chem.)* **1997**, *38(1)*, 496.
- Gaynor, S.; Greszta, D.; Mandare, D.; Teodorescu, M.; Matyjaszewski, K. *J. Macromol. Sci., Pure Appl. Chem.* **1994**, *A31*, 1561.
- Gaynor, S.; Matyjaszewski, K. *Polym. Prepr. (Am. Chem. Soc., Div. Polym. Chem.)* **1997**, *38(1)*, 758.
- Gaynor, S.; Wang, J.-S.; Matyjaszewski, K. *Macromolecules* **1995**, *28*, 8051.
- Gaynor, S.; Edelman, S.; Matyjaszewski, K. *Macromolecules* **1996**, *29*, 1079.
- Gelin, R.; Gelin, S.; Gallaud, A. *Bull. Soc. Chim. Fr.* **1973**, *12*, 3416.
- Georges, M. K.; Hamer, G. K.; Listigovers, N. A. *Macromolecules* **1998**, *31*, 9087.
- Georges, M. K.; Kee, R. A.; Veregin, R. P. N.; Hamer, G. K.; Kazmaier, M. K. *J. Phys. Org. Chem.* **1995**, *8*, 301.

- Georges, M. K.; Listigovers, N. A.; Odell, P. G.; Hamer, G. K.; Quinlan, M. H.; Veregin, R. P. N. *Polym. Prepr. (Am. Chem. Soc., Div. Polym. Chem.)* **1997**, *38* (1) 454.
- Georges, M. K.; Veregin, R. P. N.; Kazmaier, M. K.; Hamer, G. K.; Saban, M. *Macromolecules* **1994**, *27*, 7228.
- Georges, M. K.; Veregin, R. P. N.; Kazmaier, P. M.; Hamer, G. K. *Macromolecules* **1993**, *26*, 2987.
- Georges, M. K.; Veregin, R. P. N.; Kazmaier, P. M.; Hamer, G. K. *Trends Polym. Sci.* **1994**, *2*, 66.
- Giannetti, E.; Nicoletti, G.; Mazzocchi, R. *J. Polym. Sci. Polym. Chem.* **1985**, *23*, 2117.
- Goto, A.; Fukuda, T. *Macromol. Rapid Commun.* **1999**, *20*, 633.
- Grande, D.; Baskaran, S.; Baskaran, C.; Gnanou, Y.; Chaikof, E. L. *Macromolecules* **2000**, *33*, 1123.
- Granel, C.; Dubois, Ph.; Jérôme, R.; Teyssié, Ph. *Macromolecules* **1996**, *29*, 8576.
- Grassi, A.; Sacchco, S.; Zambelli, A.; Laschi, F. *Macromolecules* **1998**, *31*, 5591.
- Greene, T. W.; Wuts, P. G. M. *Protective Groups in Organic Synthesis*, 3rd Ed. Wiley-Interscience, New York, 1999, p.518.
- Greszta, D.; Mardare, D.; Matyjaszewski, K. *Polym. Prepr. (Am. Chem. Soc., Div. Polym. Chem.)* **1994**, *35*(1), 466.
- Greszta, D.; Matyjaszewski, K. *Macromolecules* **1996**, *29*, 7661.
- Greszta, D.; Matyjaszewski, K. *J. Polym. Sci. A. Polym. Chem.* **1997**, *35*, 1857.
- Griffiths, M. C.; Strauch, J.; Monteiro, M. J.; Gilbert, R. G. *Macromolecules* **1998**, *31*, 7835.
- Grimaldi, G.; Finet, J.-P.; Moigne, F. L.; Zeghdaoui, A.; Tordo, P.; Benoit, D.; Fontanille, M.; Gnanou, Y. *Macromolecules* **2000**, *33*, 1141.
- Grubbs, R. B.; Hawker, C. J.; Dao, J.; Fréchet, J. M. J. *Angew. Chem. Int. Ed. Engl.* **1997**, *36*, 270.
- Hadda, T. B.; Bozee, H. L. *Polyhedron* **1988**, *7*, 575.
- Haddleton, D. M.; Crossman, M. C.; Dana, B. H.; Duncalf, D. J.; Heming, A. M.; Kukulj, D.; Shooter, A. J. *Macromolecules*, **1999**, *32*, 2110.

- Haddleton, D. M.; Jasieczek, C. B.; Hannon, M. J.; Shooter, A. J. *Macromolecules* **1997**, *30*, 2190.
- Haddleton, D. M.; Kukulj, D.; Duncalf, D. J.; Heming, A. M.; Shooter, A. J. *Macromolecules* **1998**, *31*, 5201.
- Hammouch, S. O.; Calata, J. M. *Macromol. Rapid Commun.* **1996**, *17*, 149.
- Hammouch, S. O.; Calata, J. M. *Macromol. Rapid Commun.* **1996**, *17*, 683.
- Harrington, B. A. (Exxon). PCT Int. Appl. WO 96/40806, 1996.
- Harrington, B. A.; Hlatkey, G. G.; Canich, J. A. M.; Merrill, N. A. (Exxon). U.S. Patent 5,635,573, 1997.
- Hartney, M. A.; Tarascon, R. G.; Novembre, A. E. *J. Vac. Sci. Technol. (B)* **1985**, *3(1)*, 360.
- Hasebe, T.; Kamigaito, M.; Sawamoto, M. *Macromolecules* **1996**, *29*, 6100.
- Hawker, C. J. *Angew. Chem. Int. Ed. Engl.* **1995**, *34*, 1456.
- Hawker, C. J. *J. Am. Chem. Soc.* **1994**, *116*, 11185.
- Hawker, C. J. *Trends Polym. Sci.* **1996**, *4*, 183.
- Hawker, C. J.; Barclay, G. G.; Orellana, A.; Dao, J.; Devenport, W. *Macromolecules* **1996**, *29*, 5245.
- Hawker, C. J.; Benoit, D.; Harth, E.; Nielson, R. B.; Klarner, G.; Petro, M., A presentation held in ACS national meeting in San Francisco, 2000.
- Hawker, C. J.; Elce, E.; Dao, J.; Volksen, W.; Russell, T. P.; Barclay, G. G. *Macromolecules* **1996**, *29*, 2686.
- Hawker, C. J.; Fréchet, J. M. J.; Grubbs, R. B.; Dao, J. *J. Am. Chem. Soc.* **1995**, *117*, 10763.
- Hawker, C. J.; Hendrick, J. L. *Macromolecules* **1995**, *28*, 2993.
- Hawker, C. J.; Mecerreyes, D.; Elce, E.; Dao, J.; Hedrick, J. L.; Barakat, I.; Dubois, P.; Jérôme, R.; Volksen, W. *Macromol. Chem. Phys.* **1997**, *198*, 1553.
- Heise, A.; Nguyen, C.; Malek, R.; Hedrick, J. L.; Frank, C. W.; Miller, R. D. *Macromolecules* **2000**, *33*, 2346.

- Herman, D. F.; Nelson, W. K. *J. Am. Chem. Soc.* **1953**, *75*, 3877.
- Hindmarsh, A. C., "ODEPACK, A Systematized Collection of ODE Solvers", in *Scientific Computing*, Stepleman, R. S., *et al.* Eds., Amsterdam, **1983**, pp.55-64.
- Houghten, R. A.; Pinilla, C.; Blondelle, S. E.; Appel, J. R.; Dooley, C. T.; Cuervo, J. H. *Nature* **1991**, *354*, 84.
- Houlihan, F.; Bouchard, F.; Fréchet, J. M. J.; Willson, C. G. *Can. J. Chem.* **1985**, *63*, 153.
- Howard, J. A.; Tait, J. C. *J. Org. Chem.* **1978**, *43*, 4279.
- Howell, B. A.; Priddy, D. B.; Li, I. Q.; Smith, P. B.; Kastl, P. E. *Polym. Bull.* **1996**, *37*, 451.
- Hungenberg, K.-D.; Bandermann, F. *Makromol. Chem.* **1983**, *184*, 1423.
- Ingold, K. U. In *Free Radicals*; Kochi, J. K., Ed.; Wiley: New York, 1973; Vol. 1, Chapter 2.
- Inoue, S.; Tsuruta, T.; Furukawa, J. *Makromol. Chem.* **1961**, *49*, 13.
- Ishihara, N.; Kuramoto, M.; Uoi, M. *Macromolecules* **1988**, *21*, 3356.
- Jandeleit, B.; Weinberg, W. H. *Chem. Ind.* **1998**, 795.
- Jia, X.; Mingqian, L.; Han, S.; Wang, C.; Wei, Y. *Mater. Lett.* **1997**, *31*, 137.
- Jones, R. G.; Matsubayashi, Y. *Polymer* **1990**, *31*, 1519.
- Jousset, S.; Hammouch, S. O.; Catala, J.-M.; *Macromolecules* **1997**, *30*, 6685.
- Kaiser, E. Sr.; Tam, J. P.; Ubiak, T. M.; Merrifield, R. B. *Tetrahedron Lett.* **1988**, *29*, 303.
- Kajiwara, A.; Matyjaszewski, K.; Kamachi, M. *Macromolecules* **1998**, *31*, 5695.
- Kaminsky, W.; Arndt, M. *Adv. Polym. Sci.* **1997**, *127*, 143.
- Kaminsky, W.; Kulper, K.; Brintzinger, H.; Wild, F. *Angew. Chem., Int. Ed. Engl.* **1985**, *24*, 507.
- Kato, M.; Kamigaito, M.; Sawamoto, M.; Higashimura, T. *Macromolecules* **1995**, *28*, 1721.
- Kauffmann, H. F. *Makromol. Chem.* **1979**, *180*, 2649.

- Kazmaier, M. K.; Daimon, K.; Georges, M. K.; Hamer, G. K.; Veregin, R. P. N. *Macromolecules* **1997**, *30*, 2228.
- Kazmaier, M. K.; Moffat, K. A.; Georges, M. K.; Veregin, R. P. N.; Hamer, G. K. *Macromolecules* **1995**, *28*, 1841.
- Kennedy, J. P.; Ivan, B. *Designed polymers by Carbocationic Macromolecular Engineering. Theory and Practice*; Hanser: Munich, 1992.
- Keoshkerian, B.; Georges, M. K.; Boils-Boissier, D. *Macromolecules* **1995**, *28*, 6381.
- Keoshkerian, B.; Georges, M. K.; Quinlan, M.; Veregin, R.; Goodbrand, B. *Macromolecules*, **1998**, *31*, 7559.
- Kharasch, M. S.; Jensen, E. U.; Urry, W. H. *Science* **1945**, *102*, 128.
- Kobatake, S.; Harwood, H. J.; Quirk, R. P.; Priddy, D. B. *Macromolecules* **1997**, *30*, 4239.
- Kotani, Y.; Kamigaito, M.; Sawamoto, M. *Macromolecules* **1999**, *32*, 2420.
- Kotani, Y.; Kamigaito, M.; Sawamoto, M. *Macromolecules* **2000**, *33*, 3543.
- Kothe, T.; Marque, S.; Martschke, R.; Popov, M.; Fischer, H. *J. Chem. Soc., Perkin Trans. 2* **1998**, 1553.
- Kovtun, G. A.; Aleksandrov, A. L.; Golubev, V. A. *Izv. Akad. Nauk SSSR, Ser. Khim.* **1973**, 2197.
- Lai, S. Y.; Wilson, J. R.; Knight, G. W.; Stevens, J. C. (Dow). PCT Int. Appl. WO 93/08221, 1993.
- Lalonde, M.; Chan, T. H. *Synthesis* **1985**, 817.
- Lam, K.; Salmon, S.; Hersh, E.; Hruby, V.; Kazmierski, W.; Knapp, R. *Nature* **1991**, *354*, 82.
- Landini, D.; Rolla, F. *J. Org. Chem.* **1980**, *45*, 3527.
- LaPointe, R. E.; Rosen, R. K.; Nickias, P. N. (Dow). Eur. Pat. Appl. 0 495 375 A2, 1992.
- LaPointe, R. E.; Stevens, J. C.; Nickias, P. N.; McAdon, M. H. (Dow). Eur. Pat. Appl. O 520 732 A1, 1992.
- Le, T. P.; Moad, G.; Rizzardo, E.; Thang, S. H. PCT Int. Appl. WO 9801478 A1 980115; *Chem. Abstr.* **1998**, *128*, 115390.

- Lecomte, Ph.; Draiper, I.; Dubois, Ph.; Teyssié, Ph.; Jérôme, R. *Macromolecules* **1997**, *30*, 7631.
- Leduc, M. R.; Hayes, W.; Fréchet, J. M. J. *J. Polym. Sci., Part A* **1998**, *36*, 1.
- Leduc, M.R.; Hawker, C.J.; M.R.; Dao, J.; Fréchet, J. M. J. *J. Am. Chem. Soc.* **1996**, *118*, 1111.
- Lee, M.; Minoura, Y. *J. Chem Soc. Faraday Trans I* **1978**, *74*, 1726.
- Lee, M.; Utsumi, K.; Minoura, Y. *J. Chem Soc. Faraday Trans I* **1979**, *75*, 1821.
- Li, I. Q.; Howell, B. A.; Koster, R. A. Priddy, D. B. *Macromolecules* **1996**, *29*, 8554.
- Li, I. Q.; Howell, B. A.; Matyjaszewski, K.; Shigemoto, T.; Smith, P. B.; Priddy, D. B. *Macromolecules* **1995**, *28*, 6692.
- Listigovers, N. A.; Georges, M. K.; Odell, P. G.; Keoshkerian, B. *Macromolecules* **1996**, *29*, 8992.
- Lokaj, J.; Vlcek, D.; Kriz, J. *Macromolecules* **1997**, *30*, 7644.
- Long, W. P. *J. Am. Chem. Soc.* **1959**, *81*, 5312.
- Long, W. P.; Breslow, D. S. *J. Am. Chem. Soc.* **1960**, *82*, 1953.
- Long, W. P.; Breslow, D. S. *Liebigs Ann. Chem.* **1975**, 463.
- Lott, R. S.; Chauhan, V. S.; Stammer, C. H. *J. Chem. Soc., Chem. Commun.*, **1979**, 495.
- Lundt, B. F.; Johansen, N. L.; Vølund, A.; Markussen, J. *Int. J. Pept. Protein Res.* **1978**, *12*, 258.
- Maerker, C.; Case, F. H. *J. Am. Chem. Soc.* **1958**, *80*, 2745.
- Malmström, E. E.; Hawker, C. J. *Macromol. Chem. Phys.* **1998**, *199*, 923.
- Malmström, E.; Miller, R. D.; Hawker, C. J. *Tetrahedron* **1997**, *53*, 15225.
- Mandare, D.; Gaynor, S.; Matyjaszewski, K. *Polym. Prepr. (Am. Chem. Soc., Div. Polym. Chem.)* **1994**, *35(1)*, 700.
- Mandare, D.; Matyjaszewski, K. *Macromolecules* **1994**, *27*, 645.
- Marchand, A. P.; Weimer, W. R. Jr *Chem. Ind.* **1969**, 200.

- Marquardt, D. W. *J. Soc. Ind. Appl. Math.* **1963**, *11*, 431.
- Masui, Y.; Chino, N.; Sakakibara, S. *Bull. Chem. Soc. Jpn.* **1980**, *53*, 464.
- Mattes, H.; Benezrà, C. *Tetrahedron Letters* **1987**, *28*, 1697.
- Matyjaszewski, K. A presentation held in ACS national meeting in New Orleans, 1999.
- Matyjaszewski, K., Ed. *Cationic Polymerizations: Mechanism, Synthesis and Applications*; Marcel Dekker: New York, 1996.
- Matyjaszewski, K.; Acar, M. H.; Beers, K. L.; Coca, S.; Davis, K. A.; Gaynor, S. G.; Miller, P. J.; Paik, H.-J.; Shipp, D. A.; Teodorescu, M.; Xia, J.; Zhang, X. *Polym. Prepr. (Am. Chem. Soc., Div. Polym. Chem.)* **1999**, *40(2)*, 966.
- Matyjaszewski, K.; Coca, S.; Gaynor, S. G.; Wei, M.; Woodworth, B. E. *Macromolecules* **1998**, *31*, 5967.
- Matyjaszewski, K.; Coessens, V.; Nakagawa, Y.; Xia, J.; Qiu, J.; Gaynor, S. G.; Coca, S.; Jasieczek, C. In *Functional Polymers: Modern Synthetic Methods and Novel Structures*; Patil, A. O., Schulz, D. N., Novak, B. M., Eds.; American Chemical Society Symposium Series 704; American Chemical Society: Washington, DC, 1998; pp 16-27.
- Matyjaszewski, K.; Davis, K.; Patten, T.; Wei, M. *Tetrahedron*, **1997**, *53*, 15321.
- Matyjaszewski, K.; Gaynor, S. C.; Kulfan, A.; Podwika, M. *Macromolecules* **1997**, *30*, 5192.
- Matyjaszewski, K.; Gaynor, S. *Polym. Mat. Sci. Eng.* **1997**, *77*, 210.
- Matyjaszewski, K.; Gaynor, S.; Greszta, D.; Mandare, D.; Shigemoto, T. *Makromol. Symp.* **1995**, *98*, 73.
- Matyjaszewski, K.; Gaynor, S.; Wang, J.-S. *Macromolecules* **1995**, *28*, 2093.
- Matyjaszewski, K.; Jo, S. M.; Paik, H.-J.; Shipp, D. A. *Macromolecules* **1999**, *32*, 6431.
- Matyjaszewski, K.; Patten, T. E.; Xia, J. *J. Am. Chem. Soc.* **1997**, *119*, 674.
- Matyjaszewski, K.; Shigemoto, T.; Fréchet, J. M. J.; Leduc, M. R. *Macromolecules* **1996**, *29*, 4167.
- Matyjaszewski, K.; Wang, J. S. *WO 96/30421* **1996**.
- Matyjaszewski, K.; Wang, J.-L.; Grimaud, T.; Shipp, D. A. *Macromolecules* **1998**, *31*, 1527.

- Matyjaszewski, K.; Wei, M.; Xia, J.; McDermott, N. E. *Macromolecules* **1997**, *30*, 8161.
- Matyjaszewski, K.; Woodworth, B. E.; Zhang, X.; Gaynor, S. G.; Metzner, Z. *Macromolecules* **1998**, *31*, 5955.
- Mayadunne, R. T. A.; Rizzardo, E.; Chiefari, J.; Krstina, J.; Moad, G.; Postma, A.; Thang, S. H. *Macromolecules* **2000**, *33*, 243.
- McKay, F. C.; Albertson, N. F. *J. Am. Chem. Soc.* **1957**, *79*, 4686.
- Mecerreyes, D.; Trollsås, M.; Hedrick, J. L. *Macromolecules* **1999**, *32*, 8753.
- Minisci, F. *Acc. Chem. Res.* **1975**, *8*, 165.
- Miura, Y.; Hirota, K.; Moto, H.; Yamada, B. *Macromolecules* **1998**, *31*, 4659.
- Miura, Y.; Hirota, K.; Moto, H.; Yamada, B. *Macromolecules* **1999**, *32*, 8356.
- Miura, Y.; Nakamura, N.; Taniguchi, I. *Macromolecules* **2001**, *34*, 447.
- Moad, G.; Rizzardo, E. *Macromolecules* **1995**, *28*, 8722.
- Moad, G.; Rizzardo, E.; Solomon, D. H. *J. Macromol. Sci., Chem.* **1982**, *A17*, 51.
- Moad, G.; Rizzardo, E.; Solomon, D. H. *Macromolecules* **1982**, *15*, 909.
- Moad, G.; Rizzardo, E.; Solomon, D. H. *Polym. Bull.* **1982**, *6*, 589.
- Moad, G.; Solomon, D. H. *The Chemistry of Free Radical Polymerization*; Pergamon: Oxford, 1995; p 335.
- Mohanraj, S.; Ford, W. T. *Macromolecules* **1986**, *19*, 2470.
- Moineau, G.; Granel, C.; Dubois, Ph.; Jérôme, R.; Teyssié, Ph. *Macromolecules* **1998**, *31*, 542.
- Moineau, G.; Minet, M.; Dubois, Ph.; Teyssié, Ph.; Senninger, T.; Jérôme, R. *Macromolecules* **1999**, *32*, 27.
- Moré, J. *The Levenberg-Marquardt Algorithm, Implementation and Theory in Numerical Analysis* G. A. Watson, Ed. Lecture Notes in Mathematics 630, Springer-Verlag, 1977.
- Mullen, K.; Steenbock, M.; Klapper, M. *Polym. Prepr. (Am. Chem. Soc., Div. Polym. Chem.)* **1999**, *40(2)*, 321.

- Natta, G.; Mazzanti, G. *Tetrahedron* **1960**, *8*, 86.
- Natta, G.; Pino, P.; Mazzanti, G.; Giannini, U.; Mantica, E.; Peraldo, M. *J. Polym. Sci.* **1957**, *26*, 120.
- Nesmeyanov, A. N.; Nogina, O. V.; Freidlina, R. K. *Dokl. Akad. Nauk USSR* **1954**, *95*, 813.
- Nickias, P. N.; McAdon, M. H.; Patton, J. T. (Dow). PCT Int. Appl. WO 97/15583, 1997.
- Nielsen, R. B.; Safir, A. L.; Petro, M.; Lee, T. S.; Huefner, P. *Polym. Mater. Sci. Eng.* **1999**, *80*, 92.
- Numerical Recipes in Fortran 77: The Art of Scientific Computing, Ch.10.4, Cambridge University Press, p402.
- Odell, P. G.; Rabien, A.; Michalak, L. M.; Veregin, R. P. N.; Quinlan, M. H.; Moffat, K. A.; MacLeod, P. J.; Listigovers, N. A.; Honeyman, C. H.; Georges, M. K. *Polym. Prepr. (Am. Chem. Soc., Div. Polym. Chem.)* **1997**, *38* (2), 414.
- Odell, P. G.; Veregin, R. P. N.; Michalak, L. M.; Brousmiche, D.; Georges, M. K. *Macromolecules* **1995**, *28*, 8453.
- Odian, G. "Principles of Polymerization" 3rd Ed.; John Wiley and Sons; New York; **1991**; p230.
- Ohno, K.; Goto, A.; Fukuda, T.; Xia, J.; Matyjaszewski, K. *Macromolecules*, **1998**, *31*, 2699.
- Okuda, J. *Chem. Ber.* **1990**, *123*, 1649.
- Olah, G. A.; Narang, S. C. *Tetrahedron* **1982**, *38*, 2225.
- Otsu, T.; Kuriyama, A. *Polym. J.* **1988**, *17*, 97.
- Otsu, T.; Matsumoto, A. *Adv. Polym. Sci.* **1998**, *136*, 75.
- Otsu, T.; Yoshida, M. *Makromol. Chem. Rapid Commun.* **1982**, *3*, 127.
- Paik, H. J.; Matyjaszewski, K. *Polym. Prepr. (Am. Chem. Soc., Div. Polym. Chem.)* **2000**, *41*(1), 470.
- Pangborn, A. B.; Giardello, M. A.; Grubbs, R. H.; Rosen, R. K.; Timmers, F. J. *Organometallics* **1996**, 1518.

- Pannell, R. B.; Canich, J. A. M.; Hlatky, G. G. (Exxon). PCT Int. Appl. WO 94/00500, 1994.
- Pattern, T. E.; Xia, J.; Abernathy, T.; Matyjaszewski, K. *Science* **1996**, 272, 866.
- Pellecchia, C.; Longo, P.; Proto, A.; Zambelli, A. *Makromol. Chem., Rapid Commun.* **1992**, 13, 265.
- Penczek, S.; Matyjaszewski, K. *J. Polym. Sci., Polym. Symp.* **1976**, 56, 255.
- Percec, V.; Barboiu, B. *Macromolecules* **1995**, 28, 7970.
- Percec, V.; Barboiu, B.; Neumann, A.; Ronda, J. C.; Zhao, M. *Macromolecules* **1996**, 29, 3665.
- Percec, V.; Kim, H.-J.; Barboiu, B. *Macromolecules* **1997**, 30, 6702.
- Petro, M.; Safir, A. L.; Nielson, R. B. *Polym. Prepr. (Am. Chem. Soc., Div. Polym. Chem.)* **1999**, 40 (2) 702.
- Petrucci, M. G. L.; Lebuis, A.-M.; Kakkar, A. K. *Organometallics* **1998**, 17, 4966.
- Pozdnev, V. F.; Nishnova, I. A. *Zh. Org. Khim.* **1976**, 12, 1407.
- Puts, R. D.; Sogah, D. Y. *Macromolecules* **1996**, 29, 3323.
- Qiu, J.; Matyjaszewski, K. *Macromolecules* **1997**, 30, 5643.
- Rawal, V. H.; Jones, R. J.; Cava, M. P. *J. Org. Chem.* **1987**, 52, 19.
- Ready, T. E.; Chien, J. C. W.; Rausch, M. D. *J. Organomet. Chem.* **1996**, 519, 21.
- Rempp, P. F.; Lutz, P. J. in *Comprehensive Polymer Chemistry, Vol. 7*, Aggarwal, S. V. ed. Pergamon, Oxford, **1988**, Chapter 12.
- Rizzardo, E. *Chem. Aust.* **1987**, 54, 32.
- Rizzardo, E.; Chiefari, J.; Chong, Y. K.; Ercole, F.; Krstina, J.; Jeffery, J.; Le, T. P. T.; Mayadunne, R. T. A.; Meijs, G. F.; Moad, C. L.; Moad, G.; Thang, S. H. *Macromol. Symp.*, in press.
- Rizzardo, E.; Chiefari, J.; Mayadunne, R. T. A.; Moad, G.; Thang, S. H. *Polym. Prepr. (Am. Chem. Soc., Div. Polym. Chem.)* **1999**, 40 (2) 342.
- Rizzardo, E.; Moad, G. *Living Radical Polymerization*; Salamone, J. C., Ed.; CRC Press: Boca Raton, FL, 1996; Vol. 5, p 3834.

- Rizzardo, E.; Solomon, D. H. *Polym. Bull.* **1979**, *1*, 529.
- Rosen, R. K.; Nickias, P. N.; Devore, D. D.; Stevens, J. C.; Timmers, F. J. (Dow). U.S. Patent 5,374,696, 1994.
- Sawamoto, M.; Higashimura, T. *Macromolecules* **1978**, *11*, 51.
- Scott, J. W. *Org. Prep. Proceed. Int.* **1980**, *12*, 242.
- Sernetz, F. G.; Muelhaupt, R.; Waymouth, R. M. *Macromol. Chem. Phys.* **1996**, *197*, 1071-83.
- Shapiro, P. J.; Bunel, E.; Schaefer, W. P.; Bercaw, J. E. *Organometallics* **1990**, *9*, 867.
- Sherrington, D.; Hodge, P. Eds.; *Syntheses and Separations Using Functional Polymers*; John Wiley & Sons: New York, 1988.
- Shigemoto, T.; Matyjaszewski, K. *Macromol. Rapid. Commun.* **1997**, *17*, 347.
- Shipp, D. A.; Matyjaszewski, K. *Macromolecules*, **1999**, *32*, 2948.
- Sinn, H.; Kaminsky, W. *Adv. Organomet. Chem.* **1980**, *18*, 99.
- Skene, W. G.; Scaiano, J. C.; Listigovers, N. A.; Kazmaier, M. K.; Georges, M. K. *Macromolecules* **2000**, *33*, 5065.
- Soga, K.; Yu, C. H.; Shiono, T. *Makromol. Chem., Rapid Commun.* **1988**, *9*, 351.
- Solomon, D. H.; Rizzardo, E.; Cacioli, P. US Patent 4,581,529, 1985.
- Stahl, G. L.; Walter, R.; Smith, C. W. *J. Org. Chem.* **1978**, *43*, 2285.
- Steenbock, M.; Klapper, M.; Mullen, K.; Pinhal, N.; Hubirck, M. *Acta Polym.* **1996**, *47*, 276.
- Stevens, J. C. *Stud. Surf. Sci. Catal.* **1996**, *101*, 11.
- Stevens, J. C.; Neithamer, D. R. (Dow). Eur. Pat. Appl. 0 418044 A2, 1991.
- Stevens, J. C.; Timmers, F. J.; Wilson, D. R.; Schmidt, G. F.; Nickias, P. N.; Rosen, R. K.; Knight, G. W.; Lai, S.-y. (Dow). Eur. Pat. Appl. 0 416 815 A2, 1991.
- Stork, G.; Hudrlik, P. F. *J. Am. Chem. Soc.* **1968**, *90*, 4462.
- Szwarc, M. *Nature* **1956**, *176*, 1168.
- Takahashi, H.; Ando, T.; Kamigaito, M.; Sawamoto M. *Macromolecules* **1999**, *32*, 6461.

- Tarascon, R. G.; Hartney, M. A.; Bowden, M. J. *Materials for microlithography, ACS Symp. Ser.* **1984**, 266, 361.
- Teodorescu, M.; Gaynor, S. G.; Matyjaszewski, K. *Macromolecules* **2000**, 33, 2335.
- Teodorescu, M.; Matyjaszewski, K. *Polym. Prepr. (Am. Chem. Soc., Div. Polym. Chem.)* **1999**, 40 (2) 428.
- Tomalia, D.; Hedstrand, D.; Ferritto, M. *Macromolecules* **1991**, 24, 1435 and references therein.
- Tsuji, T.; Kataoka, T.; Yoshioka, M.; Sendo, Y.; Nishitani, Y.; Hirai, S.; Maeda, T.; Nagata, W. *Tetrahedron Lett.* **1979**, 2793.
- Turner, S. R.; Blevins, R. W. *Macromolecules* **1990**, 23, 1856.
- Uegaki, H.; Kotani, Y.; Kamigaito, M.; Sawamoto, M. *Macromolecules* **1997**, 30, 2249.
- Veregin, R. P. N.; Georges, M. K.; Hamer, G. K.; Kazmaier, M. K. *Macromolecules* **1995**, 28, 4391.
- Vogl, O.; Jaycox, G.; Hatada, K. *J. Macromol. Sci., Chem.* **1990**, A27, 1781 and references therein.
- Wang, J.-S.; Matyjaszewski, K. *J. Am. Chem. Soc.* **1995**, 117, 5614.
- Wang, X.-S.; Jackson, R. A.; Armes, S. P. *Macromolecules* **2000**, 33, 255.
- Wasserman, H. H.; Berger, G. D.; Cho, K. R. *Tetrahedron Lett.* **1985**, 26, 1411.
- Wayland, B. B.; Poszmik, G.; Mukerjee, S. L.; Fryd, M. *J. Am. Chem. Soc.* **1994**, 116, 7943.
- Webster, O. *Macromol. Symp.* **1995**, 98, 1361.
- Webster, O.W. *Science* **1991**, 251, 887.
- Willson, C. G.; Ito, H.; Fréchet, J. M. J.; Houlihan, F. *Proceedings 28th IUPAC Macromolecular Symposium, Amherst, Mass.* **1982**, p.448.
- Wulkow, M. *Macromol. Theory Simul.* **1996**, 5, 393.
- Xia, J.; Zhang, X.; Matyjaszewski, K. *Macromolecules* **1999**, 32, 3531.

- Xiang, X.-D.; Sun, X.; Briceño, G.; Lou, Y.; Wang, K.; Chang, H.; Wallace-Freedman, W. G. Chen, S.; Schultz, P. G. *Science* **1995**, *268*, 1738.
- Xu, G. *Macromolecules* **1998**, *31*, 2395-2402.
- Yamada, B.; Miura, Y.; Nobukane, Y.; Aota, M., In *Controlled Radical Polymerization*; Matyjaszewski, K., Ed.; ACS Symp. Ser. No. 685; American Chemical Society: Washington, DC, 1998; Chap. 12.
- Yamada, B.; Tanaka, H.; Konishi, K.; Otsu, T. *J. Macromol. Sci.- Pure & Appl. Chem.* **1994**, *31*, 351.
- Yoshida, E.; Ishizone, T.; Hirao, A.; Nakahama, S.; Takata, T.; Endo, T. *Macromolecules* **1994**, *27*, 3119.
- Yousi, Z.; Jian, L.; Rongchuan, Z.; Jianliang, Y.; Lizong, D.; Lansun, Z. *Macromolecules* **2000**, *33*, 4745.
- Yurramendi, L.; Barandiarán, M. J.; Asúa, J. M. *Polymer* **1988**, *29*, 871.
- Yutani, Y.; Tatemoto, M. Eur. Pat. Appl. 0489370A1, 1991.
- Zambelli, A.; Longo, P.; Pellecchia, C.; Grassi, A. *Macromolecules* **1987**, *20*, 2035.
- Zambelli, A.; Oliva, L.; Pellecchia, C. *Macromolecules* **1989**, *22*, 2129

